Recommendations for the revision of safety standards for RACHP equipment

WP 4.4, 5.1 & 5.2

life front

Public report

for the project LIFE FRONT

LIFE FRONT (Flammable Refrigerants Options for Natural Technologies) is an EU project aiming to remove barriers posed by standards for flammable refrigerants in refrigeration, heating and cooling applications

Lead authors:

Daniel Colbourne, HEAT GmbH

More information:

www.lifefront.eu

info@lifefront.eu

January 2020

LIFE FRONT is funded by the EU under the LIFE Climate Action Programme, Project number LIFE16 CCM/BE/000054

TABLE OF CONTENTS

ACKNOWLEDGEMENTS

We thank the GIZ PROKLIMA programme for contributing to this report by sharing experimental data from various projects under IEC SC61C WG4 and SC 61D WG16 as well as IKI projects. PROKLIMA is a programme of the Deutsche Gesellschaft für Internationale Zusammenarbeit GIZ GmbH, commissioned by the Federal Ministry for Economic Cooperation and Development (BMZ).

We thank the Deutsche Umwelthilfe (DUH) for sharing experimental data for various RACHP equipment and Mechanical Engineering department of University College London (UCL) for the use of their refrigeration laboratory.

LIST OF ABBREVIATIONS

ACU	Air-cooled Condensing Unit
CD	Coefficient of Discharge
CDV	Committee Draft for Vote
CENELEC	European Committee for Electrotechnical Standardisation
CRE	Commercial Refrigeration Equipment
CSL	Charge Size Limit
DN	Nominal diameter
FDIS	Final Draft International Standard
GHG	Green House Gas
GWP	Global Warming Potential
HC	Hydrocarbon
HCFC	Hydrochlorofluorocarbon
HFC	Hydrofluorocarbon
HFO	Hydrofluoroolefin
IDU	Indoor Unit
LFL	Lower Flammability Limit
LIFE FRONT Project	Flammable Refrigerant Options for Natural Technologies–Improved standards & product design for their safe use (FRONT)
NV	Natural Ventilation
ODS	Ozone-depleting substances
RAC	Refrigeration and Air conditioning
RACHP	Refrigeration, Air conditioning, and Heat Pump
RSSs	RACHP Safety Standards
UFL	Upper Flammability Limit
VE	Ventilation Equipment

EXECUTIVE SUMMARY

Background

In a setting where greenhouse gas emission (GHG) and ozone-depleting substances (ODS) are being actively reduced as countries are making a concerted effort to meet their Paris Agreement and Montreal Protocol obligations, natural refrigerants provide an important option for the refrigeration, air conditioning, and heat-pump sector (RACHP). With very low or zero greenhouse warming potential (GWP) and no effect on ozone depletion, these substances can replace the current refrigerants (HCFCs, HFCs, HFOs) effectively and at a low cost.

However, the implementation of these refrigerants faces significant barriers in established regulatory frameworks as some of them are classified as A3 substances (lower toxicity – higher flammability) in the ASHRAE classification. Regulatory frameworks relevant for RACHP relating to health and safety, construction, appliance manufacturing and servicing often prescribe limits or outright ban the use of these substances in certain settings severely curtailing their employability.

Worldwide, refrigerant use is responsible for 1,140 $MtCO_2eq$ (Green Cooling, 2020). Employing natural refrigerants like R290 (propane) with a GWP of 3, compared to R134a with a GWP of 1300, represents an excellent opportunity to reduce emissions in Europe, and through its example in much of the rest of the world.

In this context, the LIFE FRONT project aims to remove barriers posed by standards for flammable refrigerants in this sector. The project consists of three phases:

1. Literature review – to provide a detailed explanation and breakdown of safety standards and associated barriers related to refrigeration appliances, air conditioners and heat pumps.
2. Field study and laboratory tests on leakages and related mass flow – to provide detailed data on leak hole sizes, underlying causes and their frequency, as well as resulting patterns of the refrigerant mass flows and concentrations in different settings.
3. Recommendations - building on lessons learned from the field study and laboratory tests, work focused on improving product design by making modifications to current practice to accommodate for the use of larger HC charges and by evaluating options for passive and active risk mitigation measures.

This report is the result of phases 2 and 3 providing results from the laboratory testing and recommendations on measures to minimize concentrations of flammable refrigerants in the case of a leak; implementation of mitigation measures performance testing; and recommendations on increasing charge size flammability risk focusing on smaller devices as described in the access categories ‘a’ and ‘b’ in the EN 378-1 (2016) Standard.

This report consists of two main sections:

- The first section of the report discusses the charge size limitations and provides extensive analysis including focused testing on heat pumps AIT and NIBE facilities.
- The second section complements the first sections with research related to RACHP equipment and more specifically to air conditioners and small refrigeration equipment. This section compiles results and conclusions obtained in projects other than the LIFE FRONT project, as well as results from tests on refrigeration cabinets at AHT facilities. This information is presented in a series of annexes appended at the end of the report.

Together, these sections provide a comprehensive base of information on how the RACHP sector would be better able to extend the use of flammable refrigerants safely, or with a minimum level of risk increase, and be better able to realize the benefits afforded by natural refrigerants.

Estimating CSLs

The current process to estimate flammable refrigerants charging limits changes depending on the standard being employed and the type of use. For example, there are no charge limits for outside uses as there is little chance of concentrations increasing to dangerous levels in an open space. On the other hand, indoor RACHPs are limited to 4 times the lower flammability limit (LFL). Added to these, there are several incremental maximum charge limits posing a barrier to the application of A3 refrigerants.

In general, three approaches can be used to determine a refrigerant charge:

1. "Prescriptive" approaches refer to the calculation method normally adopted in Safety Standards, i.e., where the allowable charge is calculated from space dimensions, the refrigerant Lower Flammability Level (LFL) and other characteristics, including airflow and space wall openings.
2. Approaches based on testing can be applied when simple calculations are deemed incapable of handling complex situations or are found to yield too small a charge amount for the application. Such experimental tests can include concentration measurements within the space to demonstrate that concentrations do not exceed some fraction of the refrigerant's LFL. Alternatively, tests may be applied where the total amount of refrigerant that could be leaked from the system under normal conditions could be used. With any of these test methods, any combination of protective measures may be applied in any appropriate combination to provide the most cost-effective concept.
3. Finally, a risk assessment approach may be adopted, whereby details of the application, environment, protective measures, etc., are accounted for using numerical/quantitative methods. The resulting risk values can then be gauged against acceptability criteria to establish whether or not the proposed design would be deemed suitable or whether additional or alternative protective measures would need to be implemented.

Standards make a heavy use of prescriptive approaches, and this can have strong implications for the use of natural "flammable" refrigerants and realize their inherent benefits for the environment.

Charging limits and their implications

One of the biggest of outcomes of the current state of safety regulations is the limitation on the amount of the refrigerant that RACHP appliances can be loaded with: charge size. This in turn, limits the usability of these appliances in a variety of settings. However, the origin of some of these measures may not be relevant to all situations or to modern applications.

The domestic refrigeration standard EN 60335-2-24, first drafted in 1992, sets a limit of up to 150 g of "flammable refrigerant" (originally intended for R600a) in any location, irrespective of room size. This approach was then transferred to other standards and has dominated the use of these refrigerants since.

However, the 150 g limit, was originally based on a simple calculation that assumed the "smallest likely" kitchen as follows: 20% of the LFL times kitchen volume; (0.2 × 0.04) × 2.5 m × 7 m2 = approx. 150 g. Over the following years this 150 g has become the assumed boundary for "safe" and "unsafe" and has been used as a foundation for subsequent derivations of charge limits for other flammable refrigerants.

Similarly, the main methodology for estimating charging limits for air conditioners and heat pumps "comfort" applications has been widely reported to be overly restrictive (e.g., Corberan et. al, 2008; Li, 2014; Vonsild, 2014; Zhang et. al., 2013). This results in the allowable charges of flammable refrigerants being insufficient

for the effective operation of the systems. Furthermore, the use of these methodologies is even more restrictive for uses requiring higher refrigerant charges such as cold room applications.

How much charge is needed?

The heating capacity that can be delivered by a heat pump using 150 g of R290 highly depends on the technology of the components, particularly the condenser and evaporator, the heat pump is equipped with. However, the most efficient heat pump using 150g of R290 is capable of delivering approximatively 1kW of heating/cooling energy. This is very low compared to the 3 to 20kW needed to adequately supply today's average home or apartment.

As a consequence, ground source or air to water heat pumps designed to be installed indoor cannot use a flammable refrigerant as the provided heating/cooling capacity will not fit the usual heat demand of a single dwelling apartment or house in the EU. Added to this, the current standard IEC/EN 60335-2-40 does not leave any scope for innovation nor option to adopt protective measures that could effectively prevent formation of a flammable mixture using other means and thus ensure a safe usage of the equipment.

Required charge sizes are highly diverse depending on the applications and in some cases, they can be megawatts in size requiring hundreds of kilograms of refrigerant. So rather than trying to extend CSLs to a range that would satisfy all applications, a somewhat unrealistic proposition for the larger applications, it is more appropriate to determine how much refrigerant common applications would ordinarily require.

From the literature, various nominal heating/cooling loads have been collated for different applications. Similarly, required specific HC charge amounts (in g per kW of cooling or heating capacity) have been obtained from a variety of different sources. These two parameters may be combined to estimate the practical relative charge for HCs, in terms of g per m2 of room size.

The LIFE FRONT project aims to demonstrate that the risk of potential refrigerant leakage under certain flow rates does not increase the concentration of flammable substances to dangerous levels. The project provides a robust test methodology that permits to evaluate whether a heat pump using flammable refrigerant can operate without compromising safety, whatever the charge size and the room surface area.

Leak testing design

The tests conducted for this project included two prototypes designed and built by the projects' manufacturing partners. These prototypes were tested with different levels of leak rates and varying situations including the application of mitigation measures to determine if the leaks result in dangerous concentrations of refrigerant. Two rooms designed to simulate an "average" utility room were built for the test and fitted with an array of sensors to determine the concentrations of R290 at different locations and varying distances from the source.

For the purposes of the test, the team discussed the levels of concentration of refrigerant that could be considered a tolerable level of risk in the event of a leak resulting in a complete loss given different refrigerant charge sizes. It was determined that the concentration of R290 surrounding the product should not exceed 50% of the lower flammability level (LFL). It was also noted, that in the case that any of the heat-pumps parts may contain one or several ignition points, the same 50% of LFL should not be exceeded.

The test also required to assumed leak flow rates to simulate potential real situations. For this the project included an extensive review of the projects' partners records of feedback and quality control records and consultation from their decades of experience.

As part of the leak flow review, hundreds of parts provided by project partners from the manufacturing sector were also reviewed and analysed for the hole sizes, likely causes for degradation and the resulting leak flow rates. The resulting information was collated in a database that has been published and is freely available in the project website (http://lifefront.eu/databases) but the key results are summarized in table 10.

The resulting maximum assumption for the tests performed is a maximum flow rate of 65g of refrigerant per minute. While the database includes cases of 88 grams per minute leaks, these have been deemed to be solvable by product design improvements that could potentially be addressed by design requirements of the standards.

Air to water heat pump

Three R290 leak locations were identified as being the most unfavourable locations for a leak to occur: one in the evaporator enclosure and two in the condensing enclosure: one on top and one at the bottom

Similarly, three flow rates were selected to emulate leaks arising from some of the more common causes of leaks as well providing information on a wide array of the leak options:

1. 20 grams per minute – potential caused by defective bending of a pipe, a fatigue rupture, or pipe icing.
2. 45 grams per minute – corresponding to the assumed low-side R290 leak rate in the draft amendment to the IEC 60335-2-40 standard for enhanced tightness systems.
3. 65 grams per minute – highest leak rate observed in leak analysis, assuming that electric arcs can be avoided by appropriate design and construction.

Ground source heat pump

Two main locations were selected to ensure that the R290 concentration does not exceed 50% of the LFL determined by the main zones of the heat pump appliance:

1. Zone A containing the hydronic components, immersion heater, power supply, all electrical components (i.e. the main ignition points).
2. Zone C the surrounding area of the product.

The leak rates selected to test this device were:

1. 20 grams per minute as the minimum relevant rate based on the leak flow analysis.
2. 100 grams per minute was selected on the case of a catastrophic leak occurrence. While 88 grams per minute is the largest leak observed, this was rounded up.

Leak test results

The results of the air to water heat pump tests indicate that the indoor packaged air to water design is sufficient to avoid creating an explosive atmosphere around the product. However, some design improvements would be required as the 50% LFL was reached, if barely, in the test where R290 is released in the evaporating enclosure.

In the case of the ground source heat pump, the tests indicate that R290 is not penetrating zone A, where potential ignition sources could be found. The tests also demonstrate that if there is no air movement in the room, R290 settles at floor level. In addition, the ground source heat pump design is efficient in preventing the creation of an explosive atmosphere around the heat pump even in case a catastrophic leak is occurring in the refrigerating circuit as well as keeping R290 concentrations far below 50% of LFL in case a small leak is occurring.

Conclusions

The analysis and testing presented in this report prove that the current application of safety standards limits on flammable refrigerants charges are too restrictive for the application of R290 in most RACHP applications. This report further proves that with judicious application of design principles to prevent certain forms of leakage or presence of ignition points, larger charge limits could be applied for a number of applications.

A range of possible approaches for extending or introducing new approaches for determining safe charge limits are proposed including the use of calculation methods, experimental methods, and risk assessment methods. This is coupled to an analysis on how to identify how far charge limits should extend to be useful, as well as being weighed against what the legislative requirements and constraints are.

The project establishes a procedure to support the design and implementation of experimental methods. The methods focus on specific applications where a product is placed in a test space and a refrigerant leak is simulated with subsequent measurement of concentrations around the product and test space's floor are monitored for the duration of the release and for a period thereafter. Provided that the concentration does not exceed some fraction of the refrigerant LFL, the test can be deemed to pass.

The report also proposes an improved approach for calculation methods based on the construction of the RACHP enclosure, from where the leaked refrigerant then can escape into the room. The method assumes a leak rate and enclosure characteristics (internal dimensions, height and position of openings, etc.) and that by the end of the release, floor refrigerant concentration does not exceed a predetermined minimum level of safety.

By proposing these new approaches to determining charge limits, it is intended to prove that the safe application of higher charge limits is possible, and that future applications of safety standards will result in charge limits that enable a far greater and wider application of HC refrigerants without resulting in a significant risk increase for users. This will, in turn, result in reduced greenhouse gas emissions from the sector, supporting countries meet their international GHG emissions reduction obligations.

INTRODUCTION

"The LIFE FRONT project aims to remove "barriers posed by standards" for flammable refrigerants in refrigeration, air conditioning and heat pump applications. It strives to improve system design to address flammability risk and encourage thereby wider uptake of climate-friendly alternatives to fluorinated gases. "

The first activity of the project consisted in reviewing relevant literature and a study of the market and existing technology. The related report: Impact of Standards on Hydrocarbon Refrigerants in Europe – Market research report, available at the LIFE FRONT project website www.lifefront.eu provides a detailed explanation and breakdown of safety standards and associated barriers related to refrigeration appliances, air conditioners and heat pumps.

In a second step a thorough field study on leakages, and subsequent laboratory tests on gas concentration development and consequences were performed. The results are summarised in the report *Recommended leak hole size and mass flow rate by system and application characteristics* and two databases: *Refrigerant Leak Size Database* and *Concentration Database*. The report and both databases are available on the LIFE FRONT project website.

In a third step, building on lessons learned from the field study and laboratory tests, work focused on improving product design by making modifications to current practice to accommodate for the use of larger HC charges and by evaluating options for passive and active risk mitigation measures. The industrial partners of the LIFE FRONT project, AHT, AiT and NIBE, each built a prototype. All prototypes derived from an existing product of the portfolio but had been specifically designed to operate with R290. Each prototype, including a commercial refrigerating cabinet, an indoor packaged air to water heat pump and a ground source heat pump (both domestic heat pumps) were tested to:

- Assess the effectiveness of the specific design in mitigating the risk and preventing the creation of an uncontrolled explosive atmosphere
- Define a robust and reliable methodology for evaluating the safe usage of a product using flammable refrigerant.

The LIFE FRONT project aims to remove barriers posed by RACHP safety standards for flammable refrigerants in refrigeration, air conditioning and heat pump applications. In order to cover the sector of air conditioning, which was not represented by the project industry partners, results from tests undertaken by HEAT under this FRONT project and also under other projects funded by GIZ Proklima and DUH; are also included in this report. The outcome is a comprehensive summary for all equipment types which provides the basis for recommendations on:

- measures to minimise flammable refrigerant concentrations and severity of consequences
- implementation and performance testing of mitigation measures for flammable refrigerants
- assumptions for impacts on flammability risk and of flammable refrigerant charge size on risk levels

One of the main goals of the LIFE FRONT project is to feed these results into ongoing and future safety standard revisions. This report consists of two main sections:

- One related to RACHP equipment and more specifically to air conditioners and small refrigeration equipment. This section compiles results and conclusions obtained in projects other than the LIFE FRONT project, as well as results from tests on refrigeration cabinets at AHT facilities
- Another section that complements the first one and which is focussed on heat pumps and tests done within the LIFE FRONT project at AIT and NIBE facilities.

Both sections provide recommendations for revising the safety standards. The general structure of the report is reflected in the diagram in Figure 1.

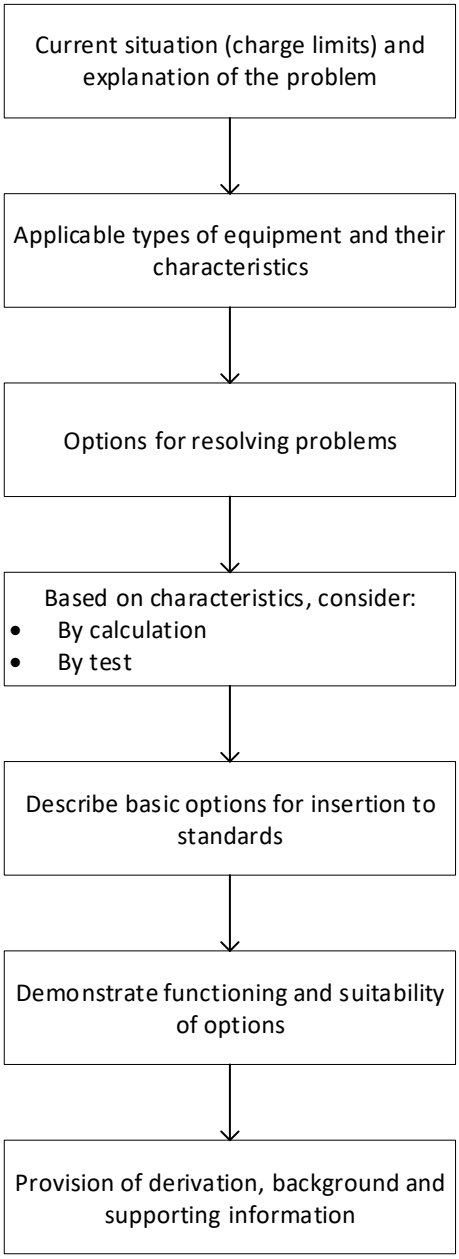

Figure 1: Logic for structure of report

This report is thus structured as follows:

- A) Section on determination by test
- B) Section on prescriptive charge size limits (CSLs) for unventilated or integral airflow
- Annex providing test and simulation data to support these approaches

1 GENERAL

The objective of this report is to recommend the following for the purpose of formulating requirements on revised RACHP safety standards:

- Measures to minimise flammable refrigerant concentrations and severity of consequences
- Implementation and performance testing of mitigation measures for flammable refrigerants
- Assumptions for impacts on flammability risk and of flammable refrigerant charge size limits on risk levels

The scope of the report is intended to be limited to "smaller" systems that are likely to be used in so-called access category 'a' and 'b', according to EN 378-1 (2016). Access category 'c' is essentially for "authorised access" personnel which currently invoke less stringent requirements. Equipment that is covered broadly includes those listed in Table 1.

Table 1: Application and system types considered

Application	System type	Large-end capacity
Residential and commercial AC	Integral room ACs	3 kW
	Window/TTW/PTAC	5 kW
	Single remote (split) AC	20 kW
	Ducted remote AC	>> 20 kW
	Ducted centralised (rooftop) AC	>> 20 kW
Commercial refrigeration	Integral storage cabinets	2 kW
	Remote storage cabinets	2 kW
	Integral display cabinets	6 kW
	Remote display cabinets	6 kW
Cold rooms	Monoblock units	>> 20 kW
	Remote system	>> 20 kW

Heat pumps	Integral hot water heating	4 kW
	Integral space heating	25 kW
	Remote space heating	25 kW

Large / industrial refrigeration, chillers and centralised (DX) retail refrigeration are excluded from the discussion, as explained in the project proposal.

1.1 Approach of this report

The approach of this public report is to:

- Summarise the charge limit requirements of RACHP Safety Standards (RSSs) and in this context to discuss demands of flammable gas safety regulations and frameworks;
- Evaluate RSSs with respect to application needs and the problems that arise from current limitations;
- Compare requirements of current limits against measurements involving real systems and similarly to consider the basis of current charge size limits (CSLs) and in regards to real systems and situations;
- Further analyse factors and variables that influence the development of potentially flammable concentrations in the event of a leak;
- Consider possible consequences of ignition of a flammable mixture;
- On the basis of this analysis devise new approaches for determining CSLs;
- Propose how these CSLs should be applied for use in RSSs.

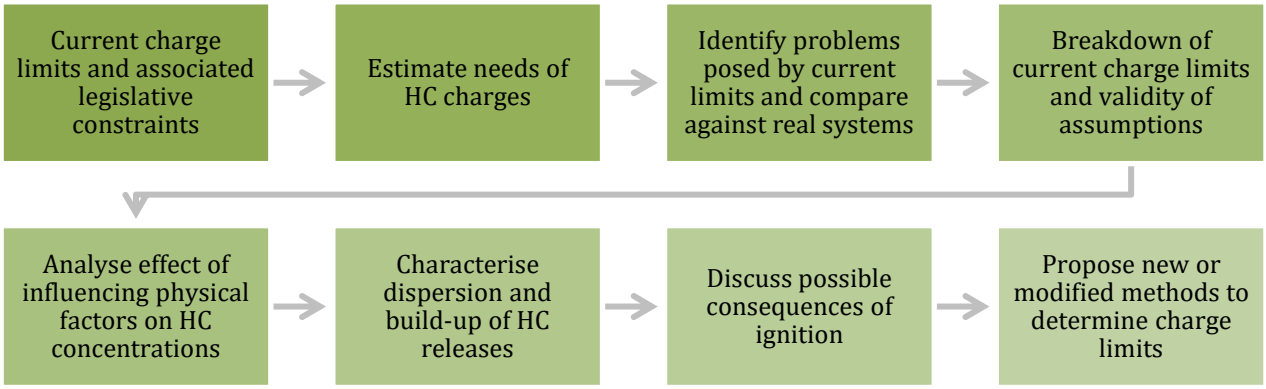

Figure 2: Work progression sequence for report.

It should be understood that RACHP safety standards are continually under revision. For instance, during the drafting of this report (May 2018 to December 2019), the revision of IEC 60335-2-89 to increase charge size limits was circulated as a CDV then FDIS and is now published. Nevertheless, current published versions of the standards are referred throughout in order to ensure the correct context and references.

1.2 Current charge size limits

The most relevant RACHP safety standards (RSS) in Europe and International level are shown in *Table 2* along with the relevant equipment type and application sectors.

There are two categories of RSS: so-called "vertical" standards, which are theoretically aimed at particular types of factory-produced serial products, although in actual fact they often cover a huge range of products and equipment. These vertical standards are generally written at international level (International Electrotechnical Commission, IEC) and are then adopted at European level (European Committee for Electrotechnical Standardisation, CENELEC), albeit usually with some minor modification to ensure harmonisation with some relevant European Directives. The "horizontal" or "group" standards are intended to cover the entire RACHP sector, ranging from small one-off units to mass-produced industrial systems. For these, there are four parts that broadly deal with basic principles and classifications, system design and construction, installation areas and system handling by workers. Historically and at present the ISO and EN standards are drafted separately and subject to different approval processes but are broadly consistent with each other.

A more detailed explanation and breakdown is provided in the report Impact of Standards on Hydrocarbon Refrigerants in Europe – Market research report, also published under the LIFE FRONT project and available at the LIFE FRONT project website www.lifefront.eu.

Table 2: Scope of different international and regional RACHP safety standards that includes A3 refrigerants

Sector	Vertical (Product Standards)			Horizontal (Group Standards)
	IEC 60335-2-24	IEC 60335-2-40	IEC 60335-2-89	ISO 5149-1,-2,-3,-4
	EN 60335-2-24	EN 60335-2-40	EN 60335-2-89	EN 378-1,-2,-3,-4
Domestic refrigeration	×			
Commercial refrigeration			×	×
Cold rooms				×
Industrial systems				×
Transport refrigeration				×
Air-to-air air conditioners & heat pumps		×		×
Water heating heat pumps		×		×
Chillers		×		×

Critical to the present discussion is that all these RSS, including CSLs are drafted by a relatively small number of persons, nominated as "experts" from national committees of member countries. Considering that the topics handled by these standards are wide-ranging, such as electrical, pressure safety, worker safety, flammability and general mechanical safety, there are seldom more than a handful of individuals that are in fact expert in any one of these particular fields. Furthermore, since the process of standards development is essentially voluntary, very drawn-out and extremely costly (i.e., given the numerous regional or international meetings in different locations each year, demanding internal R&D/development work, etc.) only organisations that recognise potential for commercial gain tend to participate.

A recent UNEP TEAP Task Force report under the Montreal Protocol (2017)[1] offers further details about the RACHP standards development process.

Across European and International RSS, the degree of stringency of CSLs differs according to the refrigerant safety classification and safety familiarity or competence of occupants (termed "access category") and the location of the refrigerating system refrigerant-containing parts in relation to those occupants. In this respect, Table 3 is an overview of how CSLs are arranged. Increasing competence permits more generous CSLs due to the assumption that occupants would have a better idea of how to react to a refrigerant release. Similarly, systems located indoors are subject to stricter CSLs on account of dilution of a release being more difficult to achieve than with an outdoor situation. Absolute values differ across the various RSS, classes of RACHP equipment and refrigerant types and actual CSLs don't always strictly adhere to this approach.

Table 3: General approach to charge size limits

Refrigerant/safety-competence of occupants associated with the area	Location of refrigerant-containing parts	
	Inside	Outside
None	Very limited	Broadly unlimited
Low	Limited	Broadly unlimited
High	Broadly unlimited	Unlimited

[1] UNEP MAY 2017 Report of the technology and economic assessment panel Volume 3 Decision XXVIII/4 Task Force Report Safety Standards for Flammable Low Global-Warming-Potential (GWP) Refrigerants

Table 4 summarises the main CSLs across the various vertical and horizontal standards and according to approximate equipment categories. There are two forms of CSL, as termed here:

- "upper charge" refers to the highest absolute mass of refrigerant permitted in any one refrigerant circuit for a given situation;
- "allowable charge" is the value that is determined according to the dimensions of the inside space within which the system is installed, but which may not exceed the maximum charge.[2]

Allowable charge limits do not apply to systems outside or in the open air, since the space is effectively of infinite dimensions. Similarly, for approaches that effectively exhaust leaked refrigerant to the outside and predominantly avoids accumulation of refrigerant within the space, the allowable charge is effectively redundant. Currently, the "ventilated enclosure" concept – that is offered in both IEC 60335-2-40 and EN 378 – permits an upper charge limit, but also prescribes additional measures, including gas detection, mechanical ventilation and a certain tightness of the enclosure.

[2] In addition to these, there are also elements of "total room limits" appearing in some standards, such as with IEC 60335-2-40 where the total mass of A3 refrigerants – irrespective of the number of separate circuits or systems – is limited to 5 kg.

Table 4: Refrigerant charge size limits for HCs according to safety standards for RACHP systems

Example equipment/application	Vertical (60335-2-24, -40, -89)		Horizontal (ISO 5149, EN 378)	
	Upper CL (UCL)	Allowable CL (ACL)	Upper CL (UCL)	Allowable CL (ACL)
Domestic refrigeration	0.15 kg	0.15 kg	n/a	n/a
Commercial refrigeration	0.5 kg	$0.01 \times V_{rm}$	1.5 kg	$0.008 \times V_{rm}$
Systems in machinery rooms or open air	n/a	n/a	2.5, 10, 25 kg, no limit	$0.008 \times V_{rm}$
ACHP: Small self-contained	0.3 kg	$0.01 \times V_{rm}$	0.3 kg	$0.01 \times V_{rm}$
ACHP: Other packaged & split	1 kg	$0.04 \times h \times A_{rm}^{0.5}$	1.0 kg / 1.5 kg	$0.04 \times h \times A_{rm}^{0.5}$
ACHP: Within vented enclosure	1 kg, 5 kg	n/a	5 kg	n/a
ACHP: In open air	1 kg, 5 kg		1.5 kg, 5 kg, 10 kg, 25 kg, no limit	

Where: V_{rm} = room volume (m3); A_{rm} = room floor area (m2) and h = unit installation height (m).

"n/a" means not applicable.

Note: for brevity, some formulae have been simplified based on a nominal HC lower flammability limit of 40 g/m3.

Two or more values within a cell refer to different access categories.

All CLs apply to individual refrigerant circuits only.

Amongst these various RSS there are no restrictions for indoor RACHPs where the refrigerant charge is lower or equal to "4 × LFL", which corresponds to 152 g (typically rounded down to 150 g) for R290.

What may be observed from Table 4 is the complexity that is introduced by the CSLs. There are several incremental maximum charge limits, ranging from 0.15 kg up to "no limit". This has proven to pose a significant barrier to the application of A3s since a deep memory of each limit for any given set of circumstances is necessary. (By comparison, there are effectively no such limits for non-flammable A1 refrigerants and thus causes consternation to less-academic design and installation engineers and technicians.)

Figure 3 provides a quantification of some of these CSLs, according to EN 378.

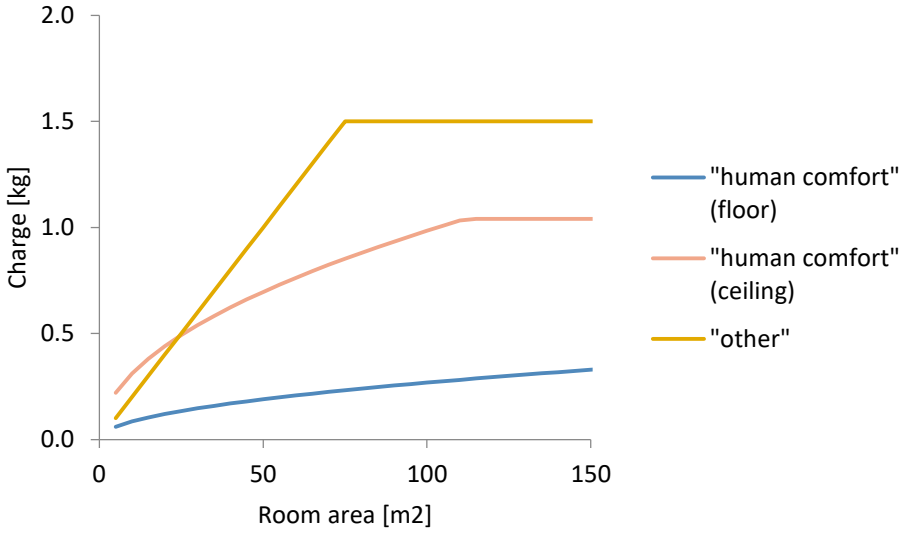

Figure 3: Example of the relationship between room size and refrigerant charge limits (for "comfort" indoor unit install height is 2.2 m for "ceiling" and 0.6 m for "floor", whilst "other" is independent of unit height).

For fixed heat pumps or air conditioners containing more than 152g of R290, the allowable charge located in an occupied space depends on the floor area and the height where the equipment is installed. Figure 4 is a graphical representation of the current formula linking the maximum charge of R290 to the floor area.

As mentioned above, a "ventilated enclosure" is defined as a separate enclosure that contains the refrigerating circuit and that does not communicate with the room. The enclosure must be under negative pressure and an airflow through the enclosure, exhausting to the open air shall be maintained at all times; the minimum airflow rate of which is stated in the standard.

Systems that employ parts of the refrigerant circuit outside of the enclosure but within the occupied space cannot comply with this exception.

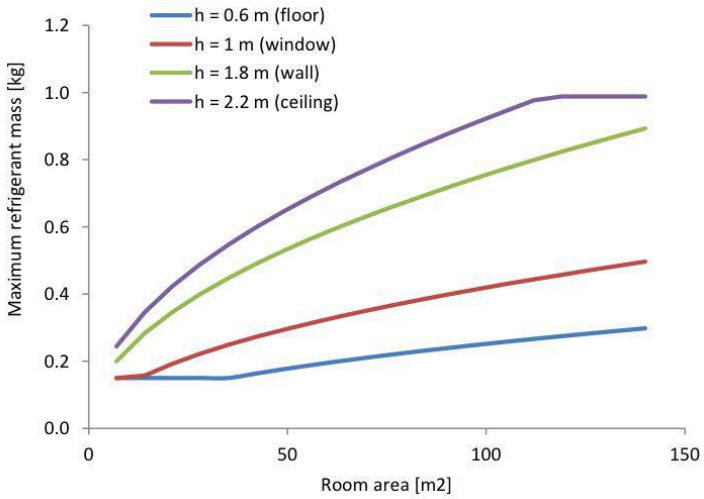

Figure 4: *Maximum R290 charge mass for a given height of the installed unit (from the base of the enclosure) and room area according IEC/EN 60335-2-40 and EN 378-1.*

1.3 Possible approaches for identifying CSLs

Broadly, there are three approaches that can be used to determine refrigerant charge, as indicated in Figure 5.

“Prescriptive” refers to the calculation method normally adopted in RSS, i.e., where the allowable charge is calculated from space dimensions, the refrigerant LFL and other characteristics, including airflow and space wall openings.

However, when simple calculations are deemed incapable of handling complex situations or are found to yield to small a charge amount for the application, approaches that are based on testing can be applied. Such tests can include concentration measurements within the space to demonstrate that concentrations do not exceed some fraction of the refrigerant’s LFL. Alternatively, tests may be applied where the total amount of refrigerant that could be leaked from the system under normal conditions could be used. With any of these test methods, any combination of protective measures may be applied is any appropriate combination to provide the most cost-effective concept.

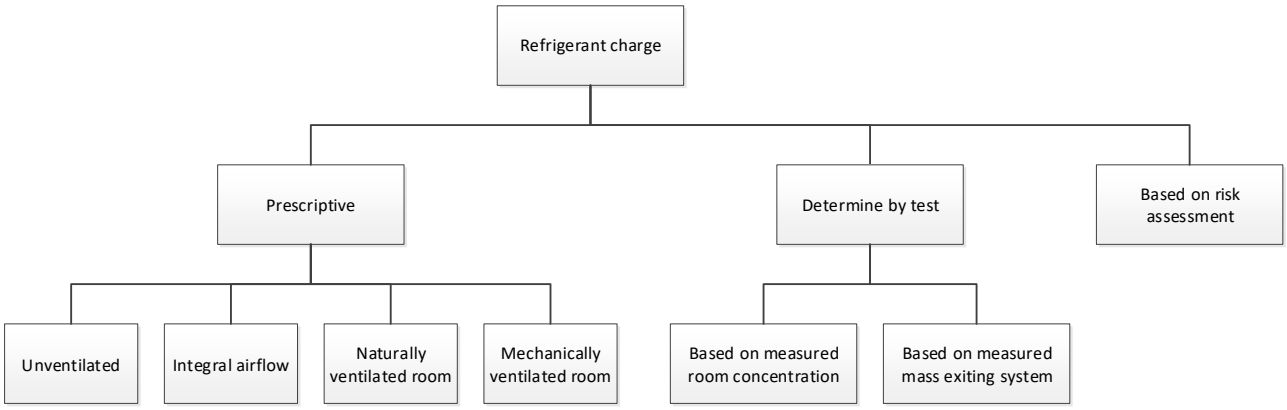

Figure 5: Approaches for determining charge size limits.

Finally, a risk assessment approach may be adopted, whereby details of the application, environment, protective measures, etc., are accounted for using numerical/quantitative methods. The resulting risk values can then be gauged against acceptability criteria to establish whether or not the proposed design would be deemed suitable or whether additional or alternative protective measures would need to be implemented.

Whilst this approach is mentioned here (for purposes of completion), it is beyond the scope of the Life Front project and will therefore not be discussed hereafter.

1.4 Outcomes

In the scope of the LIFE FRONT project, two heat pump prototypes designed to operate with R290 were built and tested. The objective of the tests was to evaluate the efficiency of the prototype design in limiting R290 concentration at 50% of LFL surrounding the product and in parts of the heat pump where an ignition source can be present, in the event of a leak is occurring within the refrigerating circuit.

The two major outcomes of the tests performed are the following:

- Mitigation measures can be implemented that permits the use of R290 in larger quantities than those imposed by the safety standards without compromising safety. The tests demonstrate that it was possible to limit the concentration surrounding the product and in heat pump parts containing potential ignition sources below 50% of the LFL.
- A suitable test method has been developed and trialled that permits the evaluation of the efficiency of the mitigation measures. The test method assesses whether the heat pump can generate an uncontrolled explosive atmosphere surrounding the heat pump in the event of a refrigerant leak.

While replacing the existing flammable refrigerant charge size limit applicable to heat pump, this test method would allow innovative heat pumps to be placed on the market without compromising safety of users and goods.

As an outcome of the work done, it is suggested that the safety standards could offer several approaches, at least a "simple" approach, based on existing requirement: 150g unless the room surface area is large enough, and an "advanced" approach that would imply that the manufacturer perform the test as described in this section.

1.5 Implications of current CSLs

Determination of limits is in principle through formulae intended to preclude the formation of large volumes of a flammable mixture. To do this a large number of assumptions are required, relating to system/equipment characteristics, nature of leaks, conditions within the room and so on. These have led to significant constraints for applicability of A3 refrigerants.

The basis and logic for equations (1), (2) and (3) is discussed below.

1.5.1 150 g limit

The domestic refrigeration standard EN 60335-2-24 which was first drafted in 1992 permits systems to use up to 150 g of "flammable refrigerant" (originally intended for R600a) in any location, irrespective of room size. This approach has since been transferred to other safety standards.

The origin of the 150 g limit in IEC 60335-2-24 was based on a simple calculation for HCs assuming the "smallest likely" kitchen, i.e., 20% of the LFL times kitchen volume; (0.2 × 0.04) × 2.5 m × 7 m2 = approx. 150 g. Over the following years this 150 g has become the assumed boundary for "safe" and "unsafe" and has also been used as a foundation for subsequent derivations of charge limits for other flammable refrigerants. For instance, in order to apply a limit to charges of non-HC refrigerants, the 0.15 kg was divided by the LFL of R290 (0.038 kg/m3) to yield a constant of value approximately 4, which may then be applied to other refrigerants with different LFLs. This then led to the expression "m1" (= 4 × LFL) in various standards.[3] Furthermore 150 g in a system with one design may be safer by a factor of 1,000 or 10,000, than another with a far poorer design (e.g., Colbourne and Esperson, 2013).

The fact that domestic refrigerators have proved to be "safe" is probably more to do with the extremely low likelihood of leakage from the factory-sealed systems, due to very few joints and in addition the extremely thorough quality control systems in place with such large appliance manufacturers. By comparison, for a

[3] It was further extended to "m2" to equate to 1 kg R290 (= 26 × LFL) and "m3" for 5 kg (= 130 × LFL). But the value of the constants has then been subject to gradual increases for A2L refrigerants only.

system using “m1” of an A2L refrigerant (e.g., 4 × 300 g/m3 = 1800 g) systems are more likely to be site-installed and charged and can comprise detachable connections and hundreds of other joints, increasing the likelihood of leakage. Thus, this may not necessarily be an appropriate approach for transposing charge limits for other refrigerants.

Nevertheless, the overall impact of this default 150 g “safe” limit has had the impact of proliferating the belief amongst the RACHP industry that any charge size about 150 g (or “m1”) may not be “safe”.

Currently[4] IEC 60335-2-89 contains the same 150 g limit for all cases (including for A2 and A2L refrigerants). CSLs for A3s in IEC 60335-2-40, EN 378 and ISO 5149 vary somewhat.

1.5.2 Limits for air conditioners and heat pumps / "comfort” applications

Within IEC 60335-2-40, EN 378 and ISO 5149, there is a charge limit formula that was originally inserted into the 2003 edition of IEC 60335-2-40 (equation 1):

$$m_{max} = 2.5 \times LFL^{5/4} h_0 \sqrt{A} \quad (1)$$

Where:

m_{max} = the allowable maximum charge in a room (kg);

A = room area (m^2);

LFL = Lower Flammable Limit (kg/m^3);

h_0 = installation height of the appliance (m);

2.5 = a semi-empirical constant of questionable origin.

Specific values were listed for this height h_0 according to the base of the unit: 0.6 m for floor-mounted units, 1.0 m for window units, 1.8 m for wall units and 2.2 m for ceiling mounted. A further constraint applied to the use of the formula was that the molecular mass of the refrigerant must be greater than 42 g/mol.

Specifically, for “non-fixed factory sealed single package units” (essentially portable ACs and humidifiers), an alternative CSL is prescribed, which can be used provided that the system charge is between $4 \times \mathrm{LFL} < m \leq 8 \times \mathrm{LFL}$:

$$m_{max} = 0.25 \times LFL \times A \times 2.2 \quad (2)$$

Where 0.25 is 25% applied to the LFL and 2.2 is the assumed room height (m). In addition, the unit must generate airflow into the occupied space corresponding to approximately four air changes per hour.

It has been widely reported that this CSL formula is overly restrictive when trying to apply it to common room air conditioning and heat pump systems (RACHPS) (e.g., Corberan et. al, 2008; Li, 2014; Vonsild, 2014; Zhang et. al., 2013). This is illustrated in an evaluation shown in Figure 6. Here, RACHPs of various efficiency levels from the Eurovent database (https://eurovent.eu/) are plotted against charge size, adjusted for R290-equivalent by using the ratio of R290 to the design refrigerant liquid densities at 45°C (GIZ, 2011). Charge limit lines for R290 are superimposed for three different installation heights, h_0 of RACHPS indoor units (IDU),

[4] As of mid-May 2019, although the 61C/792/FDIS has now been approved, leading to larger charge limits.

assuming a nominal load of 150 W m-2, which is “average” across Europe (Huang et al., 2018). For R290 to be viable, the CSL lines should be above the data-points so that the R290-charged RACHPS would be able to be installed in rooms of specific room dimensions. Whilst it is in principle possible to cool rooms with multiple RACHPS, there would be a significant cost implication, inferring a major detriment to products using A3 refrigerants. This implies that current CSLs obstruct the selection of R290 (and other A3s), especially for higher efficiency models; the consequence is even starker for applications with higher loads, i.e., above 150 W/m2. This observation is echoed in a recent report on significant barriers to the uptake of flammable refrigerants by the European Commission (2016) and the UNEP TEAP TF report (2017).

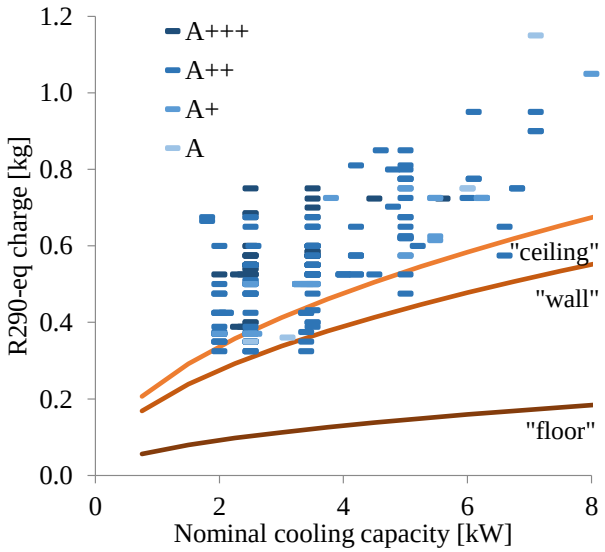

Figure 6: Comparison of RACS charge sizes (converted to R290-eq.) and current charge limits for a 150 W/m² load.

The restrictions seen here highlight the need to re-examine the validity of current approaches and assumptions to reflect practical variabilities.

Within equation (1) there are a variety of different implicit assumptions. Some of these have been examined within the wider literature that is not necessarily related to RACHP systems (for example, direction of a release and room airflow), whereas others have only originally been addressed within the standards group that originally adopted this formula. It is important to readdress many of these factors to help understand and determine whether alternative assumption should or could be made and how they can be integrated into revised CSL approach.

1.5.3 Limits for “other” applications

Whilst the equations (1) and (2) were originally proposed for use for systems within the scope of IEC 60335-2-40 and latterly for systems used for so-called “human comfort”, the horizontal standards adopt another CSL formula intended for “other” (than “human comfort”) applications. Thus, the horizontal standards follow the basic approach to limit the charge (m_{max}) according to:

$$m_{max} = 0.2 \times LFL \times V_{room} \quad (3)$$

Where V_{room} is the free room volume of the space (in m³) and 0.2 is a 20% factor is assumed to account for the stratification of the leaked refrigerant.

Whilst this approach is relatively inclusive (as can be deduced from *Figure 6*) there are several situations where it may be inappropriate. For example, when applied to a cold room or a small convenience store, it is unlikely to offer sufficient A3 refrigerant charge to satisfy the cooling demand. Conversely, with a large system that is located at floor level, even a small leak could easily result in a non-insubstantial flammable volume, and thus could be considered "unsafe". For these reasons, a more suitable approach to determining CSLs is again desired.

1.5.4 How much charge is needed?

Rather than trying to extend CSLs to any feasible level, it is probably more appropriate to determine how much refrigerant common applications ordinarily require. Ultimately any charge amount would be desirable so that all applications could be satisfied. However, given the range and extent of all systems and applications that can approach megawatts and hundreds of kilograms of charge, this is not realistic.

In general, the required charge size is highly diverse, since it depends upon the particular design and function of the system, intended temperature levels, local climate and the available technologies, in addition to the refrigerant itself. From the literature, various nominal heat loads/cooling loads have been collated for different applications. Similarly, required specific HC charge amounts (in g per kW of cooling or heating capacity) have been obtained from a variety of different sources. These two parameters may be combined to estimate the practical relative charge for HCs, in terms of g per m2 of room size. Similarly, the largest capacities of equipment ordinarily applied in a given subsector or alternatively the minimum likely available space area for certain equipment types can be used to approximate the upper boundary for these CSLs. Within this context, there are two distinct situations for which the desired charge amount may be determined:

i) Systems where the cooling or heating capacity is dictated by the dimensions and characteristics of the room(s) that it serves, and
ii) Systems where the cooling or heating capacity is broadly independent of the room(s) that it is located within.

Examples for (i) include air conditioners and cold rooms. Examples for (ii) include display cabinets and hydronic heat pumps. Cases exist that encompass both scenarios, such as "indoor" cold rooms with monoblock systems.

Table 6 provide some approximate data in terms of application heat load, specific HC refrigerant charge and room area constraints.

A fundamental aspect related to HC product development is to optimise the charge so that as much cooling or heating capacity per unit mass of charge can be achieved. For integral air conditioning systems, the best available options require about 60 g/kW or 90 g/kW for heat pump systems and for refrigeration systems the required charge is around 150 g – 250 g per kW (for chilled and freezing temperatures, respectively).

Table 5: Specific charge and specific capacity for systems or parts of systems indoors under situation (i)

Application/system	Typical load [kW/m2]	HC charge [g/kW]	Max likely capacity [kW]	Max likely sys charge [kg]	Target charge per m^2
Commercial refrigeration					
— Coldstores – monoblock	70 x $A^{0.4}$	200	10 kW	2.5	80 g/ m^2
— Cold stores – remote	70 x $A^{0.4}$	200+50 g/m pip	100's kW	10's	>80 g/ m^2
Transport refrigeration	80 x $A^{0.4}$	200	10 kW	2.5	90 g/ m^2
Cooling/heating with air conditioners					
— Self-contained	0.1 – 0.4	80	5 kW	0.5	30 g/ m^2
— Remote (split)	0.1 – 0.4	100	15 kW	2.5	40 g/ m^2
— Ducted rooftop	0.1 – 0.4	100	100's kW	10's	40 g/ m^2
— Remote multi-split*	0.1 – 0.4	100	20 kW	2.5	100 g/ m^2**

* With up to 4 indoor units; not VRF type

** based on single room served

Notation:

A = floor area of space [m2]

g/m pip = grams per metre of piping

Table 6: Specific charge and specific capacity for systems or parts of systems indoors under situation (ii)

Application/system	Typical load [kW/m2]	HC charge [g/kW]	Minimum likely area [m2]	Max likely sys charge [kg]	Target charge per m2
Commercial refrigeration					
— Plug-in retail cabinets	n/a	200	**~30 m2	1.5	50 g/m2
— Remote retail cabinets	n/a	200+50 g/m pip	** ~30 m2	>2.0 per cabinet	65 g/m2
Heating with heat pumps					
— Space heating	0.05 – 0.3	150	***~10 m2	3.0	300 g/m2
— domestic water heating*	0.03	100	*** ~10 m2	0.2	20 g/m2

* Usually only 1 – 1.5 kW, requires 100 – 200 g HC

** Small conv shop

*** Utility room/cellar

RACHP system design strategies evolve over time and charge sizes for a given capacity and temperature levels have tended to reduce correspondingly. In particular, the increased use of flammable refrigerants has led to an acceleration of charge minimisation. On the other hand, with increasing minimum efficiency rules and regulations, there can be a conflicting trend to raise charge amounts (depending upon the optimisation strategy followed). As a practical example, the average charge of ACHPs within the Eurovent database (Eurovent, 2017) varies according to energy label, as indicated in *Table 7*. Approximately 50% more charge can be used to increase the rated efficiency from A to A+++. It should be noted, though, that most of the products within the Eurovent list have not been subject to intensive charge minimisation/optimisation, so the increased specific charge are higher efficiency models may be relatively greater than what might be expected with HCs.

Table 7: Variation in specific charge with rated efficiency

Energy label	A	A+	A++	A+++
Specific charge [g/kW]	0.13	0.14	0.16	0.20
Relative charge (to class "A")	100%	108%	121%	151%

Taking the typical heat loads, HC charge sizes and target charges detailed in Table 5 and Table 6 and applying the constraints detailed in the form of upper charge limits as in Table 4, the expected cooling (or heating) capacities may be estimated. Table 8 provides the approximate cooling/heating capacity that can be reasonable achieved with A3 refrigerants for the upper charge size limits across the various RSS.

Table 8: Maximum effective cooling capacities for A3s

Type	Max capacities for upper charge mass in kW		
	EN 378	EN 60335-2-40	IEC 60335-2-40
Small self-contained (PSC)	3	3	3
Split (non-ducted) (NDS)	13	8	8
Multi-split (MS)	13	8	8
Packaged rooftop (PRT)	13	8	8
Ducted split (DCS)*	13	8	8
Space heating heat pump	TBC	TBC	TBC
Domestic water heating heat pump	TBC	TBC	TBC

The "required" charge in relation to the allowable charge for A3 refrigerants is presented in Figure 7. Dashed lines indicate values for "low heat load" (100 W/m2) and "high heat load" (300 W/m2). Lines are included for floor, window, wall and ceiling AC units. For low load applications, both floor and wall units are almost impossible and wall and ceiling units are only feasible in rooms larger than 20 m2 and 40 m2. For high load applications, all units are essentially prohibited, irrespective of available room area.

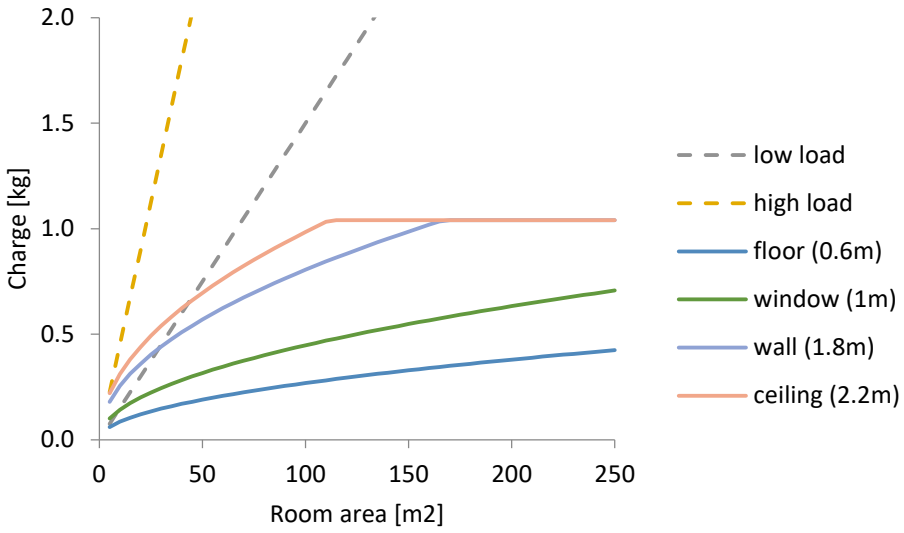

Figure 7: Comparison of required charge amount for A3 refrigerant AC systems and A3 charge size limits according to the various RSS for ceiling, wall, window and floor units; low load = 100 W/m², high load = 300 W/m², specific charge = 150 g/kW, LFL = 40 g/m³.

1.6 Legislative framework

Throughout the world most countries and/or regions have legislation that governs equipment related to potentially flammable and explosive atmospheres.

All European countries have adopted the ATEX (equipment) and ATEX (workplace) directives (2014, 1999) and in fact almost all other countries subscribe to an equivalent or similar legislative framework. Similarly, all these countries adopt the same or comparable Ex-type standards for protection of equipment used within areas where flammable mixtures could be present. It should be observed that amongst the various regulations and standards, no limits in terms of mass of flammable substance are prescribed. However, the general approach taken is to ensure that there are no potential sources of ignition (SOI) within potentially flammable zones.

In order to address this, the standard EN/IEC 60079-10-1 specifies a methodology to determine the size or the extent of a flammable zone, based on for example, the fluid flammability characteristics, pressure of the fluid that may leak, anticipated largest non-catastrophic leak hole size, ventilation in the area, etc. “Seriousness” of the zone, i.e., zone 0, zone 1 or zone 2 (in diminishing significance sequence) are classified according to the persistence of the flammable mixture. There then exist standards that define requirements for ensuring that electrical or other components do not act as SOIs, which can thus be used within the flammable zone.

In practical terms it is not feasible to impose Ex-type components within areas where RACHP systems and equipment are typically installed; this would diminish the convenience and relatively low cost of cooling (and heating) systems. Whilst this approach may be applied for within RACHP system housings and enclosures, for areas outside the housings and enclosures, the approach may be applied in the opposite direction whereby the amount of refrigerant, possibly hole size, internal pressure, etc. are limited such that the flammable zone

does not extend significantly beyond that of the RACHP equipment.[5] In this way, the principles of the various national and regional regulations and standards on controls of explosive atmospheres can be adhered to.

In addition to these, other protective measures can be applied to RACHP systems, equipment and installation areas to limit the size and extent of the flammable zones. Such measures include additional airflow, extract ventilation, natural ventilation, physical barriers within RACHP housings, etc. These are not currently available to HC refrigerants within the RSS for systems other than in machinery rooms or certain authorised access only (category 'c') spaces.

[5] The exception is for larger capacity systems installed in special machinery rooms where it is assumed that potentially large flammable zones could be created and so appropriate protective measures can be applied to the entire space, such as Ex-type electrical equipment and specialist ventilation.

1.7 Approaches for minimising extent of flammable zone

Across various RACHP and other safety standards, numerous precautionary measures are mentioned for the purpose of minimising flammability and other hazards.

Table *9* provides an overview of the various types and examples of protective measures that can be applied to RACHP equipment in order to address the flammability hazard. Each is identified as "active" (e.g., operated by electrical power source) or "passive" (e.g., without electrical or external intervention) according to their function. In addition, a rating for their effectiveness for reducing the hazard and general reliability are listed. Note that these ratings are only an indication, since they will vary according to the RACHP system and equipment configurations.

Table 9: Measures to minimise flammability hazard

Measures	Active (A)/ Passive (P)	Remarks on key implications for effectiveness/reliability
Limiting charge amount by specifying a maximum charge	P	Reliant on technician to not overcharge system
Large enough space for dilution by specifying a minimum room area/volume	P	Reliant on installer to evaluate room size correctly
Limiting releasable amount by using particular system designs or components (e.g., shut-off valves)	A/P	Long term tightness of system design and components
Limit leakage mass flow rate, such as with internal flow restrictions	A/P	Correct functioning of system components and detection if used
Encourage lower leak probability by improving the design and construction of the system	P	Technician maintains tightness when carrying out repairs
Dilution of mixture from housing into room through improved enclosure design	P	Enclosure construction is not compromised by occupants
Dilution of mixture in room by using unit circulation airflow	A	Unit fan is always available
Dilution of mixture in room by using separate circulation airflow	A	Separate fan is always available

Removal of mixture from occupied room relying on natural ventilation	P	Conditions (temperature, wind speed, direction) frequently as needed
Removal of mixture from occupied room relying on buoyancy induced exchange	P	Flow channels and openings remain unobstructed/interfered with
Removal of mixture from occupied room using mechanical ventilation	A	Fan and detection system always functioning
Removal of mixture from unit enclosure/housing by relying on natural ventilation	P	Conditions (temperature, wind speed, direction) frequently as needed
Removal of mixture from unit enclosure/housing by relying on buoyancy induced exchange	P	Flow channels remain unobstructed
Removal of mixture from unit enclosure/housing by relying on overpressure generated by refrigerant leak	P	Flow channels remain unobstructed and enclosure envelope is tight
Removal of mixture from unit enclosure/housing using mechanical ventilation (to the open air)	A	Fan and detection system always functioning
Eliminating SOIs in occupied space by terminating electrics	A	Detection system always functioning
Eliminating SOIs in occupied space by using protected electrical and other equipment throughout	P	Integrity of protected electrical/other equipment maintained
Warning personnel within the occupied space by means of audible/visual alarms and instructions	A	Detection system always functioning and occupants react as intended to alarm and have read instructions

Those which are “active” require some means to activate the mitigation measure, for example, leak detection. Incorrect technology choice or poorly designed or installed systems can compromise both effectiveness and reliability. The measures can be used individually or in combination with others an overview of the choice of protective measures are shown in Figure 8. In addition, there is an option termed “proof by test” which could include any selected measure or any combination of measures, not hitherto described.

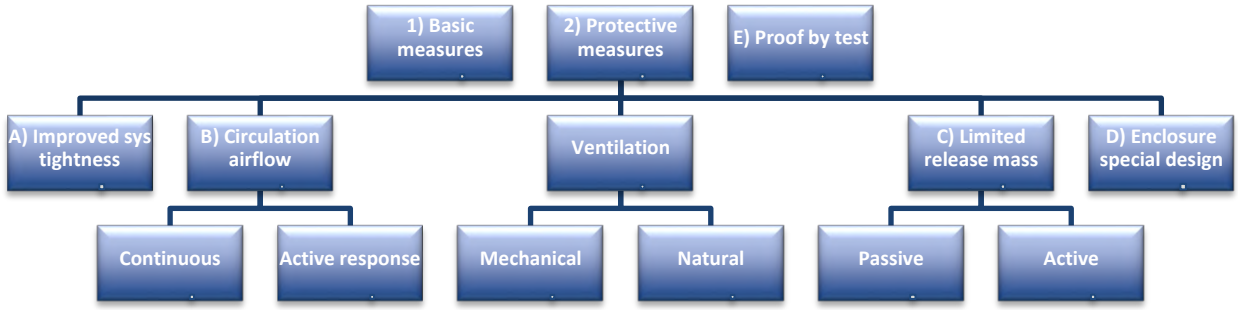

Figure 8: Overview of suitable protective measures for RACHP systems.

Critical to the active measures, there must be some form of indication of a release occurring, i.e., leak detection. There are currently three viable technologies in use: gas detection, ultrasonic leak detection and system parameter-based detection and each have pros and cons, depending upon the type of equipment and installation circumstances.

2 DEVELOPMENT OF TEST METHOD RELATED TO HYDRONIC HEAT PUMPS

2.1 Consequences of charge size limits on heat pumps

This section is focussing on hydraulic packaged heat pumps whatever heat source they may utilise. These heat pumps may provide space heating or cooling or both space heating and cooling. They may also provide domestic hot water. In this section, air to water heat pump designates a heat pump using outdoor air as heat source and ground source heat pump designates a heat pump using the ground as heat source, energy from ground to the heat pump being moved by water or brine.

Compliance to safety standards does not constitute a legal requirement, however, compliancy to product or group safety standards often ensure compliancy to EU regulation and CE marking in particular. Thus, harmonised standards are the preferred way to comply with the EU safety directives, such as the EU Pressure Equipment Directive, the EU Low Voltage Directive, and the Machinery Directive, and in practical, standard requirements are strictly followed by the industry and shape the products being placed in the EU market.

As shown in the above section, for ground source and air to water heat pumps, having floor installation the charge size cannot exceed 150 g of flammable refrigerant unless the room size exceeds 35m². The room size where the heat pump will be installed is out of the control of the manufacturer, as a consequence, 150 g is generally considered as the maximum charge size for heat pumps containing flammable refrigerant.

The heating capacity that can be delivered by a heat pump using 150 g of R290 highly depends on the technology of the components, in particular condenser and evaporator, the heat pump is equipped with. However, according to the state of the art, it is assumed that a heat pump using 150g of R290 would deliver approximatively 1kW of heating/cooling energy. To cover the heat demand of both new and existing household dwellings, the needed heating capacity varies in between 3 and 20kW.

As a consequence, ground source or air to water heat pumps designed to be installed indoor cannot use a flammable refrigerant as the provided heating/cooling capacity will not fit the usual heat demand of a single dwelling apartment or house in the EU.

As of today, IEC/EN 60335-2-40 does not leave any scope for innovation nor option for protective measures that could effectively prevent formation of a flammable mixture using other means and thus ensure a safe usage of the equipment.

Within the LIFE FRONT project, it is intended to develop a robust test methodology that permits to evaluate whether a heat pump using flammable refrigerant can operate without compromising safety whatever the charge size and the room surface area.

It is the intention to demonstrate that an obligation of providing evidence that a refrigerant leakage under a certain flowrate will not increase the concentration of flammable substances above a certain level could well replace the charge limits.

The test method applied hereafter is laid out in section 4.4 “test method for charge limits on equipment with passive or active measures”. As such this section provides a practical implement of the approach.

LIFE FRONT project experimental work is based on experiments simulating R290 leakages occurring from indoor heat pumps whereby measuring R290 concentrations surrounding the product and within the heat pump parts that contain a potential ignition source, and where the components are not Ex-type standards

Two prototypes have been tested. The prototypes have been designed and built up by the industrial partners and have been tested at the industrial partners facilities with the help of HEAT that conducted the tests. In particular, HEAT provided the gas sensors, the mass flow meter and the data collection and treatment software.

The tests aimed at:

- demonstrating that an efficient design or adapted mitigation measures can be implemented to ensure a safe usage of flammable refrigerant in heat pump equipment installed indoor whatever is the refrigerant charge size and independently of the room size.
- defining an efficient and robust methodology that can be used to evaluate whether a heat pump equipment using flammable refrigerant can operate without compromising safety whatever is the refrigerant charge size and the size of the room where the equipment will be installed.

Before performing such tests, two questions demand an answer: what is an appropriate criterion for a product to be deemed “at tolerable risk level” in regards to refrigerant charge size and which leak flow rates can be representative of “worse likely” leaks occurring from heat pump systems?

After performing the tests, one question demands an answer: is the defined test methodology robust enough to effectively evaluate whether a heat pump equipment using flammable refrigerant shows a tolerable risk level?

2.2 Definition of a “tolerable risk level”

It was needed to define the criteria to be met by a heat pump to be deemed “at tolerable risk level” in regards to the refrigerant charge size. It was decided that a heat pump is deemed “at tolerable risk level” if, in the event of a complete loss of the refrigerant charge, the R290 concentration surrounding the product does not exceed 50% of the lower flammability limit (LFL). In addition, would one or several heat pump parts contain a potential ignition source, and if the components under Ex-type standards, R290 concentration in the concerned area shall not exceed 50% of LFL.

Note that, these criteria permit to assess whether a product reaches “tolerable risk level” at its design phase. The assessment of the product safety presented in this section does not encompass a risk analysis of the product that covers its complete life cycle including manufacturing, installation, maintenance and dismantling.

2.3 Leak cause analysis and associated leak flowrate

Before starting the experimental test, it was needed to assess what could be a reasonable basic assumption for the refrigerant leak flowrate.

To answer that question, a thorough analysis of leak causes has been performed. The analysis is based on decades of experience of the project partners in manufacturing heat pumps and are based on the feedback and records from the field and after sales and quality departments. As industrial project partners manufacture hermetically sealed equipment that do not need any refrigerant piping work at installation, the leak causes that may affect the piping work done on site are not shown in Table 10.

In parallel of the leak causes analysis, hundreds of leaking parts coming from RACHP equipment installed in the field were collected and analysed by the project partner HEAT. The data has been stored in a database (http://lifefront.eu/databases). For each leak, the leak cause, leak hole size and leak flowrate are detailed so that it is possible:

- To highlight what is the typical leak flowrate occurring in the field
- To correlate leak flowrate and leak cause

The inputs that came out from both the analysis and the data collection are depicted in the table below. Every leak hole and leak flowrate shown in the table come from field measurements; some of them come from the LIFE FRONT project database and some other from the industrial partners own data bank.

Table 10: leak causes and associated leak flowrate

Component	Cause of leakage	Leak features		Associated risk	Existing mitigation measures in IEC 60335-2-89 and IEC 60335-2-40 Note that the latest version of the IEC standards have not yet be approved by the EU
		Hole size	Flowrate		
Fins and tubs heat exchanger	Any type of corrosion: galvanic, microbiological…	Small hole: 1 to 100 µm	Small : 1-2 g/day	None	No need for mitigation measures
Air to water heat exchanger (plate, co-axial…)	Crack du to frost of the heat exchanger	Large: more than 1mm²	Catastrophic: 88g/min	Refrigerant is flowing on the hydraulic system and can be ignited when hydraulic system will be vented	Disconnexion of hydraulic system from refrigerant circuit or refrigerant vented outside in case the leak occur: IEC/EN 60335-2-40/A1 section GG.6
Brazing and pipes located in the heat pump enclosure	Electrical short circuit with copper pipes	Large: more than 1mm²	Catastrophic: 88g/min	Hole is created on the pipe and refrigerant is ignited by the electrical arc: Fire or explosion	No electrical cable shall be installed close to a refrigerant pipes. For cables installed on site, cable passway shall be clearly marked. Revision IEC 60335-2-40:20xx (not published yet)
	Defective bending	0,17mm²	22g/min	Risk of fire in case of ignition source	
	Fatigue rupture due to vibration	0,17mm²	22g/min	Risk of fire in case of ignition source	Mitigation measures given in IEC60335-2-89: 2019: vibration test, section 22.108
	Defective brazing	0,7mm²	Catastrophic 65g/min	Risk of fire in case of ignition source	
	Fritting, repetitive rubbing of surface	<0,1mm²	<3g/min	Risk of fire in case of accumulation and ignition source	
	Icing of pipes	0,17mm²	22g/min	Risk of fire in case of ignition source	
Other components	Schrader valve; expansion valve, 4 way valves, pressure sensor….	Small hole	Low flowrate <3g/year	None	

One can observe that some of the causes for leakages may be eliminated already at design phase by appropriate mitigation measures, already defined in the existing or upcoming standards. However, adapted design requirements cannot prevent any leak from occurring as equipment material can be altered over time in an unpredictable manner.

The above table highlights that 88g/min is the maximum flowrate that has been identified. However, this leak flowrate has only been observed in the case of a hole created by an electric short circuit. Considering that this leak cause can be avoided by design, the first test done was based on the maximum flowrate of 65g/min which corresponds to a defective bending. For the second test, it was decided to assess the efficiency of the proposed testing method with a flowrate equal to the maximum: 88g/min (rounded to 100g/min for the sake of simplification).

It is essential to adopt a reasonable leak hole size and associated flowrate. If too small a hole is used then it is likely that the implemented protective measures will be insufficient to mitigate the hazard arising from all leaks. If too large a hole is used then the protective measures would be unnecessarily over-designed.

2.4 Test description and results

Over the project, several sets of mitigation measures and designs were implemented and tested on both the air to water and ground source heat pump prototypes. Several tries were needed to find the correct design that effectively prevent R290 concentration surrounding the heat pump from reaching higher values than 50% of LFL.

In this section, only the tests performed on the final prototypes, which designs, and the mitigation measures allow the R290 concentration to remain lower than 50% of the LFL are shown.

2.4.1 Heat pump description and main features

Both indoor packaged air to water and ground source heat pumps are hermetically sealed heat pumps, primarily designed to provide space heating through hydraulic emitters such as radiators or under floor heating/cooling systems.

These heat pumps are generally installed in garage, cellar or utility room.

The indoor package air to water heat pump is equipped with two ducts connected to the outdoor air, the outdoor air being moved through the evaporator by the mean of a fan. The main components of the refrigerating circuit are a compressor, an expansion and 4 ways valve, a brazed plates condenser and a fin and tubs evaporator.

Within the ground source heat pump, the refrigerating circuit is mainly made of a compressor, an expansion valve and two brazed plates heat exchanger, one being the condenser, the other being the evaporator. All refrigerating components are contained in an enclosure located at the lower part of the heat pump.

2.4.2 General testing features

Test space and arrangement

For both indoor packaged air to water and ground source heat pump an enclosure of a size intended to mimic a typical utility room has been built. These enclosure dimensions are: 3m x 3m x 2.5m and 3m x 2m x 2.5m height. The mock utility room enclosure shall be tight enough so as to minimise the leakage of refrigerant from the test area. The heat pump to be tested is installed in the mock utility room as prescribed in the installation manual.

R290 is supplied to the leak positions from a cylinder fed into the enclosure via refrigerant hoses (Figure 9). The hose terminates with a 1mm (0.8mm2) diameter orifice fitting in order to ensure choked flow. The mass flow rate and total released mass is modulated with a mass flow controller, calibrated for R290 (Figure 9).

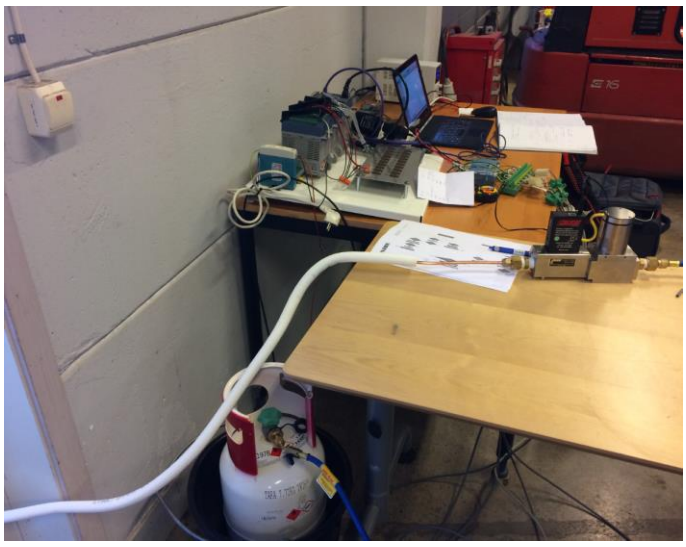

Figure 9: R290 bottle connected to the mass flow controller.

The R290 bottle is fitted in a bucket filled in with warm water that helps maintaining the R290 flowrate constant while the R290 mass contained in the bottle decreased.

Assessment of the mock utility room tightness

To assess the tightness of the enclosure mimicking the utility room, 400g of R290 were released in the enclosure. The air in the enclosure is mixed using a circulating fan. The R290 concentration was then recorded for 30 minutes. Over this period, the R290 concentration remained stable, it was concluded that the enclosure that sufficiently tight for the purpose of the tests to be performed.

Test description

To highlight the impact of the design on the heat pump safety, the first test was performed on a heat pump designed to operate with a non-flammable refrigerant such as R410A or R407C. Each test performed starts with a clean room: no R290 neither in the mock utility room nor in the heat pump enclosure. R290 is then released and the test stops after the defined R290 mass has been released. After each test, the R290 is evacuated from the testing enclosure and from the heat pump. The following test starts when the R290 sensors do not detect any R290.

Recorded data

R290 sensors are used to measure R290 concentration. Some of them are aspired sensors and others are positioned on a gas stand (as shown in Figure 10) and are diffusion operated. While tests are on-going it may happen that R290 concentration gets so high that the R290 sensors get saturated; in that event, the gas sensors are disconnected to avoid poisoning them. This is the reason why in the charts shown in the following clauses some curves are interrupted.

Figure 10: gas sensor installed on gas stand installed in the mock utility room.

2.4.3 Indoor packaged air to water heat pump prototype

An indoor packaged air to water heat pump prototype has been specifically designed for operating with R290. This prototype has been tested at the AIT technology centre in Kasendorf, Germany with the support of HEAT.

During all tests, the heat pump is not in operation, only the fan is switched on for some of the tests, the compressor is always off. Generally, the heat from the compressor will create convection currents which helps to disperse any releases, the test conditions are thus conservative.

Figure 11: prototype of indoor packaged air to water heat pump installed in the mock utility room.

Installation

The heat pump consists of three zones: the hydronic unit, which contains the hydraulic and electrical components, the condensing enclosure that contains the refrigerating circuit except evaporator, and the evaporating enclosure that contains the evaporator, the fan and the ducts. Zone C represents the surrounding of the heat pump, the zone where the R290 concentration shall not exceed 50% of the LFL. The red dots on *Figure 12* represent the R290 sensors, the orange arrows represent the location where R290 is released.

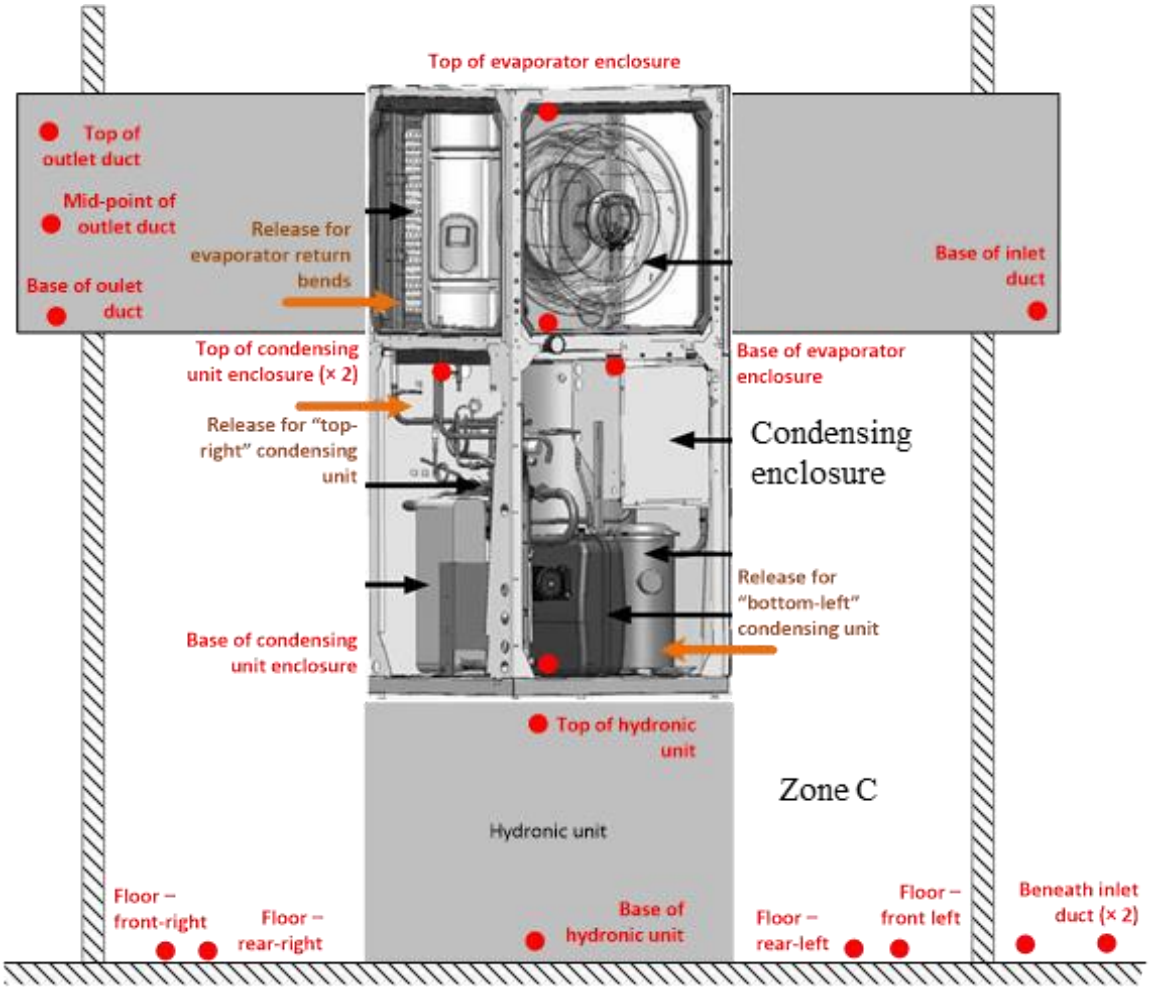

Figure 12: Rough sketch of test arrangement: red dots indicate sampling points and orange arrows are release positions.

Selection of release locations

Three R290 release locations were defined as being the most unfavourable location for a leak to occur: one in the evaporator enclosure and two in the condensing enclosure: one on top and one at the bottom. All releases involved a jet at choked flow conditions, directed horizontally, to impinge against a nearby surface in order to remove momentum from the jet and thus to minimise mixing.

Selection of flowrates and mass of R290 to be released

Three mass flowrates were selected. By performing the test using three different flowrates, the expected goal is to observe a kinetic trend and to observe preferential R290 accumulation location depending on the leak flowrate.

The three mass flowrates considered were: 20g/min, 45g/min and 65g/min. 20g/min corresponds to the leak flowrate that might be obtained in case of defective bending, fatigue rupture or pipe icing, 45 g/min corresponds to the assumed low-side R290 leak rate within the draft amendment 61D/421/CD to IEC 60335-2-40 for enhanced tightness systems and 65g/min correspond to the highest leak flowrate, considering that electrical arc can be avoided by construction.

500g of R290 was released at each test. After the 500g were released, the R290 concentration records last for another couple of minutes.

2.4.4 Test conditions

Test conditions followed those detailed in Table 10.

Table 10: test conditions for indoor packaged air to water heat pump

Test no.	Release mass flow rate [g/min]	Release location	Orifice height [m]	Evaporator fan airflow	Released quantity [g]
Tests performed on an indoor package air to water heat pump designed for R410A					
1	40	Evaporating enclosure	1.5	off	500
2	20	Condensing enclosure: bottom	0.8	off	500
Tests performed on an indoor package air to water heat pump designed for R290					
3	40	Evaporating enclosure	1.5	off	500
4	65	Evaporating enclosure	1.5	off	500
5	20	Evaporating enclosure	1.5	off	500
6	20	Condensing enclosure: bottom	0.8	off	500
7	45	Condensing enclosure: bottom	0.8	off	500
8	65	Condensing enclosure: bottom	0.8	off	500
9	20	Condensing enclosure: top	0.95	off	500
10	65	Condensing enclosure: top	0.95	off	500

2.4.5 Test results

The objective is to reach a R290 concentration at the surrounding of the equipment which does not exceed 50% of the LFL.

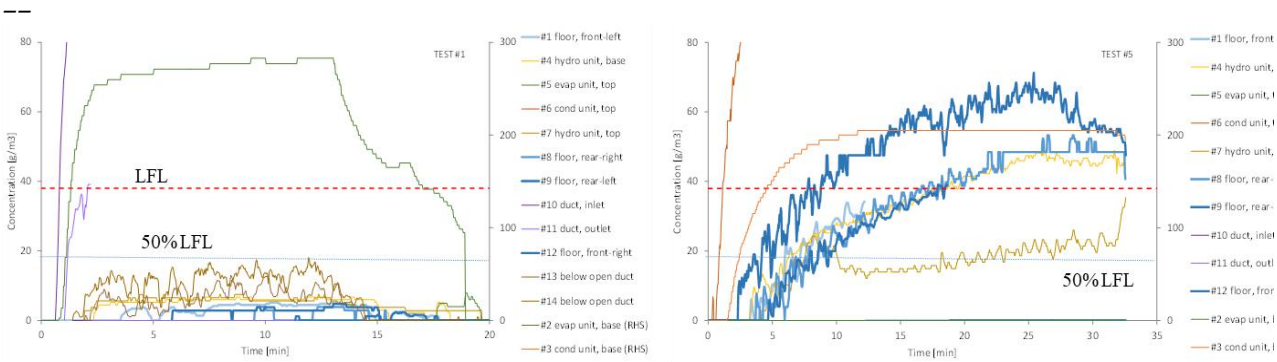

Figure 13: test 1and test 2: indoor packaged air to water heat pump designed for R410A, R290 released in the evaporating enclosure (left chart) and at the bottom of the condensing enclosure (right chart).

Test no. 1 results are shown in Figure 13. Highest concentrations were recorded in the base of the evaporator section and also at the lower part of the inlet and outlet ducts, where the concentration can be seen to rise and exceed LFL almost instantaneously. Concentrations on the floor of the test room were low, at a fraction of the LFL, whilst those directly below the duct openings (assumed to be outside) were also less than half of the LFL. Following cessation of the leak (about 13min) all concentrations fell to zero (except within the evaporator unit base).

When released in the condensing enclosure, test 2, R290 concentration get higher than LFL in zone C. No R290 is detected in the evaporating unit.

Test 1 and 2 were performed on a heat pump designed to operate with R410A, the other remaining tests are performed on the prototype, specifically designed to operate with R290.

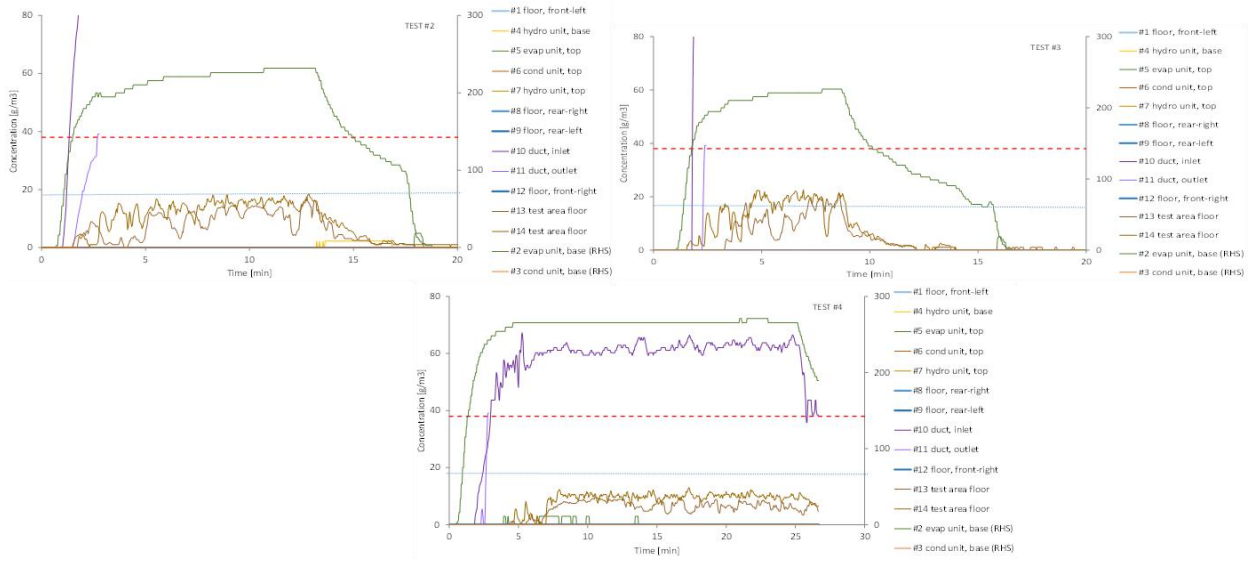

Figure 14: test 3, 4 and 5: indoor packaged air to water heat pump designed for R290, R290 released in evaporating enclosure.

When released at 65g/min, the concentration of R290 reaches 52% of the LFL in zone C. The 50% LFL criteria is not strictly met; an additional mitigation measured should be implemented in order to strictly remains below 50% of LFL. One can observe that the highest is the flowrate, the highest the R290 concentration gets at the surrounding of the heat pump.

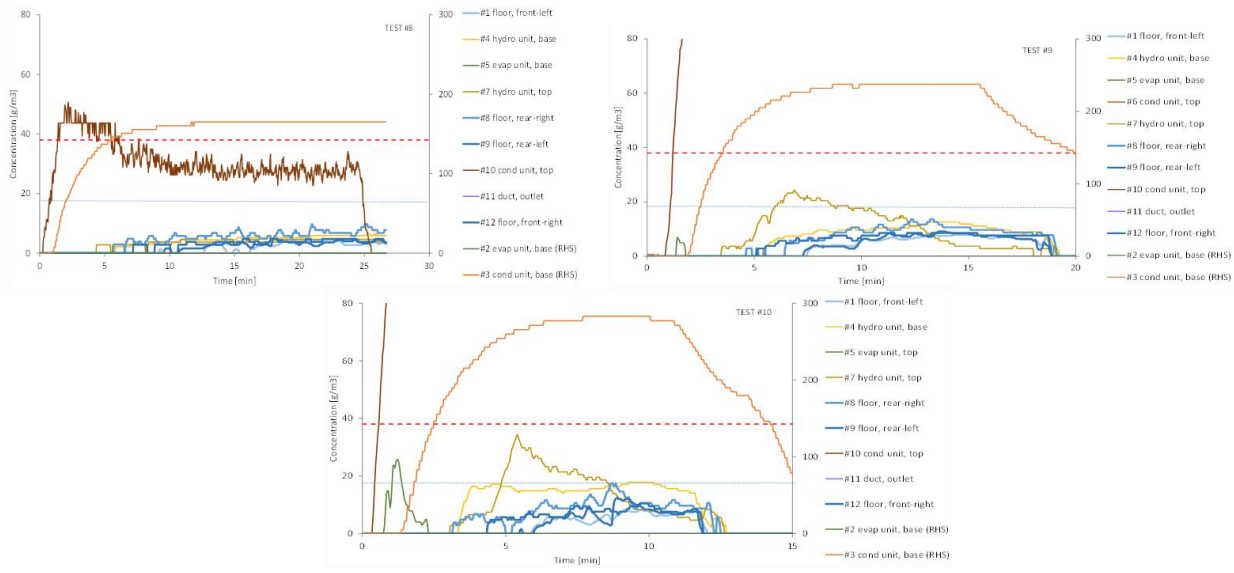

Figure 15: test 6, 7, 8: R290 released at bottom of condensing enclosure

The concentration of R290 in zone C remained below 50% of LFL for the three tested leak flowrates.

Results obtained when R290 was released at the top of the condensing enclosure, test 9 and 10 are shown *Figure 16*.

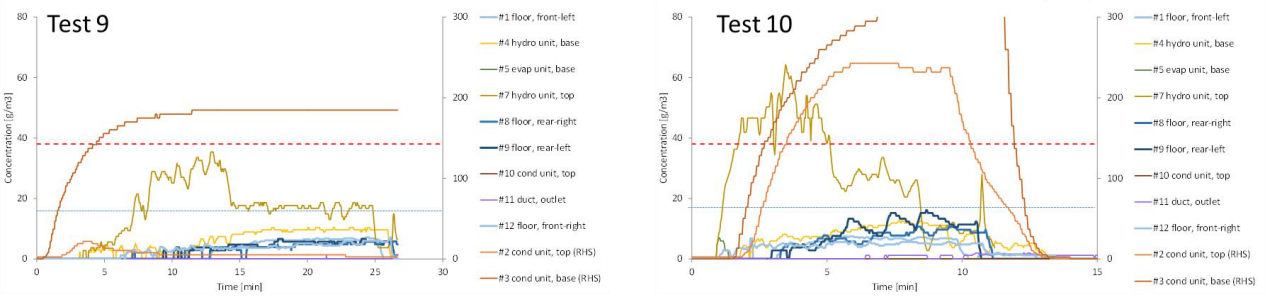

Figure 16: test 9 and 10: R290 released at top right of condensing enclosure.

From the 8 tests performed, one can conclude that the indoor packaged air to water design is sufficient to avoid creating an explosive atmosphere around the product. However, some adjustments would be needed as a little more than 50% LFL is reached where R290 is released in the evaporating enclosure.

2.4.6 Ground source heat pump prototype

A ground source to water heat pump prototype has been specifically designed to be used with R290. The prototype has been tested at NIBE AB facilities at Markaryd, Sweden with the support of HEAT. During the tests, the heat pump has not been in operation.

Installation

Three zones, represented on Figure 18, are defined: zone A: upper part of the heat pump contains the hydronic components, immersion heater, power supply and all electrical components, zone B contains the refrigerating circuit, zone C represents the surrounding of the product. Zone A and zone C represent the zones were R290 concentration shall not exceed 50% of LFL (components in zone A do not comply with ATEX legislation). The red dots represent the gas sensors.

Figure 17: prototype of ground heat pump installed in the mock utility room.

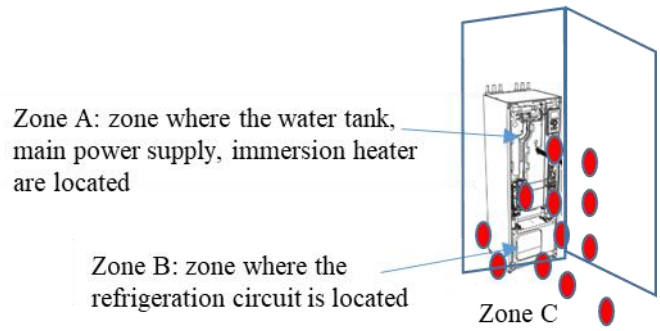

Figure 18: Rough sketch and picture of test arrangement: red dots indicate gas sampling points.

Selection of release locations

The refrigerant is contained in zone B. The leak hose is placed at the centre of zone B. For assessing whether R290 could get into zone A, the leak orifice was oriented first toward the top of zone B. Then, the leak orifice was oriented towards the side panel of zone B against the wall of the room.

Selection of flowrates and mass of R290 to be released

Two mass flowrates were selected. The two mass flow rates considered were: 20g/min and 100g/min. 88g/min is the highest leak flowrate observed according leak the cause analysis, for this test, it was decided to evaluate what will happen in case this catastrophic leak occur (88g/min was rounded to 100g/min).

800g of R290 was released at each test. After the 800g were released, the R290 concentration continued logging for several more minutes.

Test conditions

Table 11: test condition for ground source heat pump

Test no.	Release mass flow rate [g/min]	Release location	Orifice height [m]	Released quantity [g]
Tests performed on a ground source heat pump designed for R407C				
1	100	Oriented towards zone A	0.3	400
Tests performed on a ground source heat pump designed for R290				
2	100	Oriented towards zone A	0.3	800
3	100	Centre	0.3	800
4	20	Centre	0.3	800

2.4.7 Test results

In the following charts, the doted blue line represents 50% of LFL.

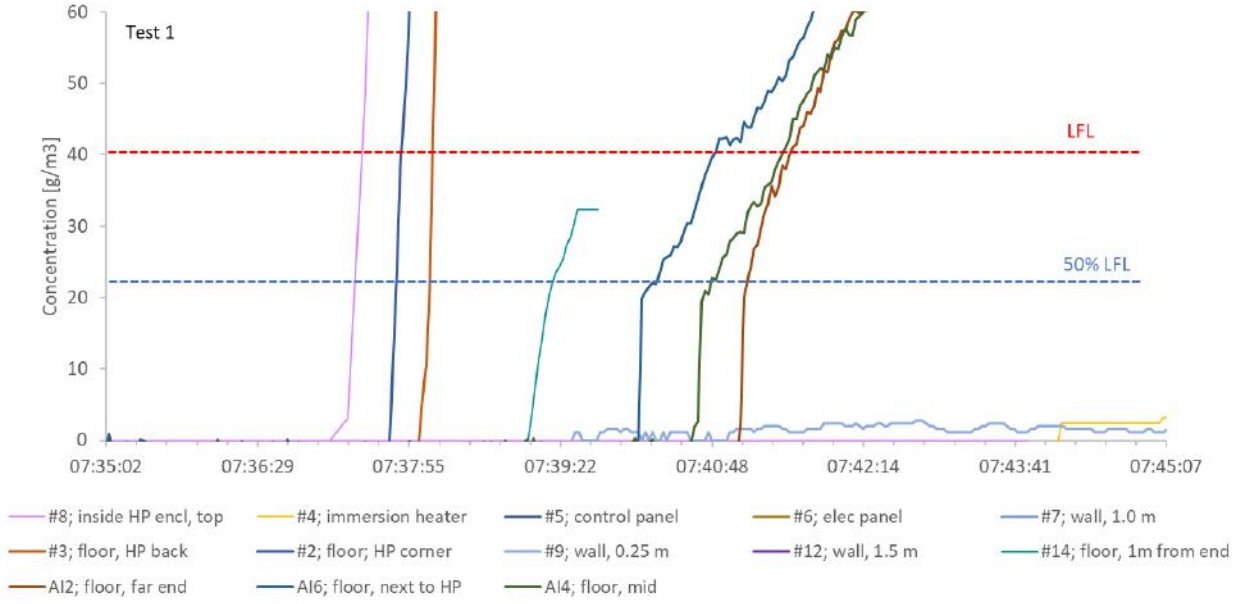

Figure 19: results of test 1 performed on ground source heat pump designed for R407C - 100g/min.

For this first test, one sensor was positioned within part B, in the refrigeration enclosure. R290 release starts at 7:36 and ends at 7:40. Only 400g were released. 50% of the LFL is reached everywhere in the room at floor level. One can notice that as there is no ventilation in the room, R290 stagnates at floor level and the concentration remains lower than 50% of LFL at 0.25m height whereas no R290 is detected by the sensors positioned at 1m and 1.5m.

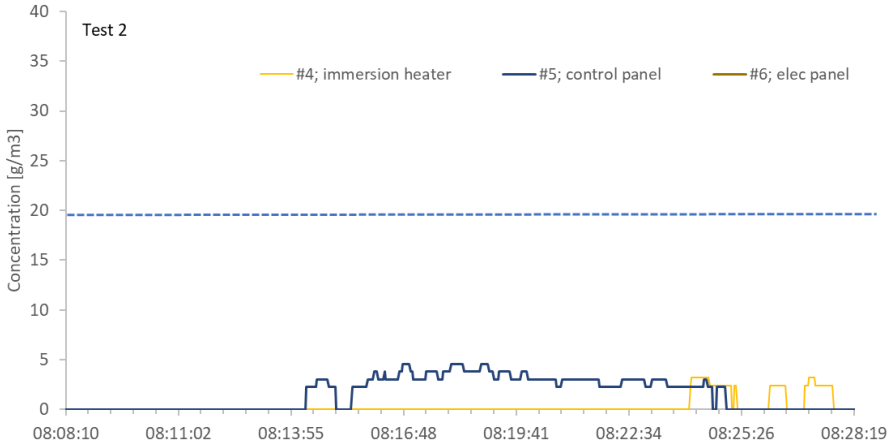

Figure 20: results of test 2 performed on the ground source heat pump prototype designed for R290 – 100g/min.

R290 release starts at 8:10 and stops at 8:22. R290 concentration remains far below 50% LFL on zone A. no R290 is detected in the electrical panel where the relays are located.

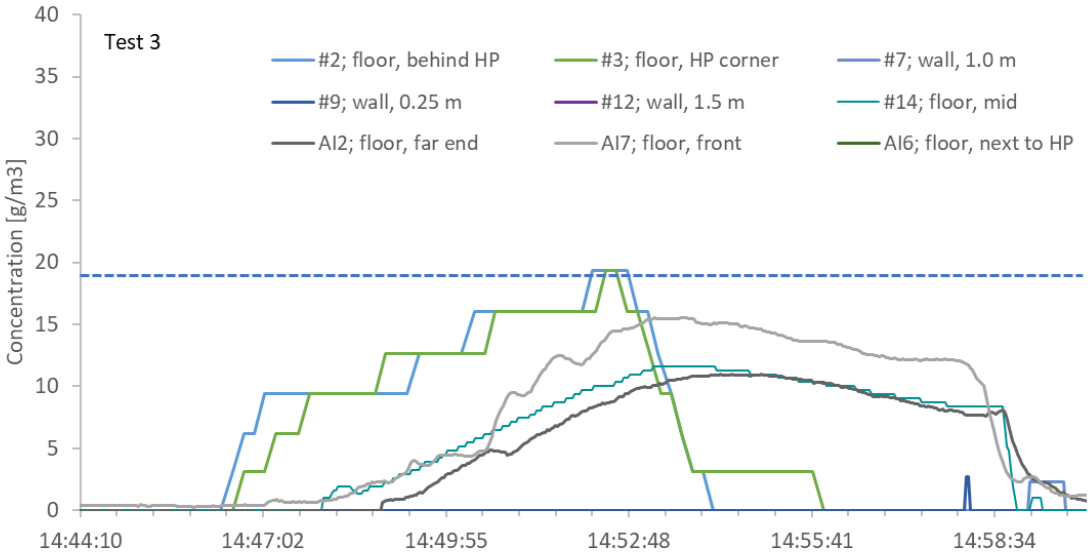

Figure 21: results of test 2 performed on the ground source heat pump prototype designed for R290 – 100g/min.

R290 is released at 14:44. The 800g are released after 8 minutes. R290 concentration increases first at the side of the heat pump which is by the wall as well as at the back. Then, the R290 is propagating into the room.

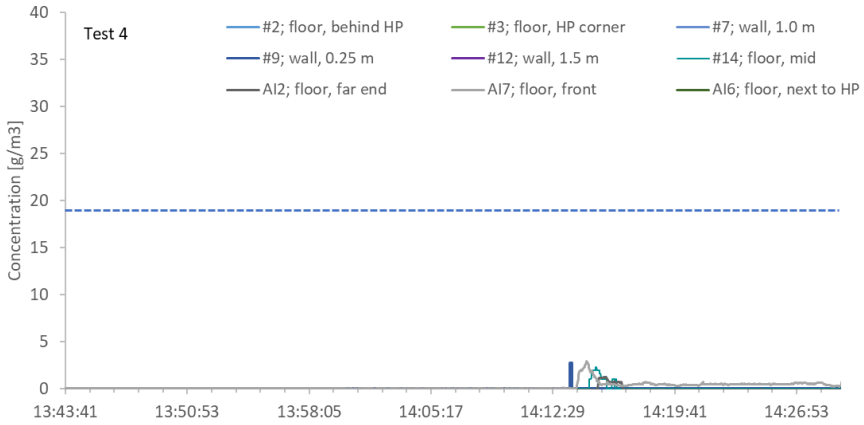

Figure 22: Results of test 3 performed on the ground source heat pump prototype designed for R290 – 20g/min.

R290 release starts at 13:43 and ends at 14:23. R290 concentration remains far below 50% of LFL.

From the three tests performed, one can conclude that R290 is not penetrating zone A, where potential ignition sources could be found. The tests also demonstrate that in case there is no air movement in the room, R290 stagnate at floor level. In addition, the ground source heat pump design is efficient in preventing the creation of an explosive atmosphere around the heat pump even in case a catastrophic leak is occurring in the refrigerating circuit. In addition, the design also permits to keep R290 concentration far below 50% of LFL in case a small leak is occurring.

The results of the performed tests show that R290 remains at the floor level. The gas sensor placed on the wall did not detect any R290 except during the first test performed on a ground source heat pump designed for R410A.

2.4.8 Assessment of the test methodology

The tests that were performed led us to the conclusion that the prototypes built during the project can operate at tolerable risk level while using R290, respectively 500g and 800g. However, it is needed to assess whether the methodology that was used is reliable and could be included in safety standard to replace the actual charge size limit rules.

In this section, the test method will be evaluated while used for testing heat pumps.

The test method aims at ensuring that in case a leak is occurring while the equipment is installed in a household dwelling, safety of persons, animals and buildings will not be compromised. To assess the relevancy of the proposed method, it is proposed to oppose each step of the test procedure to real life experience.

Room arrangement

The test method is to be applied on heat pump designed to be installed indoor. As the installation location is unpredictable as well as the ignition source that might be present in the room, it is needed to assess what could be the worst case.

The worst situation arises from an installation in a tight room where the air stagnates. In the event of a release of flammable refrigerant in such a room, the refrigerant will not be evacuated outside the room nor diluted within the room volume and may create an explosive atmosphere at some point of the room.

In order to reflect this worst case, the test shall be performed in a test room which tightness shall meet specific and well-defined criteria.

The heat pump to be tested shall be installed in the room as prescribed within the installation manual. In case several installation options are made available, the worst condition shall be chosen, considering that the worst conditions might be where the heat pump is installed alongside a wall, or in an angle of the room such as limiting the air circulation on two sides.

Equipment operation

Depending on the equipment, the worst conditions could be met while the equipment is switched on or off. In case of the tested air to water heat pump, the worst conditions are obtained when the fan is off as the fan accelerate the evacuation of R290 from the heat pump enclosure to outside.

In case of an equipment which operation does not rely on a fan, there is not much influence of the heat pump operation on the evacuation/dilution of the refrigerant. It is foreseen that there could be some thermal effects due to hot surfaces, however, the thermal effects will generate an air movement that will accelerate the flammable refrigerant dilution within the room. Again, in this case, the worst conditions will be obtained while the heat pump is switched off.

While testing heat pumps, it is quite likely that the worst case will always be obtained while the heat pump is off.

Sensors, number and positioning

The gas sensors quantity, positioning and quality are essential to evaluate the flammable refrigerant propagation within the test room and to get a reliable picture of the maximum concentration reached within the room.

The gas sensors shall be positioned in the zones where it is required to keep the refrigerant concentration lower than 50% of the LFL. Equipment surrounding constitutes one of these zones, however, additional zone, within the heat pump cabinet can be concerned and thus shall be equipped with one or several gas sensors in order to measure the refrigerant concentration when a leak occurs.

The tests performed in the scope of the LIFE FRONT project showed that the highest R290 concentration is reached at the floor level. Moreover, the tests showed than R290 concentration higher than 1m remains below 5% of LFL.

R290 being heaviest than air, where air is not moved by mean of fan, R290 will drop and stagnate at the floor level. This phenomenon of flammable refrigerant dropping at floor level will occur unless the refrigerant density is lower than these of air.

While testing a heat pumps designed to operate with a flammable refrigerant showing higher density than air, measuring the refrigerant concentration at floor level will be enough to evaluate the maximum R290 concentration reached surrounding the heat pump.

Leak generation and location

It is difficult to draw a general rule about the worst leak location. It is advised in the methodology that the manufacturer should choose the most unfavourable leak location keeping in mind that there might be need to select several leak locations. The leak should be oriented towards the direction which leads to the highest concentration at the heat pump surrounding and the heat pump parts where ignition sources might be present.

Leak flowrate and released mass

Coming from the database leak collection and leak analysis and from the experience of the industrial partners, it was demonstrated previously in this report that 100g/min is a reasonably pessimistic assumption of the maximum leak flowrate that can occur. This flowrate is reached while a catastrophic leak is occurring. Thus, it cannot be deemed to be representative from the vast majority of leak that will occur, which flowrate (according to the leak database) will remain lower than 10g/min. However, the occurrence of a major failure leading to a catastrophic leak flowrate cannot be excluded. For that reason, it is proposed, to perform two leak tests, for each leak location, one at 10g/min and one at 100g/min. it is important to perform the test using a smaller leak flowrate, 10g/min, as the flowrate may have an influence on the dilution/evacuation kinetic and may influence the refrigerant concentration at some points.

The refrigerant charge mass that can be released from the equipment cannot be higher than the charge size of the equipment. In reality, there will be refrigerant remaining within the refrigerating circuit and it is quite unlikely that the entire refrigerant charge size will be released. As the maximum releasable charge assessment is described in IEC 60335-2-40. It is recommended that either the entire charge size or the maximum reliable charge shall be released at each test.

Criteria

It was decided to align the flammable refrigerant concentration criteria to the one defined in IEC 60335-2-89 which set the maximum allowable flammable refrigerant concentration at the equipment surrounding at 50% of LFL. This criterion leaves enough room for uncertainty while ensuring consistency in between RACHP equipment.

It is added in the proposed method that the maximum refrigerant concentration shall not reached higher value than 50% of LFL in parts of the heat pump that may contains ignition sources and where components are under Ex-type standards.

2.4.9 Conclusion on the assessment of the test method

Based on the above consideration, we conclude that the described test method can effectively be used to demonstrate that a heat pump using R290 can operate without compromising safety.

2.4.10 LIFE FRONT project recommendations for heat pumps

Test method description

This method might be applicable to any flammable refrigerant and to all type of water-based heat pumps.

Room arrangement

The appliance to be tested shall be positioned within a test room. The room height shall be no less than 2.2m. The room shall be “tight” i.e., no decay in average room concentration of more than 5 g/m3 per hour. The

appliance shall be installed at a height and location as prescribed by the instructions manual, selected to yield the least favourable result.

Gas sensors: number and positioning

Sampling points to measure gas concentration shall be positioned around the heat pump, no more than 30mm above floor level. There shall be one sampling point at a distance of no more than 0.5m from each exposed side of the heat pump. *Figure 23* shows a possible arrangement of the sampling points.

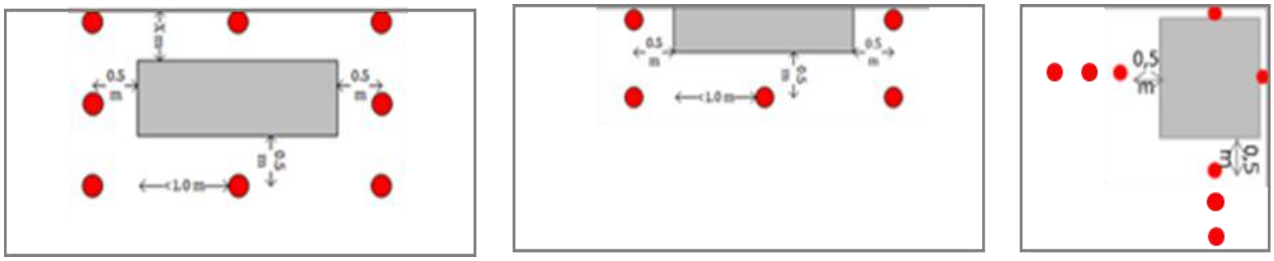

Figure 23: Possible test room set up and positioning of the sampling points; plan view showing the RACHP equipment (grey block) and floor level sensors (red dots).

The gas sensors shall be suitable for the gas to be detected and under calibration control.

Note that the gas sensor positioning is only valid where refrigerant density is higher than air density.

Leak generation and location

A simulated leak shall be made at the most unfavourable positions on refrigerant containing parts. Several locations might be chosen to be representative or to determine the least favourable one. The jet direction which leads to the highest concentration shall be chosen. The refrigerant is released through an orifice in vapour phase at a pressure of at least 2bar (gauge), or whatever is necessary for choked flow.

Leak flowrates and released mass

Two mass flowrates shall be used: 10g/min and 100g/min. It might be interesting to test an additional intermediate flowrate, 45g/min, to get the concentration developing trend around the product. The mass released shall correspond to the refrigerant charge or the releasable charge applicable for the system.

Data to be recorded

Measurements of gas concentration shall be recorded at time increments of no more than 5 seconds apart from the time at which the release begins and until the concentration at all sampling points declines for at least three minutes.

Test procedure

The tightness of the test room shall be assessed prior any test on the heat pump is performed. Sufficient tightness is demonstrated by a mass of refrigerant equating to about 50% of LFL being released into the room and mixed using a circulating fan. The average concentration at six sampling points throughout the room shall be within ±5% of the arithmetic mean and the mean value shall not decline by more than 5% within a five-minute duration.

For each flowrate and leak location, the maximum refrigerant charge or releasable charge shall be released. The test shall be repeated no fewer than three times at each flowrate and leak location. The heat pump shall be switched off during the test, only the devices that are in operation at all time (fan….) might be operating.

Pass criteria

None of the refrigerant concentration detected by the gas sensors surrounding heat pump shall be greater than 50% of LFL. In case gas sensors are installed within the heat pump enclosure, none of them shall detect a gas concentration higher than 50% of LFL.

3 ANALYSIS OF FACTORS AFFECTING CONCENTRATIONS FROM LEAKS

3.1 Introduction

There are a vast number of factors that influence the fate of a refrigerant leak and some of them are identified in Figure 24. Usually there are three main processes involved:

- Release from the pressure system;
- Flow and transfer through unit housing;
- Flow and mixing into and through the room.

Eventually once the refrigerant release is exhausted, or before a certain preventative measure initiates, a peak concentration and associated flammable volume will occur and subsequently decay. During these processes, a variety of different factors influence the quantities and ultimately the peak concentration and flammable volume to some extent. Accordingly, it is essential to understand the degree of influence of these factors, the likelihood that they are present and whether or when they need to be accounted for in charge size determination. Simultaneously, if protective measures are intended to be introduced, their influence also needs to be characterised. All should be deliberated with respect to the current CSLs.

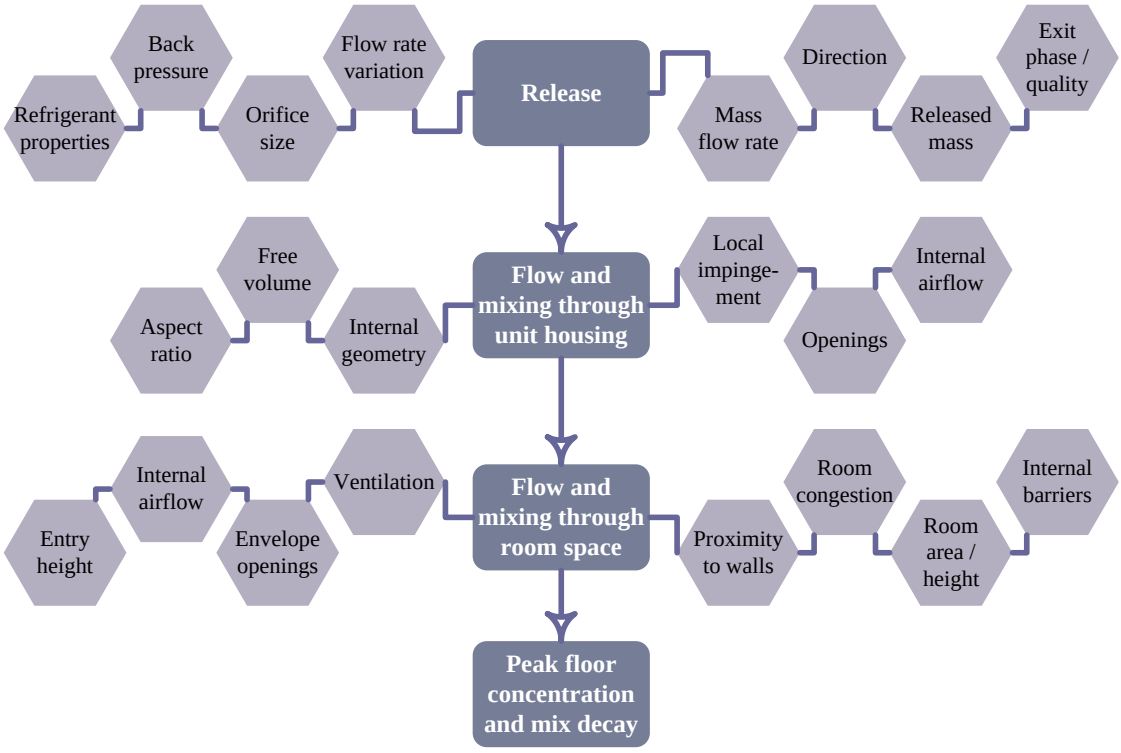

Figure 24: Main process from refrigerant release to peak concentration and eventual decay, identifying key influencing variables.

3.2 Release conditions and mass flow rates

The refrigerant release characteristics are a fundamental consideration when addressing CSLs. Within the current RSSs, assumptions on leak rates have been addressed differently. For the CSL formula in IEC 60335-2-40 (equation 1), there was an assumption made that the mass flow rate was equal to the entire charge being released over four minutes. According to the findings reported in the leak size report (Colbourne and Kanakakumar, et al. 2019), this assumption is likely to be unrealistic for the vast majority of scenarios. It is essential to use a realistic leak size in order to provide a good balance between avoidance of flammability events and cost of preventative measures.

There are several important considerations that apply to release conditions:

- Leak mass flow rate
- Leak phase (vapour or liquid-vapour mixed phase)
- Orifice shape
- Internal pressure (system operating state)
- Change in release mass flow over time

These are addressed in detail within the parallel report of leak sizes (Colbourne and Kanakakumar, et al. 2019).

The key outcomes from the leakage report are:

- Leak mass flow rate should be based on the largest hole size of the 99th quantile of the current data, i.e., excepting “extreme” errors made by technicians and component suppliers.

- Leak phase is assumed to be vapour only as this was shown to lead to higher concentrations than mixed phase
- Orifice shape should be assumed to be round
- Internal pressure is based on the maximum value for anticipated operating conditions
- Release mass flow is assumed to be constant, based on the mass flow at the beginning (1st quartile) of the release duration

3.3 Flow through housing/enclosure[6]

It is useful to understand the rationale used in the development of existing charge limitations and identify any oversights that can be discounted or alternative means of describing the processes that are deemed to have led to such restrictive requirements. In addition to reviewing the assumed leak rate (Colbourne and Kanakakumar, et al. 2019), the source condition associated with the refrigerant entering the space should also be addressed. In principle, these findings are applicable to any RACHP equipment that employs a porous enclosure to house the refrigerant-containing parts.

3.3.1 Real indoor AC units versus "diffuser" device

Whether a diffuser suitably mimics a release from an IDU was examined by simulating releases from both a diffuser device and from within an IDU and comparing floor concentrations. Each test used 310 g released at a constant 60 g/min via a 2 mm diameter capillary tube at various positions and orientations within the IDU (Figure 25), which was fixed 1.5 m above the floor with sampling points positioned at 0.5 m increments spanning out across the floor. Results for maximum mean floor concentration and "peak" concentration are given in Figure 26, enabling comparison between releases from within the IDU and the diffuser.

Highest concentration for releases from the IDU is with the capillary exit located at the lowest right-hand return bends; crucially both maximum mean and peak values were a fraction of that exhibited with the diffuser release. Maximum and peak concentrations for all positions at the left or right return bends are comparable, whereas the releases within the coil block and from the connector fitting are considerably lower. Subsequent work using a mock IDU found that the available internal sub-volume within which the release can freely pre-mix before sinking out of the IDU has a strong effect on floor concentrations.

[6] This section describes experimental work that was conducted in the refrigeration laboratory at UCL, London, partly under the EU Life-Front project and partly under the GIZ standards project.

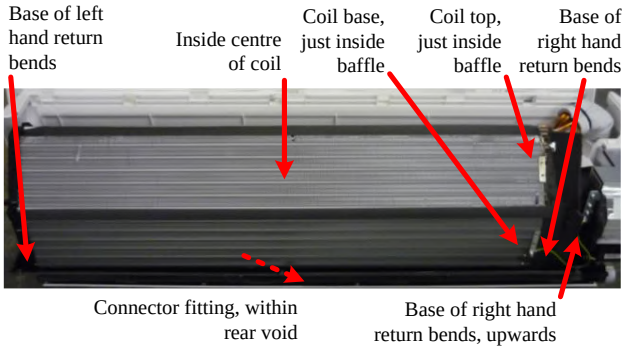

Figure 25: Comparison of theoretical minimum leak time for various flammable refrigerants.

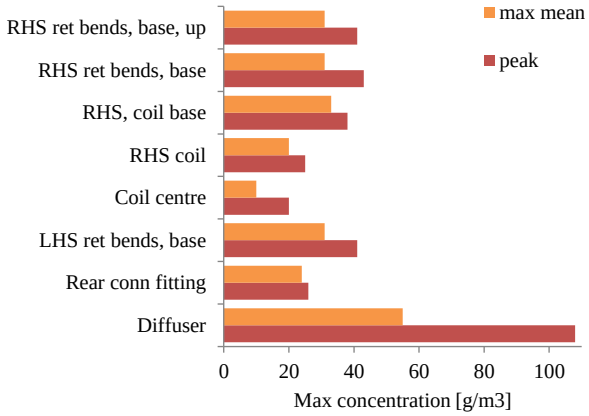

Figure 26: Comparing peak concentrations due to releases from positions within IDU and diffuser.

Further tests were carried out to broaden the assessment of differences between use of a diffuser and a real IDU (with fan off), by varying release mass flow rate and release height but maintaining a single release position within the IDU at the lowest right-hand return bends. Figure 27 presents results for the diffuser only, with the outlet positioned at 1.0 m and 1.8 m, and results for the IDU at the same heights in Figure 28. Findings from Figure 26 are replicated, where with all release heights and mass flow rates, the diffuser produces approximately double the peak and max mean concentration than with the IDU. It is seen that there is a wider difference between peak and max mean values for the diffuser. The reason for this is that the axial variation in concentration throughout the plume has not had sufficient decent distance to become as homogenised. This is not seen with the IDU release because homogenisation has already occurred through mixing inside the enclosure.

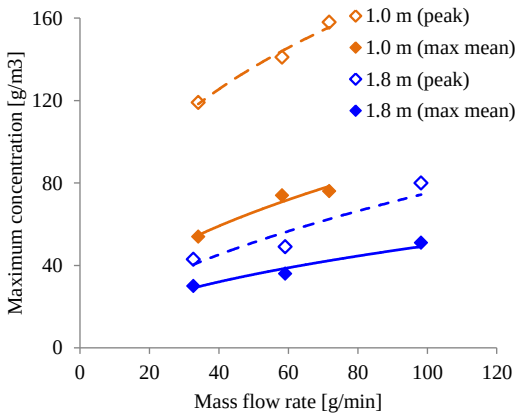

Figure 27: Floor concentrations arising from diffuser releases.

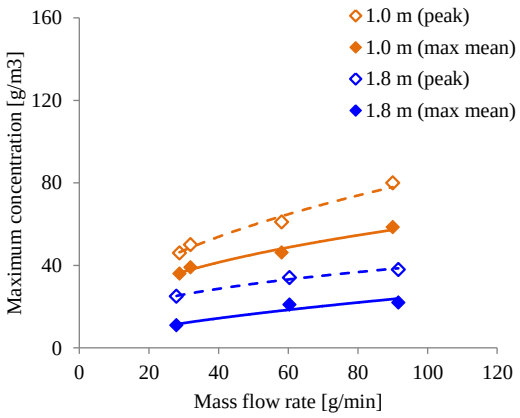

Figure 28: Floor concentrations arising from releases at IDU coil return bends.

Similar comparison is provided in Figure 29 for a release from a window type AC, where leaks were simulated from the return bends of the cooling coil, a mid-coil position and also a diffuser at the same height as the AC

was (i.e., 1.0 m). It can be seen that almost 500 g of R290 may be released from the AC, whereas only 10% of that quantity will lead to a floor concentration exceeding LFL when a diffuser is used.

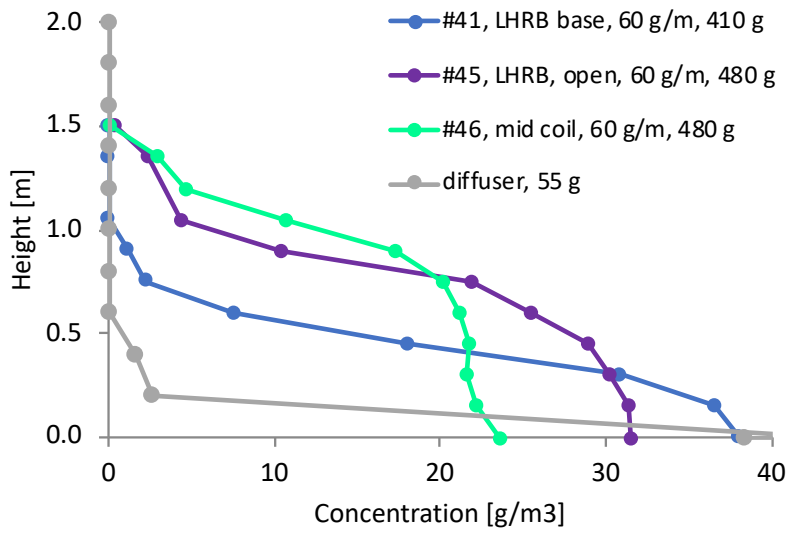

Figure 29: Vertical concentration distribution for a release from a window type AC compared against a release using a diffuser device.

3.3.2 Effect of unit enclosures/housing (UHE) on dispersion of releases

Under quiescent conditions, entrainment of surrounding air into a jet or plume of dense refrigerant is strongly influenced by its momentum; a high velocity jet into free air can easily result in near-homogenous mixing within the space whereas a low velocity descending negatively buoyant plume will often establish a stratified layer on the floor (e.g., Webber et al., 2011). Thus, the earlier study used for justification of charge limits for AC equipment was based on the assumption of a release from a so-called “diffuser” device (Kataoka et al, 2000), which is essentially a sort of packed inverted funnel that refrigerant is fed into such that the exit condition is pure refrigerant and with an outlet velocity in the order of millimetres per second. This was justified on the basis that that almost all refrigerant-containing parts of RACHP system are encased to some extent so it is reasonable to assume that any leak will impinge upon an immediate surface, thus reducing momentum from the jet leading to a plume flowing out of the UHE at low velocity. Subsequent work has demonstrated that this is a crude and detrimental assumption.

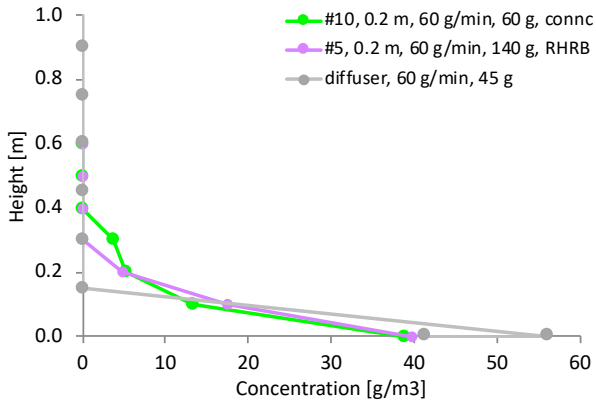

Figure 30: Vertical concentration distribution for a release from a floor type AC compared against a release using a diffuser device.

3.3.3 Release jet orientation and impingement

Under other projects, considerable work had been put into investigating the implications of the orientation of the release jet within RACHP enclosure housing and further assessing how the jet impingement on nearby surfaces/internal congestion affects floor concentrations. The findings are detailed in Colbourne and Suen (2016) and are useful to understand the influence of some of the enclosure variables and thus how to formulate surrounding concentration tests so as to account for the worst likely arrangements.

3.3.4 AC indoor unit housing geometry

To help understand the effect of IDU housing geometry on developed concentrations, a mock IDU was constructed to enable certain characteristics to be varied. External dimensions were 0.54 m long and 0.26 m × 0.26 m cross-section, with options to vary opening areas at the top, base and side, internal enclosure length and internal free volume; see Figure 31 and Figure 32.

Figure 31: Sketch of the mock IDU.

Figure 32: Photograph of the mock IDU.

R290 was injected horizontally into a small compartment to mimic the void associated with coil return bends, the volume and baffle area of which we also changeable. Throughout the mass flow rate was fixed at 70

g/min with 200 g and with the enclosure fixed at 1.0 m above the floor and against a wall panel. No forced airflow was applied.

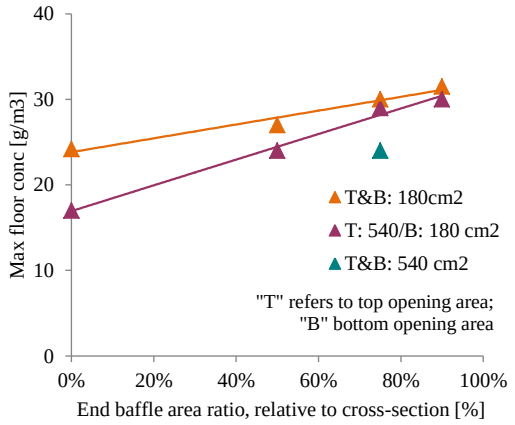

Figure 33: Effect of baffle area and top and base opening area on maximum floor concentration.

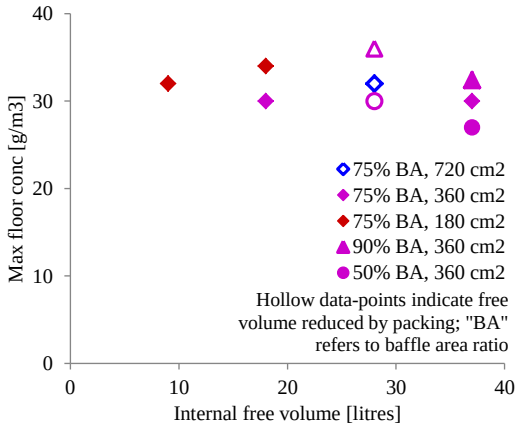

Figure 34: Effect of internal free volume and total opening area on maximum floor concentration.

Figure 33 compares maximum concentration moments after cessation of the release across for a range of end baffle to cross-sectional area ratios, where a high ratio means that the end section is almost closed off and so restricts migration of the refrigerant to the rest of the enclosure volume. Generally, the more open the path is between the void containing the release and the remaining part of the enclosure, the better the pre-mixing appears to be. Three sets are shown according to the area to the top (T) and bottom (B) openings; again, more dilution of the initial release occurs with larger openings. The influence of IDU free volume is presented in Figure 34, along with baffle area ratio and opening area (equally divided between top and bottom). For fixed baffle area ratio and opening area, the effect of internal free volume on maximum concentration appears negligible. However, when the free volume is reduced by means of internal packing (whilst enclosure volume is fixed) there is a notable increase in maximum concentration. Whether or not free volume is displaced with internal packing, both reduced baffle area ratio and increased opening area help reduce floor concentrations.

Therefore, it is considered essential to characterise this parameter so that it may be better understood. Additionally, the characteristics of the UHE can also be used to determine h^* where the UHE base height is not necessarily applicable.

3.4 Flow mixing in room space[7]

3.4.1 Enclosure location with respect to wall

Concentration measurements are typically carried out in empty rooms, with IDUs positioned centrally against one wall so as to be as symmetrical as possible and improve repeatability. In theory, a more pessimistic release position should be the corner of the room, inferring that the available surface area for entrainment would initially be reduced and thus higher concentrations. Measurements were made using a release of 440 g at 100 g/min from the right-hand return bends of an IDU at 1.0 m above the floor and positioned at three alternate locations. Figure 35 compares concentrations at cessation of the release for the same unit being positioned at the mid-point of a "short" wall (3.3 m), mid-point of a "long" wall (4.6 m) and in the corner (against the long wall). There is variation of about ±10% of the average maximum floor concentrations across the three positions, with the IDU at the corner leading to highest concentrations and the short wall position giving the lowest. For the corner position, the plume spread at floor level is more constrained thus limiting dilution, whereas for the short wall position, the plume is given the longest flow path, likely to aid dilution. Having said this, consideration must also be given to the fixed position of the gas sensors and in relation to the local distribution of the mixture.

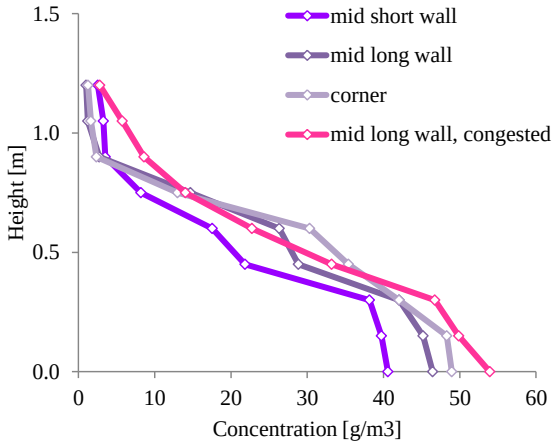

Figure 35: Effect of IDU position and congestion.

3.4.2 Room congestion

Room concentration tests normally employ empty rooms to enable reproducible measurements. Since most rooms are seldom empty it is appropriate to consider the effects of congestion within a space. With respect to the dispersion of releases there are three "forms" of congestion: one which comprises large obstructions within the space, another where larger obstructions are present within the path of decent of the plume and a third which consists of many small items. Distributed large obstructions tend to have a detrimental effect of mixing since they not only displace free volume but also act as substantial barriers preventing the flow of a plume. Where obstructions are present within proximity of a release from above floor level, previous work

[7] Whilst the experiments described in this section employed an air conditioner indoor unit (IDU), the results are considered to be applicable to any enclosure associated with an RACHP system that houses refrigerant-containing parts.

with condensing units (Colbourne and Suen, 2016) found that despite displacing free volume, they help to enhance dispersion. Theoretically, presence of many smaller objects can also help augment mixing since they can generate turbulence within a flowing mixture; investigating this case experimentally is potentially complicated and laborious given the infinite number of permutations. In order to attain a better insight of the implications of "extreme" congestion, a test was carried out by filling the test room with a much clutter as practicable; tables, chairs, cupboards, boxes, cylinders, ladders, test rigs, etc., with the majority of objects exceeding the height of the IDU and covering 45% of the room floor area. Concentrations for this test are given in Figure 35 so that they can be gauged against results for the empty room. Peak floor concentration is between 10% and 30% higher than the empty room cases and showing a much more linear transition in concentration with height. If the maximum charge is determined for an empty room, it is probably reasonable to apply to a normally partially congested room as one might encounter in practice; there is no need to apply an additional margin to account for room congestion.

Although local congestion within the room is not related to the construction of the CRA, it should be addressed since CRAs are commonly installed beside other display equipment. Tests were carried out with and without objects (sealed cupboards) of similar dimensions either side of the tested CRA in order to simulate and evaluate the impact of local congestion. Results are shown in Figure 36 and Figure 37 for C_{mp} and C_{ms}. In Figure 36 when the CU is floor-mounted (jet 'g' at 0.3 m above the floor) there is a slight difference between the congested and empty cases. Although values of C_{mp} and C_{ms} (both for 30 g and 150 g) are marginally lower for the congested case, it is generally within the uncertainty range. However, when the CU is positioned at 1.8 m, the congestion leads to a substantially lower concentration (almost half) and the difference between C_{mp} and C_{ms} is smaller. This is believed to be due to the congestion causing an obstruction and both increasing turbulence and spreading the boundary of the plume thus augmenting mixing before the mixture reaches the floor. This is supported by there being a minimal difference between Cmp and Cms (for the 1.8 m case) which implies better mixing within the descending plume and with the surroundings. This observation does not apply for releases close to the floor.

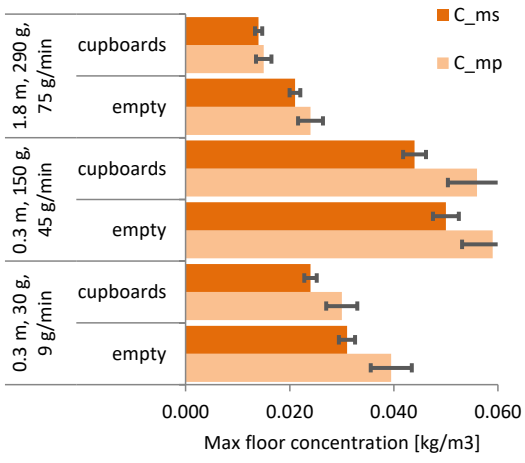

Figure 36: Effect of congestion (14 m2 room).

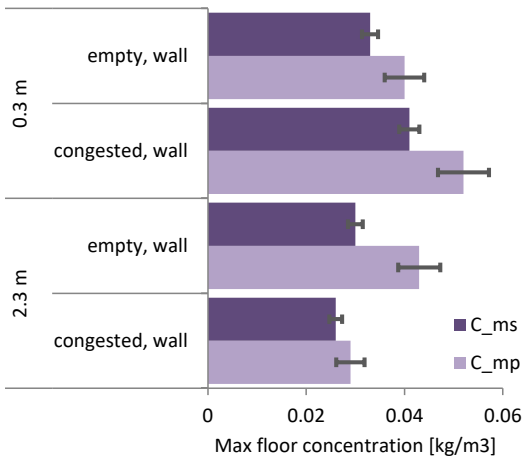

Figure 37: Effect of congestion (40 m2 room).

Further work was carried out using CFD, examining the effect on increasingly more congestion on maximum flammable concentration within the space.

3.4.3 Room openings

Airflow may originate from a number of different sources, as indicated in Table 12. For the frequently considered types of airflow such as natural and extract ventilation, there are extensive studies throughout the literature and for fan circulation, specific studies are cited. However, a brief mention on the effectiveness of the other forms of airflow is provided here.

Table 12: Different forms of airflow within a room

Type	Description	Reference
Natural/buoyancy ventilation	From thermal/wind pressure and openings	Ivings and Kelsey (2014); Figure 40
Extract ventilation	Mechanical/artificial airflow through fans	Ivings and Kelsey (2014)
Fan circulation	From IDU fan, ambient cooling fan, etc.	Colbourne and Suen (2008; 2018)
Physical movement	People walking, moving things	Figure 38
Thermal convection	Radiators, people, electrical equipment	Figure 39

Figure 40 provides some example results for a 440 g release at 100 g/min from an IDU at 1.0 m under different natural ventilation conditions. “NV opening” is a single opening of 0.2 m ×0.8 m at floor level, “T&B NV opening” is the same but with an additional opening of the same size at ceiling height and “NV+extr opening” is the first opening but also an opening at the opposite end of the room that is ducted to the outside. Values shown in the legend refer to the percentage of refrigerant mass in the room relative to that present in the baseline closed room (as determined by integration of the vertical concentration profile). By the end of the release, both “NV opening” and “T&B NV opening” led to 10% to 15% lower floor concentration and 25% to 30% less refrigerant present in the room. Having the additional opening at ceiling level does not provide a significant benefit, despite the intention that it should accentuate the static pressure head and thus allow more mixture to flow out. Conversely the “NV+extr opening” case provides a major benefit, where floor concentration is reduced the two-thirds and mass present is only about one quarter of the closed room case. Velocity measurements across the outside air ventilation opening indicated a volumetric flow rate of about 6 air changes per hour.

Figure 38 shows the effect of gentle strolling through a stratified layer of R290 moments after cessation of the release. Within a few seconds of strolling the mixture had been diluted to below LFL (red line) and after a couple of minutes the concentration is below 25% of LFL, indicating the effectiveness of any physical movement on dispersing releases.

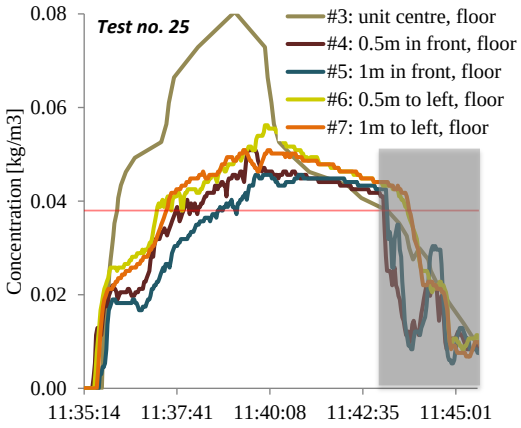

Figure 38: Effect of "strolling" through a stratified layer (during greyed duration).

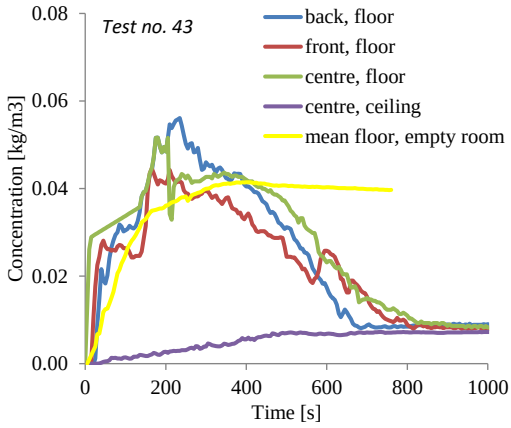

Figure 39: Effect of four thermal manikins and mock PCs on mixing of a release.

From an earlier study (Colbourne and Suen, 2003), a test was carried out where 1.2 kg of CO_2 (to mimic R290) was released into a 40 m^2 insulated room, which contained four thermal manikins and four mock PCs, each emitting 100 W of heat. In Figure 39, whilst the peak concentration was not significantly affected, rapid homogenisation of the release can be seen to occur within a few minutes, which does not happen over the same timescales with an empty room (as compared with the mean floor concentration for a similar case of 1 kg CO_2 superimposed on Figure 39). This illustrates the effectiveness of common objects helping to disperse releases.

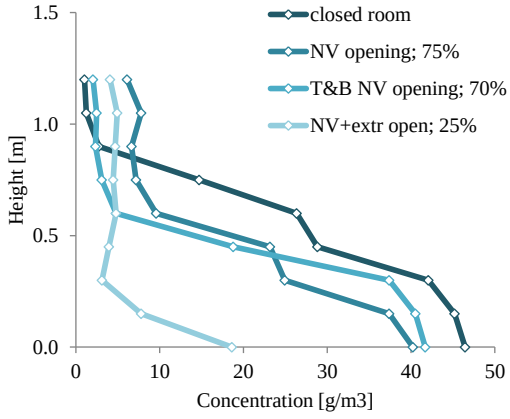

Figure 40: Effect of natural ventilation.

3.5 Concluding remarks

A large number of tests have been carried out examining the effect of RACHP equipment enclosures and housings on the surrounding floor concentrations. Specifically, enclosures and housings of a generic nature were employed so that the results could be extrapolated as far as possible to any type of RACHP equipment

within the scope of this project. Maximum charge – based on avoiding LFL surrounding the RACHP at floor level – is highly sensitive to leak time or leak mass flow rate, so appropriate consideration must be given to suitable values dependent upon refrigerant (properties), operating conditions, likely leak mechanisms and hole sizes (which should be as much as possible based on empirical field data). Adopting a single "blanket" leak time (such as four minutes) is not justified in any respect. Further, for "large" leaks, adoption of a decaying leak profile is fitting whereas a constant mass flow is apt for "small" and "medium" leaks. According to measurements so far, assumption of a vapour-only release is likely to lead to higher floor concentrations and thus smaller charge limits.

4 METHODS TO DETERMINE CHARGE LIMITS

4.1 Introduction

Considering that it is hoped that the developed requirements will eventually become established into RACHP safety standards and design guidelines, the nature of the users must also be taken into account. Such users of these requirements within the RACHP industry may include:

- Large product manufacturers
- Small product manufacturers
- Installation engineers
- Engineering contractors
- Engineering consultants
- Maintenance technicians

Amongst these stakeholders there exists a wide range of technical competence and expertise, ranging from those trained at vocational centres to those with post-graduate education at university level. As such, proposed requirements should to some extent be accessible to all such skill levels.

Conversely it may be argued that if proposed requirements demanded a higher level of understanding of certain matters then it could dissuade less competent stakeholder groups from using HCs unsafely. For instance, requirements that permit greater quantities of HC per m3 of space volume be used – or where a higher percentage of LFL concentration could arise – then requirements may be more challenging. On the other hand, such an approach could lead to a higher chance of error and thus increase flammability risk. If the requirements that permit larger quantities are coupled with a need for more substantial internal resources (such as laboratory facilities and expertise) then it is likely that only larger enterprises (with greater liability concerns) would be more prone to adopt them (and thus be more careful with their application).

The preferred approach then is to offer three branches of requirements: "simple", "involved" and "advanced", where the "advanced" impose a weightier burden on the enterprise. These branches may respectively correspond to: "calculation based", "experiment based" and "combination" (e.g., calculation based on findings of tests or vice versa). Figure 41 provides an overview.

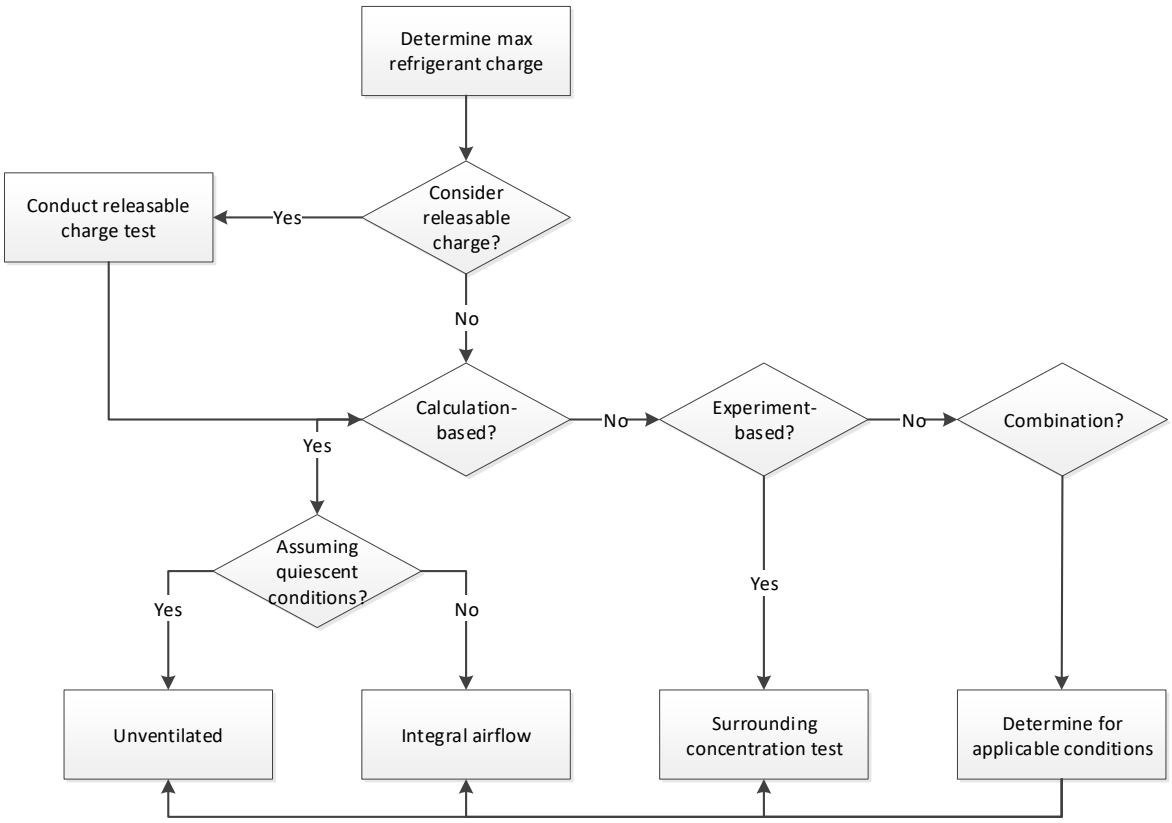

Figure 41: Flow chart for charge limit determination methods.

Due to the complexities and variations associated with construction and characteristics of RACHP systems and the need for calculation methods to be relatively simple, charges limits found by calculation tend to yield smaller numbers. This is primarily because many of the aspects that may help to reduce room floor concentration have to be accounted for in the most pessimistic manner in the calculation.

Although charge limits may be calculated, this is not necessarily done in isolation since the characteristics of the mitigation measure(s) may also need to be determined in order to validate the charge limit (e.g., minimum airflow rate).

In addition to these charge limit methods, a further element – referred to as “releasable charge” – is also described, which evaluates how much refrigerant may be actually released from a leaking system. Such a quantity can be used to determine the appropriate limits.

The following two sections describe the calculations and the tests that have been devised for identifying the maximum refrigerant charge limits. These are broadly divided into two categories:

- RACHP systems using passive methods to disperse a release;
- RACHP systems using active methods to disperse a release.

The calculation and test methods will be described. Table 13 provides a summary of those charge determination methods (and the corresponding sub-sections) along with any exceptions to the applicability of the methods.

Table 13: Summary of charge determination and supporting methods described in this section

Method	Section	RACHP exceptions
Calculation of charge limits for passive cases	4.2	Where leaked refrigerant cannot disperse in the occupied space
Calculation of charge limits for equipment with active measures	4.3	Where mechanical means cannot be used to mix a leak in occupied space
Test method for charge limits on equipment with passive or active measure: Equipment surrounding concentration test	4.4.1	None
Test method for charge limits on equipment with passive or active measure: Enclosure exiting concentration test	4.4.2	Where leaked refrigerant cannot transfer into the occupied space
Test method for determining releasable charge	4.4.3	None
Test method for confirming operation of detection systems	4.4.4	Where leak detection is not used

4.2 Calculation of charge limits for passive cases[8]

There are several approaches for passive mitigation measures. But ultimately these rely on static design measures and installation measures to ensure that a flammable concentration does not arise in the event of a leak. From

Table 9, the following mitigation measures apply:

- Limiting charge amount
- Large enough space for dilution
- Encourage lower leak probability
- Passive dilution of mixture in room
- Passive removal of mixture (including “draining”, etc.)

[8] This section describes experimental work that was conducted in the refrigeration laboratory at UCL, London, partly under the EU Life-Front project and partly under the GIZ standards project.

Of these, “encourage lower leak probability” is something that has to be integrated into circuit design and can then be used to assume a certain maximum refrigerant leak rate and as such is part of the accompanying report Recommended mass flow rates and leak hole sizes by system and application characteristics. “Passive removal of mixture” can include natural ventilation/buoyancy-induced flow between room spaces or buoyancy-induced draining from enclosures. With the former approach, there is concern over the dependability of the measures that would enable dispersion of a release (i.e., prevention of modifications to openings in room walls due to intuitive fears over heat loss/gain, etc.) and as such it will not be considered here any further. Conversely, relying on refrigerant density or pressure generated by a leak to enable draining of the mixture from an enclosure is substantially more reliable since there is no reason for operators or room occupants to inadvertently interfere with the equipment construction.

In terms of factors that affect passive dilution within a space, one of the most significant parameters is the height at which the release occurs and that path it follows to then travel into the space (when applicable). Typically, under quiescent conditions leaked refrigerant will collect within the volume below the release height (although if the release continues, the mixture will ultimately rise beyond the release height). It is thus proposed to employ a simplified expression to estimate the maximum refrigerant mass (M_{max}) based on this phenomenon (equation 4):

$$M_{max} = F_{LFL} \times LFL \times h^* \times A \qquad (4)$$

Conversely the minimum room area is desired is from equation (5).

$$A_{min} = \frac{M_c}{F_{LFL} \times LFL \times h^*} \qquad (5)$$

Where:

LFL = lower flammability limit [kg/m^3]

A = room area [m^2]

A_{min} = minimum room area [m^2]

M_c = refrigerant charge [kg]

M_{max} = maximum refrigerant charge [kg]

h^* = representative height [m] (see Figure 43)

where F_{LFL} is a factor applied to the LFL to ensure a flammable concentration is avoided, h^* is some representative the height related to the unit enclosure/housing openings above the floor (m) and A is the floor area, thus giving the free volume somewhere below the openings of the unit. In the case of an enclosure that has no openings whatsoever, then no release into the space need be considered. However, almost all enclosures do possess some opening, however small. Where an enclosure exhibits only very small openings, then that at the lowest position should be one which dictates h^*.

Figure 42 provides a graphical explanation of F_{LFL}: a large F_{LFL} is represented by a lot of mixing below the release height thus accommodating more refrigerant within the free volume below the release position,

whilst a small value is representative of a strongly stratified layer close to the floor and very little mixing above it.

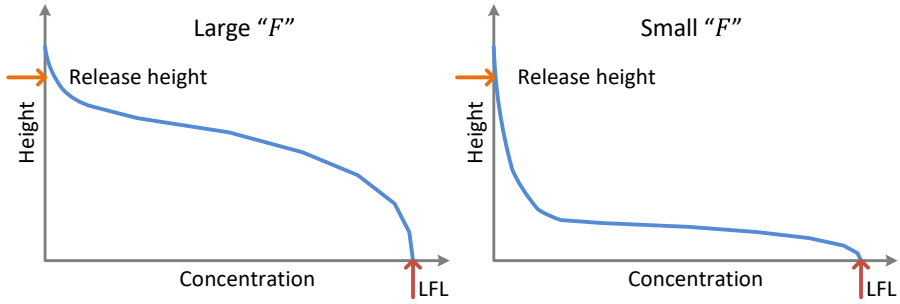

Figure 42: Graphical explanation of F_{LFL}.

As discussed later, for some types of enclosures, h^* may be taken as the height of the base of the unit (h_b), whereas in other cases h^* is somewhere between the base and the top of the unit housing. Since LFL, h^* and A are relatively easily identified, an appropriate value of F_{LFL} should be identified.

A series of experimental results and an analysis of this topic is provided in Appendix A. Based on those observations, a general rule was established to approximate the suitable value of h^*.[9]

With reference to Figure 43, if the height of the release is above the height of the top lip of the (upper) opening, i.e., $h_{rel} > h_{up,op}$, then

$$h^* = h_{base} + \frac{1}{2}\left(h_{up,op} - h_{bot,op}\right) \tag{6}$$

When the height of the release is below that of the top lip of the (upper) opening and above the lower lip of the bottom opening, i.e., $h_{bot,op} < h_{rel} < h_{up,op}$, then:

$$h^* = h_{base} + \frac{1}{2}\left(h_{rel} - h_{bot,op}\right) \tag{7}$$

But if the release is below the lower lip of the bottom opening, i.e., $h_{rel} < h_{bot,op}$, then:

$$h^* = h_{base} + h_{bot,op} \tag{8}$$

[9] Note that the approach described is universally applicable to any RACHP equipment, provided that the equipment can be characterised in a manner that is inferred here. For instance, it may include different types of air conditioners, heat pumps, refrigerated cabinets, etc.

Where h_{rel} = height of release within enclosure [m], h_b = height of unit base above floor [m], $h_{up,op}$ = height of upper opening (top lip) above the unit base [m] and $h_{bot,op}$ = height of bottom opening (bottom lip) above the unit base [m]. Figure 43 provides some example heights for an enclosure for clarification.

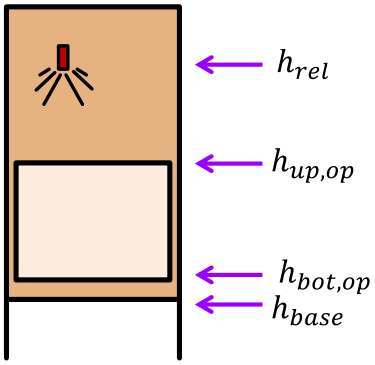

Figure 43: Example of heights.

If insufficient characteristics of the enclosure are known then default is $h^* = h_{base}$.

Note that in this last case, if the lower lip is substantially higher than the release – that is, the release is within a "bucket" – then the end result would be to underestimate m_{max}. This could be accounted for, but the method would incur additional complication that is not necessarily desired at present considering the constructional characteristics of most RACHP equipment housings.

Using these relations, F_{LFL} was determined for the entire set of tests carried out (that were relevant to this analysis) and the data in Appendix A presents the results plotted against the exiting concentration, C_{exit}.

The curves for the IDUs and VEs were correlated as equation (9) and (10), respectively.

$$F_{LFL} = 4 \times C_{exit}^{-2/5} \tag{9}$$

$$F_{LFL} = 2 \times C_{exit}^{-1/3} \tag{10}$$

Further explanation on the reasons for the two different curves is provided in Appendix A.

In the event that C_{exit} cannot be determined, then it may be set to the density of the refrigerant vapour at atmospheric pressure and room temperature.

F_{LFL} is calculated from the exiting concentration of the enclosure and depending upon whether the release plume is internally impeded before flowing from the enclosure.

Whilst the experiments and simulations to develop this correlation used R290, they have been extended to apply to any refrigerant with a different LFL. In the case of free downwards flow of the release from inside of housing/enclosure to the room floor, without directing the floor level flow in any single direction:

$$F_{LFL} = 14.8 \times \left(\frac{C_{exit}}{LFL}\right)^{-2/5} \quad (11)$$

In the case of inhibited downwards flow of release from inside unit housing/enclosure and confinement means a single direction of the exiting flow:

$$F_{LFL} = 5.9 \times \left(\frac{C_{exit}}{LFL}\right)^{-1/3} \quad (12)$$

where C_{exit} = highest concentration exiting enclosure/housing into room [g/m^3], which (again) can be: (i) calculated, (ii) determined by test, or (iii) set as pure refrigerant.

The method described for determining charge size limits is based on a set of considerations that help ensure that such procedures can be easily followed and adhered to by non-specialist engineers. Since the range of types of systems and applications and the extent of system populations that are expected to apply flammable refrigerants are vast, it is unlikely that the majority of design and application engineers will employ a sufficiently high level of expertise to be able to comprehend and interpret very detailed sets of requirements. The proposed methods herein are considered to be a "compromise" arrangement such that errors due to misunderstanding should be limited, yet sufficiently account for important characteristics of RACHP systems and installations.

A more thorough treatment of the results presented here and elsewhere may yield dependencies upon a large number of associated parameters, such that charge size limits may be better tuned to a given set of circumstances.

There are a number of other factors that influence floor concentration in the event of a refrigerant leak, including ventilation openings, mechanical ventilation, thermal sources within the room and movement from room occupants. Whilst these are not integral to the charge size determination method, additional information relating to how these factors affect concentrations is provided in Colbourne and Suen (2018).

4.3 Calculation of charge limits for equipment with active measures

There are several active mitigation measures that may be applied and integrated into RACHP equipment to avoid development of large flammable mixtures. These include:

- Limiting releasable amount
- Limit release mass flow
- Active dilution of mixture in room
- General removal of mixture
- Active removal of mixture
- Eliminating area SOIs
- Warning personnel

Of these, "limiting releasable amount" and "limiting release mass flow" are addressed elsewhere in this report. "Eliminating area SOIs" is too unreliable to consider, except perhaps in a machinery room type situation (which is out of the scope of this report). Similarly, "warning personnel" – such as through use of an alarm – has too many pitfalls.

Where it concerns "removal of mixture", there are two categories to be considered:

- mixture is removed from the wider occupied space (such as by means of extract ventilation), and

- mixture is removed from the RACHP housing directly.

Removal of the mixture from the wider space is potentially of interest, although it is more suited to ducted type systems or larger systems in situations where additional extract fans may be employed and thus will not be addressed at present. Removal of the mixture from the housing directly may be achieved using one or more techniques. However, due to the complexities associated with such techniques, it is not possible to make a reliable calculation method; instead testing needs to be used to demonstrate its effectiveness.

Finally, "active dilution of mixture in room" is a mitigation measure of primary interest for small RACHP equipment, especially since it can utilize components that are already integrated into the equipment, i.e., circulating fans.

4.3.1 Options for removal of mixture from enclosure

Where the equipment is installed in a small room and it is necessary to disperse or exhaust leaked refrigerant to the outside, several options have been identified.

A) Vertical dispersive stack to mix release throughout room

With this option, the equipment enclosure must be well sealed. A leak of refrigerant will generate an overpressure within the enclosure and this will force the refrigerant up a vertical vent stack. A possible design and results from a simulation are shown in Figure 44.

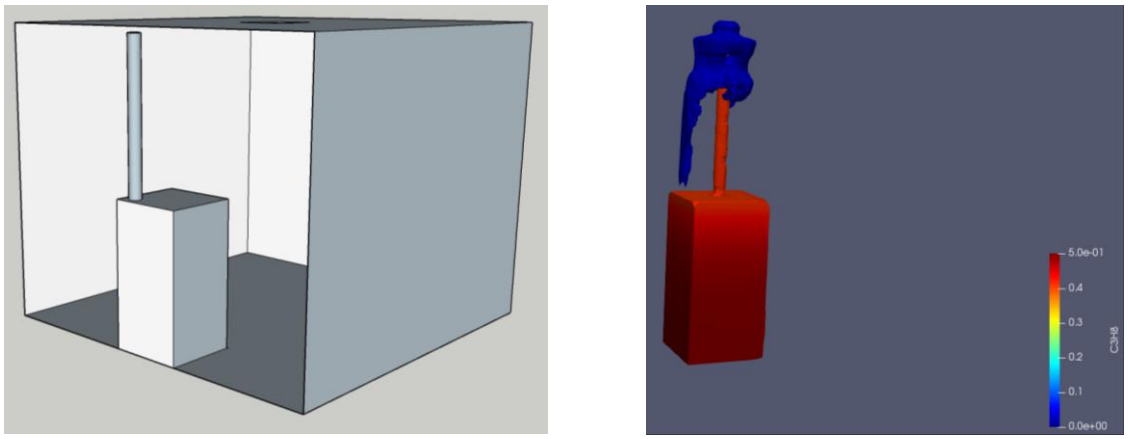

Figure 44: Vent stack design concept (left) and example simulation results (right).

B) Wind-driven extract fan to remove mixture

It is possible to fit a wind driven extract fan (e.g., Figure 45) to the top of a stack (when extending to the outside), whereby the wind generates sufficient rotational speed on the fan such that the negative pressure below it is enough to draw the refrigerant upwards in into the open air. Conversely the fan could be used to generate a positive pressure so that the mixture is forced out of a second column.

Figure 45: Example of a wind-driven fan.

C) Dual pressure pipes to drive out mixture

Another option is to fit two stack pipes to the enclosure, one near the top and one near the base (Figure 46). This arrangement may function by employing a special fitting to the top of one of the stacks. Depending upon the direction and speed of the wind, the mixture would be forced up or down pone of the stacks and fresh air through the other (similar to the use of the fan, above).

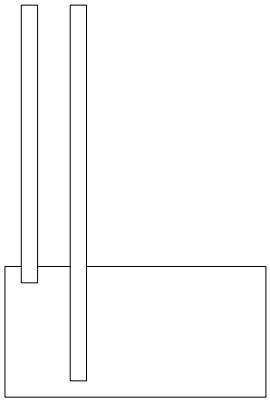

Figure 46: Enclosure with two vertical stacks.

D) Horizontal gravity drains

Provided that the enclosure is not below ground level, the dense refrigerant can simply be allowed to drain out of the enclosure through its own negative buoyancy (Figure 47). The second vertical stack is used to provide make-up air (thus encouraging the outflow of the refrigerant).

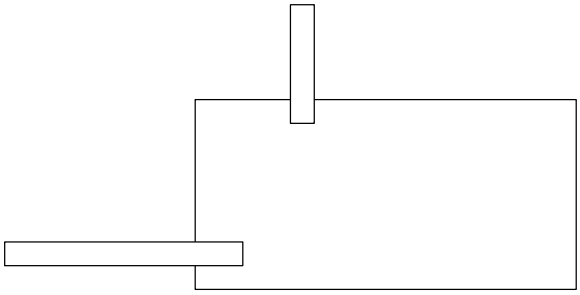

Figure 47: Enclosure with a vertical stack and a horizontal drain.

4.3.2 Calculation of charge limits when using circulation airflow

Many RACHP systems normally have a set airflow rate which is defined by the manufacturer to provide a given capacity, air throw, etc. and for certain types of equipment (e.g., air conditioners) users usually have control to some extent by means of several incremental fan speed settings, although not usually for other types of systems (display cabinets, cold room evaporators, etc.). It is necessary to identify whether the minimum airflow level is adequate to dilute a release of refrigerant in case of a leak and thus whether the manufacturer would need to assign a higher minimum airflow rate to achieve dilution. Too low airflow will result in formation of a flammable mixture at the room floor (under a given leak condition), whereas a requirement for excessively high airflow may result in unwarranted equipment costs (large fan/motor and housing) and energy costs.

As with the passive measures, the maximum refrigerant charge amount for may be determined according to a free volume within which mixing of the release may occur. However, for the case under discussion this free volume could be the entire room volume as opposed to that beneath the RACHP unit. Thus, the maximum refrigerant charge for a given space (M_{max}) may be determined from:

$$M_{max} = F \times LFL \times A_{rm} \times h_{rm} \tag{13}$$

Or alternatively, the minimum room area for a given system charge (M_c):

$$A_{min} = \frac{M_c}{F \times LFL \times h_{rm}} \tag{14}$$

where M_{max} is the maximum charge (kg), h_{rm} is the room height (m) usually assumed to be 2.2 m or 2.5 m or any other applicable height and F is a non-dimensional limit intended to avoid the entire room approaching LFL; with typical values ranging from 0.1 to 0.5 according to how much refrigerant a given RACHP system requires.

As detailed in Appendix B, a series of equations were developed to describe the extent of entrainment in an air jet and thus mixing of a release within a closed room. Formulae for theoretical minimum volumetric airflow rate from RACHP units were thus developed. Then an adjustment factor was applied to achieve consistency with a variety of experimental results, covering all sorts of different RACHP equipment, room sizes, charge amounts and so on. The two formulae proposed are for cases assuming a high leak mass flow rate (equation 15) and those with a lower leak rate (equation 16), classed as “enhanced tightness” systems.

$$\dot{V}_{o,min} = \frac{6.8\sqrt{A_o}\dot{m}_{leak}}{m_c^{1/4} LFL^{3/4}} \left(\frac{F^{1/4}}{1-F}\right) \quad (15)$$

$$\dot{V}_{o,min} = \frac{5\sqrt{A_o}\dot{m}_{leak}^{3/4}}{h_o^{1/8}[LFL(1-F)]^{5/8}} \quad (16)$$

$V_{o,min}$ is the minimum airflow volume flow rate needed to mix the release, in m3/h.

Using these formulae, some examples of minimum airflow rates according to the key variables are provided in Figure 48. It is seen that the minimum airflow is sensitive to selected parameters, where for example, high leak rates increase airflow about proportionally, doubling charge amount increases airflow by a factor of three and increasing the outlet area by four (i.e., quartering discharge velocity) doubles minimum airflow (assuming the other factors are kept constant). Also shown are typical values for high and low airflow setting on split type air conditioner indoor units, assuming a specific heat load of 200 W m^{-2} of room area.

Where active measures are applied, it is usually necessary to determine as and when they need to be initiated. Leaks may be as small as <0.001 g/min or higher. Depending upon the detection method used and the positioning of the sensor(s), some minimum mass flow may be necessary to identify whether or not a leak has occurred. As such, some minimum safe leak rate (MSLR) must be established in order to provide a boundary down to where the detection system must be able to activate yet also below the mass flow that would result in the formation of a potentially flammable mixture on the room floor. In other words, the MSLR is a tolerable leak rate under which the entire charge could be released into the space without forming a substantial flammable volume.

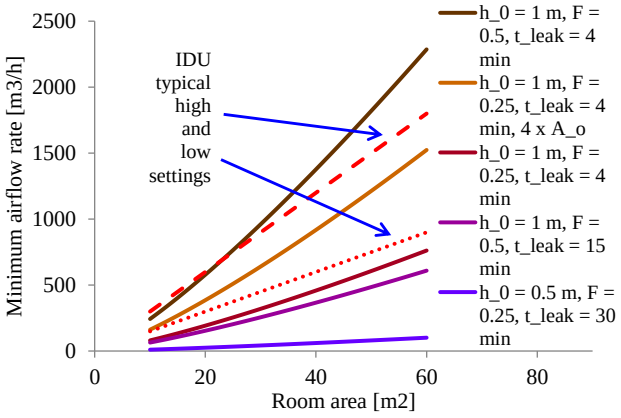

Figure 48: Example of airflow rate requirements with mean variables.

Thus, the MSLR may be determined and the analysis should consider several aspects:

- Decay in leakage mass flow in real systems
- Effect of internal air movement in real situations, such as residual air movement, from convention currents and human movement

- Observations from measurements and computations

Since the work carried out previously indicates that the majority of the released denser-than-air refrigerant accumulates below the release height (h_o), it may be argued that the MSLR ($\dot{m}_{MSLR}$ in g/min) be based on:

$$\dot{m}_{MSLR} = 60 \times \omega \times h_o A_{min,tot} \times LFL \tag{17}$$

where $A_{min,tot}$ is the total minimum room area (m^2) according to the total system charge, as in equation (5) (i.e., neglecting effect of SOSVs, etc.), LFL is in $\mathrm{kg/m}^3$ and ω is a factor used to account for the expected gradual mixing within the room. This may include diffusion, thermal convection, human-induced convective forces, etc. and ω should be determined following consideration of these factors contributing to mixing.

4.4 Test method for charge limits on equipment with passive or active measures

Studies have found that in the event of a release from RACHP equipment, the maximum concentration at the floor can be substantially different depending upon the equipment and room arrangement and inclusion of protective measures. Different designs of appliances will affect the resulting concentrations and due to the complexity and variation in the design of appliances, it is not always easy to generalise. Therefore, a test method may be used to determine the mass of refrigerant that would be insufficient to result in a flammable concentration at floor level within the room of A_{min}. Since the maximum concentration and thus allowable charge can be so sensitive to geometry of enclosure, there is a need to account for this. To date, there is no easy way to anticipate results, so in such cases there should be an option for a performance test.

Furthermore, such an approach may help to encourage equipment designers to refine the construction so that as low a concentration as possible is achieved.

4.4.1 Equipment surrounding concentration test

The following describes the proposed set-up and execution of such a test.

Within this description certain parameters may be subject to refinement, for example, exact positioning of the sensors in relation to the RACHP equipment, lateral positioning of the RACHP equipment and the acceptance criteria.

ANNEX 6 background to surrounding concentration test**Fehler! Verweisquelle konnte nicht gefunden werden.**provides some background work that contributed to the development of the test.

i) General

A leak is simulated from the most critical part of the system which is found to measure the maximum refrigerant concentration at the room floor surrounding the RACHP equipment.

ii) Room arrangement

The appliance shall be positioned within a test room. The room height shall be no less than 2.2 m.

Two example arrangements are provided in Figure 49.

The test room shall be of an appropriate area for the appliance where the length of the walls shall be the same and the height of each wall shall not differ.

The appliance shall be installed at a height and location as prescribed by the instructions and centred along one wall or within the centre of the ceiling if the appliance is intended to be ceiling mounted.

The test room shall be effectively tight. This is demonstrated by a mass of refrigerant equating to 25 – 50% of LFL being released into the room and mixing using a circulating fan. The average concentration at six sampling points throughout the room shall be within ±5% of the arithmetic mean and the mean value shall not decline by more than 5% within a five-minute duration.

The residual mean airspeed within the room shall not exceed 0.05 m/s when all of the appliance fans are switched off. This is confirmed by at least six airspeed measurements made continuously for no less than five minutes at different positions in the room using multi-directional anemometers.

NOTE Gas analysers and anemometers may be positioned at 1 m from the centre of each wall/floor/ceiling.

iii) Concentration measurements

Sampling points to measure gas concentration are be positioned around the appliance, no more than 30 mm above floor level. There shall be one sampling point at a distance of no more than 0.5 m from each exposed side of the appliance and one sampling point no more than 0.7 m from the exposed corners (or equivalent) of the appliance. Figure 49 shows a possible arrangement of the sampling points.

The gas analysers shall be calibrated for the refrigerant used. The response of the measuring system shall have a T90[10] of <20 s. Measurements of gas concentration shall be recorded at time increments of no more than 5 seconds apart.

The test shall be repeated no fewer than three times and each value of maximum mean concentration (C_{mm}) from each of the tests shall be within ±10% of the average of the C_{mm} from all tests.

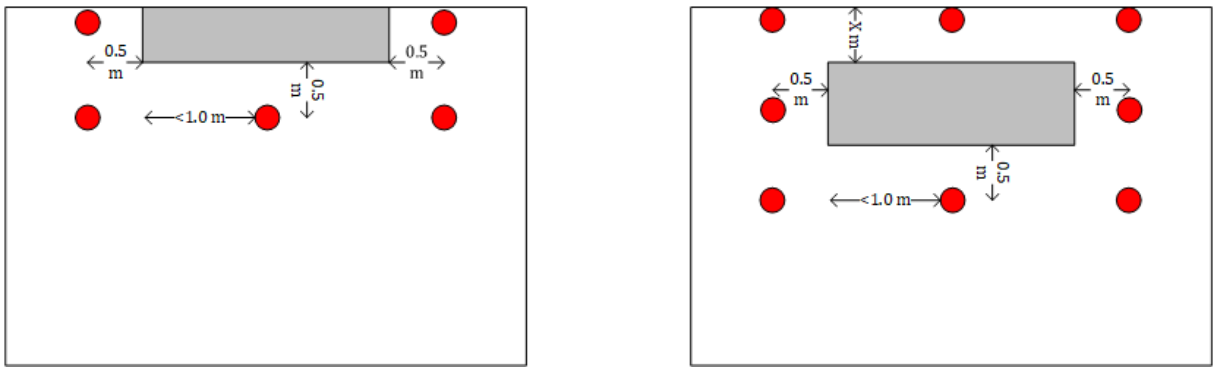

Figure 49: Possible test room set up and positioning of the sampling points; plan view showing the RACHP equipment (grey block) and floor level sensors (red circles); Note: such an arrangement can be applied to any type pf RACHP equipment.

[10] i.e., the concentration shall reach 90% of LFL within the stated time.

vi) Simulated leak

A simulated leak shall be made from the critical part and in a direction of the refrigerant-containing parts normally located within the occupied space. The critical part and direction is that which leads to the highest concentration on the room floor.

The refrigerant is released through an orifice in vapor phase at a pressure of at least than 2 bar (gauge).

The mass flow rate of the release shall be according to the defined values.

The mass released is the maximum refrigerant charge or the releasable charge applicable for the system (as determined) or as prescribed for the system.

v) Acceptance criteria

The criteria for acceptance are:

- The maximum arithmetic mean concentration (C_{mm}) across all sampling points on the floor at any time during the test shall not exceed 50% of the LFL, and
- None of the sampling points shall have a concentration that exceeds 100% of LFL.

NOTE An example result is provided in Figure 50.

The maximum charge size for a given room size or the minimum room size for a given charge size may be determined from interpolation of three or more data-points using a range of charge sizes or room sizes.

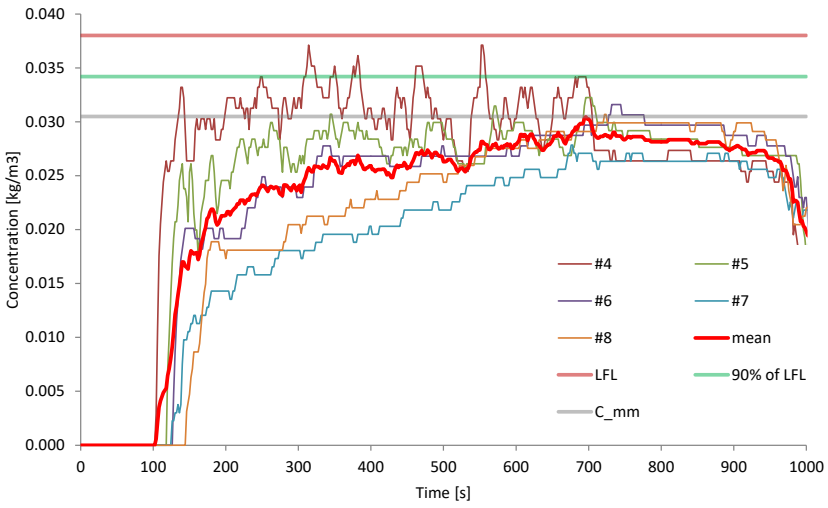

Figure 50: Example of identification of maximum mean concentration (C_{mm}) using R290.

4.4.2 Enclosure exiting concentration test

Where the exiting concentration of an RACHP enclosure is needed to calculate the maximum charge, such as for “calculation of charge limits for passive cases” (section XXX), a standardised test method should be

adopted. Whilst this is likely a more costly approach for determining exiting concentration, it is surely the more accurate option, considering the complexities associated with the insides of RACHP equipment.

i) General

A leak is simulated from the most critical part of the system which is found to measure the maximum refrigerant concentration at the exit of the enclosure.

ii) Arrangement

The enclosure/housing shall be located in a room of sufficient size so that the results are not adversely affected.

The enclosure shall be equipped with gas sensors at the base of any openings from the inside to the outside of the enclosure (see Figure 51). For enclosures of type A to D, at least six equally spaced sensors shall be used per linear-metre of opening lip and each sensor shall be positioned just on the inside of the external projection, so that any gas exiting the enclosure is unable to bypass it.

For enclosures of type E (such as where there is an opening at or below the enclosure base), sensors should be positioned below the enclosure within a conduit so that the exiting mixture will remain relatively uninterrupted. At least eight equally spaced sensors shall be used per linear-metre of opening and shall be positioned between 0.5 m and 1.0 m below the opening within the centreline of the flow path within the conduit.

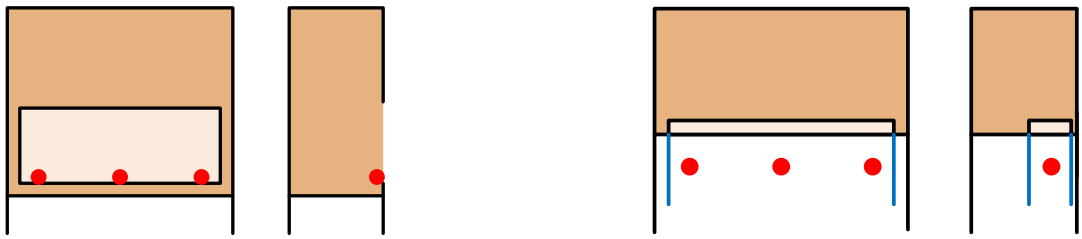

Figure 51: Arrangement of gas sensors for an enclosure types A to D with side openings (left) and enclosure type E with base openings (right).

The room within which the test is conducted shall be relatively well sealed and without air movement at a velocity exceeding 0.05 m/s. It shall be of an area approximately equal to the anticipated minimum room area for the installation of the unit.

If the unit could be installed at different heights, then tests should be done at all relevant heights according to instructions.

iii) Concentration measurements

The gas sensors should have as rapid a response time as possible, being faster than T90 = 20 s. The upper range of the sensors should be adequate to capture the highest concentrations anticipated; ideally, they should reach than 100% vol. of the refrigerant used.

Logging equipment should have a sampling interval of 5 s or less.

vi) Simulated leak

Refrigerant is fed into the enclosure through an orifice or capillary that is of a size sufficient to ensure choked flow. The orifice shall be positioned at the critical leak point and in the least favourable direction.

Note: the least favourable direction is likely to be (but not always) pointed downwards and impinging against an immediate surface.

Note: trial and error is likely to be needed in order to determine the most critical and least favourable position and direction.

The vapour release is continued at a fixed mass flow rate until steady concentrations are measured for at least two minutes at all of the sensors, or longer if this is necessary to achieve a steady exiting concentration. The mass flow rate shall be according to that the defined values.

No fewer than three identical tests shall be carried out to ensure reliable output.

v) Required output

Maximum exiting concentration shall be the maximum one-minute averaged value under steady conditions, recorded across all the sensors throughout the duration of the test.

4.4.3 Test method for determining releasable charge

In principle, if a system can be designed and controlled such that an amount less than the charged amount is released in the event of a leak, then that released amount could be used at the maximum charge.

Previous work has found that between 5% and 15% of the charge may remain in the system after a leak.

If shut-off valves are used to divide the internal volume of a self-contained system into two, the releasable charge may be between 10% and 50% of the charge amount; this can be combined with use of airflow to mix the full charge in the event of a leak when the valves are not closed.

In the case of a remote (split) system, use of valves could retain some substantial proportion of the charge outside and prevent leakage into the occupied space. If a manufacturer invests additional resources to improve level of safety there should be a benefit for doing so in terms of greater allowable charge.

The system charge should nevertheless be constrained to an amount not exceeding $0.95 \times LFL \times V_{room}$ so that in the event of a valve or other mechanism failure, the entire space will not become flammable.

The overall minimum room size for the appliance is taken as the maximum value of the individual minimum room sizes determined for each operating state.

i) General

Where the releasable charge is to be used then this quantity shall be demonstrated by one of the tests below.

NOTE If an alternative method to those described below can be shown to achieve at least the same accuracy and repeatability then it may be used as an alternative.

The test may need to be carried out for more than one operating state of the appliance (for example: off, on-cooling and on-heating).

The test shall be repeated out no fewer than three times and the test that results in the greatest released mass is used as the releasable charge.

ii) Test set-up

The appliance shall be installed within the test facility according to the instructions.

If the appliance can be installed with additional pipework, then test shall employ the maximum permissible pipe diameter and length of piping as specified by the instructions. The appliance is charged with the nominal refrigerant charge as specified in the product data.

NOTE Care should be taken to ensure that the system is fully evacuated prior to each test whilst being aware that refrigerant may be absorbed in the compressor oil.

The parts of the system within the indoor unit where a leak could occur and the refrigerant could then enter an occupied space shall be identified.

A leak orifice is positioned at the most critical location in the system that could result in refrigerant entering the occupied (indoor) space. The most critical location is the one that yields the highest releasable charge.

NOTE: The most critical location can for instance be where refrigerant pressure is highest and with greatest liquid fraction during the applicable functional state, or where a flammability risk mitigation measure takes the longest time to activate.

The orifice size shall be not less than 3.0 mm2. Where a flammability risk mitigation measure is employed a second test condition with an orifice size of 0.2 mm2 shall also be used.

NOTE Based on tests, the leak rate of 1000 g of R290 from the two-phase tube at evaporator inlet gives an average mass flow rate of about 80 g/min per mm2 (when in off-mode). An orifice of 3.1 mm2 will therefore provide about 250 g/min or a 1000 g release within 4 minutes. A 0.2 mm2 orifice will give about 15 g/min of R290 or a leak time of about 1 hour for 1000 g.

The pressure of the parts of the system that would be located within the occupied space is monitored with a sampling interval of no more than 5 s. The resolution of the pressure measurement must be no more than 0.01 bar. At least two points are monitored corresponding to that of the pipe entering and exiting the parts which have access to the occupied space.

The orifice is opened instantaneously to simulate a leak. The end of the test duration corresponds to the time at which the pressure of the refrigerant-containing parts which could leak to the occupied space are less than 0.05 bar above atmospheric pressure for no less than 3 minutes (Figure 52).

NOTE The residual mass flow of refrigerant from the leak orifice at this pressure would not contribute to an increase in floor concentration.

The mass of refrigerant released from the system within this duration shall be determined.

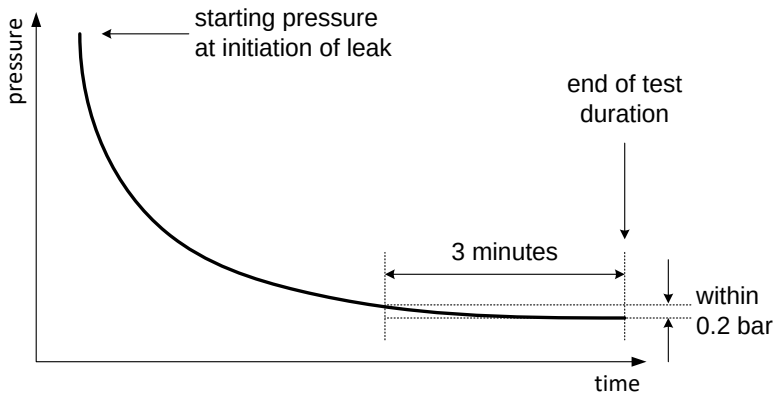

Figure 52: Diagram illustrating the tendency of sub-system pressure until approaching atmospheric pressure.

The system shall be tested under the relevant operational state and under the conditions which results in the greatest amount of charge being released.

The operational states to be considered are:

- For off-mode: the system is operated under the conditions for heating or cooling, whichever gives the most unfavourable result, for 30 minutes and then terminated and the leak is initiated after one minute
- For on-mode (cooling): the system is operated for 30 minutes where the indoor temperature shall be at 27°C ± 1 K and the outdoor parts shall be subject to a temperature of 35°C ± 1 K and then the leak is initiated.
- For on-mode (heating): the system is operated for 30 minutes with indoor temperature at 17°C ± 1 K and the outdoor parts shall be subject to a temperature of 25°C ± 1 K, and then the leak is initiated.
- For defrost mode: the system is switched into defrost mode and the leak is initiated at the latest time possible so that the leak ceases before the defrost period terminates.

NOTE If the rating conditions for the appliance are different due to their application in other climate regions, then those temperatures should be used for the tests.

NOTE Test methods A and B involve the potential formation of flammable mixtures. The tests should be carried out in a test facility and with equipment that complies with national regulations for flammable atmospheres and personnel should be sufficiently qualified to work with flammable substances.

iii) Test methods

Method A

The test shall be setup at described as above.

The mass of released refrigerant is measured by collecting it within an appropriate receptacle where the pressure within that receptacle does not exceed 0.01 bar above atmospheric pressure, using a balance with accuracy of +/- 1% of the refrigerant charge amount.

NOTE Archimedes principle must be accounted for when using this method. The following formula can be used: $M_{act} = M_{app} \times \frac{1}{1-\rho_a / \rho_r}$; Where M_{act} is the actual mass of refrigerant within the bag, M_{app} is the apparent mass, ρ_a and ρ_r are the density of the air and refrigerant vapour at the atmospheric pressure and ambient temperature of the test conditions.

Method B

The system is operated according to the functional state of the appliance. The leak is initiated from the most critical location. If the functional state involves the appliance airflow and the result can be affected by airflow rate, then the airflow rate shall be set to the least favourable setting.

NOTE For example, if there is a flammability risk mitigation measure that relies of gas detection then both the maximum and minimum airflow setting shall be considered.

If the appliance uses a protective measure, then it shall be allowed to function according to the factory settings.

The refrigerant is released directly into a gas-tight room.

When the release has ceased circulating fans are activated for the purpose of mixing the released refrigerant while the refrigerant concentration is measured at no fewer than six different points distributed evenly within the room at sampling intervals of no more than 5 s.

The mass of released refrigerant is calculated from the average concentration and the empty room volume, once the concentration of all the sampling points is within +/-1% of the average value for at least three minutes. Sampling of the concentration shall continue for at least the duration of the release and the average value does not decline by more than 3% from the beginning of the mixing as a means of demonstrating negligible loss of refrigerant from the room.

Method C

The system is operated according to the functional state of the appliance. The leak is initiated from the most critical location and vented safely to the outside. If the functional state involves the appliance airflow and the result can be affected by airflow rate, then the airflow rate shall be set to the least favourable setting.

The system is left for a period of [several] hours until all refrigerant that can leak has leaked, after which the leak orifice is sealed. Any valves or other devices are then energised or energised such that any trapped refrigerant will flow to the rest of the inside of the system. A refrigerant recovery machine is attached to the system and to an evacuated recovery cylinder. The recovery machine is switched on and so the remaining refrigerant is pumped into the cylinder. Once confident that all available refrigerant has been extracted from the system the cylinder is weighed to determine the mass of the remaining refrigerant; this is then deducted from the mass of charged refrigerant to determine the released mass.

4.4.4 Test method for confirming operation of leak detection system

If leak detection is integrated into any types of RACHP equipment as a means of initiating protective measures, then the effectiveness of the detection must be checked.

i) General

This test is applicable to appliances using flammable refrigerants with leak detection systems which initiate protective measures so as to prevent a flammable concentration occurring.

For the applicable low leak rate or the small leak orifice, the protective measures required to avoid a flammable mixture shall be completed within 90 s of the initiation of the simulated leak.

For the high leak rate or large leak orifice, the protective measures required to avoid a flammable mixture shall be completed within 30 s of the initiation of the simulated leak.

For appliances where the release height h0 as determined is less than 1 m, the protective measures required to avoid a flammable mixture shall be initiated within 10 s of the initiation of the simulated leak, such as, for circulation airflow the action is completed when the circulation airflow reaches Q_{min}.

ii) Test method for leak detection excluding detection systems based on system parameters

The appliance is modified by introducing a simulated leak through an orifice or capillary tube, as appropriate. The simulated leak shall be maintained until the equipment active protective measures function as intended.

A leak shall be simulated at the critical points of the refrigerant-containing parts of the appliance intended to be located indoors. The test shall be conducted at a "low" and a "high" leak rate as defined.

The composition of the refrigerant used for the test shall be taken as the nominal composition as specified in ISO 817. Where LFL is referenced in this annex, the LFL shall be taken at the nominal composition as specified in ISO 817.

NOTE Sound and thermal insulation may affect the result of ultrasonic detection.

The low leak rate shall be:

$$\dot{m}_r = 13 \times h_o \times LFL \tag{18}$$

Where

$\dot{m}_r$ = the leak rate in g/s;

h_0 = height of the installation (m);

13 = a constant;

LFL = lower flammability limit in kg/m^3.

The high leak rate shall be according to the value determined for the improved tightens or normal tightness system.

$$m_r = 4{,}17 \times m_c \tag{19}$$

Where

4.7 = a constant;

mc = is the charge size

A leakage of refrigerant in the refrigerating system is simulated by injecting vapour at the critical points for detection of the leak. A critical point is a joint in the refrigerant system tubing, *a bend* of more than 90 degrees, or other point judged to be a weak point in the refrigerant containing system due to the thickness of the metal, exposure to damage, sharpness of a bend or the manufacturing process.

The refrigerant shall be released such that the pressure at the inlet to release orifice is not less than 300 kPa (gauge) in order to achieve choked flow.

Care shall be taken that the installation of the orifice or capillary does not unduly influence the results of the test.

During this test, following appliance operating states shall be tested, when applicable:

- *Fan OFF and*
- *Fan ON,*

If the actions required by Annex GG in the event of detection of a leak are circulation airflow and/or mechanical ventilation, and the minimum airflow specified by the manufacturer is not less than the minimum airflow specified in Annex GG testing in the fan ON mode is not required.

Appliances that can be installed in different positions shall be tested in all positions allowed by the instructions. The supply and return openings shall not be covered and the recommended air-filters shall be installed per instructions.

The test is conducted in a room that is of sufficient size to conduct the test without influencing the results by accumulation of leaked refrigerant into the room during the test.

The minimum room area $\mathrm{A_t}$ is:

$$\mathrm{A_t} \geq \frac{2{,}4 \times \mathrm{m_r}}{\mathrm{LFL} \times \mathrm{h_t}} \tag{20}$$

where

A_t is the minimum room area for the test in m2;

h_t is the height from the floor to the bottom of the unit in the test set-up in m;

m_r is the refrigerant leak rate in g/s;

LFL is the lower flammability limit in kg/m3;

2,4 is the conversion factor based on limiting the test room concentration to 5% LFL at the end of a 120 s refrigerant release at a release rate of $\dot{m}_r$.

iii) Test method for leak detection using system parameters

The appliance is modified by introducing a leak orifice in the system. The leak shall continue until the actions required by Annex GG are completed.

The orifice shall be positioned at the least favourable location of the refrigerant-containing parts of the appliance intended to be located indoors. The test shall be conducted with each of the leak orifices defined in PP.3.2 and PP.3.3.

The system shall be charged with the refrigerant type and amount as stated in the instructions.

The composition of the refrigerant used for the test shall be taken as the nominal composition as specified in ISO 817. Where LFL is referenced in this annex, the LFL shall be taken at the nominal composition as specified in ISO 817.

The small leak orifice to within ±0,1 mm² shall be:

$$A_o = \frac{4{,}6 \times LFL}{1{,}7} \tag{21}$$

where

A_o = orifice area in mm² and shall be no less than 0,1 mm²;

4,6 = a constant;

1,7 = nominal mass flux [g/(s mm²)];

LFL = lower flammability limit [kg/m³].

The length of the orifice bore shall be no longer than 1 mm.

The large leak orifice to within ±0,1 mm² shall be:

$$A_o = \frac{4 \times m_c}{0{,}8} \tag{22}$$

where

A_o = orifice area in mm^2 and shall be no less than 0,1 mm^2;

4 = a constant;

0,8 = nominal mass flux in g/(s mm^2);

m_c = refrigerant charge in kg.

The length of the orifice bore shall be no longer than 1 mm.

The system shall be operated in the following operating states as appropriate:

- Compressor off with indoor temperature 27 °C and outdoor temperature 35 °C, with Indoor fan ON
- Compressor off with indoor temperature 27 °C and outdoor temperature 35 °C, with indoor fan OFF
- Cooling mode with
- the compressor running at maximum speed allowed by the controls at the specified temperature, and
- highest outdoor air temperature and highest airflow, or highest entering fluid temperature and highest fluid flow rate, and
- highest indoor air temperature and highest indoor fan airflow or highest entering fluid temperature and highest fluid flow rate.
-
- Heating mode with
- the compressor running at maximum speed allowed by the controls at the specified temperature, and
- highest outdoor air temperature and highest airflow, or highest entering fluid temperature and highest fluid flow rate, and
- highest indoor air temperature and highest indoor fan airflow or highest entering fluid temperature and highest fluid flow rate.

The test is for the condition where the leak orifice is positioned at the most critical location, being the one that yields the greatest time before the actions required by Annex GG are completed.

Care shall be taken that the installation of the orifice does not unduly influence the results of the test.

5 FINAL REMARKS

Existing RACHP safety standards prescribe limits on refrigerant charge that are in general rather restrictive and prevent application of R290 in a great proportion of systems and equipment that would normally be installed – partly or entirely – indoors. The offending standards include IEC and EN 60335-2-24, IEC and EN 60335-2-40, IEC and EN 60335-2-89, ISO 5149 and EN 378. These standards generally include allowable charge limits (i.e., broadly proportional to the size of the occupied space) and upper charge limits, beyond which the allowable limits cannot exceed. The origin, source and logic of these charge limits have been examined, with particular attention to the underlying assumptions (if any).

Further, a range of possible approaches for extending or introducing new approaches for determining charge limits has been discussed, including use of calculation methods, experimental methods and use of risk assessment. This discussion has been coupled with a discussion on how to identify how far charge limits should extend to be useful, as well as being weighed against what the legislative requirements and constraints are.

For the experimental determination methods, a procedure has been established, where a product is placed in a test space and a refrigerant leak is simulated. Concentrations around the product on the floor are monitored for the duration of the release and for a period thereafter. Provided that the concentration does not exceed some fraction of the refrigerant LFL, the test can be deemed to pass.

For the calculation methods, an improved approach has been devised based on the construction of the RACHP enclosure, where the leaked refrigerant then pours into the room. The method assumes a certain leak rate and particular enclosure characteristics (internal dimensions, height and position of openings, etc.) and that by the end of the release, floor concentration does not exceed a fraction of the LFL.

These new approaches to determining charge limits will enable a far greater and wider application of HC refrigerants, without resulting in a substantial increase in flammability risk.

REFERENCES

1. ADL, 1998. Risk assessments of flammable refrigerants. Report for Calor Gas Ltd. Arthur D. Little, Cambridge, UK
2. ATEX (equipment): DIRECTIVE 2014/34/EU OF THE EUROPEAN PARLIAMENT AND OF THE COUNCIL of 26 February 2014 on the harmonisation of the laws of the Member States relating to equipment and protective systems intended for use in potentially explosive atmospheres (recast)
3. ATEX (workplace): DIRECTIVE 1999/92/EC OF THE EUROPEAN PARLIAMENT AND OF THE COUNCIL of 16 December 1999 on minimum requirements for improving the safety and health protection of workers potentially at risk from explosive atmospheres (15th individual Directive within the meaning of Article 16(1) of Directive 89/391/EEC)
4. Beyler, C. L., 2002. Fire hazard calculations for large, open hydrocarbon fires. In SFPE Handbook of Fire Protection Engineering, NFPA, USA
5. Colbourne D., Hühren R., Vonsild A. 2012. Safety concept for hydrocarbon refrigerants in split air conditioner. Proc. 10th IIR-Gustav Lorentzen Conference on Natural Working Fluids, Delft, The Netherlands.
6. Colbourne D., Liu Z. X. (2012) R290 leakage mass flow rate from a refrigerating system. Proc. 10th IIR-Gustav Lorentzen Conference on Natural Working Fluids (GL2012). Delft, The Netherlands.
7. Colbourne D., Rajadhyaksha D., Sahu A. (2013) HC-290 as an alternative refrigerant for split air conditioning systems in high ambient temperatures. Proc. IIF-IIR. Compressors 2013: 8th International Conference on Compressors and Coolants, Častá – Papiernička.
8. Colbourne D., Rajadhyaksha D., Sahu A. 2013. HC-290 as an alternative refrigerant for split air conditioning systems in high ambient temperatures. Proc. IIF-IIR. Compressors 2013: 8th International Conference on Compressors and Coolants, Častá – Papiernička.
9. Colbourne D., Suen K. O. 2008. Risk analysis of flammable refrigerants. 1. Correlations for concentrations from leaks. Proc. 8th IIR-Gustav Lorentzen Conf. nat. Working Fluids, Copenhagen.
10. Colbourne D., Suen K. O. 2016. R290 concentrations arising from leaks in commercial refrigeration cabinets. Proc. 12th IIR Gustav Lorentzen Conference, Édimbourg, United Kingdom.
11. Colbourne D., Suen K. O. 2018. Minimum airflow rates to dilute R290 concentrations arising from leaks in room air conditioners. Proc. 13th IIR Gustav Lorentzen Conference, Valencia, Spain.
12. Colbourne, D., Espersen, L., 2013. Quantitative risk assessment of R290 in ice cream cabinets. Int. J. Refrig., Vol. 36, Issue 4, pp 1208–1219.
13. Colbourne, D., Kanakakumar, V., Oppelt, D., Pätzold, B. Recommended leak hole size and mass flow rates by system and application characteristics. LIFE FRONT Interim Report under EU Climate Action Programme, 2019.
14. Colbourne, D., Liu, Z. X., 2012. R290 leakage mass flow rate from a refrigerating system. Proc. 10th IIR Gustav Lorentzen Conf, Delft, The Netherlands
15. Colbourne, D., Suen, K. O. 2014. Characterisation of a leak of flammable refrigerant within equipment enclosures. Proc. 11th IIR Gustav Lorentzen Conf. (GL2014), Hangzhou.
16. Colbourne, D., Suen, K. O., 2004. Appraising the flammability hazards of hydrocarbon refrigerants using quantitative risk assessment model Part I: modelling approach, Int. J. Refrig. Vol. 27, pp. 774–783.

17. Colbourne, D., Suen, K. O., 2004. Appraising the flammability hazards of hydrocarbon refrigerants using quantitative risk assessment model Part I: modelling approach, Int. J. Refrig. Vol. 27, pp. 774–783.
18. Colbourne, D., Suen, K. O., 2008, risk analysis of flammable refrigerants, Part 2: Methodology for calculation of risk frequencies and flammable quantities, Proc. 8th IIR Gustav Lorentzen Conf., Copenhagen, Denmark
19. Colbourne, D., Suen, K. O., 2014. Characterisation of a leak of flammable refrigerant within a small enclosure. Proc. 11th IIR Gustav Lorentzen Conf., Hangzhou, PR China
20. Colbourne, D., Suen, K.O. 2003. Equipment design and installation features to disperse refrigerant releases in rooms-Part 1: Experiments and Analysis. Int. J. Refrigeration, vol. 26, pp. 667–673.
21. Corberan, J. M., Seguradoa, J., Colbourne, D., Gonzalvez, J. 2008. Review of standards for the use of hydrocarbon refrigerants in A/C, heat pump and refrigeration equipment. Int. J. Refrigeration, vol. pp748–756.
22. DCLG, 2010. English Housing Survey – Housing stock report 2008. Department for Communities and Local Government, London, UK
23. DCLG, 2014. Fire Statistics: Great Britain April 2012 to March 2013. Department for Communities and Local Government. Office for National Statistics, London, UK
24. Deutsche Gesellschaft für Internationale Zusammenarbeit (GIZ), 2011. Operation of split air conditioning systems with hydrocarbon refrigerant. Proklima International, Eschborn, Germany.
25. Elbers, S. J., Verwoerd, M., 1997. Quantitative Risk Assessment of a Heat Pump System with Propane Refrigerant. Final Report of TNO, R97-238. Apeldoorn, The Netherlands
26. EN 378-1: 2016. Refrigeration Systems and Heat Pumps – Environmental Requirements – Basic requirements, definitions, classification and selection criteria
27. EN 60079-10-1: 2015. Explosive atmospheres – Part 10-1: Classification of areas – Explosive gas atmospheres.
28. EN 60335-2-40: 2003+A2, 2009. Specification for safety of household and similar electrical appliances. Safety. Particular requirements for electrical heat pumps air-conditioners, and dehumidifiers.
29. EN 62502: 2011, Analysis techniques for dependability – Event tree analysis, BSI, London, UK
30. EN TR 14739: 2004. Scheme for carrying out a risk assessment for flammable refrigerants in case of household refrigerators and freezers. BSI, London
31. Etheridge, D., Sandberg, M. 1996. Building ventilation: theory and measurement. British Gas Research and Technology, John Wiley & Sons, UK.
32. European Commission, 2016. Report from the Commission on barriers posed by codes, standards and legislation to using climate-friendly technologies in the refrigeration, air conditioning, heat pumps and foam sectors. COM(2016) 749 final. Brussels, 30.11.2016.
33. Fleck, N. A. 1985. Fatigue crack growth due to periodic underloads and overloads. Acta Metall., vol. 33, No. 7, pp. 1339-1354.
34. Hall, J. R., 2012. Home fires involving air conditioning, fans or related equipment. National Fire Protection Association, USA
35. Hawkins, G., 2011. Rules of Thumb – Guidelines for building services. 5th Edition, BG9/2011, BSRIA, Bracknell, UK
36. HSE 2014. http://www.hse.gov.uk/statistics/sources.htm
37. HSE, 2001. Reducing risks, protecting people. Health and Safety Executive, HMSO, Norwich, UK
38. Huang, B., Hansen, P. M. S., Viegand, J., Riviere, P., Asloune, H., et al. Air conditioners and comfort fans, Review of Regulation 206/2012 and 626/2011 Final report. [Research Report] European Commission, DG Energy. 2018.
39. Hymes, I., Boydell, W., Prescott, B., 1996. Thermal radiation: Physiological and pathological effects. Institution of Chemical Engineers, Rugby, UK
40. IEC 60335-2-24:2010+A1: 2012 Household and similar electrical appliances – Safety – Part 2-24: Particular requirements for refrigerating appliances, ice-cream appliances and ice makers.
41. IEC, 2005. Summary Report - Refrigeration Incidents. 61C/322/INF. International Electrotechnical Commission, Geneva.
42. International Electrotechnical Commission (IEC). 2015. IEC 60079-10-1: Explosive atmospheres. Classification of areas – Explosive gas atmospheres.
43. International Electrotechnical Commission (IEC). 2017. 61D/386/FDIS. IEC 60335-2-40 ED6: Household and similar electrical appliances – Safety – Part 2-40: Particular requirements for electrical heat pumps, air-conditioners and dehumidifiers.
44. ISO 5149-1:2014+A1:2015 Refrigerating systems and heat pumps — Safety and environmental requirements
45. Ivings, M. J., Kelsey, A. 2014. Technical input on ventilation effectiveness for area classification guidance EI15. Health and Safety Executive, United Kingdom.
46. Kataoka, O., Yoshizawa, M., Hirakawa, T. 2000. Allowable Charge Calculation Method for Flammable Refrigerants. International Refrigeration and Air Conditioning Conference, Purdue, USA.

47. Kosonen, R, Duplessis, G., Mustakallio, P. 2013. The effect of building characteristics and climatic zone on sensible and total cooling demand in an office building. Proc. CLIMA 2013 Congr., Prague, Czech Republic
48. Lee's loss prevention in the process industries. 2005. Lee, F., Mannan, S (Ed). Elsevier Butterworth, UK
49. Li, T. 2014. Indoor leakage test for safety of R-290 split type room air conditioner. Int. J. Refrig. Vol. 40, pp. 380-389.
50. Vonsild A. L. 2012. Safety standards for hydrocarbon refrigerants. Proc. 10th IIR-Gustav Lorentzen Conf. Delft, The Netherlands.
51. Wang, Z., Yang, Z., Li, J., Ren, C. X., Lv, D., Wang, J., Zhang, X., Wu, W. 2013. Research on the flammability hazards of an air conditioner using refrigerant R-290. Int. J. Refrig., Vol. 36, pp. 1483-1494.
52. Webber, D. M., Ivings, M. J., Santon, R. C. 2011. Ventilation theory and dispersion modelling applied to hazardous area classification. J. Loss Prevention in the Process Industries, vol. 24, pp. 612-621.
53. Wolfer, M., Seiler, H., 1999. Ammoniak und Kohlenwasserstoffe als kaltemittel: riskoanalyse, produktehaftpflicht und strafrecht. Bundesamtes fur Energie, Switzerland
54. Zhang, W., Yang, Z., Li, J., Ren, C-x., Lv, D., Wang, J., Zhang, X., Wu, W., 2013. Research on the flammability hazards of an air conditioner using refrigerant R-290. Int. J. Refrig., Vol. 36, Issue 5, pp. 1483-1494

ANNEX 1 OBSERVATIONS ON RELEASES FROM REAL UNITS

A1.1 Introduction

According to section 1.2, current RSS impose CSLs according to room size (provided the A3 charge is >0.15 kg). Section 1.5 indicates through computational methods that these CSLs are more stringent than are probably necessary. Further work was carried out – both as a part of the current study and under other projects[11] – to evaluate whether RACHP systems could create substantial flammable mixtures when releasing greater quantities of A3 refrigerants. Whilst some of the data was previously reported, it has been repeated here for the purpose of completion in terms of the range of RACHP equipment.

Measurements on R290 releases associated with the following are presented:

- Display cabinets
- Condensing units
- Wall AC units
- Window AC units
- Floor AC units
- Ducted AC systems
- Cold rooms

A1.2 Display cabinets

A large number of concentrations measurements have been made for releases from within display cabinets, ranging from single door to five door cabinets, open fronted and so on. Under this EULF project both multideck display cabinets (with and without doors) and a mock cabinet have been examined.

As part of some earlier work, a 3.75 m multideck cabinet was tested under several different conditions with a release of 500 g of R290. Figure 53 shows maximum floor concentration for the multideck cabinet in a 40 m2 room under different scenarios with releases at 60 g/min from the base-mounted evaporator coil.

With evaporator airflow on the concentration is always substantially lower than when they are off (for example, if they have been temporarily terminated during defrost). When fans are off, the cabinet with doors leads to a notably lower concentration, although the effect of doors seems to be negligible if the fans are operating. CRAs are normally loaded and this also results in higher concentrations under all circumstances; this is likely to occur due to the displacement of air inside the cabinet leading to a richer mixture before it pours out of the cabinet.

[11] These include GIZ Proklima C4, DUH-DMT Leakage project, UNIDO-Thermotar project and other privately funded projects by RACHP manufacturers.

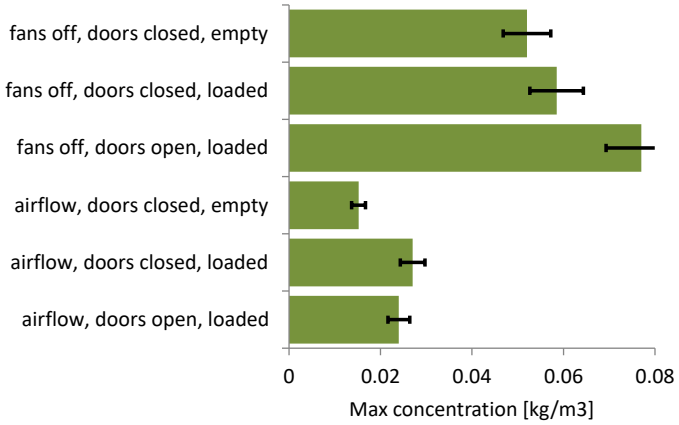

Figure 53: Effect of cabinet doors and airflow on a leak from evaporator; A = 45 m2.

Releases of 500 g R290 at 22 g/min were also made from a similar multideck cabinet of 3.75 m in a test room of 24 m2 (see Figure 54 and Figure 55). Concentrations were measured at positions surrounding the cabinet.

Figure 54: Leak position at lower point of evaporator.

Figure 55: Cabinet loaded.

Tests with the cabinet fans off and where there are no cabinet doors, are shown in Figure 56[12] and with closed cabinet doors in Figure 57. Maximum and average surrounding concentrations are marginally lower for closed door case, except for a small elevation at 23 mins, just after the released was stopped. Also apparent is the wider span of surrounding concentrations, largely influenced by the percolating of the mixture from within the cabinet to the outside. The most apparent difference is the substantially higher concentrations inside the cabinet.

[12] The figures in this section are indicative to demonstrate behavior patterns. Full data can be found in D Colbourne, A Arango, E Dickson. SAFE DESIGN OF R290 DUCTED AIR-CONDITIONING EQUIPMENT, Proc. 13th IIR Gustav Lorentzen Conference, Valencia, 2018.

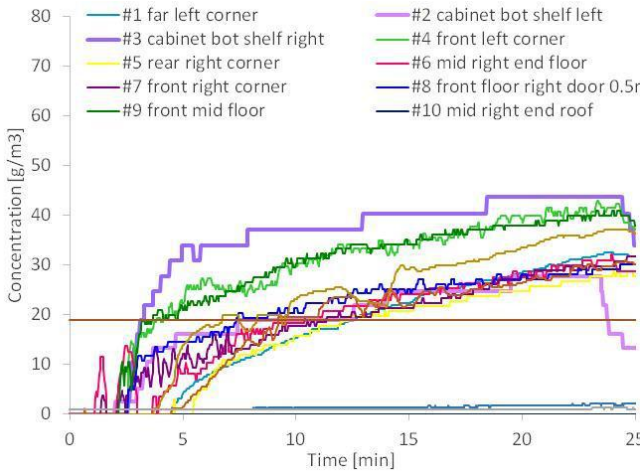

Figure 56: Conc surrounding cabinet with release at 0.3 m, fans off and no doors (#16); A = 24 m2.

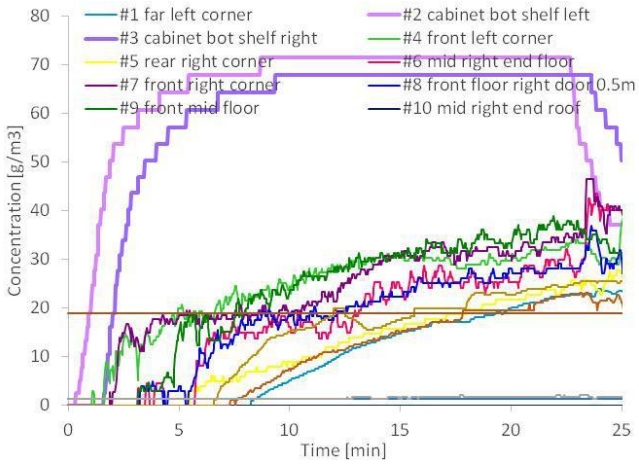

Figure 57: Conc surrounding cabinet with release at 0.3 m, fans off and with closed doors (#18); A = 24 m2.

Tests with evaporator fans switched on and release orifice at 0.3 m are shown next. Figure 59 has results for closed door case and without doors in Figure 58. Surrounding concentrations are seen to be substantially lower than the "fan off" examples, whilst those for the 'fans on with closed doors' case appears – as with the fan off cases – leads to a marginally lower surrounding-concentrations. Note that the jump in concentrations close to the end of the release in Figure 58 is not due to any door opening (since there were no doors), but on account of the cabinet fans switching off arising from a high temperature alarm. Conversely, the test in Figure 59 did involve door opening after termination of the release, but as can be seen here, the increase in floor concentration is in fact minimal.

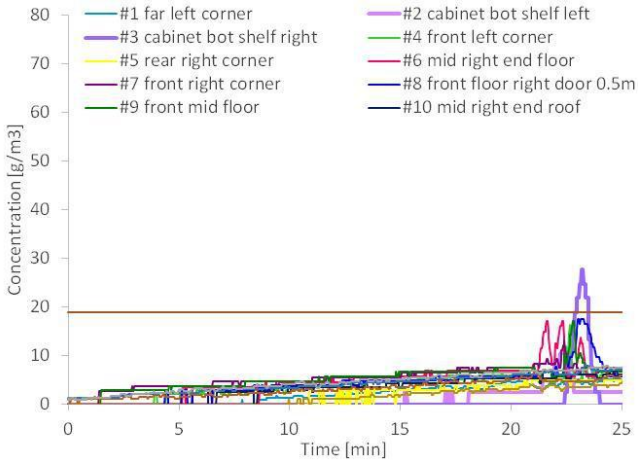

Figure 58: Conc surrounding cabinet with release at 0.3 m, fans on and no doors (#15); A = 24 m2.

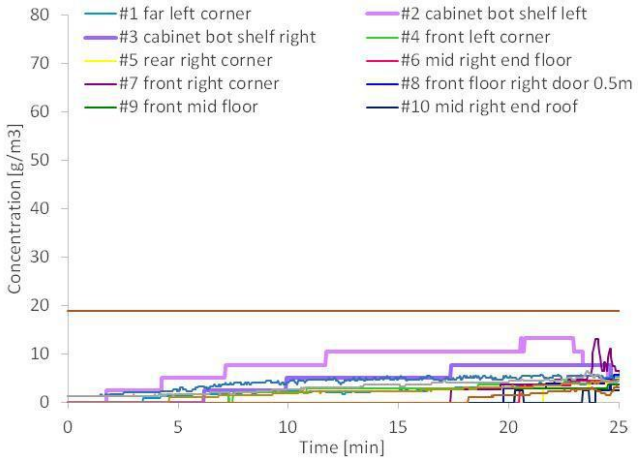

Figure 59: Conc surrounding cabinet with release at 0.3 m, fans on and with closed doors (#19); A = 24 m2.

A1.3 Air cooled condensing units (ACU)

The construction of ACU housing, positioning and function varies widely. For those that are integral to the RACHP units, such as part of the display cabinet or coldstore monoblock unit, they may be installed at or close to floor level or at a higher level (on top of the RACHP system). The results presented below illustrate

these two cases: one where a ACU is positioned such that the release occurs at 1.7 m (Figure 60) and another at 0.2 m (Figure 61).

Figure 60: Elevated condensing unit at 1.7 m release height.

Figure 61: Floor level condensing unit at 0.2 m release height.

Results are included in Figure 62 for a release of 1000 g from the ACU at 1.7 m and with the condenser fan off. Here, no floor level sensors reach or exceed LFL. Conversely in Figure 63 where 300 g has been released from the ACU at 0.2 m above the floor are seen to exceed LFL by a substantial margin.

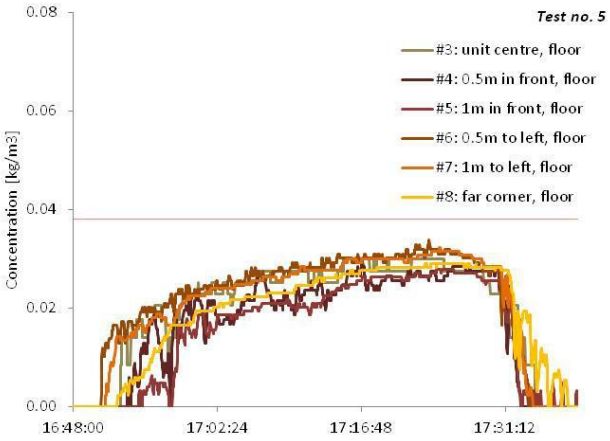

Figure 62: 1000 g at 35 g/min from CU at 1.7 m; A = 13.5 m2.

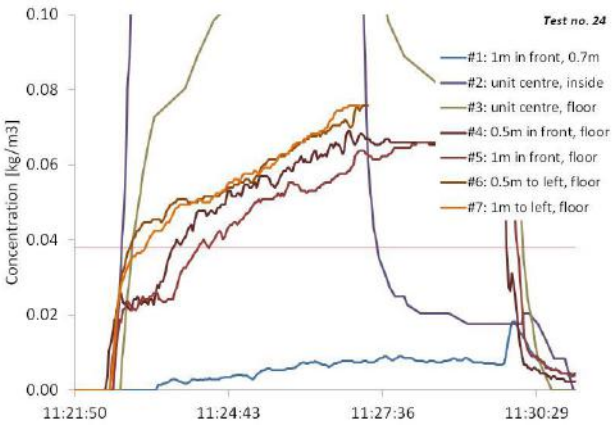

Figure 63: 300 g at 60 g/min from CU at 0.2 m; A = 13.5 m2.

Similar test are seen with the results in Figure 64 and Figure 65, where 320 g and 1000 g are released from a ACU located in both cases at 0.2 m above the floor. For these tests, the ACU fan was operating and a significant difference is observed, compared to the “fan-off” tests, where nowhere does the floor concentration reach LFL.

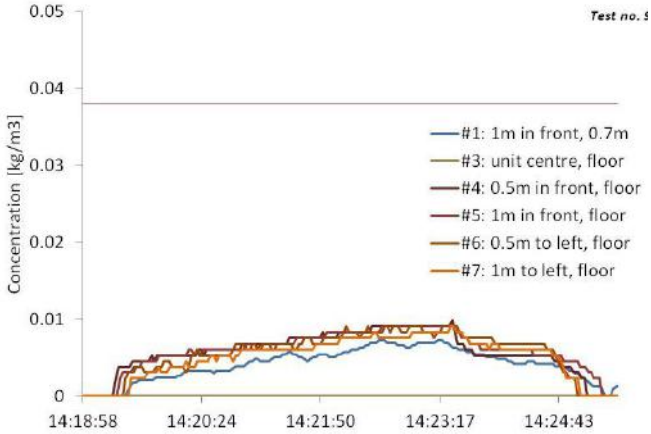

Figure 64: 300 g at 80 g/min from ACU at 0.2 m with fan operating; A = 13.5 m2.

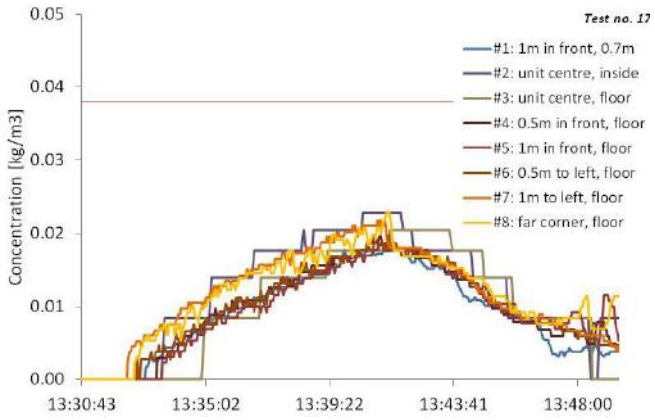

Figure 65: 1000 g at 110 g/min from ACU at 0.2 m with fan operating; A = 13.5 m2.

A1.4 Wall AC units

A series of measurements with wall AC indoor units were conducted. IDUs were mounted at 1.0 m, 1.5 m and 1.8 m, as seen in Figure 66, Figure 67 and Figure 68, respectively. Releases of R290 were simulated via a capillary tube at the far-right end of the IDU at the lowest point within the housing (on the opposite side from the louver).

Figure 66: Wall IDU at 1.0 m.

Figure 67: Wall IDU at 1.5 m.

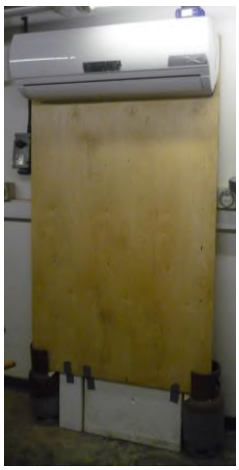

Figure 68: Wall IDU at 1.8 m.

Concentration data is given in Figure 69, Figure 70 and Figure 71 for the three incremental IDU heights. All three tests used a released mass was 300 g at a flow rate of 60 g/min. Sampling points were directly beneath the IDU and then at 0.5 m steps in an outwards direction perpendicular to the rear wall. There is a clear trend seen, where a higher IDU leads to lower floor concentrations.

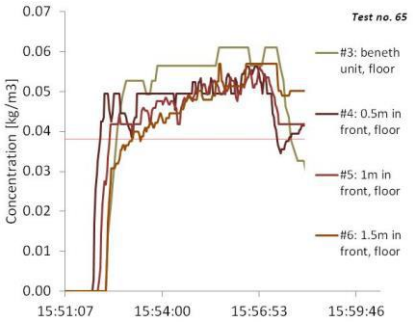

Figure 69: Conc data for release from IDU at 1.0 m; A = 13.5 m2.

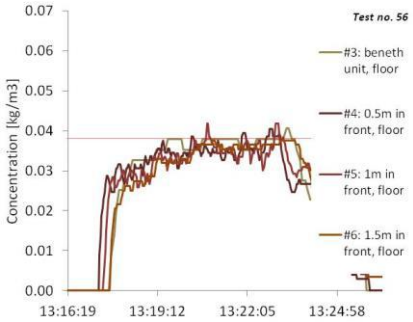

Figure 70: Conc data for release from IDU at 1.5 m; A = 13.5 m2.

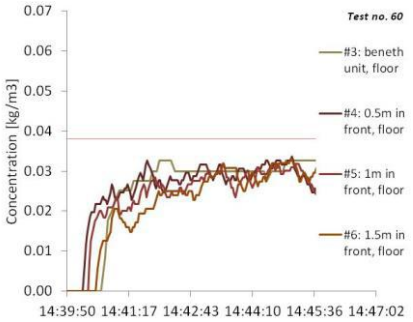

Figure 71: Conc data for release from IDU at 1.8 m; A = 13.5 m2.

Based on the current RSS (EN 378 and IEC 60335-2-40), the maximum charge calculated would be 85 g for the IDU at 1.0 m, 175 g for a 1.5 m IDU and for the 1.8 m IDU, 260 g.

Additional tests (using the same set-up but with a smaller IDU) were carried out where the release of R290 was terminated at the time that the floor concentration at the centre of the room approached LFL. In this way, it is possible to determine the maximum releasable quantity before a flammable layer is formed. These measurements enable generation of height-concentration graphs to provide an understanding of the vertical distribution of the refrigerant within the room.

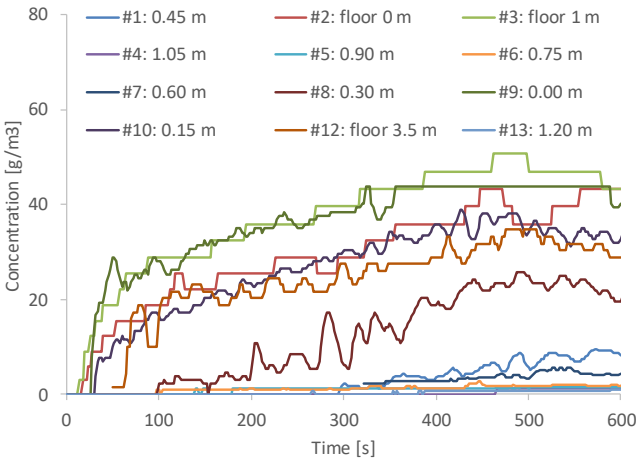

Figure 72: 240 g of R290 released at 30 g/min from 0.5 m to achieve LFL at room floor centre (#17); A = 13.5 m2.

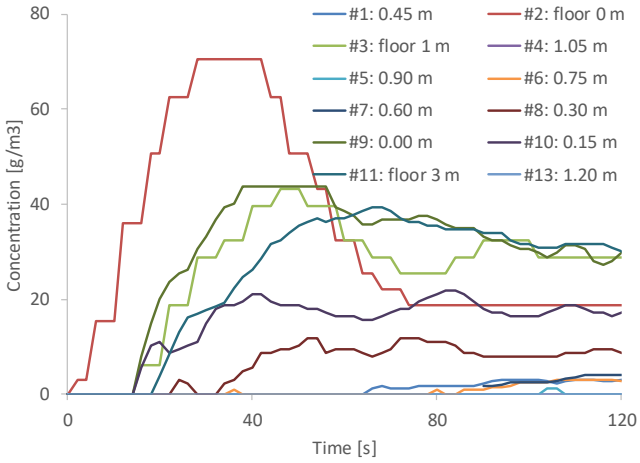

Figure 73: 115 g of R290 released at 150 g/min from 0.5 m to achieve LFL at room floor centre (#14); A = 13.5 m2.

Figure 77 gives the local concentration data for incremental heights within the centre of the room at the time when the floor concentration approaches LFL, for three different IDU heights (0.5 m, 1.0 m, 1.5 m) and two release mass flow rates (30 g/min or 60 g/min and 150 g/min). The release mass is also listed in the legend. This data indicates clearly that the higher the IDU, the more refrigerant that can be released before reaching LFL and similarly with a lower mass flow.

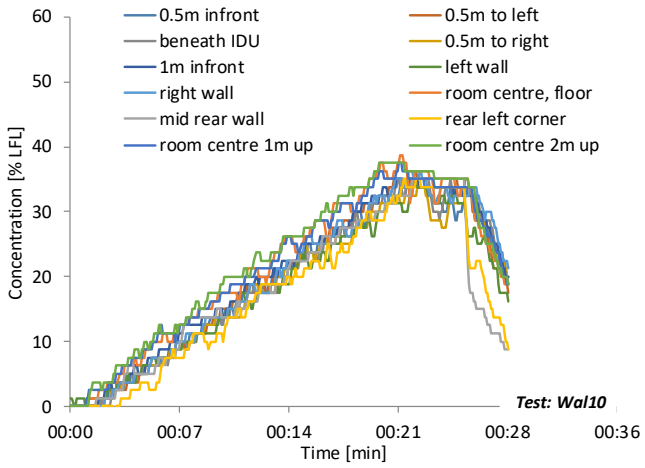

Figure 74: 1000 g of R290 released at 60 g/min from 1.8 m wall IDU with fan on "low" setting (#wal10); A = 40 m2.

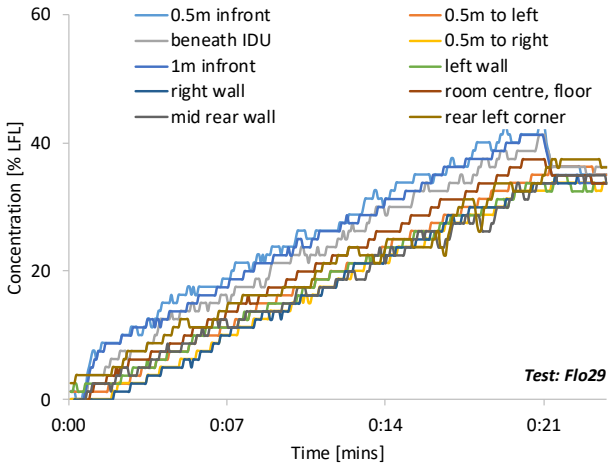

Figure 75: 1000 g of R290 released at 60 g/min from a floor IDU with fan on "low" setting (#flo29); A = 40 m2.

Figure 76 shows results from the same tests where the released mass is plotted against release mass flow rate. This equally shows a distinct increase in released mass with lower mass flow. Also included in the figure are (dashed) lines showing the maximum charge according to equation (1).

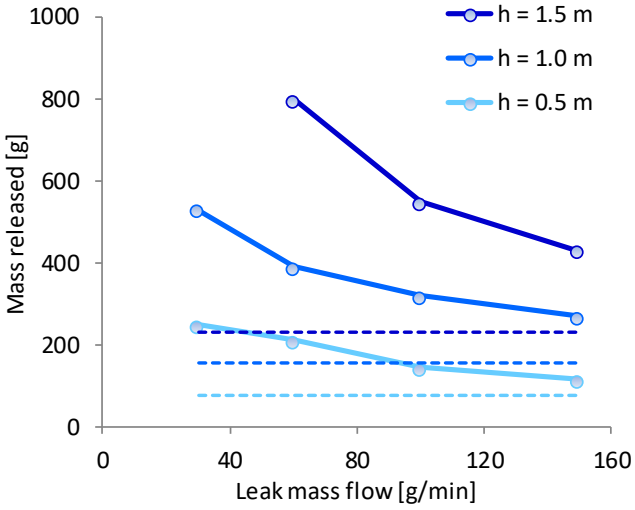

Figure 76: R290 released mass to achieve LFL at room floor centre with IDU at different heights and various release mass flow rates A = 13.5 m2.

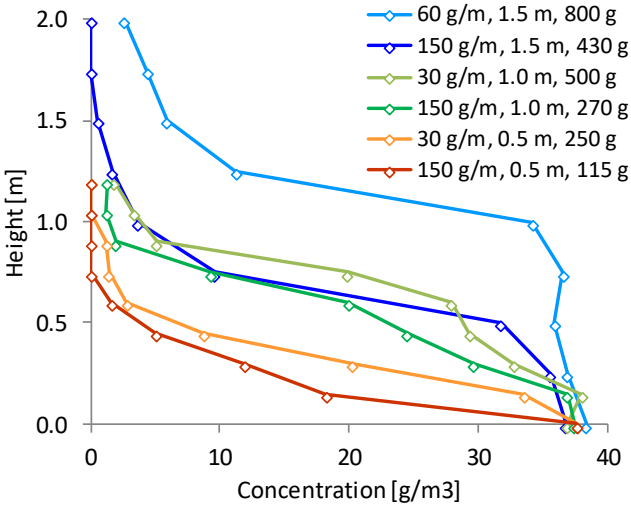

Figure 77: Vertical concentration distribution of R290 release with IDU at different heights and with various mass flow rates A = 13.5 m2.

A1.5 Window AC units

A series of tests were carried out with a window AC. The entire unit was placed within the test room and leaks simulated from different positions within the housing. Certain tests were conducted by sealing the

outer housing with plastic so as to force all refrigerant out of the front of the unit, instead of allowing a proportion to flow to the outside space (as with an actual installed unit).

Figure 78 illustrates the basic construction of a window AC. The key observation is that the refrigerant-containing parts of the evaporator are open to both the inside and outside. As such, in the event of a release from the evaporator, refrigerant will migrate to both the inside space and the outside. In the event of a leak from the condenser parts of the system refrigerant will only travel to the outside space.

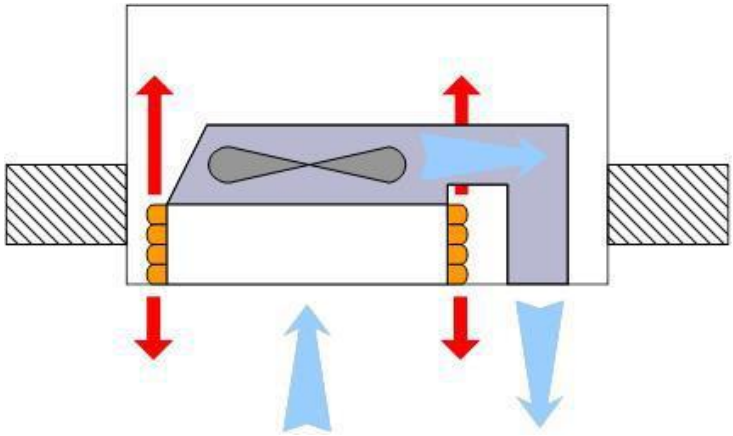

Figure 78: Sketch of window type AC construction.

Figure 79 shows the entire unit and the release directions (inside the housing) are indicated in Figure 80.

Figure 79: Window AC with plastic sealing to top and all sides, except front grille.

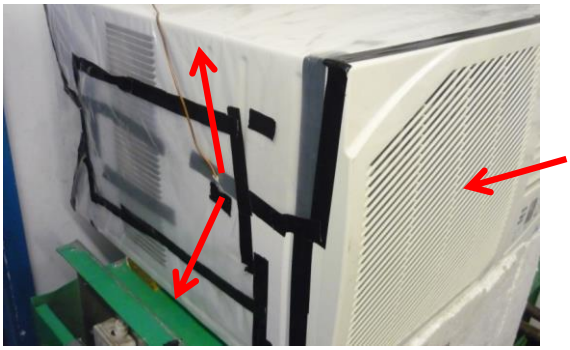

Figure 80: Release directions within AC housing at left hand return bends (left arrows) and mid-coil (right arrows).

For each test, concentrations were measured at 0.15 m vertical increments and the values and Figure 81 presents the resultant concentration profiles corresponding to the end of the releaser period. The situations that lead to the highest floor concentrations are when the release occurs from the return bends within the side panel between the evaporator and housing side panel; whether the jet is directed upwards or downwards, the result is similar. For the case where the plastic sheet on the rear housing openings was removed, the floor concentration was substantially lower and a more even vertical mixing occurred. For a

release in the centre of the evaporator coil (directed backwards) floor concentrations were much lower again and again with better room mixing. Again, since the side and rear parts of the housing would ordinarily be outside, it is much more likely that room concentrations would be lower still.

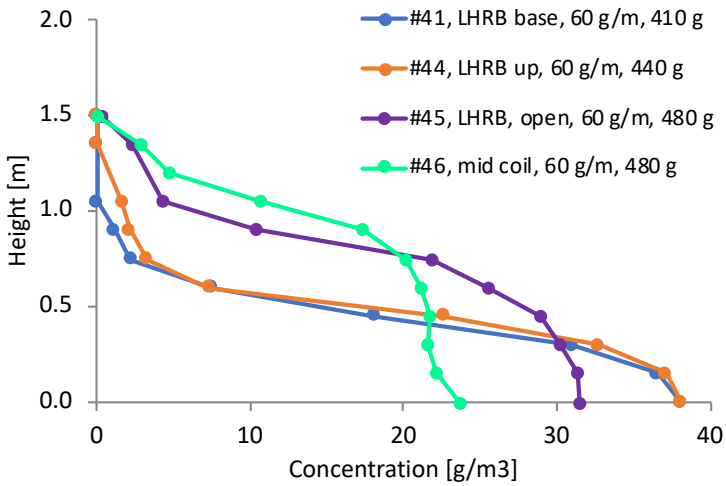

Figure 81: vertical concentration profiles for different release scenarios at the end of the release period; A = 13.5 m2.

In general, the window unit has rather particular behaviour and it requires a relatively large release of refrigerant until the local floor area reaches or exceeds the LFL. This is due to most of the release exiting from the housing from the condenser-side openings. An important question is how much of the release actually flows into the conditioned space and how much actually flows to the outside – this could have a major implication on the allowable charge. Finally, it is clear that use of a diffuser is totally unrepresentative of releases from the real unit and as such it should not be used to mimic release and dispersion behaviour.

A1.6 Floor AC units

Several tests were carried out with a floor type split AC IDU. For some tests the IDU was placed at 0.15 m above the floor (Figure 82) and then also at 1.0 m above (Figure 83).

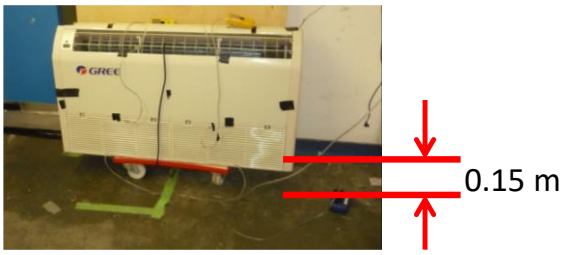

Figure 82: Floor unit positioned just above the floor.

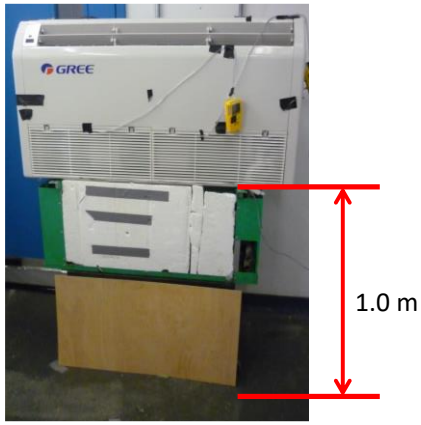

Figure 83: Floor unit positioned 1 m above the floor.

There are also two main potential leak points: one close to the inner base where there is usually a connection to the interconnecting piping (Figure 84; about 0.2 m above the base) and a second at the return bends (Figure 85; about 0.5 m above the base), either end of the evaporator. Releases from the connector were made beneath the pipe insulation, which usually is to the detriment of good mixing as it tends to muffle the release. Due to the close proximity to the floor, all releases were of 150 g and mass flow rates were at 20 g/min, 40 g/min and 60 g/min.

Figure 84: Release position at the connector.

Figure 85: Release position at the evap return bends.

Results from the tests when the IDU was positioned close to floor level are shown in Figure 86 for the release from the connector and Figure 87 for releases from return bends. Under some conditions, the maximum floor concentration easily reached or exceeded LFL. Surprisingly, although the release from the return bends was at a higher elevation than the connector, the mixing within the room tended to be better. This is likely due to the much smaller internal volume of the side panel where the return bends are and the “channelling” effect that the side panel provides to the release, leading to the majority of the release actually exiting much closer to the floor. Interestingly, in both cases the mass flow does not tend to dictate the maximum concentration. In fact, the higher and lower mass flow seem to provide comparable concentrations at the floor.

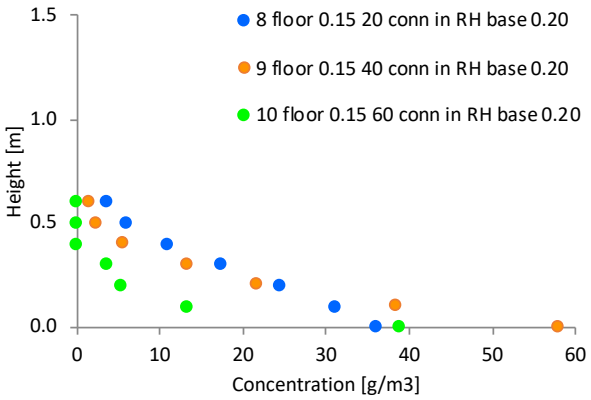

Figure 86: Vertical concentration profiles for releases from the connector when the IDU is at 0.15 m; A = 13.5 m2.

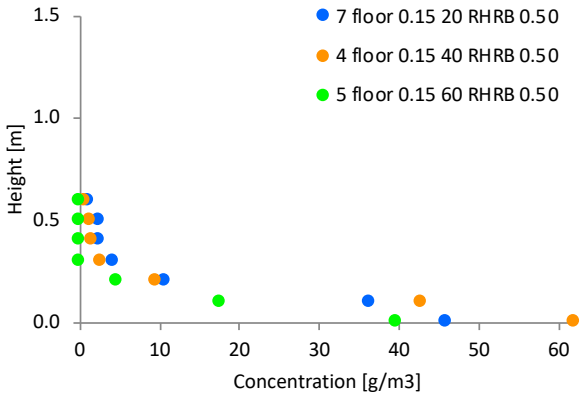

Figure 87: Vertical concentration profiles for releases from the return bends when the IDU is at 0.15 m; A = 13.5 m2.

As one would expect, when the IDU is positioned at 1.0 m above the floor, the maximum concentrations are notably lower then when the IDU was at 0.15 m. Results are in Figure 88 for releases from the connector and in Figure 89 for return bend releases. For these tests the released mass was greater, being 200 g for a 20 g/min release rate, 300 g with 40 g/min, 400 g with both 60 g/min and 90 g/min.

For the connector releases, the higher mass flow rates lead to higher concentrations but considering the differences in released mass, these differences may be considered relatively small. For instance, the 60 g/min and 90 g/min release both involved 400 g, yet the maximum floor concentrations are only about 10% higher with the greater mass flow. A similar observation is apparent with the releases from the return bends.

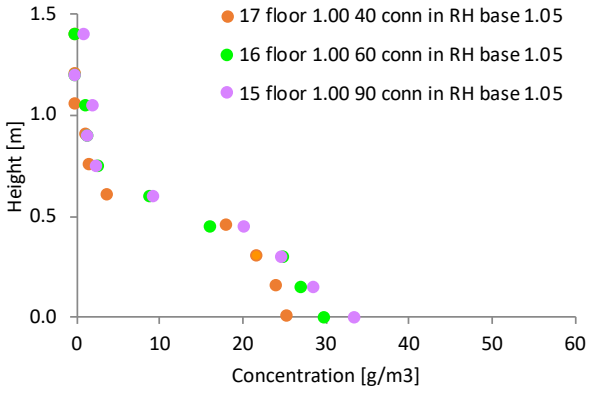

Figure 88: Vertical concentration profiles for releases from the connector when the IDU is at 1.0 m; A = 13.5 m2.

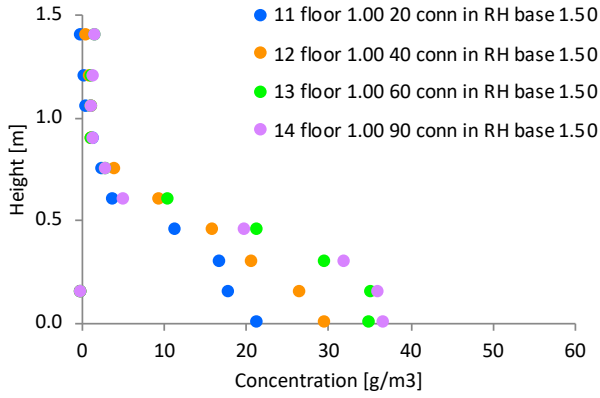

Figure 89: Vertical concentration profiles for releases from the return bends when the IDU is at 1.0 m; A = 13.5 m2.

It is evident that when the IDU is situated on or just above the floor, the concentration is likely to easily exceed LFL, suggesting that other mitigation measures need be applied for such units.

A1.7 Ducted AC systems[13]

When the AC system utilises ducting, such as with a ducted split system or a rooftop type ducted system, additional considerations are required. Depending upon the type of unit, ducting may take one of several arrangements; a summary of the principle configurations is shown in Figure 90 for both rooftop and ducted split units. Amongst these, a release from within an AHU may travel horizontally, vertically downwards or vertically upwards along a duct into the room. If there is no airflow, refrigerant will not travel upwards due to its negative buoyancy.

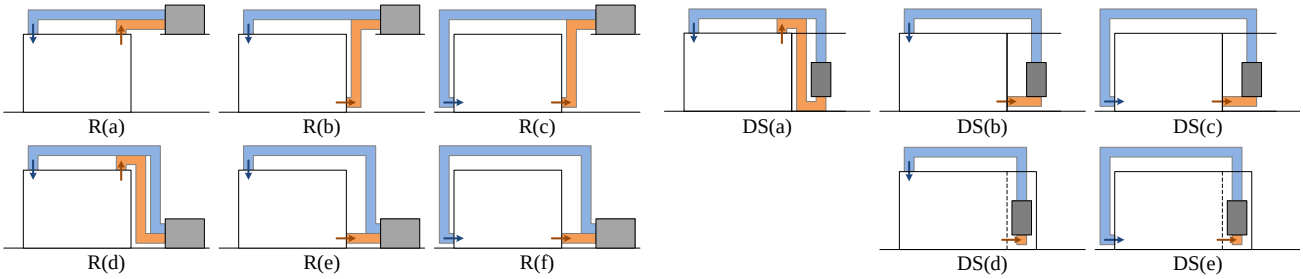

Figure 90: Different possible ducting arrangements for rooftop (left) and ducted split (right) systems.

As part of another project (Colbourne et al, 2018) measurements were taken at openings of both flow and return ducts with and without airflow as applicable, to characterise concentrations in mixtures exiting duct openings. To this end, vertical and horizontal ducting was prepared, either as a single main or with four branched outlets; examples of the setups are shown in Figure 91 and Figure 92.

Figure 91: Experimental set up to mimic arrangement "R(b)" and "R(e)" in Figure 90.

Figure 92: Experimental set up to mimic arrangement "R(c)" and "D" in Figure 90.

Measurements were made with duct systems both with single and with multiple outlets.

Firstly, Figure 93 shows the cross-sectional distribution of the mixture as it flows along the main duct. Importantly this shows that the flow is almost entirely homogenous and there is no maldistribution.

[13] Work carried out under UNDP project, but included here for completion.

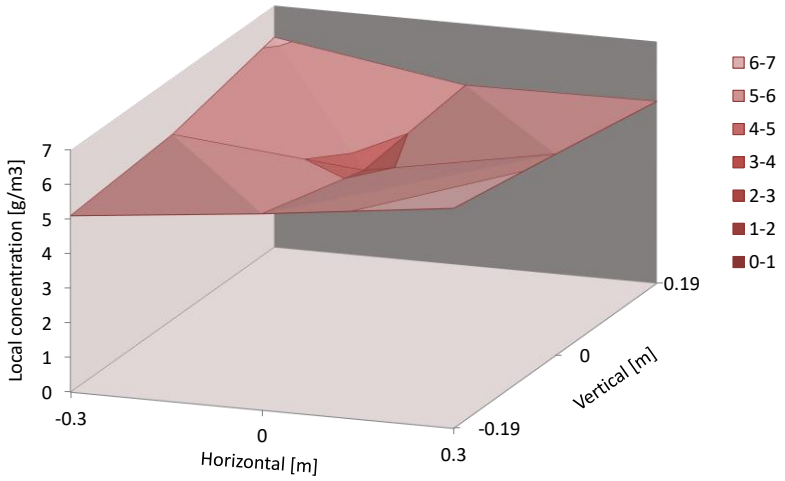

Figure 93: Concentrations across a main duct at 1.5 m from evaporator, with release at 200 g/min and "low" airflow at 0.78 m3/s.

Using a vertical-upward duct with airflow, the maximum concentration was found to be almost the same across all outlets (Figure 96), indicating there is no significant maldistribution. The disparity between the two sampling positions for ach outlet in Figure 96 is due to local eddy currents partially drawing in and recirculating room air on account of the misbalanced duct configuration.

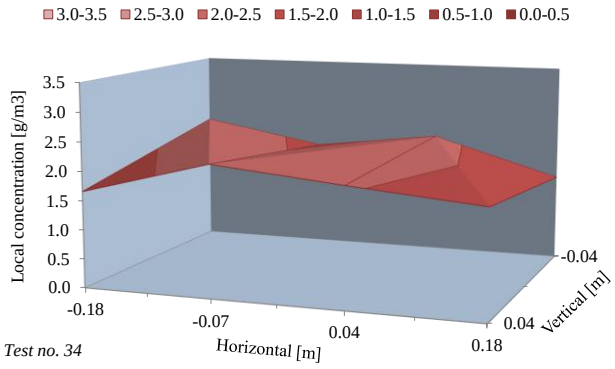

Figure 94: Concentrations across single outlet with "low" airflow (0.78 m3/s) and 120 g/min release.

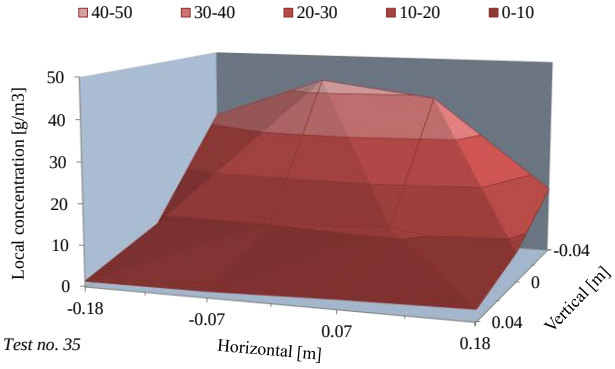

Figure 95: Concentrations across main outlet with no airflow, 4 mins into a 120 g/min release (500 g).

With a rooftop AHU feeding horizontal ducting without airflow (Figure 97), several variations were tested, including simulated leaks at the top and base of evaporator coil and with the return air opening open, partially blocked and fully blocked so as to force more or less refrigerant into the supply duct. These variations have a significant influence on the concentrations at the outlet openings, ranging from very low values with a release at the bottom of the coil and return opening unblocked, to values approaching LFL when the release is at the coil top and return opening to fully blocked. Interestingly, there is no clear distinction between concentrations at near outlets (1st LH/1st RH) and those at the far end (2nd LH/2nd RH).

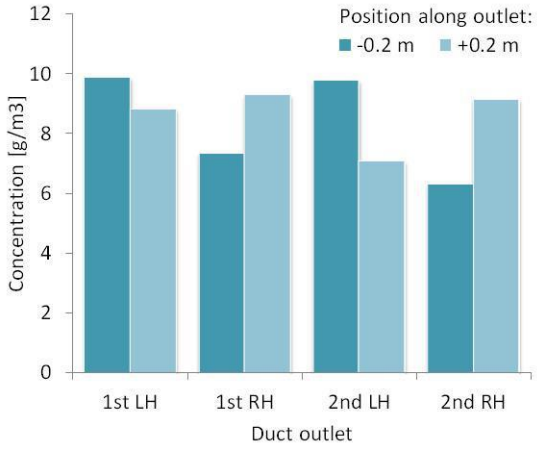

Figure 96: Concentration before termination of a 1000 g release at 150 g/min with airflow on; A = 35 m2.

One further situation that may arise is if the connecting flow and return ducting are elevated (i.e., forming a "bucket") and there is a refrigerant leak whilst airflow is off, the accumulated mixture may then be propelled out of the housing and through the ducting almost instantaneously. It is noted that this would have to occur fairly soon after cessation of the leak since the AHU is not gas-tight so refrigerant will eventually fully drain from the AHU to the surroundings. Several tests were carried out by positioning sampling points at successive distances from a single main outlet, along the air discharge centreline and also incrementally above, below and beside the centreline in order to establish the extent of any flammable region.

Provided there is airflow, concentration within and at duct inlets and outlets is always a fraction of LFL. When airflow is off and ducting is horizontal or downwards-vertical, concentration within part of the duct will most likely be above LFL. The special situation where airflow initiates soon after a release produces a flammable mixture at and beyond the duct outlet but lasts only for a few seconds.

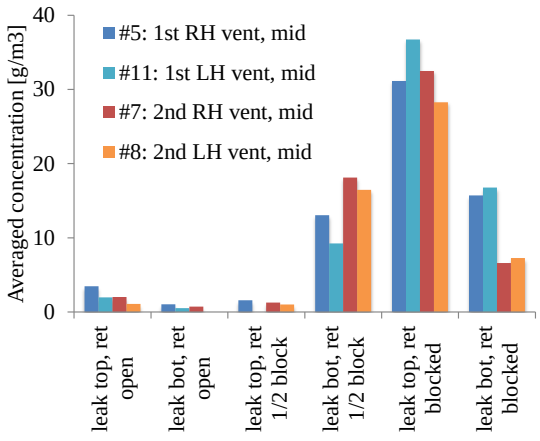

Figure 97: Concentrations at duct outlets for 350 g at 50 g/min for release locations/AHU confinement; A = 35 m2.

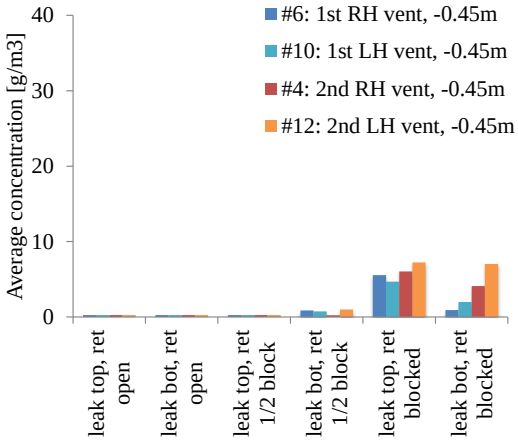

Figure 98: Concentrations at 0.45 m below duct outlets for 350 g at 50 g/min for different conditions; A = 35 m2.

Beyond supply and return duct opening

With airflow operational it was seen above that concentrations throughout the ducting is fairly homogenous and generally a fraction of LFL. Absence of AHU airflow can result in concentrations exceeding LFL at inlet and outlets of horizontal or downward-vertical ducts.

Duct openings at floor level were found to generate potentially flammable mixtures across the surrounding area, in the same way as with the ducted split AHU. In order to minimise occurrence of concentration above LFL, use of an elevated plenum chamber was similarly evaluated, terminating from a 6 m horizontal/downwards-vertical duct fed by a rooftop unit. A similar effect arises with the ducted AHU, although for the same release mass and flow rate concentrations tend to be lower likely due to the additional momentum generated from the 3 m drop, thus accelerated the flow and producing better mixing at the outlet.

For refrigerant flowing along horizontal ducts to the outlets the concentration can exceed LFL. Measurements were also made at collection points about 0.5 m below the outlets to see how far the flammable mixture may extend. Figure 98 shows some results for the same tests in Figure 97, where the concentration is seen to dilute by a factor of five to ten over the 0.5 m descent. This also provides confidence that any potentially flammable mixture is unlikely to extend more than a few centimetres beyond the inlets and outlets.

Example results are provided in Figure 94 and Figure 95 for a single outlet at the end of a horizontal main duct 5 m from the AHU, with and without airflow, respectively. With airflow, the planar distribution is fairly even, with a variation of ±0.5 g/m3 from the average. These results were replicated with vertical ducting and also at the cross-section 1.0 m from the AHU; provided there is airflow through ducting any refrigerant release is always well mixed. Conversely, when airflow is off (Figure 95), concentrations exceeding LFL occur along the base of the ducting, although values are a small a fraction of the LFL a few centimetres above the base. According to the various tests, the maximum concentration tends to halve after each subsequent two metres of ducting. The inference is that with sufficient duct length, concentrations above LFL at outlets can be avoided.

A1.8 Hydronic heat pumps

Hydronic heat pumps – whether for hot water or space heating – are often considered to be a concern due to their installation in small utility rooms or cellars. A number of tests were conducted on such a product. Figure 99 is a photograph of the HP and the room arrangement (3 m × 2 m) within which tests were carried out.

Leaks were simulated with 20 g/min, 45 g/min and 65 g/min from the evaporator return bends (top section) and from within the condensing unit part (base section) and involved a 500 g of R290.

Figure 99: LWC HP with connected duct.

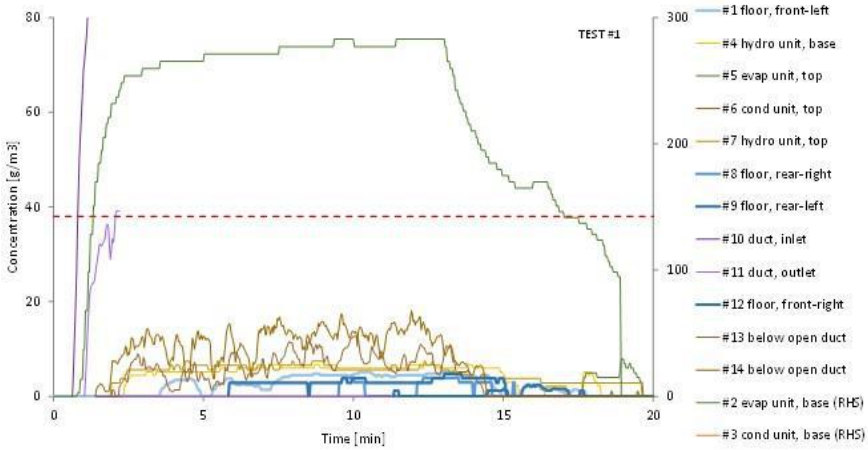

Figure 100: Test no. 1; 40 g/min release from evaporator return bends; A = 12 m2.

Figure 100[14] shows concentration measurements from an evaporator leak. All sampling points at floor level show values less than 20% of LFL. However, refrigerant does flow into the evaporator compartment and out along the ducts to (normally) the outside. Beneath the duct outlets at floor level the concentration is around one-third of the LFL (although obviously there is far less airflow within the lab environment). Concentrations at various other locations within the HP assembly exceed LFL, such as at the inside base of the ducting and within the evaporator compartment.

A leak was simulated at the base of the condensing unit section and results are in Figure 101, but without any modifications to the housing, etc. Concentrations inside the enclosure approach or exceed LFL but also concentration at the floor, surrounding the HP eventually rise above LFL (especially at the far rear corner, where there is a cable entry gap in the housing).

A further result is shown in Figure 102, where the test employs a 5 cm diameter hole between the condensing unit and evaporator enclosures and the fan operating at 150 RPM such that air is drawn up through the hole and blown through the ducting. This has a huge effect on reducing surrounding concentrations. Except for the concentration within the unit enclosures, all others – including within the ducting – are well below 20% of LFL.

[14] The figures are indicative to demonstrate behavior patterns. Full data can be found in D Colbourne, A Arango, E Dickson. SAFE DESIGN OF R290 DUCTED AIR-CONDITIONING EQUIPMENT, Proc. 13th IIR Gustav Lorentzen Conference, Valencia, 2018.

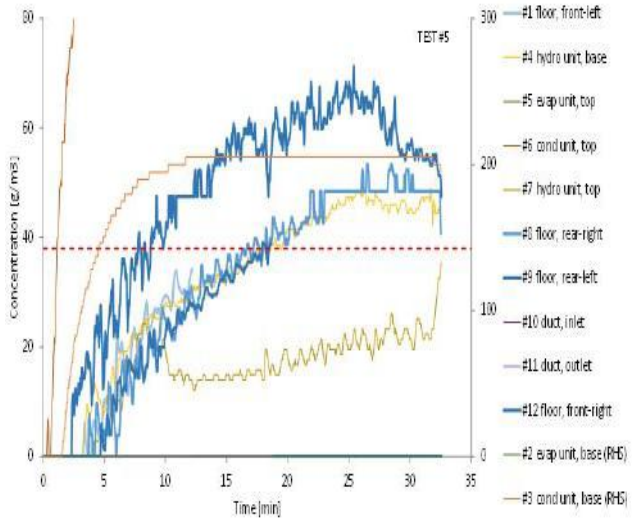

Figure 101: Test no. 5: 20 g/min within condensing unit enclosure; A = 12 m2.

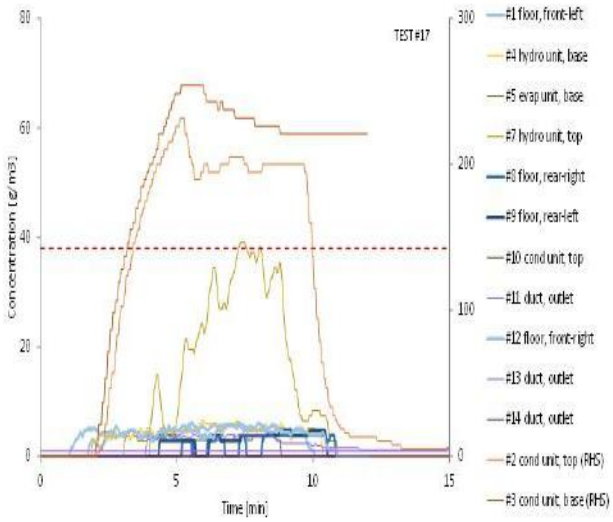

Figure 102: Test no. 17: 65 g/min within condensing unit enclosure but with evaporator fan on at 150 RPM and a 5 cm diameter hole in base; A = 12 m2.

A1.9 Concluding remarks

RACHP equipment. Release mass flow rates range from around 20 g/min to 200 g/min, but are mostly around 60 g/min and charge amounts are from about 100 g to 1000 g. These results help to give an impression about how R290 releases disperse from different types and arrangements of RACHP equipment and conditions under which more attention should be paid to minimise the flammability risk.

However, in general it is seen that except with equipment mounted close to or on the floor, concentrations at or above LFL are avoided.

Nevertheless, different approaches should be made available to suit the equipment, the circumstances and available preventative measures.

ANNEX 2 IMPLICATIONS OF HIGHER HC REFRIGERANT ON FLAMMABILITY RISK

A2.1 Introduction

There are a vast number of factors that influence the fate of a refrigerant leak. and some of them are

An analysis has been carried out to provide an indication of the impact of larger charge sizes on flammability risk.

This is based on R290 since computational output data was already available.

This analysis involves several steps:

- Generation of flammable time and volume data for a release
- Calculation of
  - probability of flammable volume
  - probability of ignition source(s)
  - frequency of ignition
- Determination of severity of ignition event
- Calculation of risk

Calculations are based on increasingly large released mass of R290.

The evaluation is based on a release or R290 emanating from an indoor unit enclosure housing refrigerant-containing parts, from wherein the leak occurs. As such the analysis it is directly applicable to those equipment types identified in the far-right column of Table 14. For the case of ducted systems, the calculated risk is likely to be lower than estimated for IDUs (within the bounds of the stated assumptions) since refrigerant will exit the duct outlet at lower concentrations, less than 100% of the leaked refrigerant will flow into one room (assuming more than one room is served) (Colbourne, Arango and Dickson, 2018) and the presence of ducts act to provide pressure relief for any overpressure arising from deflagrations.

Table 14: Configurations of air conditioner types applicable to risk evaluation

Type		Primary configuration	System layout	Applicable to analysis
Hermetically-sealed unit (HSU)	double duct*	Small self-contained	Self-contained	Y
	single duct**	Small self-contained	Self-contained	Y
Duct free split (NDS)		Ducted free split	Remote	Y
Multi-split (MS)		Multi-split including VRF	Remote	Y*
Ducted split (DS)		Residential/small cap	Remote	N
		Commercial/large cap	Remote	N
Packaged rooftop (PRT)		Ducted commercial	Self-contained	N
Exhaust air-to-air heat pump		Inside / outside	Self-contained	Y

* Assuming that the refrigerant flows freely from other indoor units to the one with a leak

Several modes have been considered, during when a leak is assumed to occur:

- Unit off
- Airflow on
- Unit on or off with detection to initiate airflow
- Unit off with liquid line solenoid valve closed
- Unit on or off with detection to close solenoid valves

A2.2 Calculations and assumptions

Generation of flammable time and volume data

Computational fluid dynamics (CFD) code[15] was used to generate flammable volume and time data. General set-up of the model was rhoreactingbuoyantfoam solver, no turbulence modelling and a mesh ranging from 0.015 – 0.06 m. Turbulence models were excluded to (a) yield more pessimistic results and (b) to increase calculation time.

A room of 3 m × 4.5 m × 2.5 m high was used with an AC IDU positioned on the wall at the narrow end of the room (see Figure 103) – although this could equally be any other RACHP enclosure of comparable location and dimensions. An opening of 0.2 m2 was located in the ceiling directly above the IDU to avoid pressurisation of the room. Pre-mixing of the release within the IDU was accounted for by assigning a nominal exiting concentration within the IDU enclosure, in order to mimic observations from measurements (Colbourne and Suen, 2018a). All releases were taken to be in vapour-phase only.

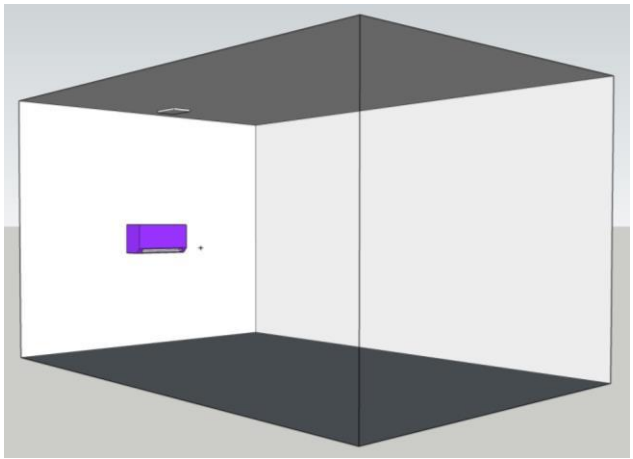

Figure 103: Domain for computations; IDU is at 1 m above floor.

In addition, the effect of infiltration, residual air movement and thermal convection were entirely neglected, again, leading to an unrealistically pessimistic quantification of flammable volume and times.

[15] https://sim-flow.com/

Probability/frequency calculations

For calculating the frequency of ignition, the approach developed in Colbourne and Suen (2004; 2008) was utilised, as it is especially targeted towards the case of flammable refrigerants in RACHP systems indoors. The frequency of ignition is the likelihood that ignition is expected to occur per year.

The ignition frequency of a single leak under a particular set of conditions ($f^*_{l,i}$) is calculated from equation (23).

$$f^*_{l,i} = f_{leak,l,i} \sum_{h=1} P^{F*}_{h,l,i} \tag{23}$$

where $f_{leak,l,i}$ and $P^{F*}_{h,l,i}$ are leak frequency and probability of ignition of a flammable mixture by an active SOI, respectively. $f_{leak,l,i}$ refers to a specific leak size in term of duration (l) under a set of conditions and is largely related to the construction/installation of the system and compressor operating mode (on- or off-cycle), and is normally based on empirical (and anecdotal) data. i represents each individual set of operating and environmental conditions. $P^{F*}_{h,l,i}$ is evaluated with respect to a vertical element/region (h) within the room so that sources of ignition are linked to local formation of a flammable mixture (in light of the relative buoyancy of the gas). $P^{F*}_{h,l,i}$ is determined from equation (24).

$$P^{F*}_{h,l,i} = \sum_{N=1}^{Nsoi} \left\{ 1 - \left[(1 - P^{F}_{V,h,l,i}) + P^{F}_{V,h,l,i} (1 - P_{soi,h,l,i}) \right]^{N_E} \right\}_{N_{soi}} \tag{24}$$

where P^F_V is the probability of a flammable volume, P_{soi} is the probability of an active source of ignition, N_{soi} is the number of SOI, and N_E is the number of active events of each SOI. P^F_V, and therefore P^{F*}, is a function of the size and duration of a flammable mixture which may be influenced by many parameters, including charge size, leak duration and airflow conditions, arising from infiltration, convection by thermal sources, evaporator and/or condenser fans, etc., and requires modelling of a release to determine relevant characteristics.

The probability of the flammable volume is given by (equation 25).

$$P^F_{V,h,l,i} = (\bar{V}^F_h / V'_h) P_{sys} P_{perc} \tag{25}$$

where the reference volume V' corresponds to the horizontal levels chosen for grouping local SOI ($V'_h = A_{Rm} h_{Rm} / N_h$), and $\bar{V}^F_h$ is the mean flammable volume existing within that reference volume. P_{sys} is the probability of a system to release its charge, also interpreted as "annual leak rate" or the ratio of total mass leaked from a given population of systems to the refrigerant bank. P_{perc} is percolation probability which is failure to ignite a C^F due to small pockets of unmixed gas or air within a cloud (Rew and Spencer, 1998).

To account for the dynamic nature of equipment operation and/or associated environment, $f^*_{l,i}$ is normally evaluated for each set of conditions, such as compressor operating mode and the presence of alternate or multiple airflow types. Consequently, the overall ignition frequency (f^*) is the sum of the individual ignition frequencies for all leak sizes, weighted with the corresponding time fraction for each combination of conditions – compressor operating mode (φ_{op}) and each airflow type – that is present (equation 26).

$$f^* = \sum_{i=1} \left[\sum_{l=1}^{Nleak} \left(\sum_{k=1} f^*_{l,i} \varphi_{k,i} \right) \right] \tag{26}$$

with each $\varphi_{k,i}$ referring to different operating modes, infiltration rate, presence of thermal currents, mechanical ventilation, and so on.

The ignition event can result in one or more "primary" consequences, which depend upon the local conditions: a jet fire, a flash fire, and/or an explosion (which is characterised by the development of sufficient

overpressure from the expansion of the gases). For simplicity, the only consequence accounted for is maximum overpressure, which is assumed to occur in a confined volume; equation 27.

$$\Delta p = 8 \times \frac{\bar{V}^F}{V_{room}} \tag{27}$$

Where the constant 8 is the maximum pressure rise ratio from ignition of a hydrocarbon and V_{room} is the confined room of the room (m^3). Note that this is a vast oversimplification of the process and also results in drastically pessimistic results, since in real cases there is heat transfer to the surroundings, escape of gas through the room fabric and pressure relief through failure of windows, doors, etc.

Finally, the overall risk (of overpressure) is expressed as equation (28).

$$R = f^* \times \Delta p \tag{28}$$

For quantifying these sets of equations, ten SOIs are assumed per 10 m^2 of room floor area and are located randomly within the space. Each SOI event lasts for 1 s and occurs once per hour throughout a 24 h period.

Flammable mixture quantities are obtained from the CFD calculations, as described above.

For leak frequency, a nominal value of 0.0001 per year is used for the “smallest” leak size, but this is reduced by a factor of 10 for each doubling of the leak size; this follows the current findings of the leak hole size survey (Colbourne and Kanakakumar et al, 2019).

Table 15: Frequency bands of holes with main leak rates (for R290)

Leak size	Leak frequency
60 g/min	1.0E-04
120 g/min	1.0E-05
180 g/min	2.0E-06

A2.3 Results

Generated data and formulae described in section 4 were used to calculate ignition frequency and then risk of overpressure. Results are expressed with released mass as a function of percent of the entire room space reaching LFL.

Assumptions for the occurrence of the various failure modes are listed in Table 16.

Table 16: Selected failure frequencies

Event(s)	Failure frequency (y-1)
No mains electrical supply[16]	0.045
AC unit electrical fault	0.02
Fan failure or major duct blockage	2.0E-06
Failure of valve to close[17]	0.01
Failure of detection to function[18]	0.005

An example of the concentration gradients from the CFD output is shown in Figure 104.

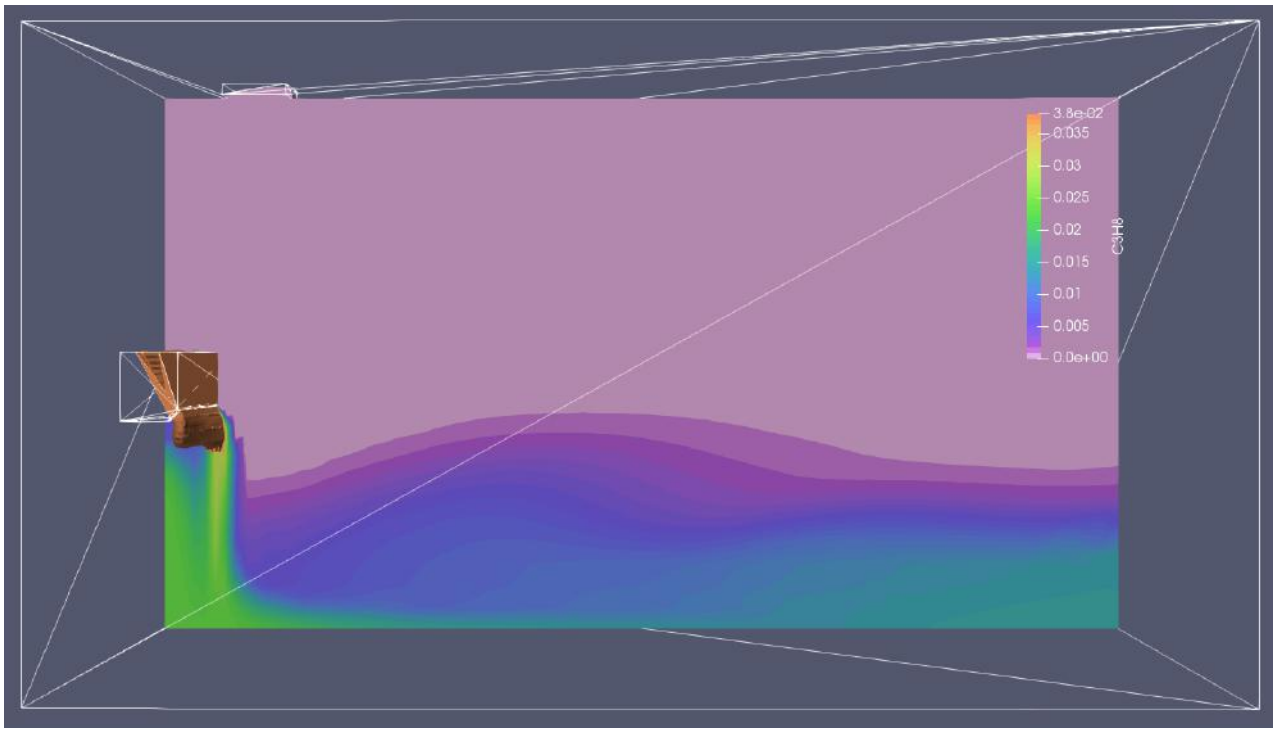

Figure 104: Example of CFD output; the flammable region is shown as the 3D scalar at the IDU on the left side.

[16] https://www.entsoe.eu/publications/statistics-and-data/#statistical-yearbooks
[17] http://www.hse.gov.uk/landuseplanning/failure-rates.pdf
[18] http://www.hse.gov.uk/researcH/rrpdf/rr029.pdf

A2.3.1 "Unventilated" room

Overall results are presented in Figure 105, covering a number of cases for a unit at 1 m in a 13.5 m2 room. Each of the cases listed represent a range of release mass flow rates and degree of pre-mixing within the unit (leading to different exiting concentrations).

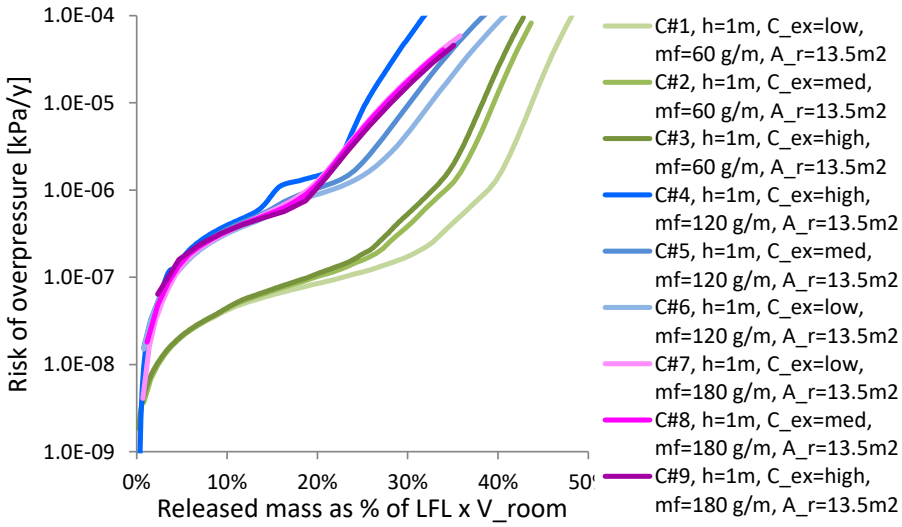

Figure 105: Risk of overpressure as a function of released mass (as a % LFL for the entire room) and different leak rates and internal IDU pre-mixing.

The following observation may be made:

- Significant differences in risk between the cases are apparent.
- For a release corresponding to 30% LFL a wide range in risk may be observed between low (60 g/min), medium (120 g/min) and high (180 g/min) leak rates. Differences between medium and high leak rates are relatively small but are considerable between low and medium leak rates – in the order of about two to three orders of magnitude.
- There is substantial difference between cases having a high degree of release pre-mixing (within the indoor unit) and those with a low degree of pre-mixing, of about one order of magnitude (but only once notable mixing within the room space has already begun). This does not apply to the high leak rate case, where the pre-mixing seems to have minimal effect.

Figure 106 present similar results to the above, except with selected cases for the AC unit being installed at 0.5 m and 2.0 m (in addition to 1.0 m). The same patters as those seen in Figure 105 are also present here.

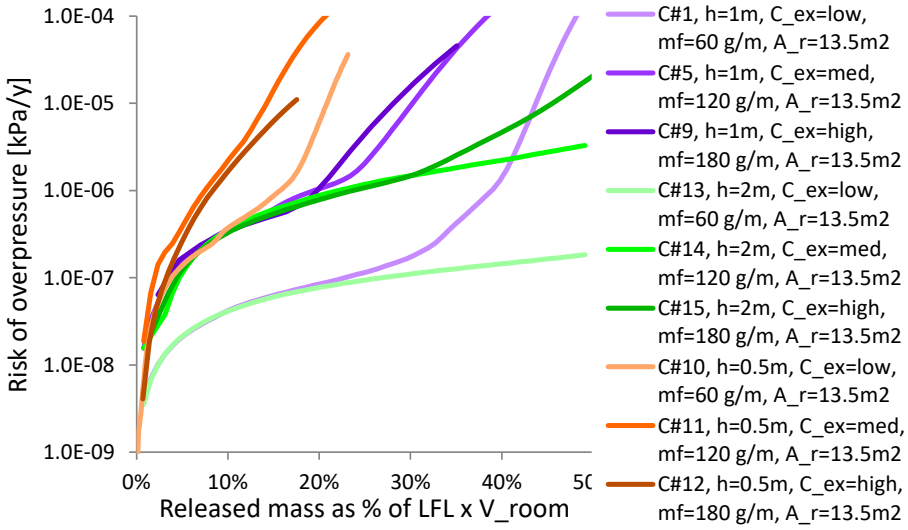

Figure 106: Risk of overpressure as a function of released mass (as a % LFL for the entire room) and different unit installation heights.

The following observations may be made:

- For all cases for a gives release mass flow and degree of pre-mixing, risk follows the same curves up to a certain mass (% of room LFL). Eventually there is a divergence in the risk with values for units installed at a lower height indicating an escalation in risk sooner than with releases occurring at a higher level.
- Again, those with lower release mass flow and higher degrees of pre-mixing, exhibit substantially lower risk.
- The difference in risk between low mass flow/low exiting concentration and high mass flow/high exiting concentration seems to be constant or even diminishes with low installation height units, whereas with those installed at higher levels the risk values tend to diverge with increasing release mass. In other words, units installed at lower heights become more sensitive irrespective of the mitigation measures.

Figure 107 evaluates the same conditions but comparing the effects of room size; 13.5 m2 vs. 56 m2.

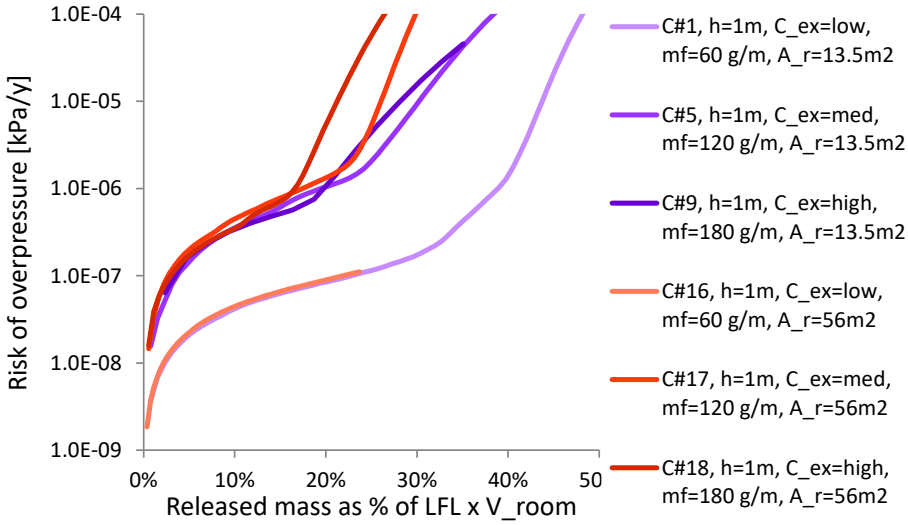

Figure 107: Risk of overpressure as a function of released mass (as a % LFL for the entire room) and different room sizes.

The following observations may be made:

- As with installation height, for a gives release mass flow and degree of pre-mixing, risk follows the same curves up to a certain mass (% of room LFL). Again, there is a divergence in the risk with values for units installed in smaller rooms escalating in risk sooner than with releases occurring at a higher level.

Some results may be deemed as somewhat counter-intuitive. This is due to certain simplifications that would ordinarily be challenging to account for. As such this quantification is relatively crude considering that:

- Local concentration within the flammable volume is not taken account of.
- Probability of ignition is assumed not to be influenced by the local concentration of R290 (which it is).
- Severity of ignition event is not influenced by the flammable concentration, which is taken as stoichiometric.
- Venting from the space and heat transfer to the room surfaces is neglected.

A2.3.2 System with circulation airflow

If a system is constructed with circulation airflow as a mitigation measure, the risk may be estimated from assuming:

- Airflow is operating continuously (except when there is a system electrical failure or the fan experiences a fault), or
- There is a failure of mains electrical supply, or
- When airflow is initiated by leak detection, which may also be subject to a fault.

Assumptions for these various failure modes are listed in Table 16.

Figure 108 shows the risk for two reference cases C#1 and C#5 in comparison with two cases using continuous circulation airflow and airflow initiated by detection, with two different release rates and corresponding airflow rates.

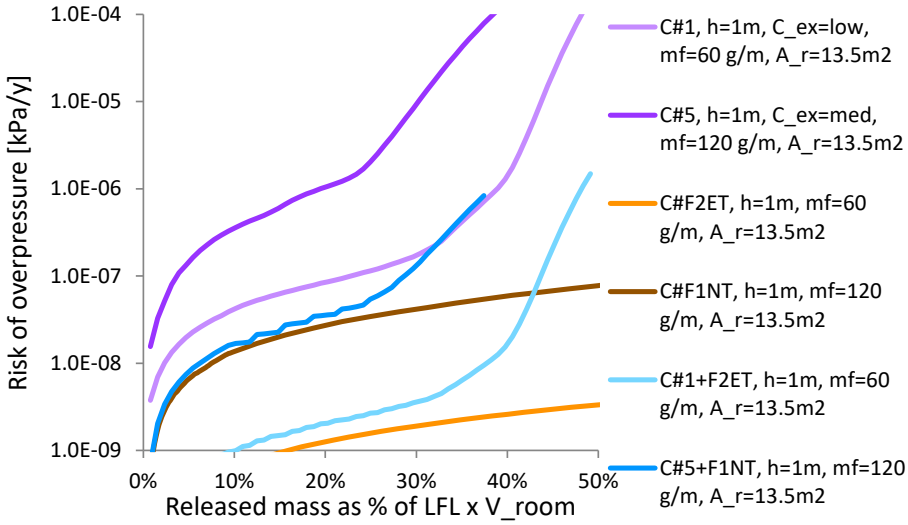

Figure 108: Risk of overpressure as a function of released mass (as a % LFL for the entire room) for with and without continuous airflow.

For the cases where circulation airflow is initiated by detection and assumption has to be made about the probability of failure on demand (FOD) of the airflow. Such a failure may be due to problems with the detection itself or a fault with the fan or airflow. An assumption for the overall FOD probability of 1% has been used.

The following observations may be made:

- Below a released mass of 20 – 40% of LFL, the risk when using continuous airflow is about two orders of magnitude lower.
- The benefit of circulation airflow on reducing risk relative to releases under quiescent conditions is substantial for larger quantities.
- Up to a charge of 30% of LFL, the risk closely follows that of the circulation airflow only, however, thereafter it begins to increase since that of the unventilated case dominates, but nevertheless remains about two orders of magnitude lower.

A2.3.3 System with shut-off valves

Where system shut-off valves (SSOV) are included within the system construction in order to limit the releasable mass of refrigerant into the space, estimation of the impact on risk is fairly straight-forwards.

Figure 109 presents some results for cases C#1 and C#5 where 15% and 40% of the refrigerant charge is retained.

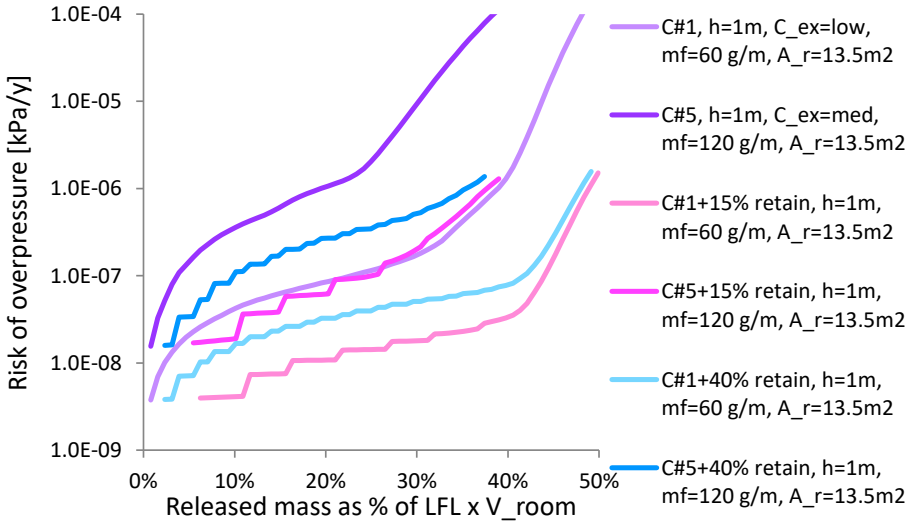

Figure 109: Risk of overpressure as a function of released mass (as a % LFL for the entire room) for with and without use of SOSVs (Note: the "stepped curve" is due to increments arising from use of look-up table for calculations).

As with the circulation airflow case, an assumption must also be made on the FOD on the SOSVs – a probability of 1% has again been used.

The following observations may be made:

- For all cases evaluated, retaining some refrigerant inside the system reduces the risk (as one would expect). Similarly, the greater the proportion retained, the lower the resultant risk.

An additional consideration is a combination of (ii) and (iii), i.e., whilst the system is operating, it is assumed that the indoor unit fan must also be operating with at least a moderate airflow rate and when switched off, whilst the fan is likely to be off, the SSOV may be automatically closed (normally closed) or closed in response to a signal from a leak detection system. [No results generated for this]

A2.4 Concluding remarks

According to CENELEC Guide 32 / IEC Guide 116, some value of tolerable risk should be identified, from which the effectiveness of risk reducing measures can be gauged.

For the purposes of the current discussion, this may be assumed to be based on:

- Background fire risk of cooling appliances in the order of 1×10-6 to 1×10-5 per year
- Overpressure that does not result in significant personal harm, being around 10 kPa[19]

[19] 10 kPa is taken as a reasonable "non severe" value based on the various data within "Methods of approximation and determination of human vulnerability for offshore major accident hazard assessment" from UK Health and Safety Executive (HSE); http://www.hse.gov.uk/foi/internalops/hid_circs/technical_osd/spc_tech_osd_30/spctecosd30.pdf

Thus, for the present discussion, the tolerable level of risk can be assumed to be the product of 10 kPa and 1×10-6 equals 1×10-5 kPa per year.

Note that thermal dose may also be considered as a harm indicator, but this is less convenient to apply as it depends very much upon the distance that the target (person) is from the deflagration, the duration (seconds) that they are present and the type and thickness of clothing they are wearing at the time. To limit disagreement over values and interpretation, overpressure was therefore selected.

For the various cases illustrated above, the mass that corresponds to the assumed tolerable risk may be compared against the limits prescribed within the current safety standards; see Table 17. From the standards, the limit in terms of % of LFL is illustrated in Figure 110.

Table 17: Comparison of mass corresponding to tolerable risk level and limit in standard.

Case	Unit height [m]	Release mass flow [g/min]	Room area [m2]	Unit exiting conc [g/m3]	% LFL mass at tolerable risk level	% LFL limit in standards, Figure 110	Min potential charge multiplier
1	1 m	60	13.5	225	44%	14%	3.1
2	1 m	60	13.5	450	40%	14%	2.9
3	1 m	60	13.5	900	39%	14%	2.8
4	1 m	120	13.5	1200	27%	14%	1.9
5	1 m	120	13.5	540	32%	14%	2.3
6	1 m	120	13.5	270	34%	14%	2.4
7	1 m	180	13.5	1200	28%	14%	2.0
8	1 m	180	13.5	600	28%	14%	2.0
9	1 m	180	13.5	300	28%	14%	2.0
10	0.5 m	60	13.5	225	22%	7%	3.1

11	0.5 m	120	13.5	540	18%	7%	2.6
12	0.5 m	180	13.5	1200	14%	7%	2.0
13	2 m	60	13.5	225	>50%	27%	1.9
14	2 m	120	13.5	540	>50%	27%	1.9
15	2 m	180	13.5	1200	47%	27%	1.7
16	1 m	60	56	225	>30%	7%	4.3
17	1 m	120	56	540	26%	7%	3.7
18	1 m	180	56	1200	21%	7%	3.0
F1NT	1 m	120	13.5	n/a	>50%	14%	3.6
F2ET	1 m	60	13.5	n/a	>50%	14%	3.6

In all the cases listed, it is estimated that charge limits within the standards are at least a factor of two smaller than the minimum “necessary” charge to meet the tolerable risk level and in some cases could be increased by a factor of four or more.

This is despite the analysis including a series of inherently pessimistic assumptions, including:

- Neglection of turbulence within flammable volume modelling
- Higher than likely exiting concentration from the unit housing
- No infiltration
- No residual air movement within room
- No thermal convection
- No air movement arising from room occupants
- Vapour only release (two-phase release with the same mass flow tends to give in lower concentrations)
- Relatively high SOI density
- Severity of the consequence is based on adiabatic deflagration and unvented overpressure

Conversely, certain assumptions may lead to other outcomes:

- Room is empty; depending upon the positioning of objects and relative to the release a room full of clutter may result in a larger or smaller flammable volume
- Consequence does not consider thermal dose from the deflagration

From a practical perspective, note that installation of the unit may result in over-charging (or indeed under-charging) of the system and that the installer may overestimate (or underestimate) the dimensions of the room.

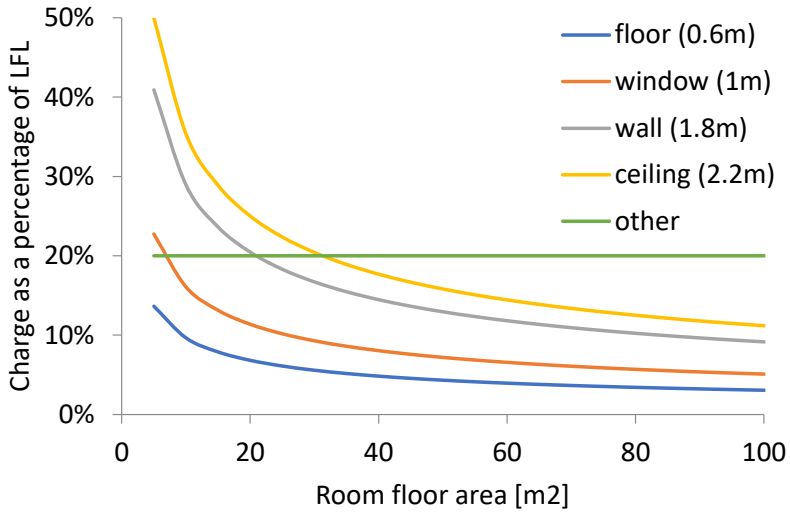

Figure 110: Current maximum charge size of A3 as a function of LFL within a room of 2.2 m high.

Overall, on a risk basis, the charge size limits (% LFL ×room volume) seems to be unnecessarily stringent. In addition, there are several other factors that seem to have a notable influence on risk that could be taken into account when determining appropriate charge size limits.

ANNEX 3 BACKGROUND FOR DETERMINATION OF CHARGE LIMITS FOR UNVENTILATED SITUATIONS

A3.1 Introduction

As was described above, one of the most significant parameters that affect room floor concentration – or inversely the maximum allowable refrigerant charge within that room – is the height at which the release occurs.

Typically, under quiescent conditions the refrigerant will collect within the volume below the release height (although if the release continues, the mixture will ultimately rise beyond the release height.

It is thus proposed to employ a simplified expression to estimate the maximum refrigerant mass (m_{max}) based on this phenomenon (equation 4):

$$m_{max} = F_{LFL} \times LFL \times h^* \times A \qquad (29)$$

where F_{LFL} is a factor applied to the LFL to ensure a flammable concentration is avoided, h^* is some representative the height related to the unit enclosure/housing openings above the floor (m) and A is the floor area, thus giving the free volume somewhere below the top of the unit.

Figure 111 provides a graphical explanation of F_{LFL}: a large value is represented by a lot of mixing below the release height thus accommodating more refrigerant within the free volume below the release position, whilst a small value is representative of a strongly stratified layer close to the floor and very little mixing above it.

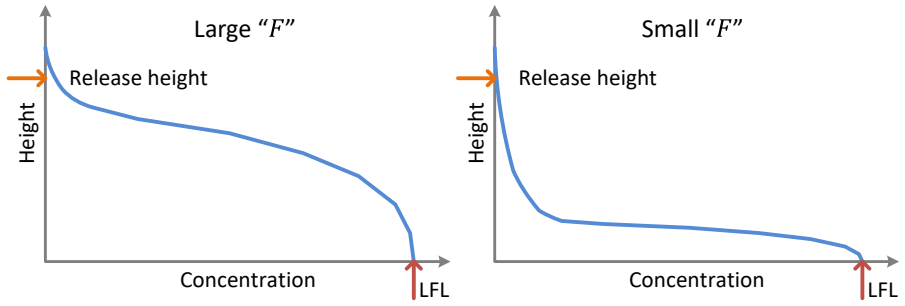

Figure 111: Graphical explanation of F.

As discussed later, for some types of enclosures, h^* may be taken as the height of the base of the unit (h_b), whereas in other cases h^* is somewhere between the base and the top of the unit housing. Since LFL, h^* and A are relatively easily identified, the question is what the appropriate value of F_{LFL} is?

A3.2 Outflow concentrations

Further work was carried out with the intention of characterising $\bar{C}_{exit}$ as a function of UHE configuration. Several types of equipment were examined in this respect: three different IDUs (a small and large wall unit

and a large floor unit), a small condensing unit and a so-called “variable enclosure” which was constructed such that its internal volume and location and size of openings could be modified.

A3.2.1 AC wall IDUs

IDU’s were prepared with several frusta sealed to the open discharge grille, extending downwards for 0.5 m so as to channel all refrigerant-air mixture that pours from the IDU openings with the intention of obtaining steadier readings (as opposed to erratic readings caused by internal turbulence). Additional casing was attached around the perimeter of the inlet grille to collect any mixture spilling out of the top opening. Sampling points were positioned at the base of each channel of the frusta. R290 was released at different constant mass flow rates from the base of the right-hand return bends for the large IDU and various positions about the return bends for the small IDU (all with the fan de-energised). A diagram of the arrangement and example photographs are provided in Figure 112. The left-hand image is a schematic of the casing and positioning of sensors used to capture the exiting concentration from the IDU with the centre photograph being the actual set-up. Positions of the release (within the end space of the IDU) are indicated on the right-hand image.

Figure 112: Diagram and photographs of the test arrangement.

Average concentrations for each of the mass flow rates at each successive linear location along the discharge opening are given in Figure 113 and Figure 114, with the release position indicated by an arrow. Figure 115 summarises those results and also for the mixture flowing out of the top inlet opening. Local data in Figure 113 shows a significantly higher proportion of the mixture exiting closer to the release point than at the opposite end of the IDU (about 40 times higher at 10 g/min) but as release rate increases, a more even distribution develops (e.g., only four times higher at 100 g/min). It may also be noted that the direction of the release also has an influence on this distribution. For example, other tests (not shown) with a different release orientation (but same location) resulted in the pattern in Figure 113 being reversed, where highest values occurred at the opposite end of the IDU; the momentum of the jet “pushed” the refrigerant away from the immediate openings.

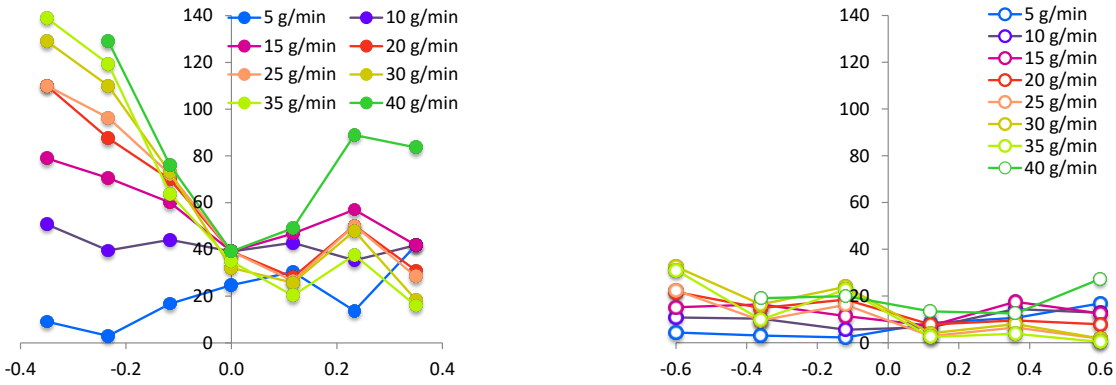

Figure 113: Example concentration profiles for IDU outlet (left) and inlet (right) for leak position (i).

As seen in Figure 115, not-insignificant quantities of refrigerant migrate out of the top (inlet) of the IDU, once there is sufficient volume of refrigerant vapour to act against the negative buoyancy of the mixture within the IDU; this observation was found computationally in previous work (Colbourne and Suen, 2014). Refrigerant mixture must only be flowing upwards from a proportion of the inlet opening area given that fresh air must be simultaneously drawn downwards through the opening it to enable the mixture to flow from the base (exit). Importantly, this phenomenon should assist with the dilution mixing process as it increases the area of the plume-air interface.

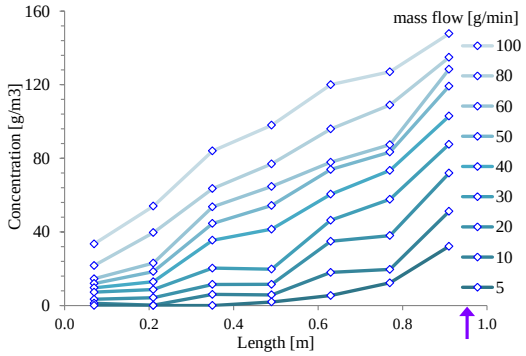

Figure 114: R290 concentrations at different mass flow rates along large IDU discharge opening length.

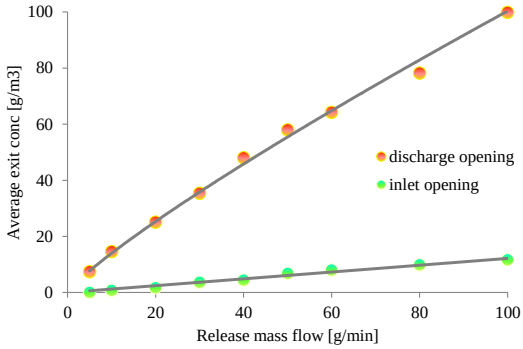

Figure 115: Average concentration of R290 exiting IDU.

A3.2.2 Variable enclosure (VE)

Similar measurements were carried out with enclosures where exiting concentrations were recorded for different configurations and geometries. Approximately 100 sets of measurements were conducted across the range of variables. The setup was slightly different, where sensors were positioned both laterally along the (lower) opening and vertically in order to characterise the vertical distribution (Figure 116).

Releases were made from different positions within the enclosure, generally from the centre of the rear wall at three different heights and also at the left side. A so-called “diffuser-impinger” was used (also in Figure

116, centre-right) that was designed to mimic the situation in real equipment where a high velocity jet impinges on a nearby surface and thus reduced the momentum of the jet.

Openings of the VE indicated ranged from 0.1 m to 1.3 m high but also with an additional opening at the top part of the enclosure was introduced when appropriate. It can also be seen that the opening sensor positions were just on the inside of the VE envelope, since earlier tests found that sensors located any more than a couple of millimetres outside of the lip missed the exiting mixture.

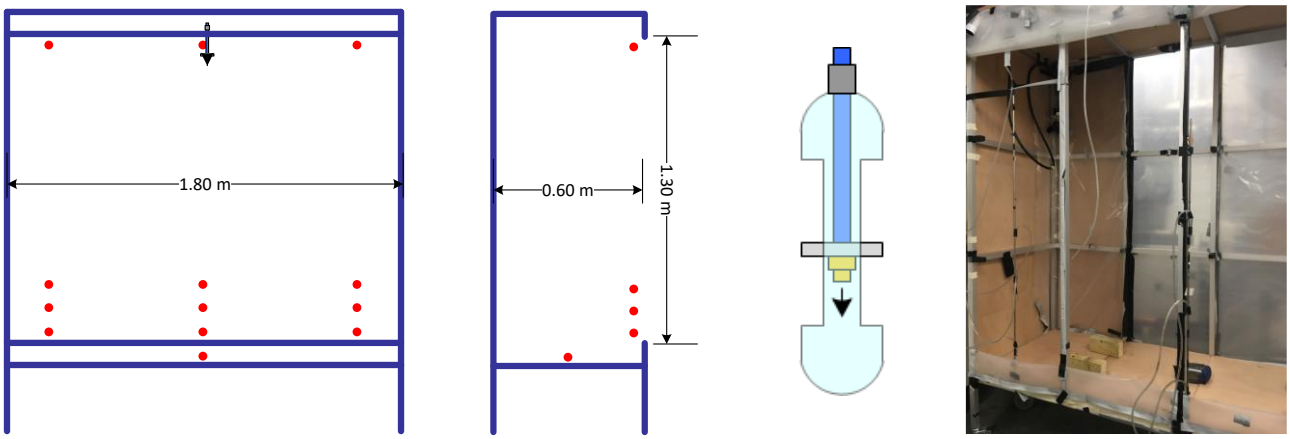

Figure 116: Diagram and photographs of example test arrangement for variable enclosure.

Figure 117 shows how the data was extracted from each test. For mixture exiting the enclosure the concentration at each sampling point was averaged across the minute prior to cessation of the release (yellow box). Then starting about one minute after cessation of the release

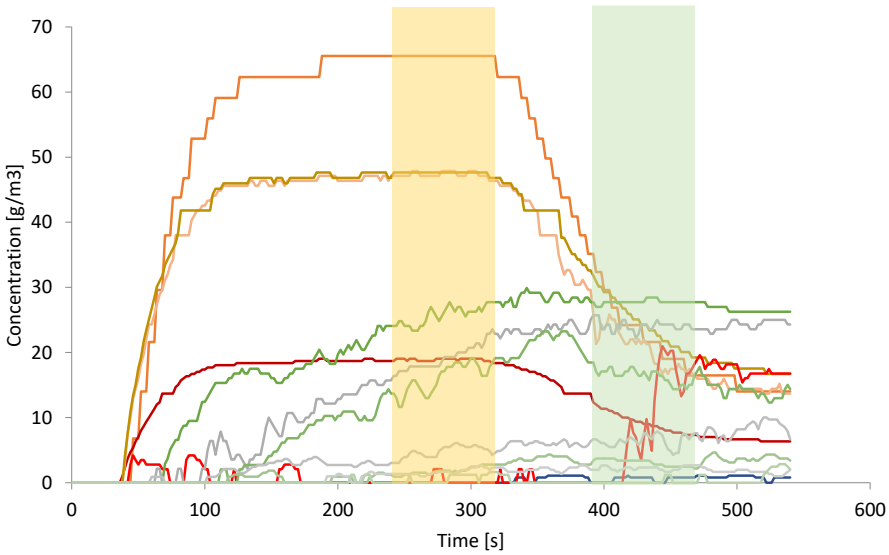

Figure 117: Extracting values for C_f and C_{exit}; orange and yellow lines at enclosure openings, green and grey lines at vertical tower at centre of room.

An example of developing floor concentrations arising from a 300 g and 30 g/min release under different VE configurations is shown in Figure 118. Both the positioning and size of the release and openings can have a significant impact on C_f, for instance, with a high release position and large opening $C_{f,max} \cong 15$ g/m3 whereas a low release position irrespective of the opening size or a low opening irrespective of the release position, gives $C_{f,max} \cong 30$ g/m3.

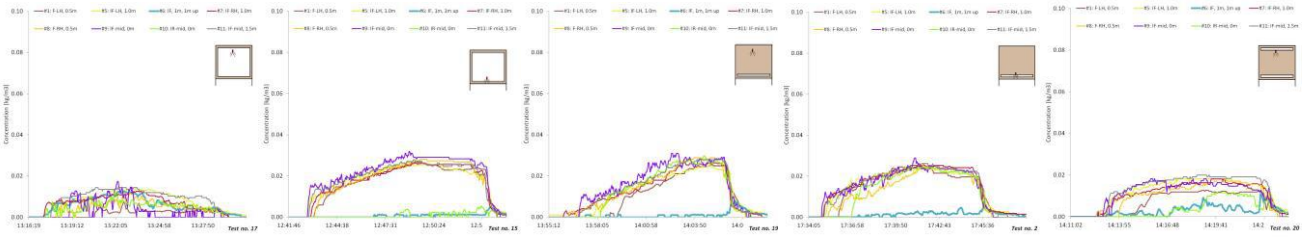

Figure 118: Comparison of floor concentrations with different VE configurations. This figure is to indicate the general behaviour under different conditions.

Across the entire set of tests, a lower exiting concentration tends to result in lower C_f; a basic correlation is seen in Figure 119, which covers all VA sizes, opening positions and dimensions and also the cases with internal (within the VE) airflow. Considering the breadth of variables, this may be deemed a functional correlation, which provides confidence in utilising a charge limit approach based on UHE C_{exit}.

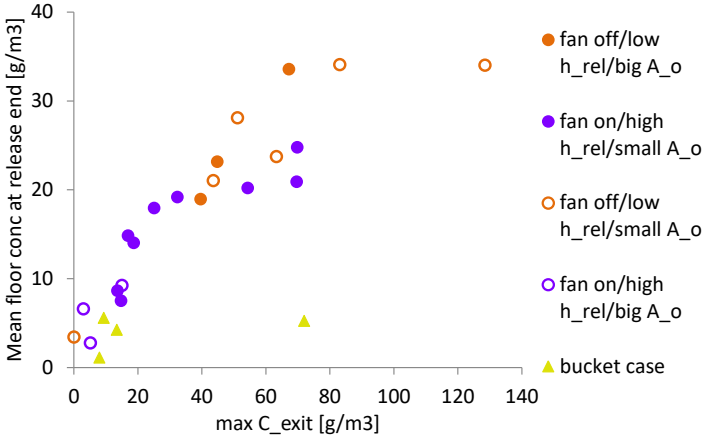

Figure 119: Comparison of C_f and C_{exit} for different VE configurations.

A3.3 Effect of UHE configuration

To help understand the conditions associated with the mixture exiting the UHE, a number of tests were carried out first using a closed enclosure. The structure referred to previously was sealed with plastic sheet and downwards impinging releases at three different mass flow rates were made from three heights (indicated with green arrows) within one corner of the UHE. R290 concentrations were measured at 0.1 m vertical increments. The results in Figure 120 show a marked difference between the vertical distributions arising from the various both mass flow and release height.

For releases at the top of the UHE, the vertical distribution is effectively identical for all release rates and in fact there is almost no variation in concentration within the height of the UHE; the internal concentration is virtually homogenous and this occurs at least whenever the mass flow exceeds a few g/min. With the release

point halfway down the UHE, there is a slightly greater departure from homogeneity compared to the release at the top. The concentration falls off about 4/5ths of the distance to the top of the UHE and whilst the two faster mass flow rates are almost identical, the slower one indicates a higher concentration at the base and reduced value from slightly above the release point. Releases at the base level result is the most pronounced differences, where concentrations at the base are two to three times higher than the previous release heights and the layer height never extends above half of the UHE height. Particularly significant is the impact of mass flow, where a slower release tends to give much higher base concentrations whereas the faster release results in a lower base concentration. This observation is contrary to the observations of releases in (larger) rooms where the higher mass flow always causes higher C_f. In the present case, there is a greater momentum of the release relative to the UHE volume thus generating more turbulence/mixing than if it was in a large space; this phenomenon was also reported by Cleaver et al (1994). Such an effect would be more pronounced in cases where the UHE was smaller and/or the mass flow was faster.

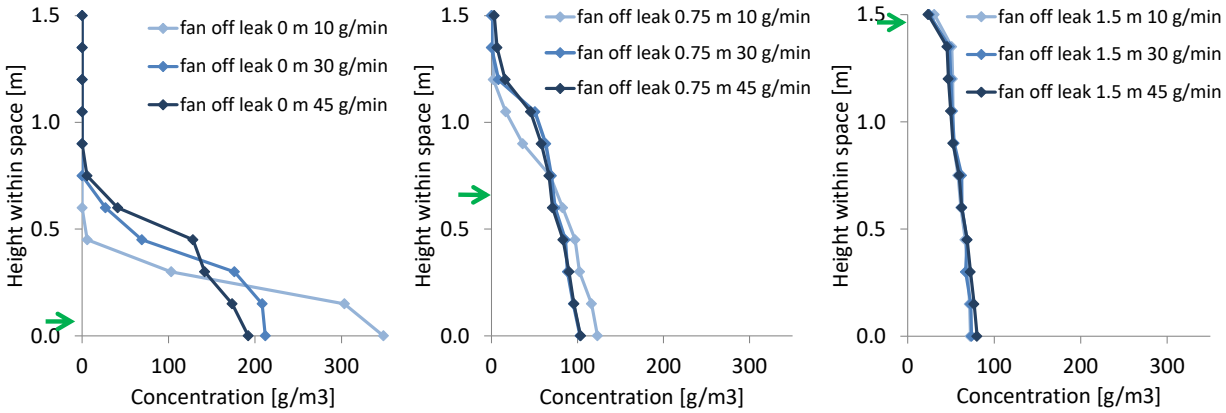

Figure 120: Vertical concentration distribution within sealed enclosure 135 g into a release from three different release heights and three different mass flow rates.

There are several implications arising from these observations.

- Whenever releases occur from the upper part of an UHE, it is likely that it will exit in a well-mixed condition, irrespective of any opening location.
- If releases occur towards the base of the UHE, and depending upon the internal volume and release mass flow, it is possible that the exiting concentration be higher with lower mass flow releases when openings are also close to the base; this is somewhat counter-intuitive0
- Any openings below the top of the UHE will result in internal dilution at different rates.

ANNEX 4 EXPERIMENTAL AND COMPUTATIONAL ASSESSMENT OF F_{LFL}

F_{LFL} was determined from measurements across a range of different conditions.

Critical to this work is consideration of the concentration of the mixture exiting the unit housing or enclosure; this is handled in more detail in the next section.

A4.1 Experimental

There are two approaches to this. The first is to carry out measurements within a room using sensors located vertically at appropriate spacing intervals so that the room concentration can be integrated to estimate the mass of refrigerant below the representative height (e.g., h_b). This approach requires the assumption of a fairly even lateral distribution of mixture concentration across the room (in the event of a limited number of sensors). The second approach is to carry out a number of tests in rooms involving a range of released masses and unit heights and iteratively identify F_{LFL} according to the circumstances that do not result in $\bar{C}_f \geq$ LFL. Whilst this is less precise (that is, it is effectively a trial-and-error scheme) is employed as a means to cross-check the findings from the first approach.

A4.1.1 Test set-up

Both AC IDUs and mock RACHP enclosures/housings were used to determine the concentration distribution. Two IDUs used were typical wall units, one of 8 kW and one of 2.5 kW nominal capacity and were positioned at 0.5 m, 1.0 m and 1.5 m above floor level, mostly at the narrow end of the room, but also on a few occasions along the long wall and at one room corner. Measurements using the variable enclosure had the unit positioned against the centre of the long wall and with its base typically at 0.3 m above floor level. The variable enclosure was designed so that a range of different unit configurations (generally mimicking commercial refrigeration appliances) could be tested.

Except where specified, air was at quiescent conditions.

A4.1.2 Results

Figure 121 includes some example measurements of concentration-height profiles (CHP) at the end of the release. The data on the left for a small (2.5 kW) wall IDU and on the right for a large (8 kW) wall IDU. The shape of the profile remains about the same irrespective of release mass flow, where a higher or lower flow will result in more or less proportionally higher or lower concentrations at a given height.

The graph in Figure 121 shows different profiles for three different VE opening arrangements. Where there is a single opening at the VE base (“0.1”) the CHP indicates a lot of refrigerant close to the floor and very little above about half a metre, similar to the “small F” case in *Figure 122*. However, where there is one large opening covering the height of the VE (“1.3”) the CHP is steeper, mimicking the “large F” case in *Figure 123*. Importantly, it can also be seen that despite the situation with two small openings (“2×0.1”) being geometrically similar to the one small opening (“0.1”), the CHP is almost identical to that with the single large opening.

Throughout all tests with IDUs, the CHP generally converges with zero refrigerant at or just below h_b. This is to be expected following the plume-filling box hypothesis of Baines and Turner (1969). However, with the VE there is no obvious height at which the CHP approaches zero concentration, so therefore a more detailed approach is required.

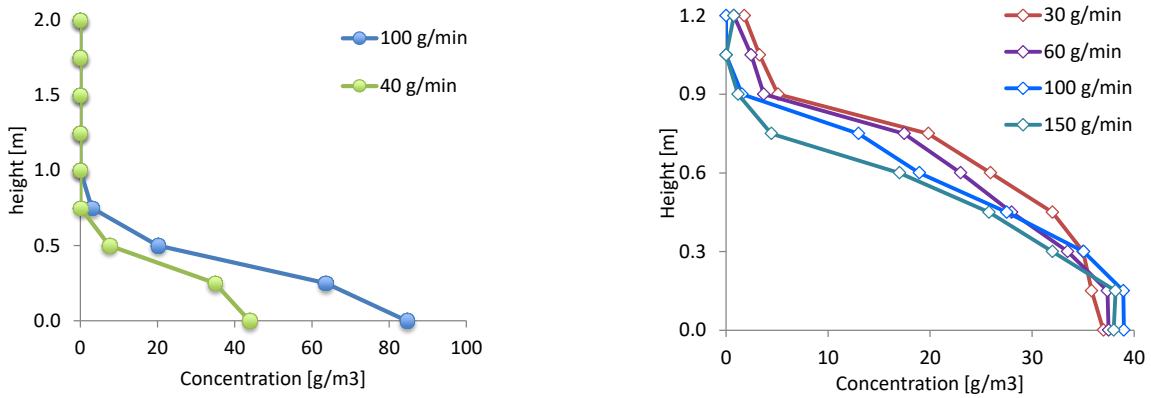

Figure 121: Examples of vertical concentration distribution in room centre for a release from a small 2.5 kW IDU (left) and a large 8 kW IDU (right) both with h_b = 1 m.

As described above equation 4 is proposed for determination of maximum charge, which is a function of some representative height. For the IDU it seems reasonable to set h^* as h_b. Thus F_{LFL} may be determined from experimental data using equation 30:

$$F_{LFL} = \frac{\sum_{i=1}^{h} C_i}{LFL} \tag{30}$$

An example of the determination of F_{LFL} from experimental data using IDUs is shown in Figure 123. Here it can be seen that irrespective of the IDU height (and the same IDU C_{exit}), F_{LFL} always has about the same value.

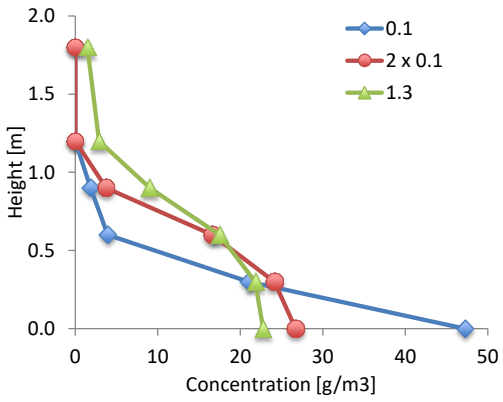

Figure 122: Examples of vertical concentration distribution in room centre for a release from a VE with different openings at h_b = 0.3 m.

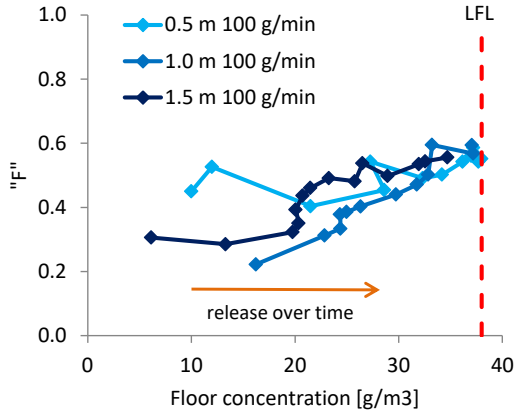

Figure 123: Experimentally determined F for IDUs at different install heights.

Some examples of the layer height behaviour are shown in Figure 124 for four different mass flow rates (and corresponding C_{exit}), where the release position (height) is represented by the red arrow. Generally, the height of the layer is seen to asymptote close to below the IDU, from which point onwards only the floor concentration continues to rise.

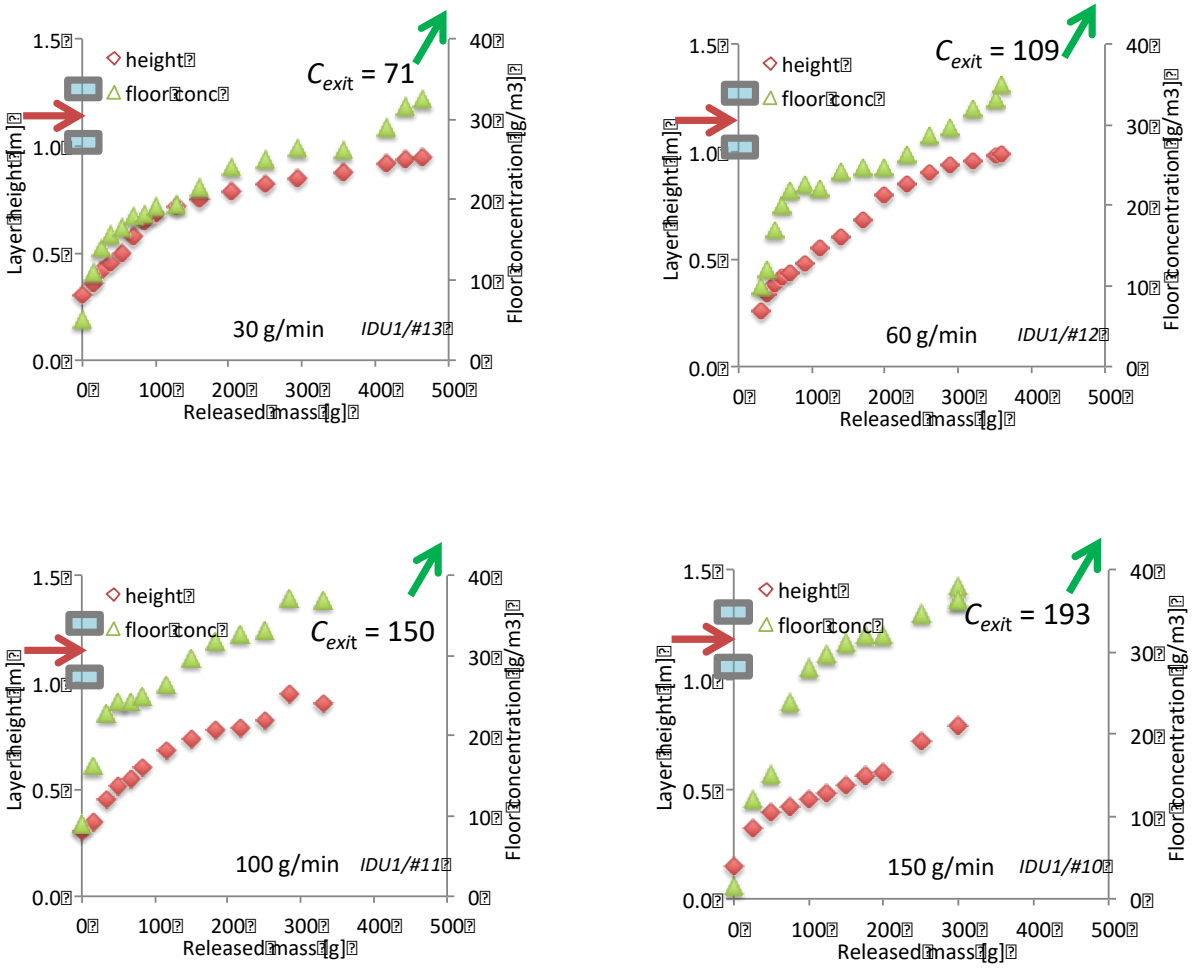

Figure 124: Change in layer height (where CHP à 0) over time for different IDU exit conditions.

For the VE, the situation is a little more complicated.

Some examples of behaviour are shown in Figure 125 for various VE configurations, where the release position (height) is represented by the “spray” graphic. In most cases the height of the layer is seen to asymptote after an initial period, from which point only the floor concentration continues to rise.

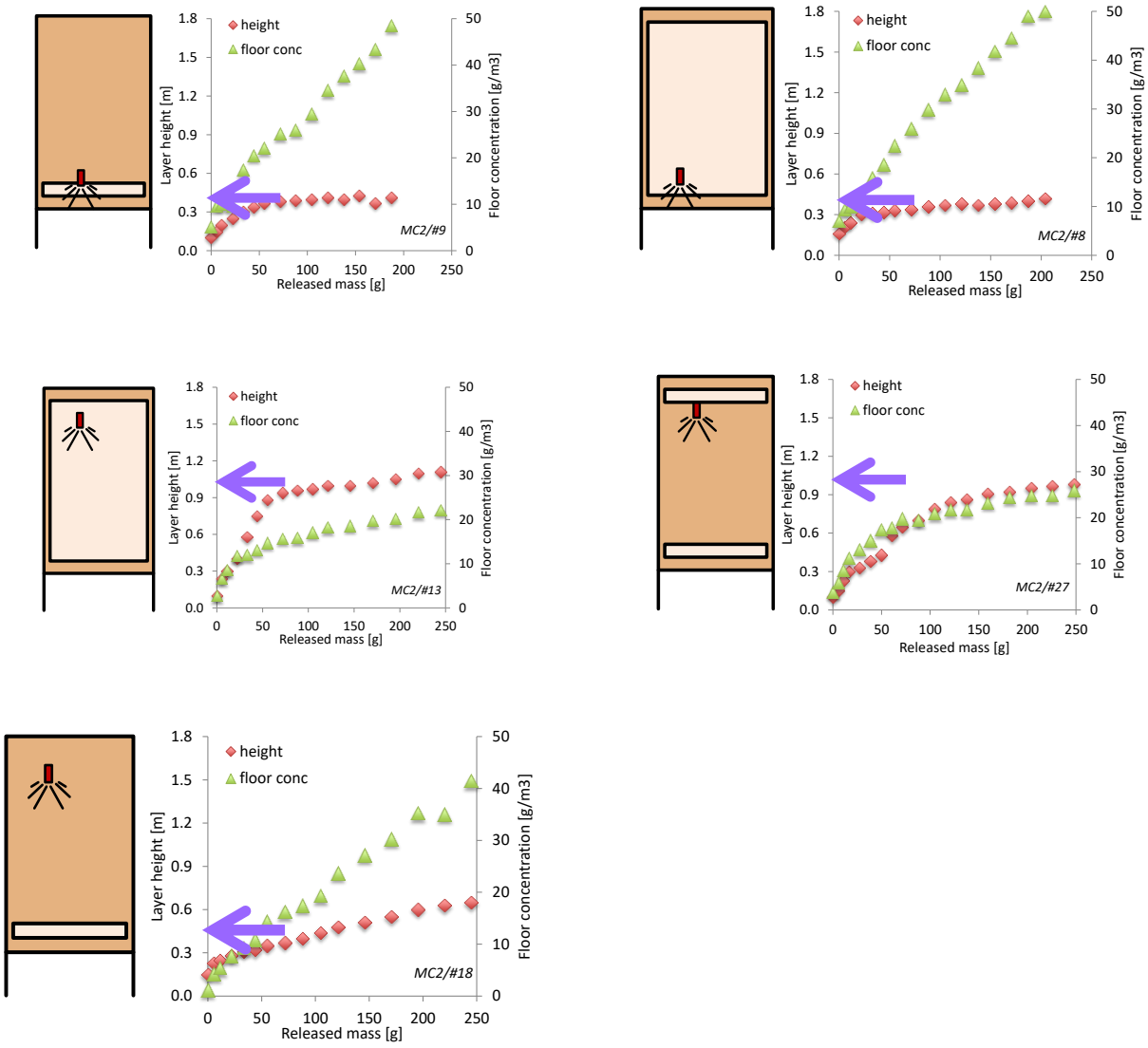

Figure 125: Change in layer height (where CHP à 0) over time for different VE configurations.

Based on these observations, a general rule can be established to approximate the value of set h^*.

If the height of the release is above the height of the top lip of the (upper) opening, i.e., $h_{rel} > h_{up,op}$, then

$$h^* = h_{base} + \frac{1}{2}\left(h_{up,op} - h_{bot,op}\right) \quad (31)$$

When the height of the release is below that of the top lip of the (upper) opening and above the lower lip of the bottom opening, i.e., $h_{bot,op} < h_{rel} < h_{up,op}$, then:

$$h^* = h_{base} + \frac{1}{2}\left(h_{rel} - h_{bot,op}\right) \quad (32)$$

But if the release is below the lower lip of the bottom opening, i.e., $h_{rel} < h_{bot,op}$, then:

$$h^* = h_{base} + h_{bot,op} \quad (33)$$

Note that in this last case, if the lower lip is substantially higher than the release – that is, the release is within a "bucket" – then the end result would be to underestimate m_{max}.

Using these relations, F_{LFL} was determined for the entire set of tests carried out (that were relevant to this analysis) and Figure 126 presents the results plotted against the exiting concentration, C_{exit}.

The curves for the IDUs and VEs were correlated as equation (34) and (35), respectively.

$$F_{LFL} = 4 \times C_{exit}^{-2/5} \tag{34}$$

$$F_{LFL} = 2 \times C_{exit}^{-1/3} \tag{35}$$

The reason for there being two different curves is that certain housing constructions (e.g., VE) are less favourable to better dispersion of the plume whereas others (e.g., IDUs) tend to assist dispersion of the plume. This is believed to be primarily related to the "channelling" effect that an open front enclosure has, whereas a plume that emanates from a wall IDU tends to spread in a 180° span and thus dilutes more readily.

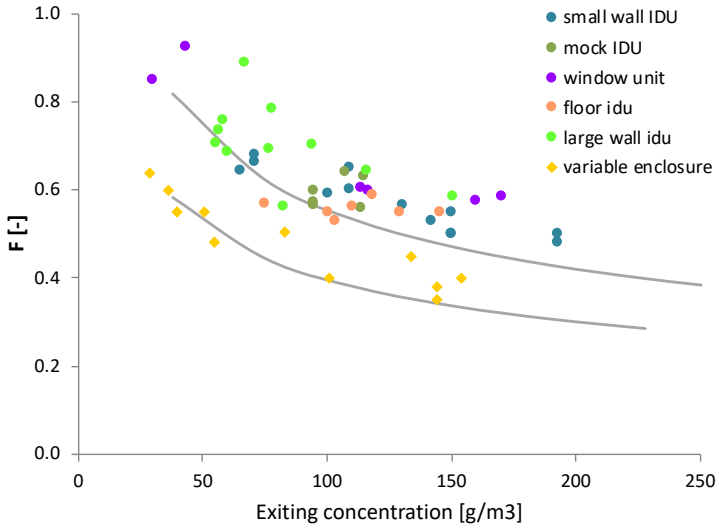

Figure 126: Experimentally determined F_{LFL} using IDUs and VE.

A4.2 Computational analysis

Experimental determination of F_{LFL} can be constrained due to availability of test facilities, such as room size, unit dimensions and refrigerant availability. Therefore, a parametric assessment of F_{LFL} was carried out using CFD, across a range of room sizes, unit characteristics, installation heights and release conditions.

A4.2.1 Model

For the computational work, the CFD package Simflow[20] – which is based on OpenFOAM[21] and Paraview[22] for post-processing – was used. The rhoreactingbuoyantFOAM solver was used, primarily with a laminar model and a mesh ranging from 0.015 m to 0.06 m, according to the spatial location. Entire geometry was isothermal, thermal radiation was neglected, diffusion was disabled (to increase calculation time) and a small opening at the top of the room above the unit from where the release occurs was used to avoid pressurisation. Calculation time steps were set at 0.01 s. For all other parameters, the default values were maintained, such as for transport models, solver solutions and discretisation/interpolation options.

Turbulence was not applied for two reasons. The main reason was for purposes of increasing calculation time whilst the second was to minimise the damping effect turbulence has on mixing so that situations leading to significantly different values of F would become more obvious.

An example of the differences in results arising from inclusion of turbulence models is shown in Figure 127 and Figure 128, with respect to $\bar{C}_f$ and F, respectively. It is evident that turbulence models lead to a representation of better mixing (as would be expected) and thus a higher F_{LFL}, for a given set of conditions. As such, neglecting turbulence leads to a more pessimistic result.

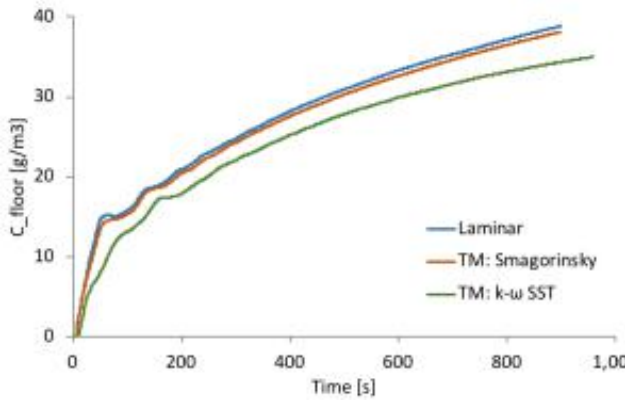

Figure 127: Comparison of laminar and selected turbulence models on $\bar{C}_f$.

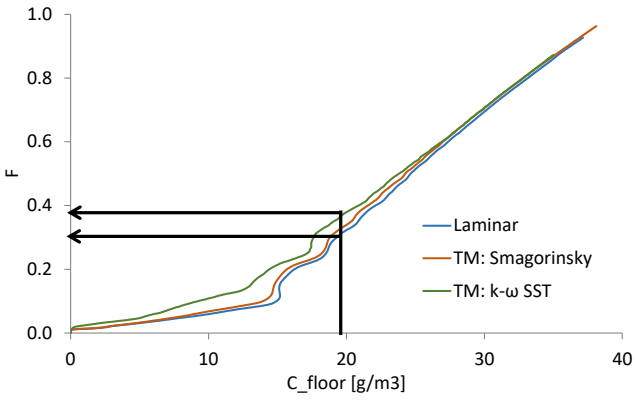

Figure 128: Comparison of laminar and selected turbulence models on F.

In addition to calculating the mass and concentration of refrigerants, the volume of the flammable mixture throughout the release duration was also quantified for purposes of further analysis.

Note that the model was not necessarily calibrated against measurements. Whilst reasons for this are elaborated later, the purpose of the calculations was to "amplify" the most pessimistic outcomes to help identify any important trends and therefore an accurate model was not deemed essential to this stage of the work.

[20] https://sim-flow.com
[21] https://openfoam.com
[22] https://www.paraview.org

A4.2.2 Configuration and geometry

To minimise the extent of complicating variables, a simple arrangement was chosen, where an AC IDU was positioned on a wall of an empty room and a specified dilute refrigerant-air mixture was released at a fixed mass flow rate from within the IDU, until $\bar{C}_f$ > LFL.

About 20 cases were calculated, as listed in Table 18, all of which used R290 except for two which additionally employed selected other flammable refrigerants. Through these various cases, it was considered that the inputs represented a wide range of conditions that could be anticipated with common RACHP equipment.

Table 18: Parameters used for the various CFD cases.

Case	Unit size	Height [m]	A_room [m2]	Condition	Mf [g/min]	C_{out} [g/m3]
#1	8 kW	1	13.5	v2	60	489
#2	8 kW	1	13.5	v3	60	245
#3 *	8 kW	1	13.5	v4	60	98
#4	8 kW	1	13.5	v5	120	152
#5	8 kW	1	13.5	v6	120	380
#6 *	8 kW	1	13.5	v7	120	759
#19	8 kW	1	13.5	v8	180	196
#7	16 kW	1	13.5	v4	60	98
#8	16 kW	1	13.5	v7	120	759
#11	8 kW	1	54	v4	60	98
#12	8 kW	1	54	v7	120	759
#9	4 kW	1	13.5	v4	60	98
#10	4 kW	1	13.5	v7	120	759

Case	Unit size	Height [m]	A_room [m2]	Condition	Mf [g/min]	C_{out} [g/m3]
#11	8 kW	2	13.5	v4	60	98
#12	8 kW	2	13.5	v7	120	759
#13	8 kW	0.5	13.5	v4	60	98
#14	8 kW	0.5	13.5	v7	120	759
#17	8 kW [tall] #	1	13.5	v4	60	98
#18	8 kW [tall] #	1	13.5	v7	120	759

* Also with R600a, R32, R1234yf and R152a

The "tall" unit is with a 1 m high body as opposed to 0.3 m

Details of the IDU geometry are shown in Figure 129, where C_{out} is the defined outlet concentration of the IDU, but C_{exit} is the resulting exiting concentration due to entrainment of gas from above the IDU and subsequent internal mixing. These inputs were selected to help reflect the measured C_{exit} reported below/above. Additionally, this "flow through" arrangement was chosen to mimic recirculation of mixture back into the IDU and the associated dilution.

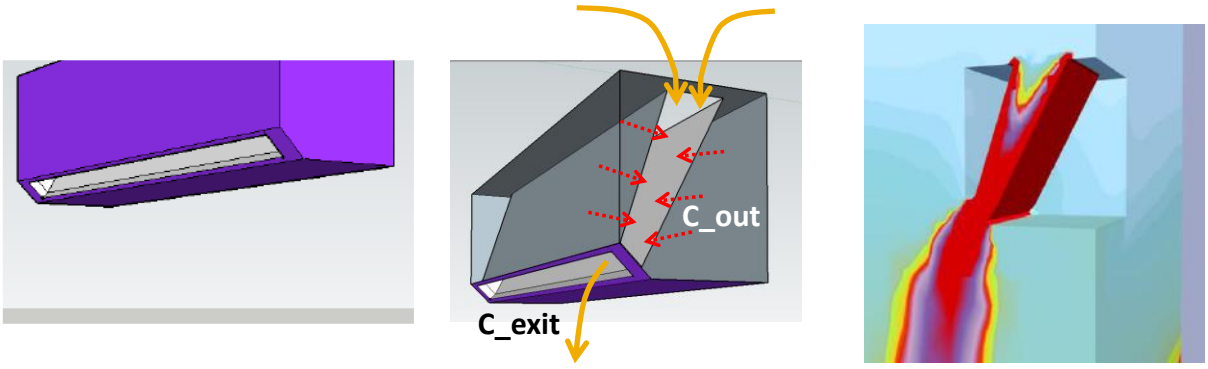

Figure 129: Illustration of IDU external geometry (left) where the exterior is removed to show the internal faces from where a fixed concentration mixture is released (centre) and a screen-grab of concentration contours to demonstrate the flow path (right).

Each case calculation proceeded until $\bar{C}_f$ exceeded LFL. Data was extracted to determine the mass of refrigerant and free volume below h_b and below 0.05 m above the floor (see Figure 130, left), at each time-step. Thus, F_{LFL} is determined by:

$$F_{LFL} = \frac{\int_0^h C_r dh}{LFL \times h_b \times A} \tag{36}$$

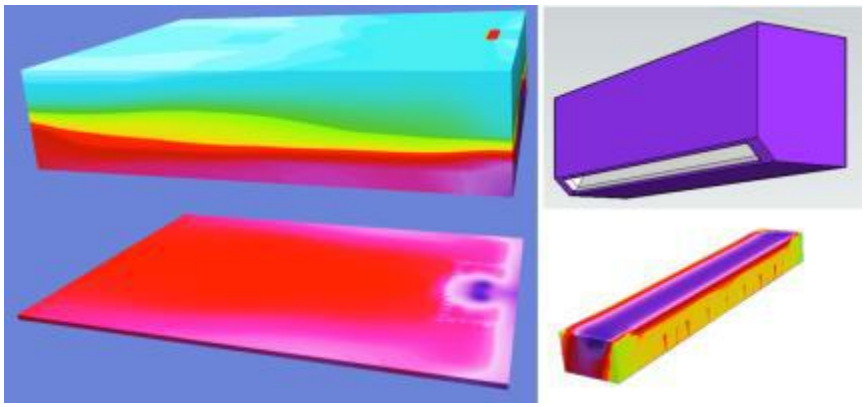

Figure 130: Elements integrated to determine mass of refrigerant at relevant spatial regions.

In addition, the same procedure was carried out for a small volumetric element at the IDU outlet (see *Figure 130*, right) in order to determine the average exiting concentration, $\bar{C}_{exit}$. Example results are shown in *Figure 131* for Case #3 and #4. Whilst $\bar{C}_{exit}$ is seldom constant for the release duration (i.e., until $\bar{C}_f = LFL$) the variation is always within ±5 g/m^3 once the initial transients have settled. Averaged values of $\bar{C}_{exit}$ are latterly used to correlate with the case results. Note that although $\bar{C}_{exit}$ is influenced by $\bar{C}_{out}$ there is no such correlation between the two since the IDU geometry affects the internal mixing and thus $\bar{C}_{exit}$.

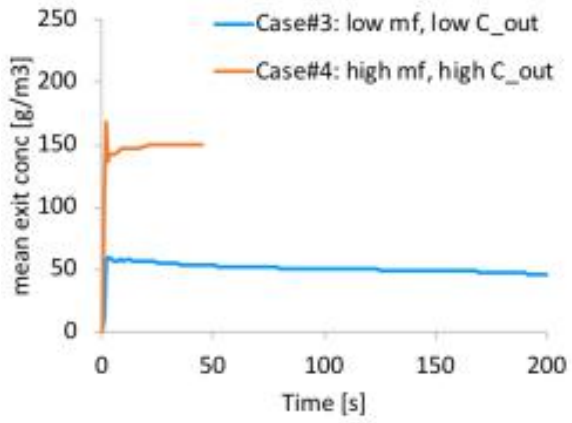

Figure 131: Example results for mean exit concentration for Case #3 and Case #4 (x-axis limited to 200 s only to help display case #4 more clearly).

A4.2.3 Calculation outputs

Some example results for mean floor concentration ($\bar{C}_f$) and F_{LFL} are provided in Figure 132. The left graph shows $\bar{C}_f$ for Case #3 and Case #6 over time, corresponding to a low $\dot{m}_r$ and C_{out} and high $\dot{m}_r$ and C_{out}, respectively. The right graph is for the two same cases but for F plotted against $\bar{C}_f$. F_{LFL} is determined at the

point when $\bar{C}_f = LFL$, thus for the two cases shown, F_{LFL} = 0.29 and F_{LFL} = 0.95 for Case #3 and Case #6, respectively.

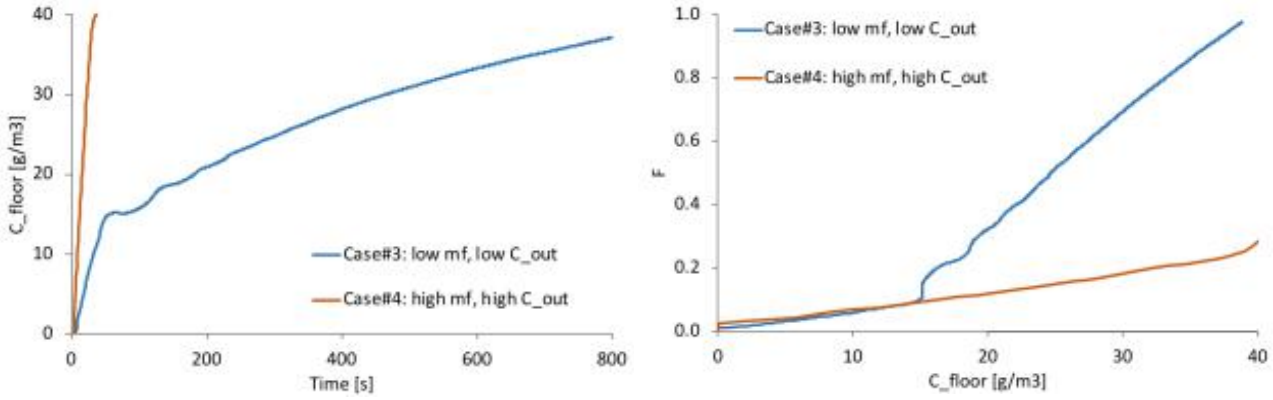

Figure 132: Example plots of C_f and F for cases #3 and #6.

Values for F_{LFL} for R290 across all cases are presented in Figure 133. A similar trend to that established for the experimental analysis is observed, where F_{LFL} reduced from almost unity when $\bar{C}_{exit} \sim LFL$ and reduces as $\bar{C}_{exit}$ increases and at these higher values of $\bar{C}_{exit}$ a wider relative deviation develops. This suggests that any correlation should be more cautionary towards higher $\bar{C}_{exit}$.

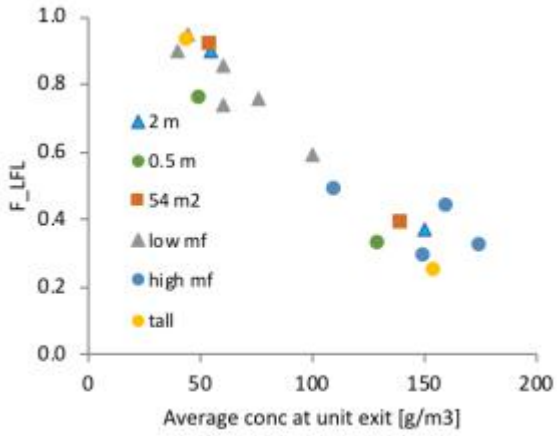

Figure 133: Compilation of CFD results for R290, plotting F_{LFL} against $\bar{C}_{exit}$.

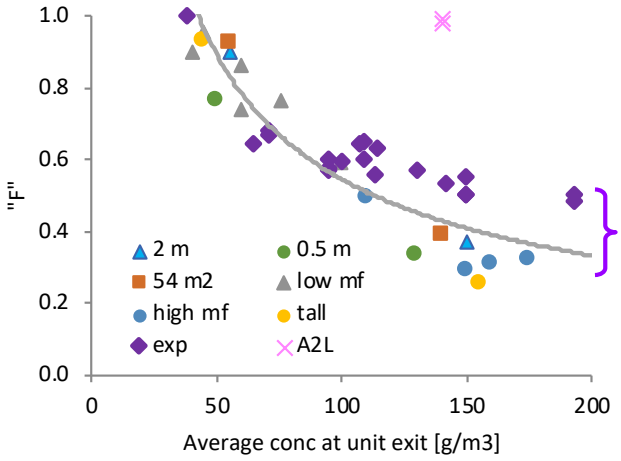

Figure 134: Results from Figure 133 but with data points from experimental work (Figure 126) superimposed.

ANNEX 5 CHARGE LIMITS FOR EQUIPMENT WITH INTEGRAL CIRCULATION AIRFLOW

A5.1 Introduction

Many RACHP systems normally have a set airflow rate which is defined by the manufacturer to provide a given capacity, air throw, etc. and for certain types of equipment (e.g., air conditioners) users usually have control to some extent by means of several incremental fan speed settings, although not for other types of systems (display cabinets, cold room evaporators, etc.). It is necessary to identify whether the minimum airflow level is adequate to dilute a release of refrigerant in case of a leak and thus whether the manufacturer would need to assign a higher minimum airflow rate to achieve dilution. Too low airflow will result in formation of a flammable mixture at the room floor (under a given leak condition), whereas a requirement for excessively high airflow may result in unwarranted equipment costs (large fan/motor and housing) and energy costs.

Various methods for determining minimum airflow rate for prevention of flammable mixtures have been proposed elsewhere. A formula is provided within IEC (2015) that can be transposed for minimum airflow rate of extract ventilation (equation 37), for the presumption that a given continuous release does not form a flammable mixture greater than 1% of the room volume.

$$\dot{V}_{min} = \frac{\dot{m}_{leak}}{\rho_g} - \frac{f \times \dot{m}_{leak}}{\rho_g \phi LFL_v} \tag{37}$$

where $\dot{V}_{min}$ is the minimum airflow rate (m^3 s^{-1}), $\dot{m}_{leak}$ is the release mass flow rate (kgs^{-1}), ρ_g is the gas density (kg m^{-3}), ϕ is a dimensionless multiplier for the lower flammability limit (LFL), dictating the ventilation outlet concentration (i.e., <1 to ensure the mixture is non-flammable), LFL_v is LFL as volume fraction and f is a factor used to account for the internal mixing efficiency that may range from 1 (e.g., an empty room) up to 5 (e.g., a highly congested room). Alternatively, Colbourne and Suen (2008) proposed an expression for determining maximum floor concentration arising from a refrigerant release due to several installation and equipment characteristics which can be transposed to estimate minimum airflow rate. More recently the proposal of IEC (2017) for "A2L" refrigerants defines a minimum airflow rate (equation 38) and discharge velocity of 1.0 m s^{-1}.

$$\dot{V}_{min} = 30 \times m_c / LFL_m \tag{38}$$

where $\dot{V}_{min}$ is the minimum airflow rate (m^3 h^{-1}), m_c is system refrigerant charge (kg), LFL_m is LFL as mass per volume (kg m^{-3}) and 30 is a constant relating to assumed refrigerant leak mass flow rate.

There are several shortcomings with these approaches. IEC (2015) assumes infinite release duration and that the airflow removes some of the mixture from the room whilst replenishing with fresh air; this does not suitably represent the case of a RACS in a closed room. Colbourne and Suen (2008) is based on a variety of highly pessimistic assumptions, such as the release originating from outside the unit housing and at low momentum and very high release mass flow rates, and the application of the formula itself is possibly too unwieldly for use in a standard. IEC (2017) only accounts for a fixed and similarly high release rate but also neglects the effect of RACS discharge or room air speed on mixing. Thus, there is a clear need for a broadly universal approach for determining the minimum airflow rate of RACS, taking account of the various construction and installation characteristics of RACS as well as being relatively simple to apply for non-specialists. In order to do this, the airflow conditions associated with a RACS are identified and the applicable principles for airflow mixing are introduced. This leads to the development of a general formula, which is

then examined with respect to practicalities experimentally and eventually the formulae are adjusted to account for empirical findings.

A5.2 Concept development

When a jet of air (e.g., from a RACHP enclosure outlet grille) discharges into a free volume it entrains air from the surroundings so that that total volumetric airflow rate of the field gradually increases (*Figure 135*). If that jet comprises a stream of leaked refrigerant then the concentration of refrigerant within the flow field should also gradually decrease as more air is entrained, assuming that the flow within the jet remains turbulent. Greater discharge volume flow rate increases rate of entrainment and therefore leads to more dilution. Eventually the flow will terminate, either at the opposite wall or on the room floor, depending upon whether the buoyancy effects or the momentum effects of the jet dominate; also indicated in *Figure 135*. Thus, the maximum concentration observed at the opposite wall or floor would correspond to the mean concentration within the cross-section of that jet at the point that it terminates. If this maximum concentration at jet termination is set to refrigerant LFL, then the corresponding minimum airflow rate and jet outlet characteristics may be determined.

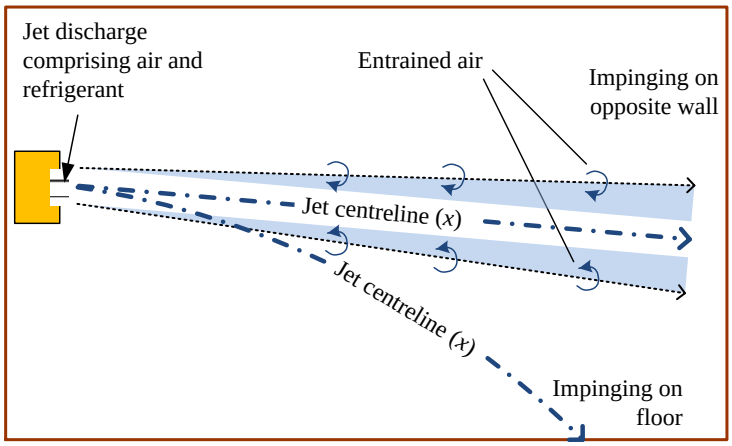

Figure 135: Schematic of entrainment process and jet termination.

The analysis requires a number of assumptions: that there is negligible air exchange between the room and its surroundings, conditions are isothermal, .that the refrigerant vapour is denser than air, leak is of constant mass flow rate, negligible transit time for an element of refrigerant to flow from the IDU to the floor or wall, and – for the present work – the air discharge direction is horizontal.

A5.3 Entrainment

Classical entrainment hypothesis is that the rate of entrainment of surrounding fluid across a jet or plume boundary is proportional to the average centreline velocity and perimeter of the flow field:

$$\frac{d\dot{V}}{dx} = P\alpha\bar{u}_c \tag{39}$$

where $\dot{V}$ is volume flow rate (m^3 s^{-1}), x is distance along the jet (m), P is perimeter around the flow field (m), α is entrainment coefficient and $\bar{u}_c$ is centreline velocity along x direction (m s^{-1}). From this, Etheridge and Sandberg (1996) derive closed equations for volume flow rate of neutrally buoyant jets at some distance from the jet exit. Since most RACS IDUs have high aspect ratio outlets, their model for plane jets is selected:

$$\dot{V}(x) = b\dot{V}_o\sqrt{\frac{\alpha x}{A_o}} \tag{40}$$

where the constant $b = 2^{5/4} \approx 2.4$ and A_o is the area of the jet outlet aperture (m^2).

At any distance x from the outlet, the flow rate $\dot{V}(x)$ is the sum of the outlet airflow rate ($\dot{V}_o$) and the additional airflow that has been entrained until distance x. Therefore, the total entrained airflow, $\Sigma\dot{V}_e$ until x is $\dot{V}(x)$ minus that from the outlet:

$$\Sigma\dot{V}_e(x) = b\dot{V}_o\sqrt{\frac{\alpha x}{A_o}} - \dot{V}_o \tag{41}$$

A5.4 Jet termination

A negatively buoyant jet is discharged horizontally comprising denser than air refrigerant will eventually impinge on the floor. From Etheridge and Sandberg (1996), using the constants for a plane jet with identical boundary for flow and concentration fields, the expression for the distance travelled until termination (x_T) along an unobstructed jet centreline is:

$$x_T = \left\{h_o \frac{3.75A_o}{f(I)Ar_o b\sqrt{\alpha}}\right\}^{0.4} \tag{42}$$

where Ar_o is the non-dimensional Archimedes number based on the outlet conditions, as given below, h_o is the centre height of the jet outlet (m) and $f(I)$ is a combination of volume, momentum, energy and buoyancy flux integrals determined analytically by Etheridge and Sandberg; $f(I)$ = 0.39. Archimedes number for the IDU discharge condition is:

$$Ar_o = g'\frac{\sqrt{A_o}}{u_o^2} \tag{43}$$

where g' is the reduced gravity (m s^{-2}) and u_o is the velocity at IDU air discharge (m s^{-1}).

Note that as the jet proceeds into the surroundings and more air is entrained the average concentration will reduce, so g' and thus Archimedes number become smaller; the result is the trajectory becomes less steep so lengthening x_T. Were this aspect to be accounted for in the model it forms an implicit solution and

therefore difficult to compute. Since using Ar_o must produce a more pessimistic result (higher floor concentration) then it was opted to adopt this simplification of using IDU discharge Ar_o. Since $u_o = \dot{V}_o/A_o$:

$$Ar_o = g' \frac{A_o^{2.5}}{\dot{V}_o^2} \tag{44}$$

Since to be in a useable form g' must be based on the IDU discharge condition, i.e., at the start of the release where surrounding air is uncontaminated and discharge concentration (C_o) is known:

$$g' = g\left(\frac{\rho_m - \rho_a}{\rho_a}\right) \tag{45}$$

where g is gravity, ρ_m is density of the refrigerant-air mixture (kg m^{-3}) and ρ_a is air density (kg m^{-3}). The mixture density may be approximated as $\rho_m \cong C_o + \rho_a$, where C_o is refrigerant concentration (kg m^{-3}) in the discharged air.

For the time being, assuming that the release mixes homogenously with the entire airflow within the IDU housing, bulk mean concentration of the discharged jet would be:

$$C_o = \frac{\dot{m}_{leak}}{\dot{V}_o} \tag{46}$$

Substituting (46), (45) and (44) into (42), and combining the constants yields:

$$x_T = \left\{h_o \frac{9.6\dot{V}_o^3 \rho_a}{g\dot{m}_{leak} A_o^{1.5} b\sqrt{\alpha}}\right\}^{1/2.5} \tag{47}$$

However, if the room is sufficiently small then the jet can impinge on the opposite wall of the room in which case termination distance is taken as the representative distance across the room:

$$x_T = \sqrt{A_{rm}} \tag{48}$$

where A_{rm} is the room floor area (m^2).

With higher refrigerant leak rates or lower airflow rates the distance to the floor is generally less than $\sqrt{A_{rm}}$. Therefore, it is reasonable to use the approach for a negatively buoyant jet impinging on the floor for the analysis.

A5.5 Dilution process

Refrigerant concentration within the IDU air discharge was defined in equation (46). At the time that the release begins (say, at time = $t1$) and assuming the jet enters an uncontaminated space and that the refrigerant continues to mix homogenously within the progressing jet, concentration at some distance (x) along the jet is:

$$\bar{C}(x) = \frac{\dot{m}_{leak}}{\dot{V}(x)} \tag{49}$$

Over time, the discharged refrigerant will mix within the room and therefore the entrained air comprises an increasingly richer mixture, peaking at cessation of the leak. Thus, the total volume of air that has been entrained into the jet for the duration of the leak, or the volume of air within the room, whichever the smaller, is used to estimate the average concentration of the surrounding air at the time of cessation of the release (time = $t2$), i.e.:

$$\bar{C}_{sur,t2} = \frac{m_r}{min\{\Sigma\dot{V}_e t_{leak}, V_{rm}\}} \tag{50}$$

where m_r is the total mass of refrigerant released (kg) and t_{leak} is the time over which it is released (s), i.e., $t2 - t1$.

In practice, there is usually a minimum IDU airflow rate associated with a given capacity (typically in the order of 75 $m^3\ h^{-1}$ per kW) and thus room size on account of the associated heat load and a certain air discharge opening area to ensure the necessary air throw. Quantifying the term $\Sigma\dot{V}_e t_{leak}$ across a wide range of conditions, including leak time, indicates that V_{rm} will always be exceeded by up to a factor of five. Whilst this does not guarantee that the released refrigerant will be perfectly distributed throughout the entire room, it does provide some confidence that the term $min\{\Sigma\dot{V}_e t_{leak}, V_{rm}\}$ can simply revert to V_{rm}; thus $\bar{C}_{sur,t2}$ is the mean room concentration. This assumption has been further supported by CFD simulations over a wide range of scenarios (see Figure 137).

For any given time, the maximum concentration at floor level must correspond to the concentration within the jet as it approaches the floor or wall. At the beginning of the release ($t1$), that maximum concentration corresponds to the termination position of the jet as in equation (46), when setting $x = x_T$, i.e.:

$$\bar{C}_{max,t1} = \frac{\dot{m}_{leak}}{\dot{V}(x_T)} \tag{51}$$

As mentioned above, moments before cessation of the release the entrained air along the trajectory of the jet will also comprise refrigerant mixed within the room and in addition the refrigerant within the air drawn into the IDU suction. Thus, at cessation of the leak the maximum concentration will be:

$$\bar{C}_{max,t2} = \frac{\dot{m}_{leak}+\dot{m}_{sur}+\dot{m}_{suct}}{\dot{V}(x_T)} \tag{52}$$

where $\dot{m}_{sur}$ is the mass flow of refrigerant from the surroundings (kg s^{-1}), i.e. from the entrained mixture, is:

$$\dot{m}_{sur} = \bar{C}_{sur,t2}\Sigma\dot{V}_{e,t2} \tag{53}$$

And $\dot{m}_{suct}$ is the mass flow of refrigerant into the IDU suction (kg s^{-1}); since the volume flow of air into the IDU must be the same as that being discharged ($\dot{V}_o$), then:

$$\dot{m}_{suct} = \bar{C}_{sur,t2}\dot{V}_o \tag{54}$$

Substituting equations (50), (53) and (54) into (52), the maximum concentration at cessation of the release can be expressed as a function of exit airflow rate:

$$\bar{C}_{max,t2} = \frac{\dot{m}_{leak}}{\dot{V}(x_T)} + \frac{m_r}{V_{rm}} \tag{55}$$

Introducing equation (40) into (55) enables $\bar{C}_{max,t2}$ to be determined as a function of IDU airflow in the case of full room mixing (equation 56).

$$\bar{C}_{max,t2} = \frac{\dot{m}_{leak}}{b\dot{V}_o\sqrt{\frac{\alpha x_T}{A_o}}} + \frac{m_r}{V_{rm}} \tag{56}$$

By setting $\bar{C}_{max,t2}$ = LFL_m and rearranging, plus with the introduction of a new dimensionless term (R) to account for heterogeneity of the discharged refrigerant-air mixture (see section A 5.7), equation (56) provides an explicit formula (equation 57) for determining minimum required airflow rate.

$$\dot{V}_o = \frac{\dot{m}_{leak}}{Rb\sqrt{\frac{\alpha x_T}{A_o}\left(LFL - \frac{m_r}{V_{rm}}\right)}} \quad (57)$$

Finally, equation (47) or (48) can be inserted into equation (57) and combining constants (including R = 1/3), yields equations (58) and (59), respectively.

$$\dot{V}_{o,min} = \frac{5.6\dot{m}_{leak}\sqrt{A_o}}{A_{rm}^{1/4}\left(LFL - \frac{m_r}{V_{rm}}\right)} \quad (58)$$

$$\dot{V}_{o,min} = \frac{4\dot{m}_{leak}^{3/4}\sqrt{A_o}}{h_o^{1/8}\left(LFL - \frac{m_r}{V_{rm}}\right)^{5/8}} \quad (59)$$

Under some situations, the jet will terminate on the opposite wall of the room, i.e., $x_T > \sqrt{A_{rm}}$, where equation (58) is applicable. When lower leakage mass flow rates are assumed (which implicitly results in lower $\dot{V}_{o,min}$) and the IDU is closer to the floor, the trajectory of the negatively buoyant jet veers towards the floor before reaching the opposite wall ($x_T < \sqrt{A_{rm}}$); in this case equation (59) needs to be applied. Through extensive evaluation of all applicable variables, equation (59) need only be applied when the R290 leak mass flow rate is less than, $\dot{m}_{leak} = m_r/(145 \times h_0 + 180)$.

Assessment of the approach was also carried out with CFD software (Simflow/OpenFOAM[23]), evaluating a range of conditions typical for RACS (airflow rate, discharge area, release mass and mass flow, unit height, discharge direction and room size). On average (e.g., over a several second duration to smooth out the "flapping" phenomenon), the trajectory of the jet was mostly less pronounced than equation (47) inferred. The exception was with units close to the floor where the Coandă effect helps draw the jet closer to the floor. But in all cases the extent of the LFL boundary was further from the floor or wall as anticipated by the model; examples are provided in Figure 136, Figure 137 and Figure 138.

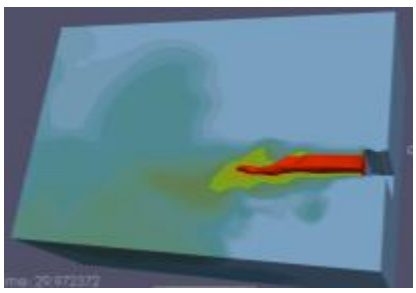

Figure 136: Contours showing trajectory, A_o = 0.20 m2, 500 g at 141 g min-1; x_T = 5.5 m.*

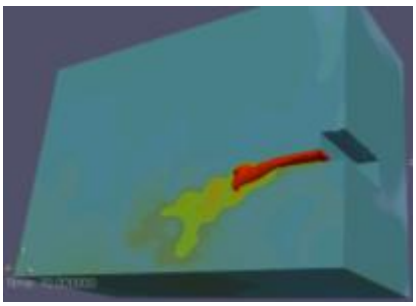

Figure 137:Contours showing trajectory, A_o = 0.05 m2, 500 g at 141 g min-1; x_T = 5.5 m; nearly all room air mixed within 70 s.*

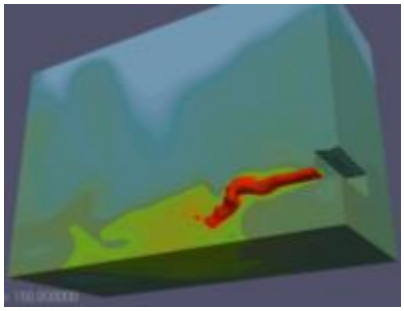

Figure 138: Contours showing trajectory, A_o = 0.05 m2, 500 g at 141 g min-1; x_T = 4.1 m.*

[23] https://sim-flow.com/; solver: rhoreactingbuoyantFOAM, turbulence model: RANS RNG κ-ε; mesh: 0.015 – 0.06 m

* Red contour is region above LFL; green is 0.5×LFL to LFL; pale blue is <5% of LFL; room length = 4.5 m

A5.6 Measurements

A series of measurements were conducted to clarify several aspects, such as understanding the heterogeneity of the mixture at IDU discharge, the lateral distribution within the room and also a variety of different conditions to help validate the proposed formulae.

A5.7 IDU exit condition

An initial assumption was that a release of refrigerant within an IDU is fully mixed within the airflow, before being discharged. Experiments were carried out in order to examine the validity of this assumption. Two types of IDU's were considered: three typical "wall" units and a "floor" unit. R290 releases of various constant mass flow rates were made from different positions within the IDUs over a range of airflow rate settings.

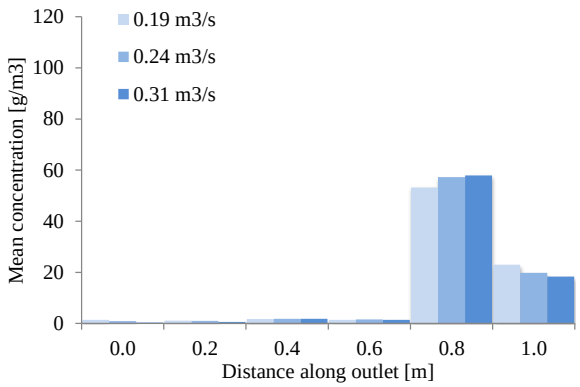

Figure 139: Measurements of R290 concentration within air discharged from an IDU at varying airflow rates.

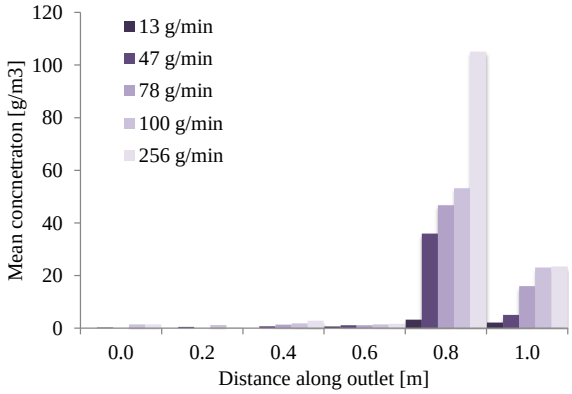

Figure 140: Measurements of R290 concentration within air discharged from an IDU at varying release mass flow rates.

With the floor IDU, R290 concentrations were measured at six equidistant positions along the centreline of the air discharge outlet. Figure 139 shows results with a 100 g/min release simulated from the coil right hand return bends and airflow rates of 0.19, 0.24 and 0.31 m3 s-1, whilst the results in Figure 140 used a fixed 0.19 m3 s-1 airflow and release rates ranging from 13 to 256 g min-1. These indicate that irrespective of the conditions, refrigerant remains within about one-third of the discharged air, with the majority being within 1/5th.

Releases were simulated at four other locations, as indicated in Figure 141. Positioning and orientation of the releases were intended to create as much pre-mixing within the IDU as possible before the R290 was discharged with the air. Whilst most of these alternative release positions did lead to a wider distribution of refrigerant across the discharged air (Figure 142), full homogeneity could not be achieved.

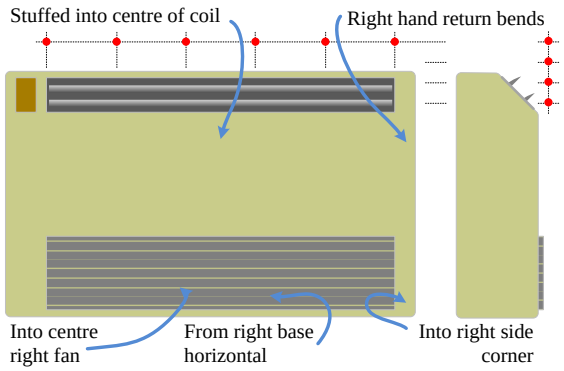

Figure 141: Positions/direction of additional release points and position of sampling points (red dots).

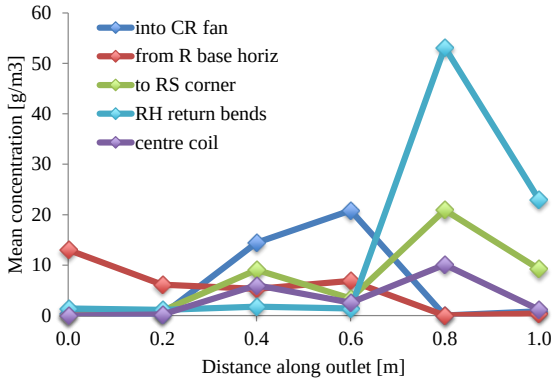

Figure 142: Average concentration at linear distances along air discharge arising from different release points.

Further measurements were carried out on wall IDUs in a similar fashion, but with a finer distribution of sampling points (40 mm apart) and covering the width of the outlet at five angular locations relative to the horizontal (270°). Figure 143 and Figure 144 show local R290 concentrations for a low (480 m3 h-1) and high (1260 m3 h-1) IDU airflow rate arising from a 30 g min-1 release rate from the coil return. A similar tendency with the floor IDU is seen, where the majority of refrigerant is discharged from about half of the discharge opening (about 225° to 270°) and about one-quarter of the length. This pattern was replicated in both 2.5 kW and 8 kW IDUs and over several different leak positions and orientations about the right-hand return bends.

Maximum local values along the length are given in Figure 145 for four different airflow rates. As with the floor IDU, increasing airflow rate does not help homogenise the exit concentration. Comparing the peak concentrations against the bulk mean concentration (as expressed in equation 46) Figure 146 indicates a large discrepancy in the order of eight to 15, inherent in the assumption of homogenous mixing inside the IDU.

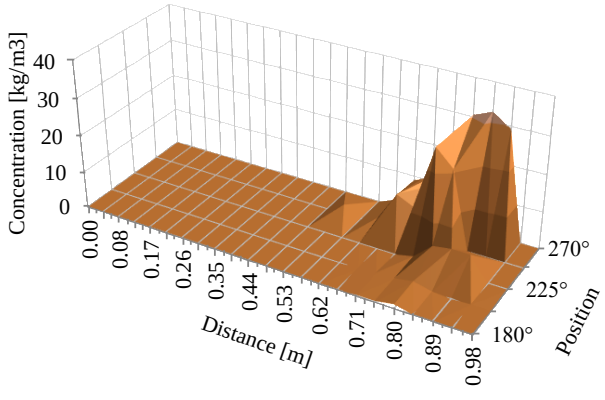

Figure 143: Local R290 concentration at wall unit discharge with 30 g/min and 480 m3/h airflow.

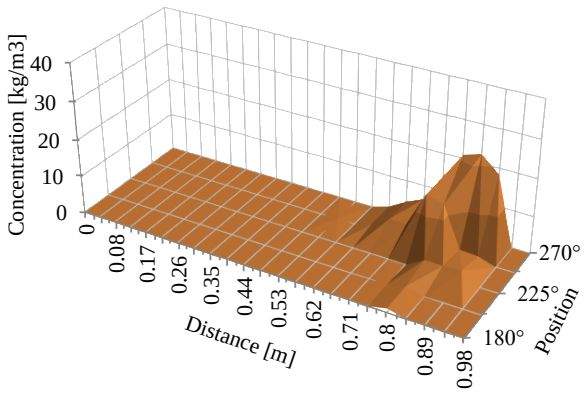

Figure 144: Local R290 concentration at wall unit discharge with 30 g/min and 1260 m3/h airflow.

Based on these results, it is evident that the majority of the discharged air is not directly useful for dilution of a release. An approximation from these data suggests that broadly two-thirds of the discharged volume airflow may be neglected. Accordingly, the term applied to equation (57) was set at R = 1/3.

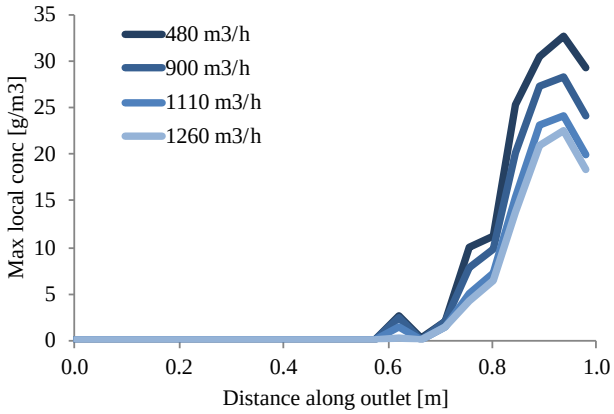

Figure 145: Maximum R290 concentration along discharge for different airflow rates.

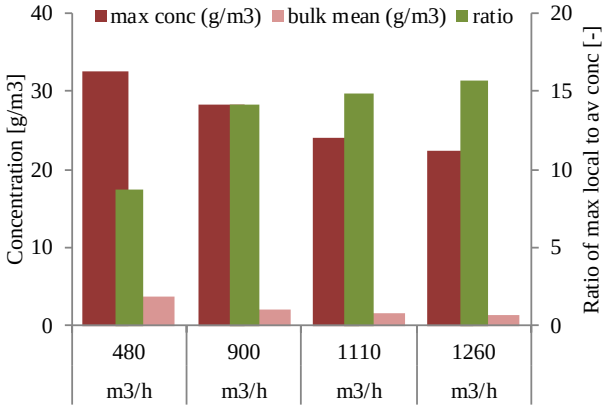

Figure 146: Comparison of maximum concentration and bulk mean concentration.

A5.8 Spatial distribution of discharged mixtures

Whilst the measurements described above were made immediately after the IDU outlet, it may be possible that refrigerant mixing occurs across the entire jet prior to approaching the floor or opposite wall. Measurements were used to help provide confirmation of the validity of equation (47) for determining x_T and the usefulness of the term. Two arrangements were prepared to investigate this further. *Figure 147* shows (a) incrementally spaced sampling points (purple) at floor level in order to indicate x_T and (b) a matrix of sampling points arranged at the same height as the IDU outlet ("h_H" in the graphs) and also at 0.15 m below ("h_L") to indicate both vertical and lateral distribution of the refrigerant within the discharged air.

Figure 148 plots local floor concentration (in line with the release position), with the respective coloured arrows indicating the result for x_T from equation (47). There is fairly good agreement, especially when considering the variability of the release conditions.

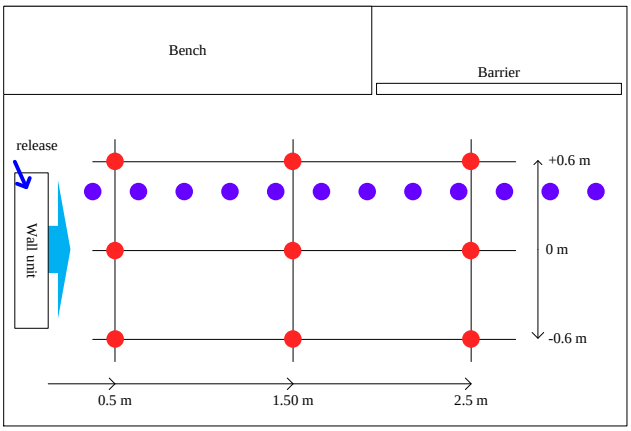

Figure 147: Layout of test room (3.5 m × 4 m) with sampling points indicated.

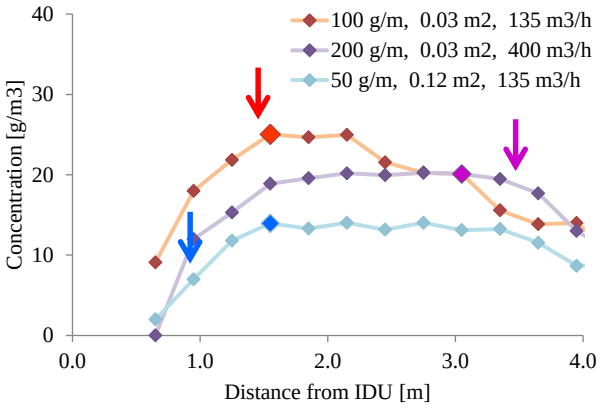

Figure 148: Floor concentrations during a release (g/min) within the IDU with outlet opening (m2) and airflow (m3 h-1) at different conditions.

Two sets of results are shown in *Figure 149* and *Figure 150*, which are from identical test arrangements, except for different airflow rates. (Note data for -0.6 m is not included since it matches that of 0 m.) Concentrations along the 0 m line are about the same, irrespective of height and distance from the IDU and approximately correspond to mean room concentration. Concentrations directly in front of the release start at a high value and then decrease towards the background concentration at the far end of the room. Crucially, concentrations at 0.15 m below the plane of air discharge are found to be higher in the centre of the room, inferring a downward trajectory of the refrigerant-rich part of the jet. Results for the lower airflow rate suggest a steeper trajectory on account of the more pronounced decline in concentrations towards the far end of the room.

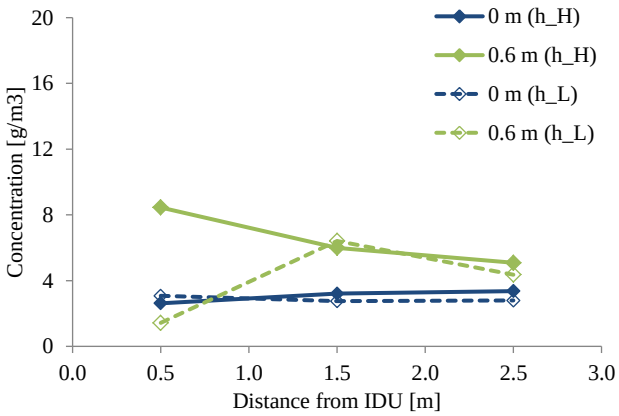

Figure 149: Local concentrations in front on air discharge; 1260 m3 h-1, 120 g min-1 and 200 g.

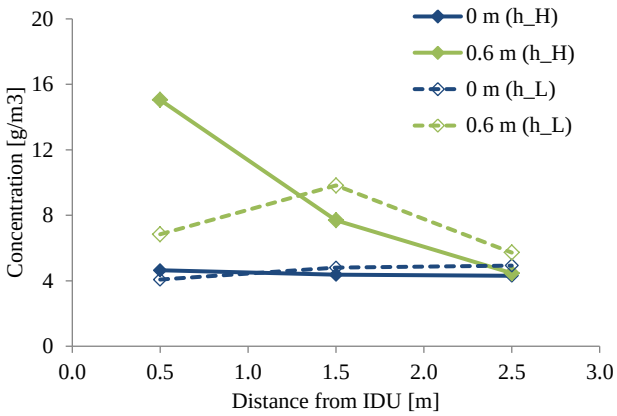

Figure 150: Local concentrations in front on air discharge; 480 m3 h-1, 120 g min-1 and 200 g.

A5.9 Validation

Equations (58) and (59) (rearranged as a function of $\bar{C}_{max,t2}$) were compared against maximum measured concentrations across a large number of experiments from our database, involving different RACS and also commercial refrigeration equipment (CRE). Across the database, tests used a wide range of variables, such as airflow rates, outlet areas, unit height/positioning, released masses and mass flow rates, room sizes and also density and distribution of sampling points. Figure 151 shows comparison between the measured and calculated values with approximately 250 data-points, which shows that the equations under predict in most cases. However, since the primary purpose of the task is to determine a minimum airflow rate to guarantee against a flammable mixture forming, a positive adjustment factor of 1.2 was applied to minimise the number of data-points remaining to the left of parity (Figure 152).

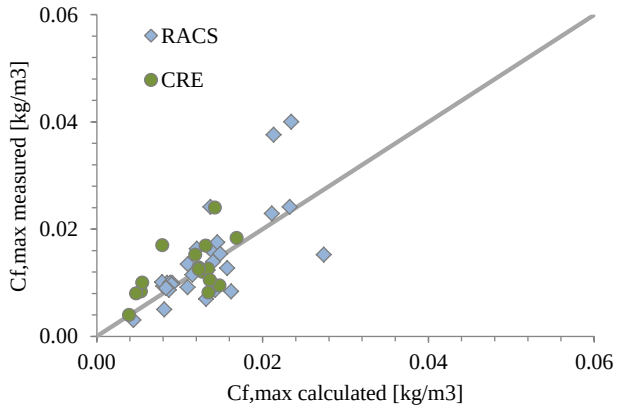

Figure 151: Comparison of measured maximum concentrations and unadjusted proposed formulae.

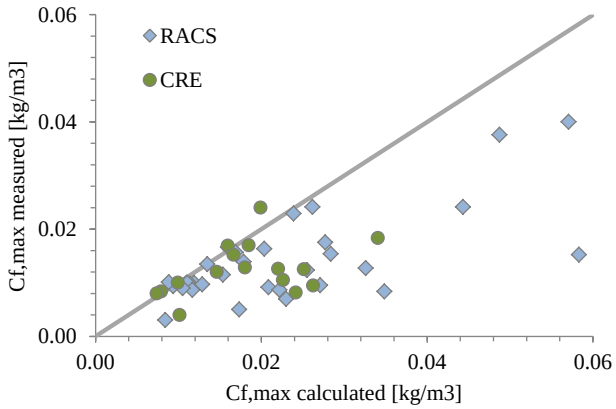

Figure 152: Comparison of measured maximum concentrations and proposed formulae adjusted to "catch all".

A5.10 Initiation of airflow

The minimum airflow rate determined in the previous section may apply under continuous operation or alternatively it may in principle operate only upon response to a refrigerant leak.

There are several possible means by which a leak may be identified, including detection of the refrigerant using a gas sensor, response of system parameters to a deficit of charge and receipt of ultrasound waves generated by a leak under choked flow conditions. Each of these options have both advantages and disadvantages with respect to initiating airflow (or any other mitigation action); here the most critical features should be reliability and time of response from the start of the leak.

This section analyses released under quiescent conditions in order to determine the required response time to initiate airflow and also to check whether the specified airflow in the previous section is sufficient to disperse an already stratified layer of refrigerant.

A5.10.1 Required response time

Correct timing for initiating airflow is critical for minimising the size and duration of a flammable mixture. Thus, work was carried out to help determine when the onset of a flammable mixture occurs and how long it takes to spread. To support this, measurements were made with releases from floor and wall units to observe flow speeds of the mixture front under different release rates. Sensors were positioned along the centreline of the room floor at 0.7 m increments in line with the middle of the IDU.

Figure 153 and Figure 154 show some example measurements of floor concentration for a slow release rate from a floor IDU and a high release rate from a 1 m wall IDU, respectively. Concentration data for sampling points inside the base of the IDU are also shown; from these it can be seen that there is a delay between the concentration front hitting the first sensor with a release from the wall IDU compared to the floor IDU, on account of the additional distance from the IDU outlet.

With the floor IDU there is a rapid rise in local concentration whereas the rise is more gradual with the wall IDU, which is due to the more dilute front from the wall IDU. However, the rate of local concentration rise decay more rapidly with the floor IDU the further the sensor is from the IDU; at the far end of the room the local concentration struggles to reach 50% of LFL.

One further observation is that for each sampling point, to different rates of concentration rise occur. The first rapid rise is due to the mixture front passing over the sampling point, whereas the second arises from the subsequent "filling" process where the floor concentration simply becomes richer.

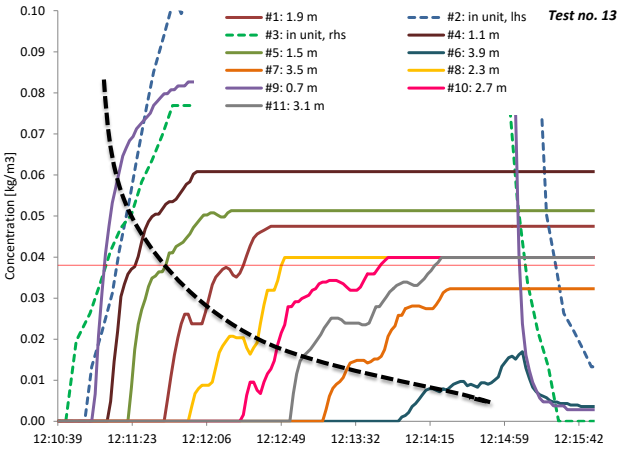

Figure 153: Concentrations across the floor due to a 15 g/min release from a floor unit.

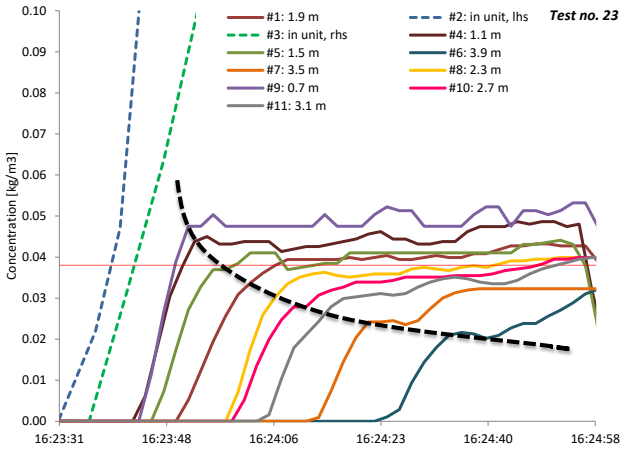

Figure 154: Concentrations across the floor due to a 95 g/min release from a 1 m wall unit.

Speed of the spreading mixture was calculated according to the time some concentration took to pass between two sampling points. (Note that the accuracy of the result is affected by the 2 s sampling interval – as seen when two sampling points 0.7 m apart display a result almost simultaneously – and slightly different response time of the analysers. Nevertheless, it is seen that these factors become less significant as all the data is aggregated.)

Two reference concentrations were used to determine the speed: 1 g/m^3 to represent the plume front itself and 50% LFL (19 g/m^3). Considering these two reference values, a sort of "slip" may be observed as the speed of the lower concentration front is faster than the 50% of LFL front.

Rate at which concentration increases at a given location becomes slower at distances further away from release

Figure 155 and Figure 156 show the time taken for the front to travel from the first analyser to the subsequent ones at the stated distance, for the two different IDUs at various release rates.

In general, the higher the mass flow, the faster the front flow likely due to the greater "dynamic/static" pressure head forcing a faster spread. For the same mass flow, the flow front from the wall IDU tends to travel at about twice the speed, which is probably due to the greater momentum generated by the 1 m plume fall prior to hitting the floor. However, once the mass flow approaches the higher end of the range tested, there is little difference between them.

Arguably the floor IDU tends to exhibit a smoother relationship, likely due to less dilution and less turbulent behaviour prior to onset of lateral flow.

Curves in Figure 155 and Figure 156 have a slightly exponential shape (particularly for the lower mass flow rates) inferring deceleration as the front moves away from the IDU; the decline in momentum being caused by the increasingly dilute mixture at the front. This deceleration is expected to be accentuated if the unit/room orientation has higher aspect ratio, i.e., the floor plume would have a wider spread and thus loose velocity sooner.

Nevertheless, it was chosen to assume a constant front flow velocity to simplify the subsequent steps.

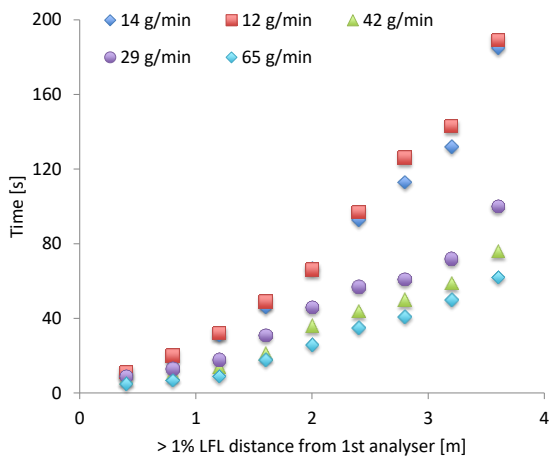

Figure 155: Mixture front travel time for releases from floor IDU.

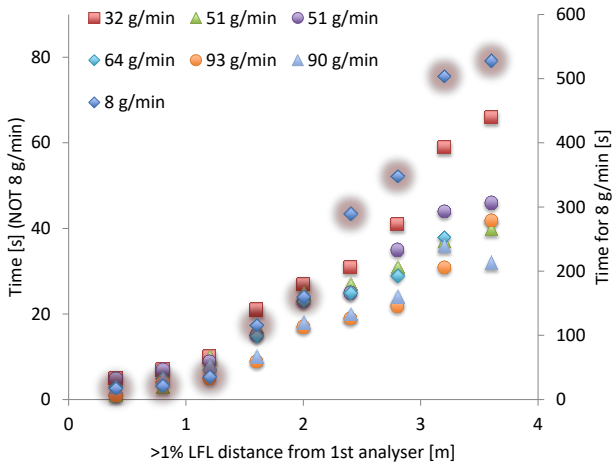

Figure 156: Mixture front travel time for releases from wall unit at 1 m.

The plot in *Figure 157* provides the average front velocity of 1 g/m^3 and 19 g/m^3 mixture fronts over a range of release mass flow rates. Data is presented for both floor and wall IDUs.

As indicated previously, the average velocity is higher for larger leak rates, where more refrigerant leads to a denser flow so more momentum and greater static pressure differential across front, thus forcing a faster flow. However, at smaller release rates, the velocity appears similar irrespective of IDU height or the concentration used to define the mixture front. Whenever the release rate is greater than about 15 – 20 g/min, the wall IDU always produces higher velocities.

If one extrapolates these observations to IDUs at higher levels, say 2 m, it could be argued that the average front flows marginally faster than releases from the 1 m IDU.

Whilst the 19 g/m^3 front travels slower than the 1 g/m^3 front concentration front for the 1 m wall IDU, the difference is almost indistinguishable for releases from the floor IDU.

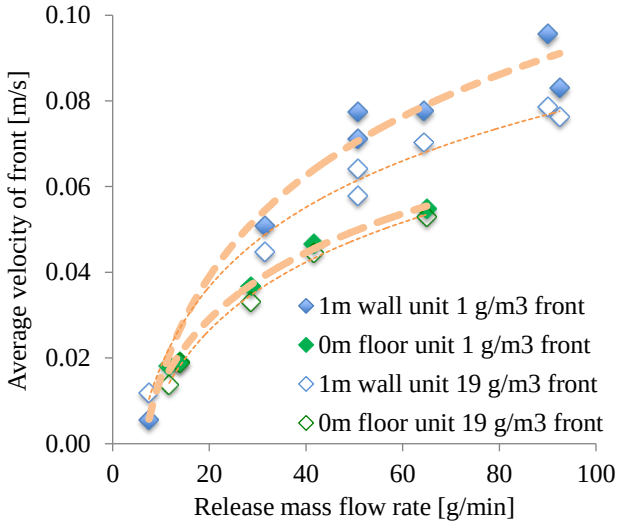

Figure 157: Average velocity of a 1 g/m3 and a 19 g/m3 mixture front over all test conditions.

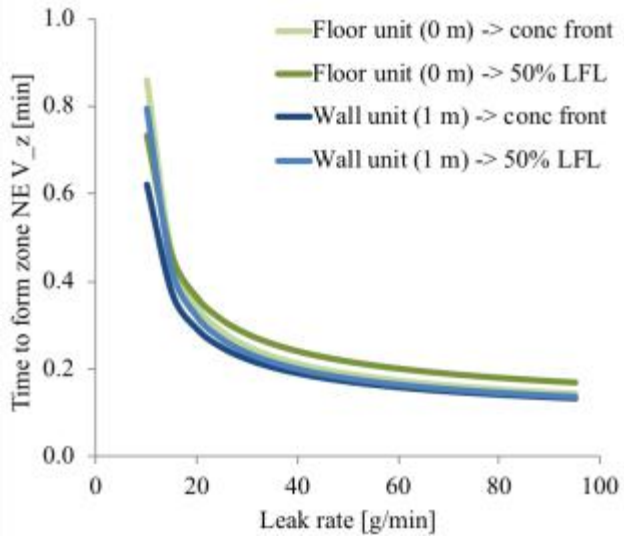

Figure 158: Recommended maximum response time to avoid a mixture reaching the limit of NE.

The calculated average front velocity may then be used to estimate the response time permitted for the mitigation action before a "dangerous" mixture develops.

With reference to IEC 60079-10-1, there is a concept "zone of negligible extent (NE)" that represents a certain sized (0.1 m^3) mixture of flammable gas and air, which, if ignited, would not result in significant harm or damage. This quantity will thus be used as a boundary for the subsequent analysis.

Using the curves for the 50% LFL front velocity and assuming a spreading plume height of 0.5 m for the 1 m wall IDUs and 0.2 m for the floor IDUs (based on measurements) the time taken to develop a certain mixture volume can be estimated. The results of this calculation are shown in *Figure 158*, where two distinct gradients can be observed, corresponding to a "low" release rate and a "high" release rate. Taking the low release rate as 15 – 20 g/min, the minimum time to reach zone NE is about 0.4 min and about 0.2 min with the high release rate. Thus, the response time should be about 25 s and 10 s for the low and high release rates.

A5.10.2 Other refrigerants

R290 is relatively light compared to other flammable refrigerants; for instance, R1234yf has vapour density about 2½ times that of R290 at STP. Thus, it is appropriate to take account of such differences to understand the possible variation amongst refrigerants.

In general, it may be expected that denser refrigerants will lead to a faster flow front on account of the greater static pressure difference across the front.

CFD calculations with R12 (having the same molecular weight as R1234yf) (*Figure 159*) are compared with R290 (*Figure 160*) for a 60 g/min release from a 1 m high wall IDU. Corresponding front flow velocities are shown in *Figure 160* for both, relative to the distance at which the "touchdown" of the plume occurs. For the flow across the floor the average velocity is about 0.07 m/s for R290 (this corresponds almost exactly to the R290 measurements above) but 0.09 m/s with R12, being 30% faster than R290. Note that after the first half metre the velocity decelerates from about 0.25 m/s to 0.05 m/s, which corresponds to the situation when the isotropic flow ceases due to coverage between three of the walls.

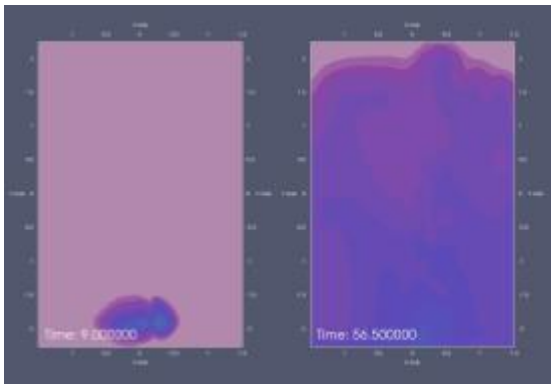

Figure 159: Floor spread of R290-air mixture 9 s and 56 s after release from 1 m wall IDU.

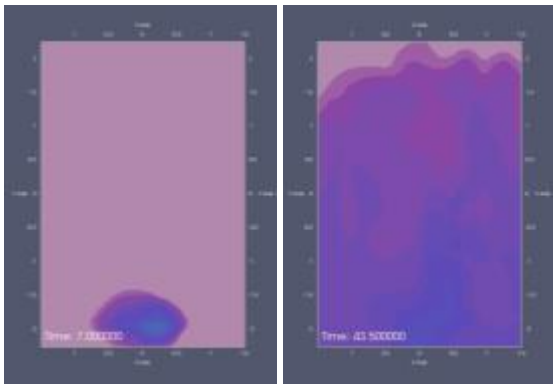

Figure 160: Floor spread of R12-air mixture 7 s and 43 s after release from 1 m wall IDU.

Also considering the downwards plume, R290 takes 8.5 s to descend the 1 m from IDU to the floor, whereas the R12 plume takes 6.5 s (using 0.5 s time increments). Thus, the descending velocity is also about 30% faster for the denser refrigerant.

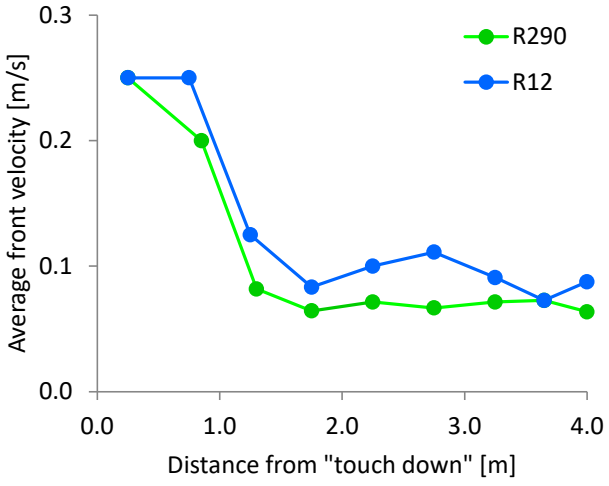

Figure 161: Average velocity of a 1 g/m3 mixture front flowing across the floor.

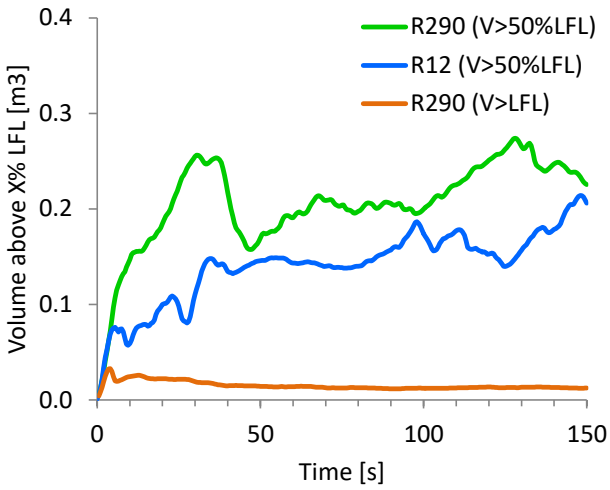

Figure 162: Volume of mixture above 50% of the LFL of R290 and above LFL for R290.

Additional calculations were made to determine the volume of the mixture at a concentration above 50% LFL of R290 with the results shown in *Figure 161*, where it is evident that the higher travel velocity assists in increasing the rate of dilution. Here, the volume for R12 is notably smaller than with R290, on average by about 35% for the 150 s.

Comparing the values in Figure 159 for a 60 g/min release provides a reasonably good match to the values in Figure 162, inferring a response within 10 s to 15 s would be appropriate. *Figure 162* also includes the R290-air mixture volume above 100% of LFL, which is typically about 5% to 10% of the volume above 50% of LFL, suggesting that a delay in excess of 150 s would probably be acceptable (for the case and conditions under evaluation here).

A5.11 Practical assessment

An initial assumption was that a release of refrigerant within an IDU is fully mixed within the airflow, before being discharged. Experiments were carried out in order to examine the validity of this assumption.

In Figure 163 and Figure 164, the floor concentration rises rapidly, so the delay time for a fan starting dictates how much of the floor area exceeds the LFL. Once the fan starts, the release becomes well mixed within 10 – 20 seconds. This mixing equally effective whether 30 g or 100 g has already been released; the majority of the inertia to be overcome by the fan is the inertia of the still air in the room (approximately 50 kg), so an addition few grams of refrigerant has a negligible influence.

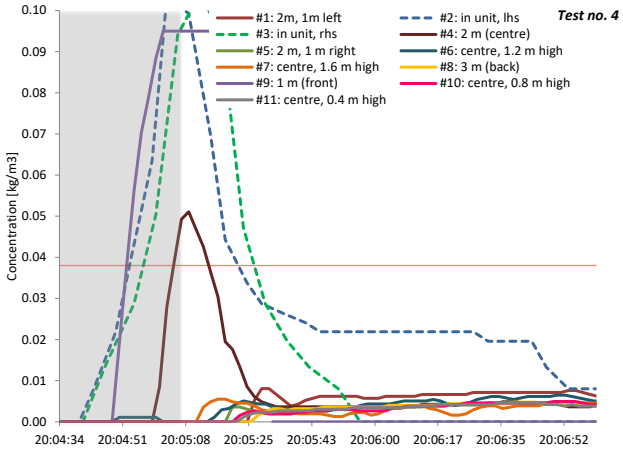

Figure 163: Floor unit, 60 g/min, horizontal air discharge, 350 m3/h after 30 s delay.

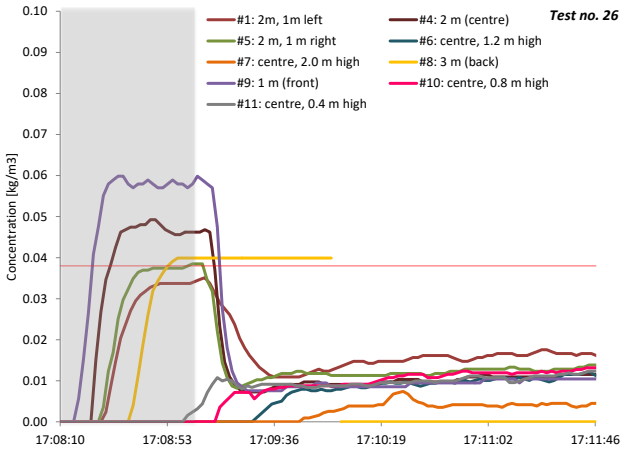

Figure 164: Wall unit (1 m), 100 g/min, horizontal air discharge, 480 m3/h after 45 s delay.

Generally, a delayed initiation of airflow is still effective in mixing a release, once the fan has started. For longer delays with lower airflow rates, subsequent “ripples” occur as airflow begins to mix the stratified layer. Layering persists with lower airflow rate, but higher airflow mixes well.

Based on the experimental results, it can be observed that the minimum airflow rate from the proposed formula is adequate for mixing a release following delayed initiation of fan. In fact, the data suggests formula gives higher airflow than is necessary.

Of most Importance is the response time to initiate the airflow, i.e., activation time for the sensor. This is especially the case for units located on or close to the floor, where a slower response leads to a greater proportion of room floor area being covered by flammable mixture (… assuming instantaneous leak, no ambient airflow, etc.)

This situation is simulated in Figure 165 and Figure 166, where a release of R290 is allowed to continue in quiescent conditions for 1½ minutes. Subsequently the airflow is initiated and within about 10 s effective mixing takes place. Initiation of sufficient airflow dilutes “accumulated” flammable mixture within a few seconds. This replicates observations from experiments.

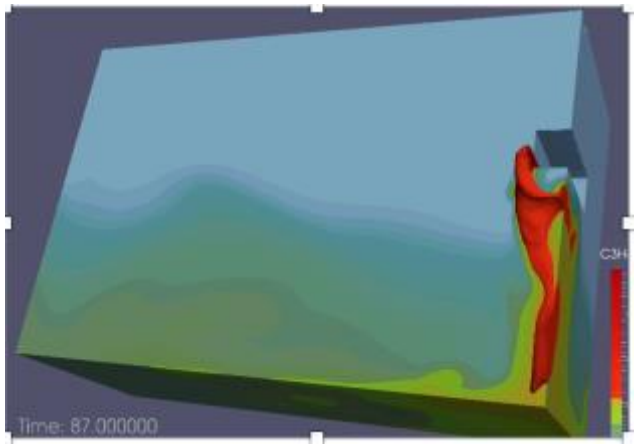

Figure 165: Moments before fan starts.

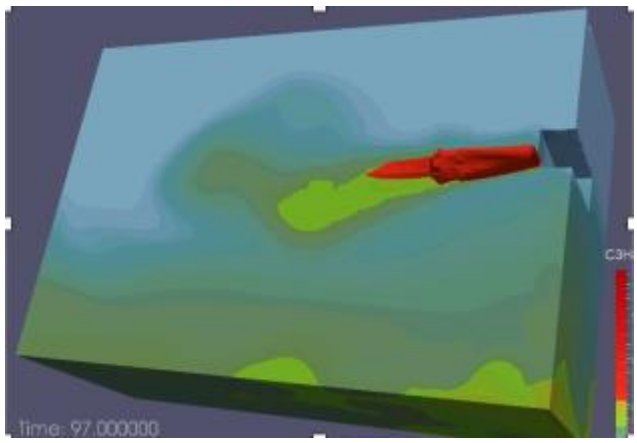

Figure 166: Moments after fan starts.

Figure 167 illustrates the evolution of flammable volumes with the same release occurring at different heights. With releases from units at 1.0 m and 2.0 m, the flammable volume remains more or less constant until the fan initiates. This is because – at least within the 90 s time frame – the R290 plume manages to dilute to below LFL before it reaches the floor. Conversely with the unit at 0.5 m there is a gradual increase in flammable volume until the fan is switched on and this is due to the plume remaining above LFL by the time it hits the floor and travels some distance across the floor. Again, this was also found with experiments. In such a case, the response time of the detection should be faster (for example, 20 s).

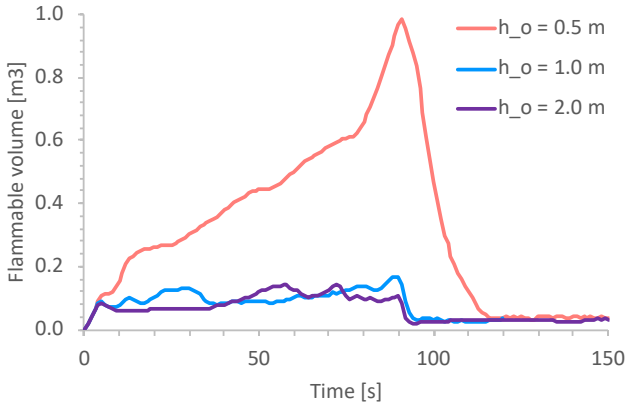

Figure 167: Flammable volumes with quiescent releases at 0.5 m, 1.0 m and 2.0 m prior to fan starting at 1½ minutes.

A5.12 Final remarks

Usually, refrigerant charge amount for a RACHP system is determined according to the room size into which the IDU will be installed and the LFL of the refrigerant:

$$m_{max} = F \times LFL \times A_{rm} \times h_{rm} \tag{60}$$

Or alternatively, the minimum room area for a given system charge (m_c):

$$A_{min} = \frac{m_c}{F \times LFL \times h_{rm}} \tag{61}$$

where m_{max} is the maximum charge (kg), h_{rm} is the room height (m) usually assumed to be 2.2 m or 2.5 m and F is a non-dimensional limit intended to avoid the entire room approaching LFL; with typical values ranging from 0.1 to 0.5 according to how much refrigerant a given RACS requires.

In order to make equations (60) and (61) more directly and practically applicable, equation (13) is substituted in (and including the 1.2 adjustment factor), giving:

$$\dot{V}_{o,min} = \frac{6.8\sqrt{A_o}\dot{m}_{leak}}{m_c^{1/4} LFL^{3/4}} \left(\frac{F^{1/4}}{1-F}\right) \tag{62}$$

$$\dot{V}_{o,min} = \frac{5\sqrt{A_o}\dot{m}_{leak}^{3/4}}{h_o^{1/8}[LFL(1-F)]^{5/8}} \tag{63}$$

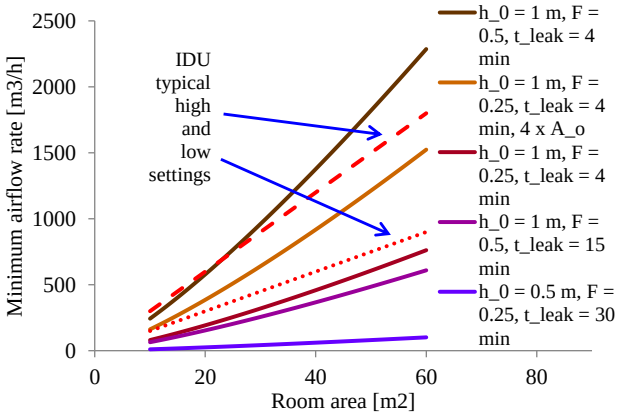

Figure 168: Example of airflow rate requirements with mean variables.

Using these formulae, some examples of minimum airflow rates according to the key variables are provided in Figure 48. It is seen that the minimum airflow is rather sensitive to the selected parameters, where for example, high leak rates increase airflow about proportionally, doubling charge amount increases airflow by a factor of three and increasing the outlet area by four (i.e., quartering discharge velocity) doubles airflow, assuming the other factors are kept constant. Also shown are typical values for high and low airflow setting on IDUs, assuming a specific heat load of 200 W m^{-2} of room area. Evidently, under some conditions IDU airflow may need to be raised to the high setting to ensure flammable mixtures are avoided and occasionally redesign of the RACS may be necessary.

Compared to the methods mentioned in the introduction, use of the above equations are attractive in several respects. In particular, the need to make judgement on certain variables is eliminated, they account for discharge velocity of IDUs, absolute mass of releasable refrigerant charge and installation height of IDU (where applicable) as well as enabling the choice of assumed leak rate. Moreover, they have been extensively validated against database of measurements specifically using RACHP systems.

ANNEX 6 BACKGROUND TO SURROUNDING CONCENTRATION TEST

Different designs of appliances will affect the resulting concentrations and due to the complexity and variation in the design of appliances, it is not always easy to generalise. Therefore, it is preferable to develop a test method that may be used to determine the mass of refrigerant that would be insufficient to result in a flammable concentration at floor level within a room of a given size. Since the maximum concentration and thus allowable charge can be sensitive to geometry of enclosure, there is a need to account for this. Furthermore, such an approach may help to encourage equipment designers to refine the construction so that as low a concentration as possible is achieved. Analysis of many previous tests involving simulated leaks from RACHP equipment helps identify the most appropriate test methodology.

A series of test data were used to analyse the behaviour of the released refrigerant around the RACHP equipment – or around the floor projection of it – to help identify the most important positions for measuring gas concentration in such a test.

Numerous test results were analysed in terms of sensitivity of location. In general, the most important positions tended to be within 1 m of front and sides (towards wall) of the unit under test and 0.5 m from the unit perimeter projection.

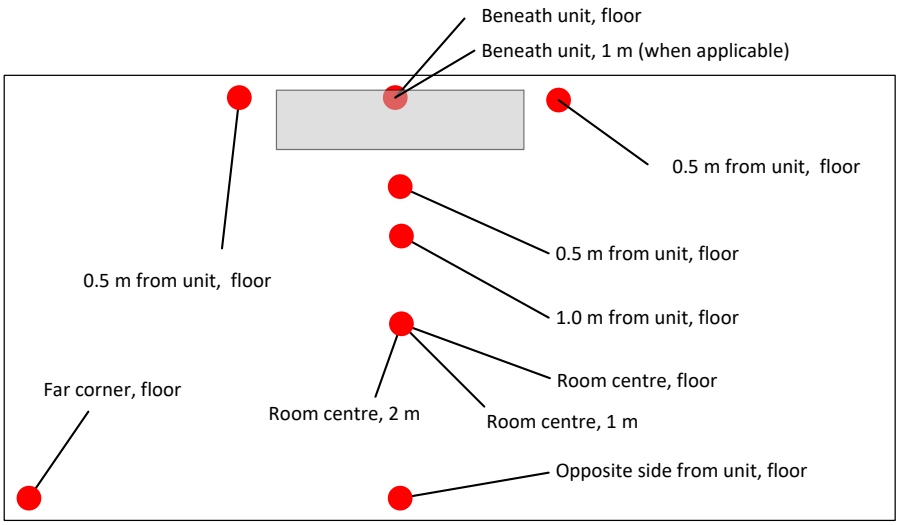

Figure 169: Arrangement of gas sensors.

Peak concentrations for each sampling position were taken and compiled to identify the most critical; these are indicated in Figure 170, Figure 171 and Figure 172.

For window unit, highest concentrations (except those directly below unit) were:

- 0.5 m in front, 0.5 m to left, at left wall (when the leak is made from LH side)
- 0.5 m in front of unit (but 1.0 m in front was never higher than 0.5 m in front)

For wall unit, highest concentrations (except directly below unit) were:

- 0.5 m in front, 0.5 m to left, at left wall (when the leak is made from LH side)
- 1.0 m in front of unit (but 1.0 m in front is never higher than 0.5 m in front)

For the floor unit, highest concentrations (except directly below unit) were:

- 0.5 m in front, 0.5 m to left, at left wall (when the leak is made from LH side)
- 1.0 m in front of unit (but 1.0 m in front is never higher than 0.5 m in front)

Thus, these positions help indicate the preferred sensor locations for subsequent surrounding concentration tests.

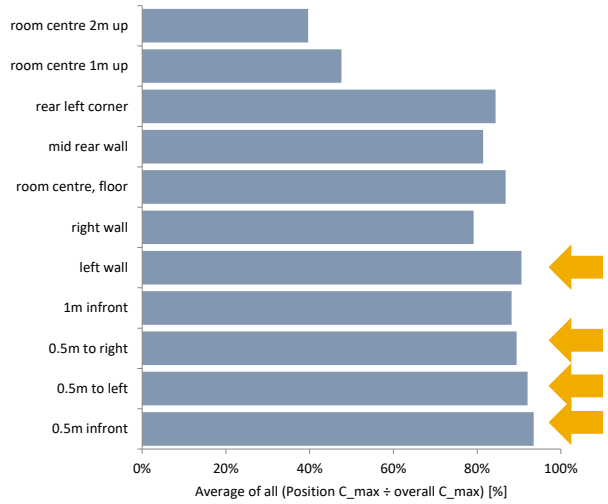

Figure 170: Results for window unit; orange arrows indicating positions with highest four concentrations.

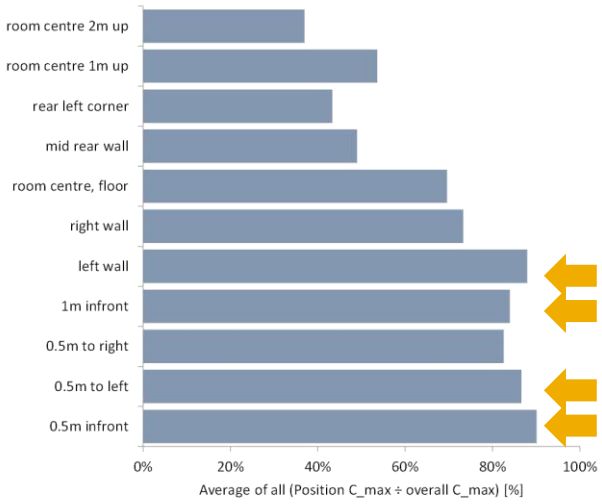

Figure 171: Results for wall unit; orange arrows indicating positions with highest four concentrations.

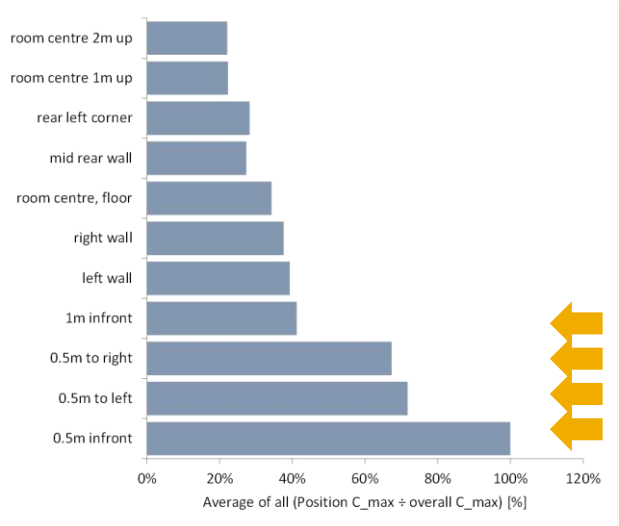

Figure 172: Results for floor unit; orange arrows indicating positions with highest four concentrations.

ANNEX 7 LEAK DETECTION METHODS

A7.1 Introduction

There are three common forms of "leak detection", which could be employed to initiate airflow if needed:

- Refrigerant gas detection
- Ultrasonic receiver
- System parameter response to charge deficit

Table 19 provides a summary of the key characteristics of the detection methods.

Table 19: Summary of detection method characteristics

	Gas detection	System parameters	Ultrasonic
Technology	Various means to sense presence of gas at a certain concentration range	Pressure, temperature, vapour quality, etc. corresponding to off-design operation	Receipt of sound waves above about 20 kHz generated by choked flow
Cost	High	Medium to high depending upon chosen parameters	Low
Response time	Slow to fast, depending upon sensing technique	Medium to slow, depending upon system design and chosen parameters	Fast
Calibration	Necessary at 3 – 12 months	Once, factory calibrated	Once, factory calibrated
Reliability	Vulnerable to poisoning from other substances, dust accumulation, being painted over, easily damaged, etc.	Sensors generally reliable, but changes in system construction, operating conditions, other tinkering, etc. could result in misinterpretation.	Generally, very reliable but could receive false signals, e.g., from bats, insects, dog-whistles, etc.

Apart from for industrial situations, all of these technologies are largely untested in small RACHP systems and equipment. Gas detection is the most widely used but typically using high cost instrumentation that is unlikely to be suitable for smaller systems (i.e., the cost and maintenance of the technology should not exceed more than a few percent of the system cost).

Using system parameters as a detection technology could be effective, depending upon the parameter(s) monitored and the operating mode of the system. For instance, if the system is operating it may take a loss of 20% to 30% of the charge to be "noticed", i.e., to be able to distinguish it from other factors such as increase in heat load, reduction in ambient temperature and so on. With a 1 kg system charge and assuming

a “safe” leak rate of 20 g/min, this would mean it could take 10 min to 20 min to identify the leak which may not be acceptable under certain circumstances. Nevertheless, there are some prototype R290 systems that employ this technique and have been proved to be effective. Perhaps the most suitable application though is using pressure as the indicator within indoor parts of the system during off-mode, since even a relatively small leak hole will result in a rapid reduction in system pressure (in the order of 1 bar per 5 s to 15 s, depending upon hole size). A more detailed evaluation of this can be found in Colbourne et al. (2013).

Use of an ultrasonic transducer for leak detection has historically been used in the RACHP industry for on-site, handheld detection purposes, although it does not have a positive reputation. Fixed ultrasonic detectors have also been used occasionally for industrial gas applications, alongside other detection methods.

A7.2 Ultrasonic leak detection

A7.2.1 Introduction

Initial trials were carried out using a relatively low-cost handheld ultrasonic leak detector (USLD)[24], where a release of a specified mass flow was simulated at one end of an IDU and the USLD was moved gradually closer to the release until the audible indicated became apparent. Figure 173 illustrates the boundary (red shading) within which the USLD was effective in terms of providing an output signal. The same range applied to sensing the underside of the IDU. It is noted that only a single leak direction was used as well as a fixed diameter orifice capillary tube so at least for the lower flow rates the exiting velocity is likely below sonic. No other directions were tested. Nevertheless, the trials indicated that preliminarily the concept is viable.

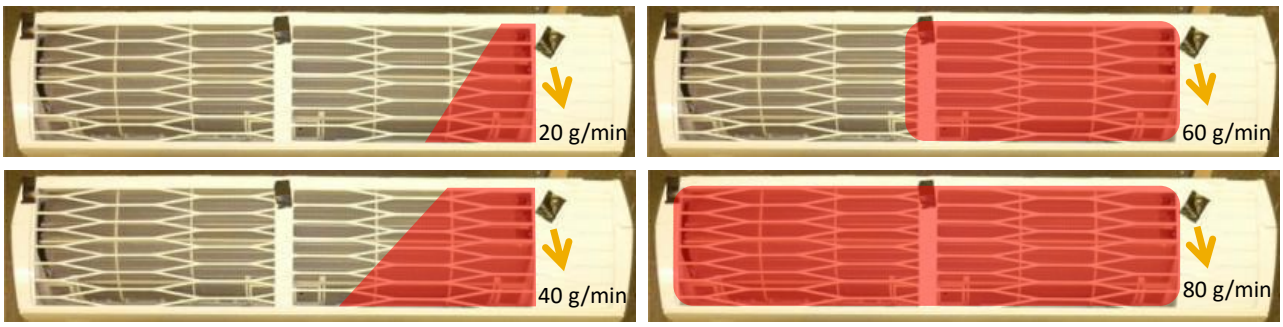

Figure 173: Location of releases (red arrows) and sensor positioning (green circles) within wall IDU.

A7.2.2 Measurements

Further trials were carried out with an NHBS Ltd ultrasonic range microphone, M500-384, which has a frequency range of <10 kHz – 384 kHz. As an example of the output Figure 174 shows a spectrogram of sound power level across the range of frequencies. Also indicated here, is the typical range for human hearing and also the range of ultrasonic receivers (USRs) that can be found “off the shelf”.

[24] e.g., https://www.sitebox.ltd.uk/sealey-pp4-ultrasonic-leak-detector-osealey_PP4

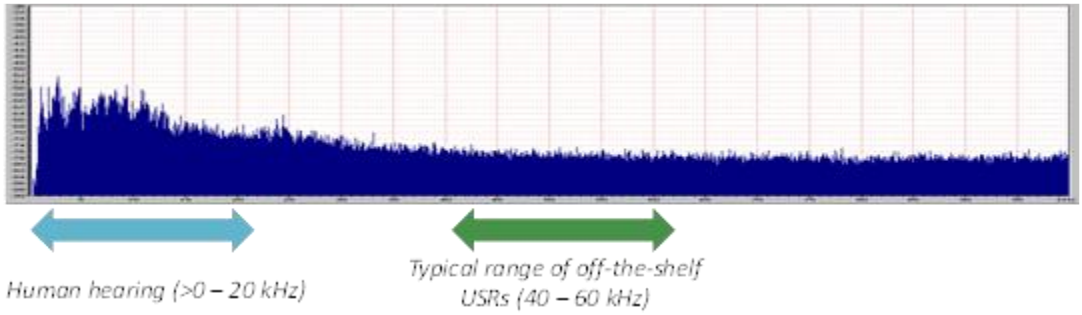

Figure 174: Example of sound power density output from the microphone.

Initially measurements were carried out with different R290 release rates using a 1 mm diameter orifice positioned in an open room perpendicular to the microphone that was 0.5 m away (Figure 174). Example sound power-frequency spectrograms (SPFS) for each incremental mass flow rates are shown in Figure 176. Compared to the no release ("pottering in room") case, a significant sound power level was recoded for all release rates.

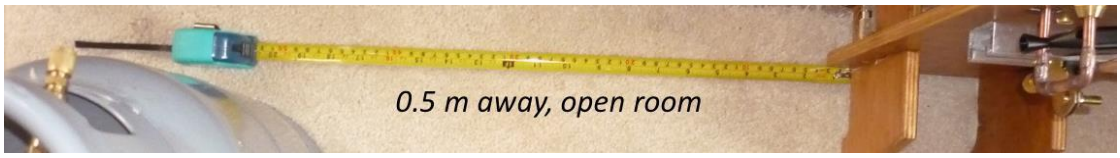

Figure 175: Example of release-microphone trial arrangement.

Compared to the no release ("pottering in room") case, a significant sound power level was recoded for all release rates.

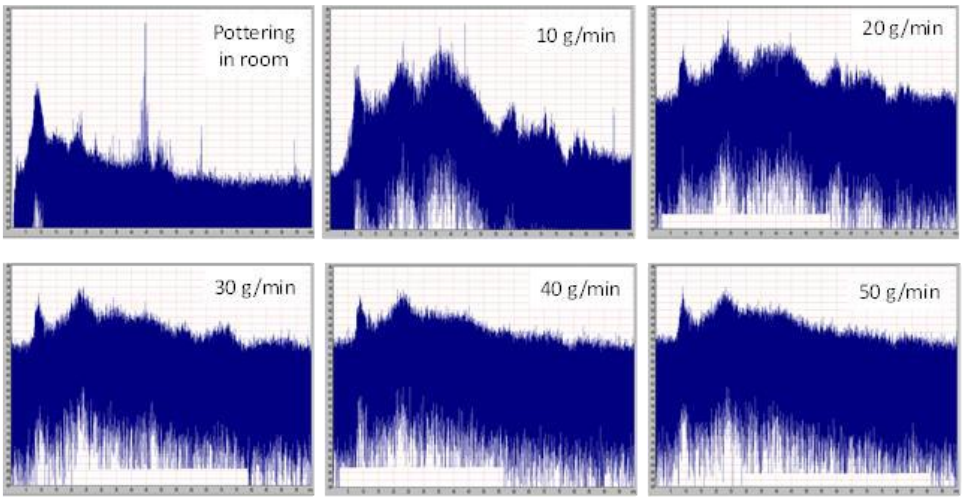

Figure 176: Sound power-frequency spectrogram; dB on y-axis and frequency on x-axis (cut off at 100 kHz).

Next, measurements were carried out with different leak rates with an orifice positioned inside a wall AC unit, as shown in Figure 177. For all measurements R290 was released from a 1 mm diameter orifice inside one end of the IDU at a perpendicular direction to microphone. The microphone was directed towards the far end of the IDU so as to represent a pessimistic situation.

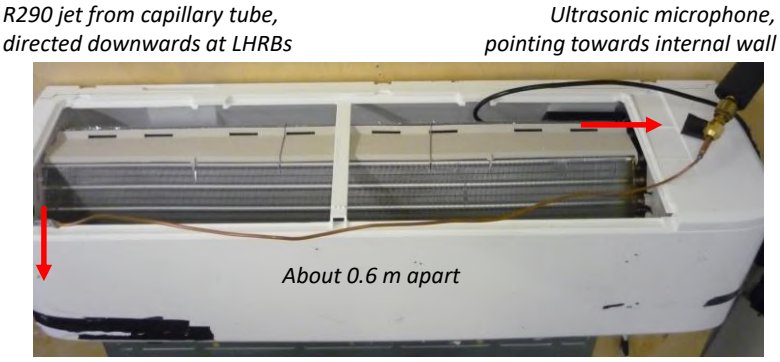

Figure 177: Arrangement for SPFS measurements with a wall AC unit.

Example SPFS for each incremental mass flow rates are given in Figure 178. There is a significant signal recorded up to about 40 – 50 kHz with a 10 – 30 g/min release rate. For larger leaks there is a stronger signal across the entire frequency range.

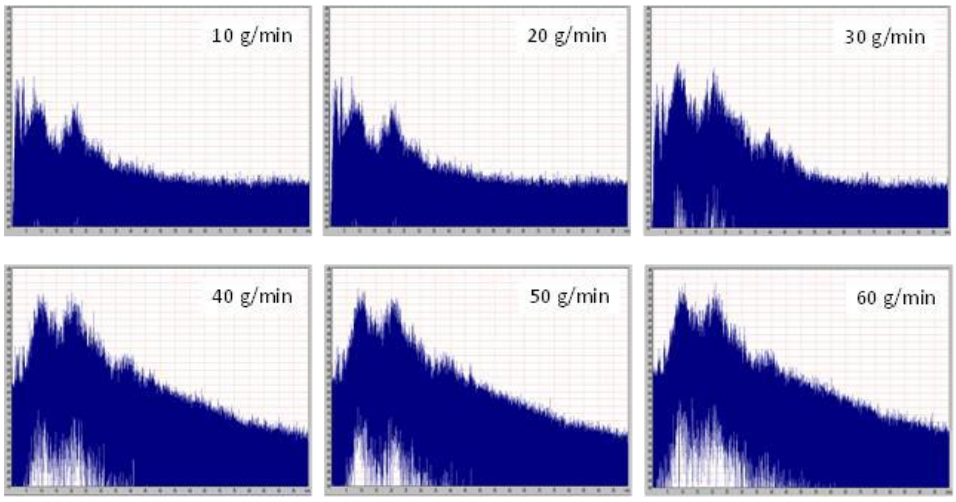

Figure 178: Sound power-frequency spectrogram; dB on y-axis and frequency on x-axis (cut off at 100 kHz).

The same measurements were repeated using a floor type AC unit, as shown in Figure 179. In this case, the release was directed downwards as was the microphone, but at the opposite end of the unit.

Figure 179: Arrangement for SPFS measurements with a floor AC unit.

SPFS are presented in Figure 180 for incremental release mass flow rates. The patterns are similar to that of the wall AC unit, if not a little more pronounced.

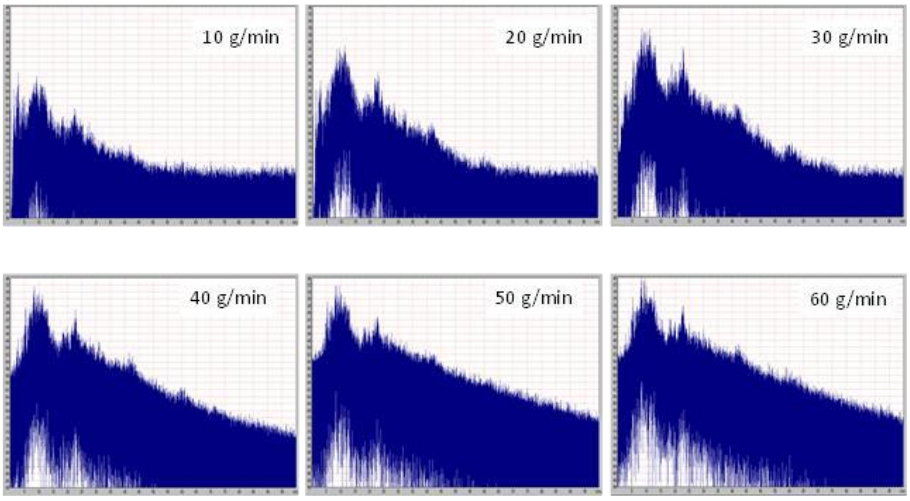

Figure 180: Sound power-frequency spectrogram; dB on y-axis and frequency on x-axis (cut off at 100 kHz).

Across these various tests a significant increase in SPL is observed when release rates are at above 10 g/min. Measurements from inside IDUs seem to show some damping, especially at the higher frequency range. However, since most "off-the-shelf" transducers cover the range 25 – 55 kHz, the "important" frequencies are not detrimentally affected.

Whilst these tests involved R290 only, it is anticipated that similar results would be observed for all refrigerants. However, since there are variations in fluid thermodynamic properties, such as speed of sound, it would be important to evaluate all candidate fluids.

A7.2.3 Practical trial

As part of an implementation project running in parallel to the EULF project, USLD was integrated into a new product developed with R290 (see Colbourne, Arango and Dickson, 2018[25]). The RACHP equipment was a 20 kW indoor air handling unit (AHU) of a ducted split system, as in the Figure 181 photograph.

Two USD sensors[26] were positioned at the upper and lower parts of the AHU (Figure 182) and upon detection of the target frequency above a certain sound power level, the indicator LED on the PCB illuminates (Figure 183) and the blower within the AHU starts.

Three different orifice sizes were used to simulate leaks from within the AHU: 0.5 mm^2, 1.0 mm^2 and 2.0 mm^2 and this yielded release mass flow rates of about 15 g/min, 40 g/min and 120 g/min. Two release locations were used; one at the middle and one at the bottom of the evaporator coil. Tests were carried out both whilst the system was operating and switched off. Concentrations were measured within the AHU to assess the effectiveness of the concept.

Figure 181: Ducted AC indoor unit trialled.

Figure 182: Positioning of ultrasonic receivers within unit.

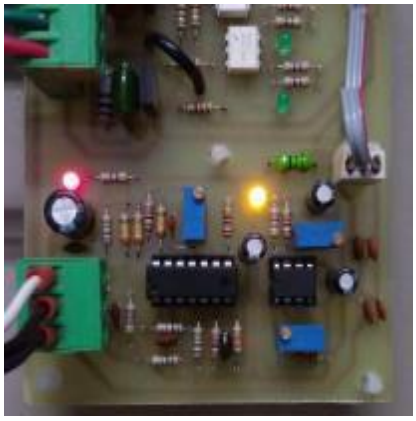

Figure 183: PCB including USD output indicator.

Out of 42 tests, the USD identified leaks in all but three. Whenever there was a positive response, it occurred within 5 s of the start of release. Local concentration never reached 25% of LFL.

There were three cases in which the system did not detect the releases. Two were with 15 g/min when the blower was already operating and one case was also with 15 g/min when the blower was off. These negative responses were resolved by relocating the ultrasonic receiver(s) and adjusting sensitivity of sensor on the PCB. Subsequent tests all responded positively.

An example of the concentration measured within the AHU is shown in Figure 184.

[25] http://conf.montreal-protocol.org/meeting/oewg/oewg-40/events-publications/Observer%20Publications/DEVELOPMENT%20OF%20THERMOTAR%20R290%20DUCTED%20SPLIT%20AND%20ROOFTOP%20AIR-CONDITIONING%20UNITS.pdf

[26] At a cost of $0.75 each

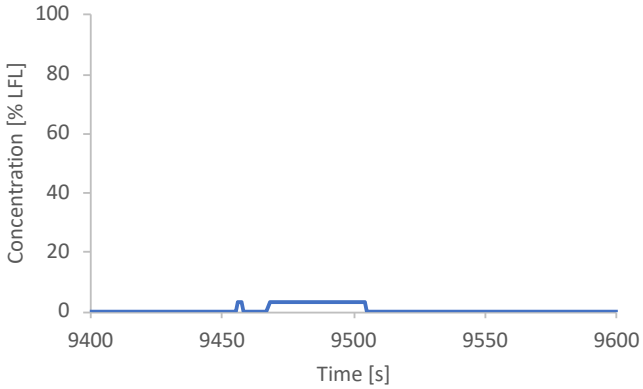

Figure 184: Concentration within the AHU.

A7.2.4 Final remarks

These practical trials indicated favourable results with application of the USD technology. Importantly the response time was extremely fast – much faster than what is usually experienced with gas detection. As mentioned above, ultrasonic receivers are relatively low cost and measurements are entirely repeatable. The most important consideration seems to be good positioning of receivers, based on simulated release locations and orientations. Another factor key to their effectiveness is related to the construction of the internal surface of the AHU. For instance, where the walls are covered by thermal insulation, effectiveness of the USD tends to be reduced and a hard or metal internal surface layer greatly helps (for low release rates). These tests were carried out on the factory floor, surrounded by loud machinery (e.g., metal punching, brazing and arc welding, conveyors, trolleys, pipe benders, etc. and these did not seem to interfere with the USD.

In conclusion USD seems to offer a low-cost and reliable means of leak detection that could be applied throughout RACHP equipment where refrigerant-containing parts are located within unit housing.

A7.3 Gas detection

The effectiveness of using gas sensors for potentially activating mitigation measures was also investigated, specifically during periods without fan operation. Ten different release positions were selected and six different sensor locations, as indicated in Figure 185.

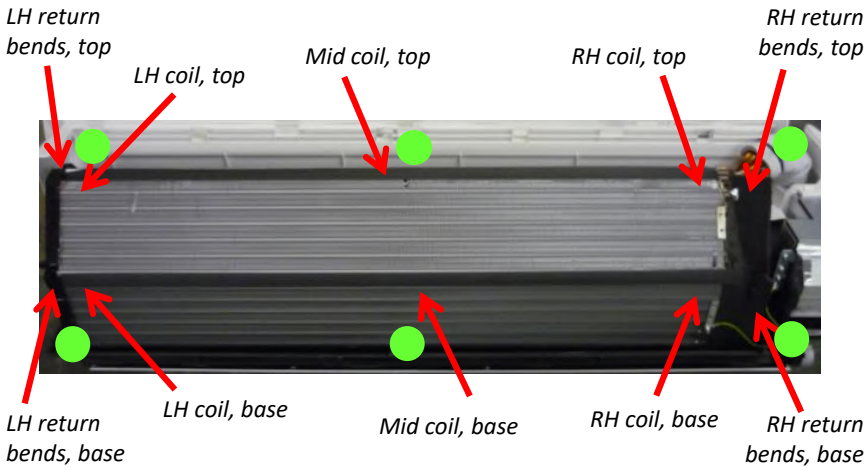

Figure 185: Location of releases (red arrows) and sensor positioning (green circles) within wall IDU.

After "cleaning" the room, the release was initiated and continued until sensors achieved at least 20% LFL or until 1½ minutes had elapsed. Two separate vapour mass flow rates were used: 15 g/min and 90 g/min, to mimic "small" and "large" leaks, respectively. Table 20 presents an overview of the results, being expressed as the number of seconds until a given sensor reached 20% LFL. Note that all durations were adjusted according to the measured response time of each of the sensors.

Table 20: Time (seconds) from start of release to 20% of LFL for different sensing and release positions

Release location	Mass flow (g/m)	#8: LH end, top	#1: LH end, base	#5: Mid, top	#6: Mid, base	#7: RH end, top	#4: RH end, base
LH ret bends, mid	90	1	1	10	12	13	9
LH ret bends, mid	15	1	1	13	18	18	19
LH ret bends, top	15	1	1	18	12	24	8
LH ret bends, top	90	1	1	52	17	a	8
LH ret bends, base	90	1	1	13	11	15	[forgot]
LH ret bends, base	15	1	1	39	27	30	13
LH coil, top	15	18	a	a	59	a	a
LH coil, top	90	14	17	19	58	a	29
LH coil, base	90	11	12	13	11	16	3
LH coil, base	15	11	a	a	11	a	10
Mid coil, top	15	a	a	10	5	a	a
Mid coil, top	90	a	a	8	5	13	16
Mid coil, base	90	a	a	a	45	a	a
Mid coil, base	15	a	a	a	a	a	a
Mid coil, base	15	a	a	a	a	a	a
Mid coil, top	15	a	a	a	8	a	a
RH coil, top	15	a	a	14	a	9	8
RH coil, top	90	15	15	10	11	11	6
RH coil, top	90	16	a	a	7	11	7
RH coil, base	15	a	a	a	8	a	18
RH coil, base	15	a	a	a	a	20	12
RH coil, base	90	a	a	a	7	a	10
RH ret bends, top	90	14	16	9	10	1	1

RH ret bends, top	15	29	[a]	[a]	30	1	1
RH ret bends, base	15	[a]	[a]	[a]	[a]	1	1
RH ret bends, base	90	17	[a]	[a]	53	1	1
RH ret bends, base	15	[a]	[a]	[a]	[a]	1	1

[a] *Concentration at position did not reach 20% of refrigerants LFL within test duration of 1.5 minutes*

In general, the findings were:

- No one gas sensor position was universally applicable, based on the conventional IDU design as used in the tests;
- Several sensor positions took longer to register a response (to 20% LFL) with a "large" leak than a "small" one;
- Some release positions did not result in any gas concentration reaching 20% LFL within the 1½ minute period, whereas others achieved a rapid response in all positions.

The basic conclusions are that one single sensing position is probably insufficient. Therefore at least two sensors should be used, or alternatively eliminate the concern of certain potential leak positions (such as creating a conduit from one region to another so as to transfer some leaked refrigerant). Nevertheless, based on these results the most preferable position seems to be that below the right-hand return bends at the base of the enclosure.

Ultimately this sort of exercise would be necessary for each RACHP unit housing for which gas detection is required.

A7.4 System parameters

RACHP system operating parameters may be used to indicate a deficit of refrigerant charge. There have been a variety of studies examining possible approaches for this, primarily measuring certain system parameters and comparing them against previously logged values. Software then uses fuzzy logic or artificial neural networks to determine whether the system operation is deviating sufficiently from the intended behaviour to justify warning of a possible refrigerant leak.

Such methods normally demand comprehensive monitoring of several parameters, such as pressures, temperatures, compressor current/power, possibly refrigerant flow rate, etc. Ordinarily this would be costly and cumbersome for smaller RACHP systems. Additionally, current methods tend to consider only deviation from steady operation, whereas for safety purposes the critical deviation in transient changes in operation, that arise from rapid refrigerant leakage; in the order of minutes to tens on minutes rather than over hours or days.

Two previous projects under the International Climate Initiative (IKI) involved the development of parameter-based leak detection systems; one with Transfrig in South Africa for transport refrigeration[27] and another with Godrej for R290 split air conditioners[28].

Figure 186 shows results of testing for the transport refrigeration system, where the leak detection scheme was used to close off an EEV so as to prevent refrigerant leaking into the refrigerated space. Parameters monitored were degree of EEV opening, suction superheat and suction pressure and observations from the initial testing were used to programme the control logic to react under the right conditions. Two different leak holes were tested as well as the two temperature levels (low and medium storage temperature). As well as "on" mode, the tests were also carried out during (hot gas) defrost mode. It can be seen that at least 50% of the charge can be retained, although with LT a greater proportion of refrigerant is held in the receiver. During cooling mode, the larger leak holes resulted in a more rapid response.

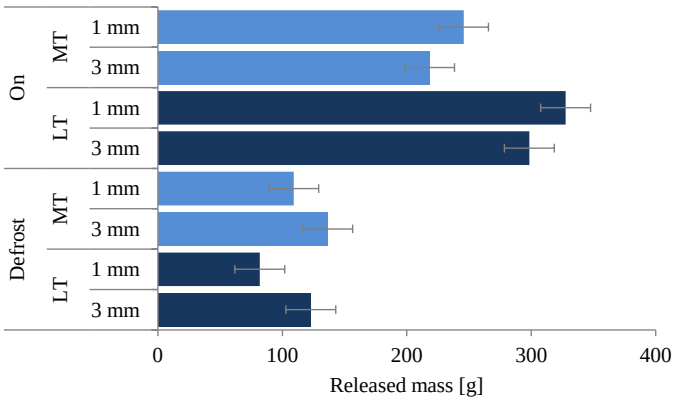

Figure 186: Released mass under different conditions; no intervention results in 650 g released.

For the R290 split ACs, similar testing was carried out both during on-mode and off-mode. Only pressures and temperatures were recorded, since the units did not use EEVs and in addition the variation in compressor power/current was found to be too small to identify a leak. Figure 187 provides some example results for off-mode, where there is a rapid decline in evaporating temperature and suction pressure within a half-minute of the release starting and this continues at a rapid rate until the system is almost empty. Again, the larger leak holes yield a faster decline in pressure and temperature.

[27] https://www.international-climate-initiative.com/en/nc/details/project/development-of-innovative-logistics-and-supply-structures-in-the-refrigerated-transport-sector-in-south-africa-12_I_148-443/

[28] https://www.international-climate-initiative.com/en/news/article/new_production_plant_for_climate-friendly_air_conditioners_in_india/

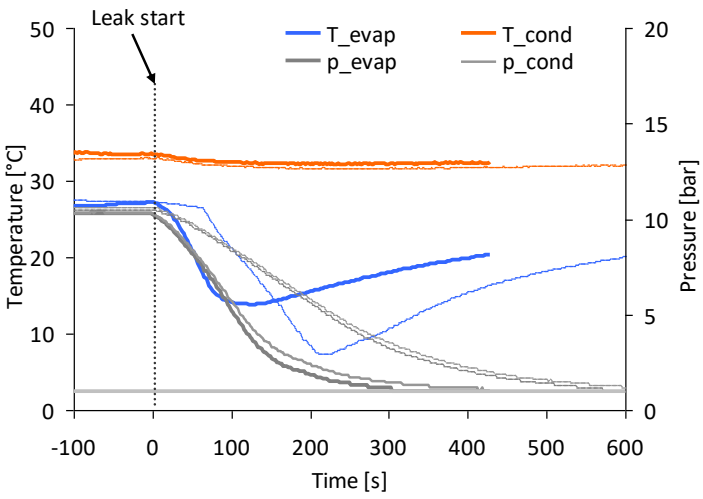

Figure 187: Pressure and temperature profiles for release with system in off-mode; thick lines 1.6 mm hole, thin lines 1.0 mm hole.

Similar tests were carried out on an 8 kW window type AC in off-mode, with three different hole sizes and starting charges as seen in Figure 188, Figure 189 and Figure 190. The graphs clearly show the decline in system pressure, which could be used for leak detection.

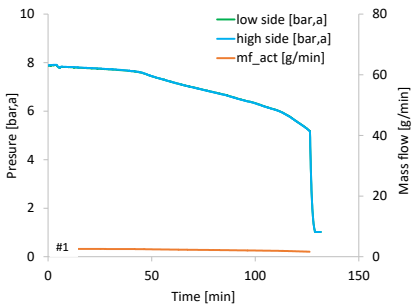

Figure 188: 260 g; 0.2 mm diameter (0.03 mm2).

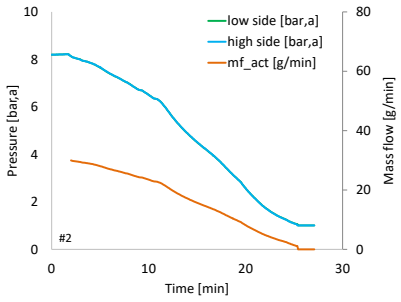

Figure 189: 400 g; 0.5 mm diameter (0.2 mm2).

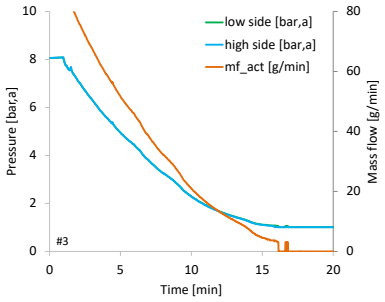

Figure 190: 500 g; 1.0 mm diameter (0.8 mm2).

Additional results are shown in Figure 191, Figure 192 and Figure 193, but taken from a simulation model (Colbourne and Zhu, 2012).

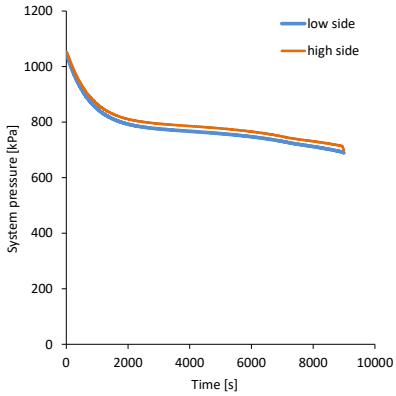

Figure 191: 1000 g; 0.3 mm diameter (0.07 mm2).

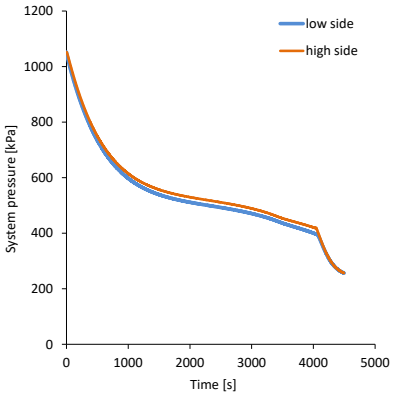

Figure 192: 1000 g; 0.5 mm diameter (0.2 mm2).

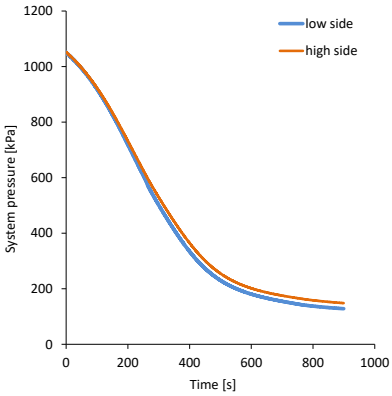

Figure 193: 1000 g; 1.0 mm diameter (0.8 mm2).

Across these various results it is clear that again, specific characteristic measurements are necessary for each different system (including expansion device).

ANNEX 8 CONSIDERATIONS FOR MAXIMUM SAFE LEAKAGE RATE (MSLR)

A8.1 Introduction

As previously discussed, some minimum mass flow rate of a leak must be specified. This Annex highlights some of the discussions associated with the selection of the MSLR.

A8.2 Decay in leakage mass flow

As shown in section 2.3, all leaks (under a fixed set of ambient conditions) start at the highest mass flow and decay to zero. Thus, whatever MSLR that is chosen would be based on some initial flow rate but would nevertheless decay to lower values thereafter. Whilst it could be argued that the median flow rate be used, the results indicate that the highest value is broadly the most important, even in the event that it persists only for a relatively short period.

A8.3 Residual air movement

Measurements using high sensitivity omnidirectional anemometers as part of a previously reported study (Colbourne and Suen, 2003) found that despite a room being totally sealed with plastic film and the insulated room being enclosed within a second insulated room so as to eliminate as much as possible thermal gradients, residual air movement was recorded. The data in Figure 194 is from about 23 equally distributed anemometers measuring air speed in between release tests with forced airflow. The residual air speed never falls below 0.03 m/s at any of the sensors.

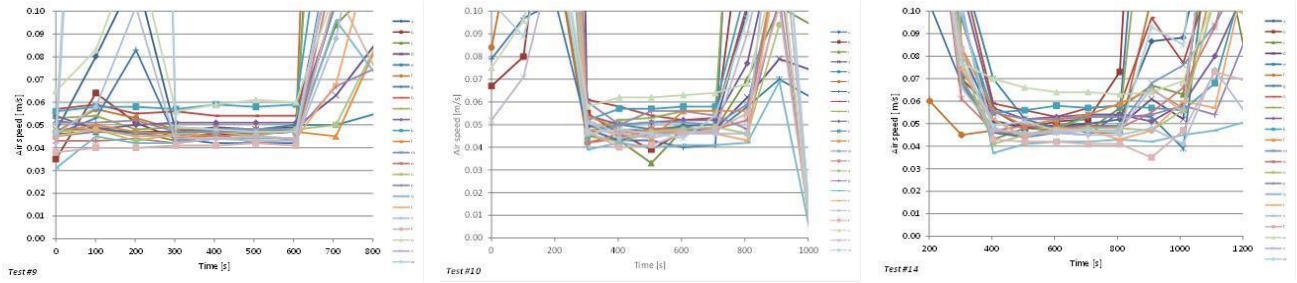

Figure 194: Measurements of residual airflow within the room.

It is difficult to integrate such residual air movement into computational models, given that the direction and local velocity is somewhat random due to there being no defined source. In this respect it should simply be borne in mind that whatever output arise from computations for a certain scenario will likely represent an unrealistically pessimistic result.

A8.4 Room air changes

All occupied spaces have some degree of ventilation – be it intended or unintended – due to openings in the space envelope and permeable construction materials. Temperature difference between inside and outside air generates static pressure gradients and pressure difference caused by wind speed both contribute towards air volume exchange across the space. Figure 195 give some example data for air change rates for a compilation of European dwellings (Orme, M., et al 1998) based on weather conditions for central UK.

Using a range of typical air change rates and a simple box model, average concentration following a release of R290 in the bottom third of a 100 m^3 room is shown in Figure 196. It can be seen that even with a relatively small air change rate of 0.5 room changes per hour, the average concentration is about half of the "tight" (0.0 air changes per hour) case. Since 99% of buildings within Europe will have an air change rate of at least 0.2 per hour, this infers that in the vast majority of cases the actual average and local concentration arising from a leak will be substantially lower than what computations may suggest.

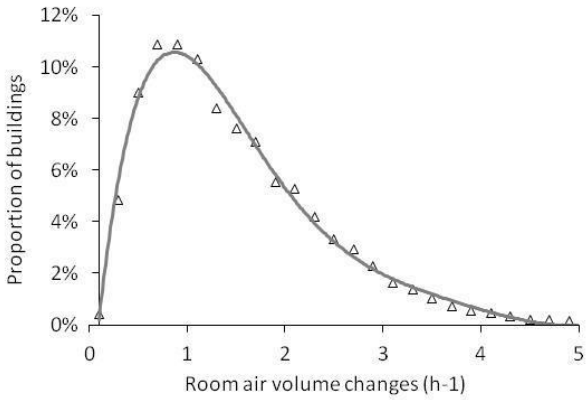

*Figure 195: Example air charge rates arising from temperature difference (*Orme, M., et al 1998*).*

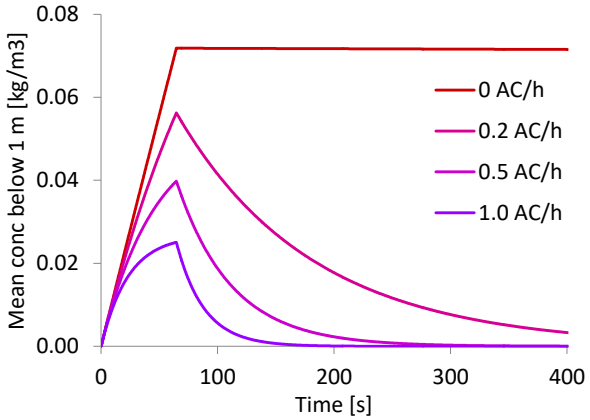

Figure 196: Effect of selected air change rates on average R290 concentration in bottom third of room.

A8.5 Thermal sources

In addition to room leakage and residual air movement, presence of thermal sources can also lead to additional air movement within a room. As an example, Figure 197 presents test results (Colbourne and Suen, 2003) for a release into a 100 m^3 room containing four thermal manikins and four mock PCs, each with a 100 W thermal output; these give an average thermal load of 20 W per m^2 of floor area. Superimposed on the data is the average concentration for the case without thermal sources.

The data shows that whilst the rise in floor concentration is similar in both cases, the presence of thermal sources results in a rapid decline in floor concentration and also mixing at ceiling level. Eventually these thermal convection currents lead to homogenisation of the entire release throughout the room within a few minutes. Thermal loads in the order of 20 W/m^2 are likely in most occupied spaces.

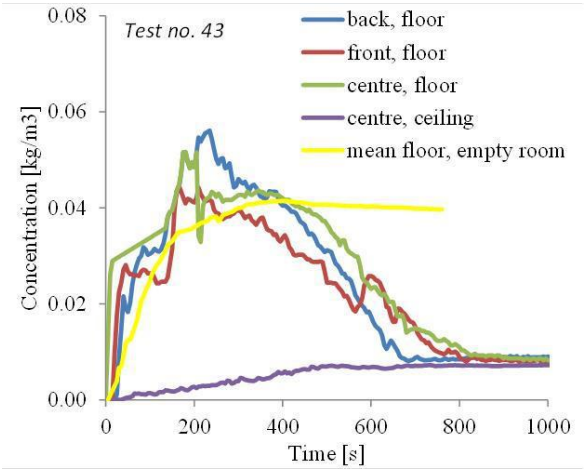

Figure 197: Room concentrations arising from releases into a room with thermal sources.

This effect was further investigated for spaces within which relatively slow leak rates were assumed to occur. Two cases were examined:

i) Heat flux from one heating wall (+15 W/m2 = 170 W total) and one cooling (-15 W/m2) for thermal balance (Figure 198);
ii) Heat flux from two persons (+100 W each = 200 W total) and cooling (-2.6 W/m2) at each vertical wall for thermal balance (Figure 199).

Releases were simulated from an IDU located at one narrow end of the room and at a height of 0.5 m so as to minimise the benefit of full room mixing. Various low mass flow releases were evaluated, where calculations start simultaneously at 0 s for both release and heat flux.

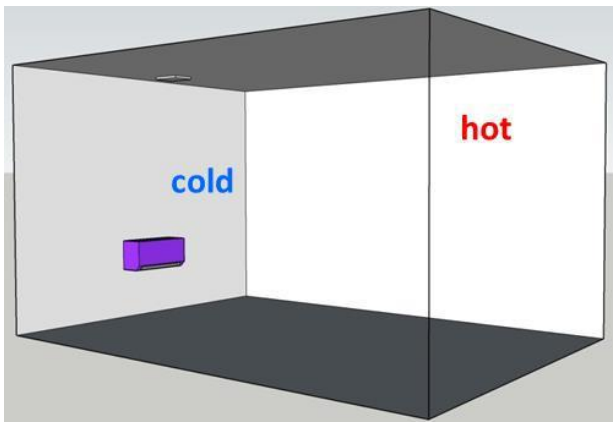

Figure 198: Case with one heated opposite and one cooled wall.

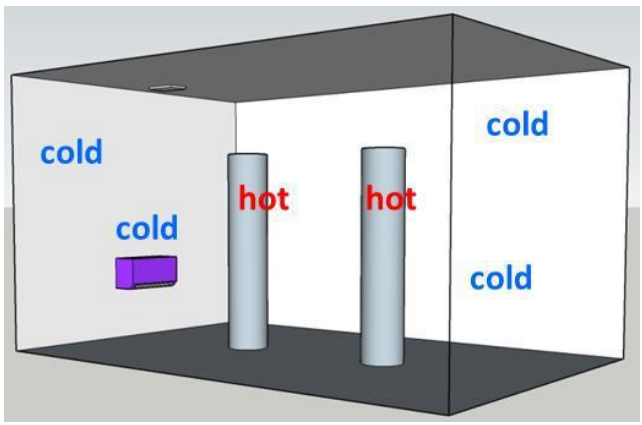

Figure 199: Case with four cooled walls and two heated columns (to mimic people).

Calculations were carried out for release rates of 5 g/min, 10 g/min and 15 g/min, with Figure 200 and Figure 201 showing results for the 15 g/min case.

Figure 200 shows iso-concentration contour images at 100%, 75%, 50% and 25% of the LFL at 325 g release mass. At 75% of LFL a uniform layer at the floor does not occur and instead the layer is “pushed” towards the hot wall and at 50% additional layers are seen about 1 m above the floor and again at ceiling level. The entire space contains a mixture of at least 25% LFL throughout.

Room mid-line concentrations are in Figure 201 taken at 150 g increments, for both the thermal and isothermal (inset) cases. As indicated by Figure 200, there are significant differences arising from the thermal convection where significant vertical mixing is apparent compared to the isothermal case. The bottom-left image shows 100% LFL contour at 450 g release mass, again with thermal convection and isothermal (inset) cases. Here, there is a significant difference in both the floor area across which the flammable mixture has spread and also the formation of total flammable volume, illustrating the substantial impact of thermal sources on mixing of the release. Analysis of the results shows that local shear velocities of up to 0.13 m/s are present, which correspond to the high degree of mixing.

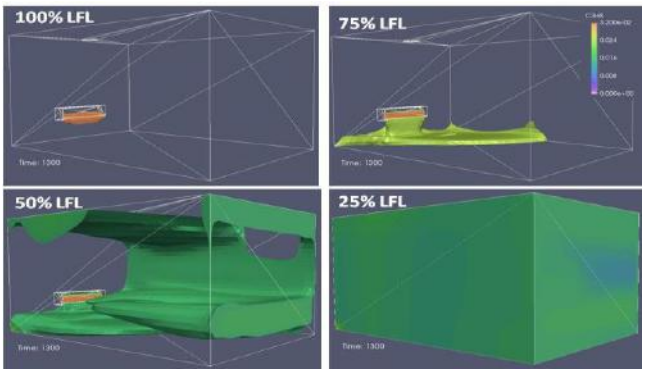

Figure 200: Iso-concentration images at 100%, 75%, 50% and 25% of LFL for 325 g at 15 g/min release rate in room with two thermal walls.

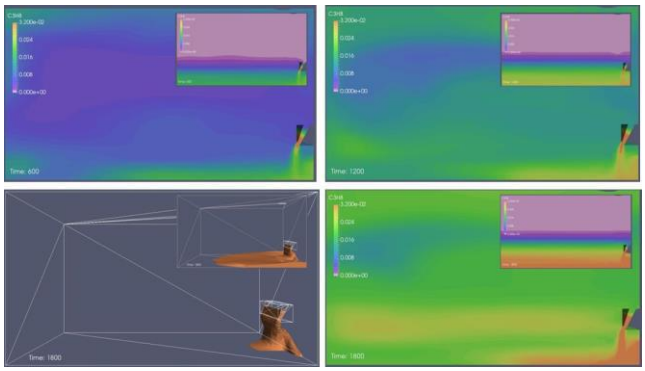

Figure 201: Images of mid-line concentration at time steps corresponding to 150 g increments with insets showing result for isothermal conditions.

Figure 202 and Figure 203 provide equivalent results for the second case with the thermal columns.

Iso-concentration contour images at 100%, 75%, 50% and 25% of the LFL at 325 g release mass are included in Figure 202; the distribution of the volumes are somewhat different from those in Figure 200. At 75% of LFL almost no flor layer is present and at 50% of LFL an elevated layer is apparent again at about 0.5 – 1.0 m above the floor and “hugging” the thermal columns. Again, the entire room contains at least 25% LFL mixture.

Mid-line concentrations for both the thermal and isothermal (inset) cases in Figure 203 at 150 g increments similarly show extensive mixing throughout the room volume. In the bottom-left image with 100% LFL contours at 450 g release mass, there is an even more substantial effect on the decrease of flammable volume due to thermal convection. Shear velocities within the space were also up to about 0.13 m/s.

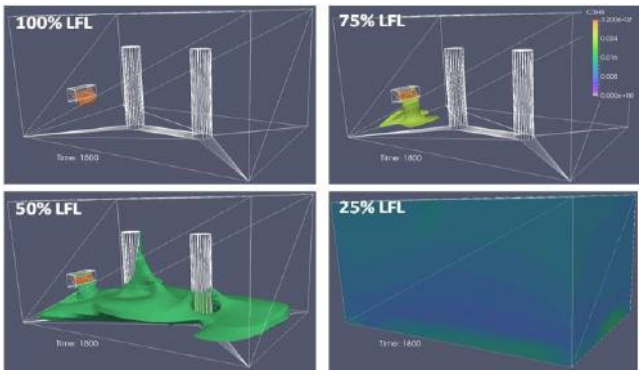

Figure 202: Iso-concentration images for 100%, 75%, 50% and 25% of LFL for 15 g/min release rate in room with two thermal columns and four walls.

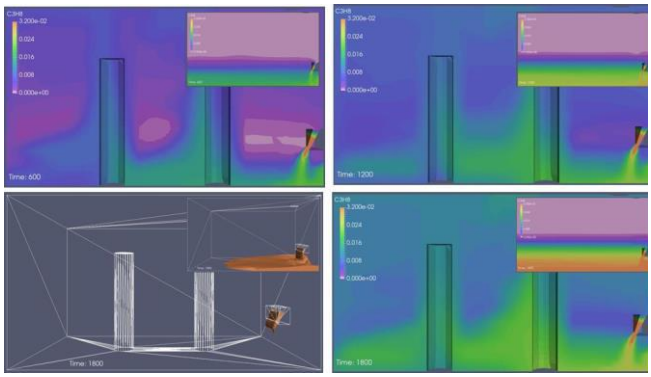

Figure 203: Images of mid-line concentration at time steps corresponding to 150 g increments with insets showing result for isothermal conditions.

These results highlight that even though heat flux through the space is relatively small thermal convection currents can almost entirely neutralise formation of flammable layers within the room, when leak rates approach those of MSLR.

A8.6 Movement of personnel

A final contribution to mixing of a small mass flow release within a space is that of moving personnel. To illustrate this, Figure 204 and Figure 205 show measurements made in the UCL lab, where a mass of R290 was released and moments after cessation of the release, one person began to slowly stroll around the lab floor for about three minutes, as indicated by the grey box. Within about two minutes the average flor concentration reached half the LFL and approach homogeneity by about three minutes. It is evident that gentle movement of a room occupant effectively easily mixes and dilutes stratified layers.

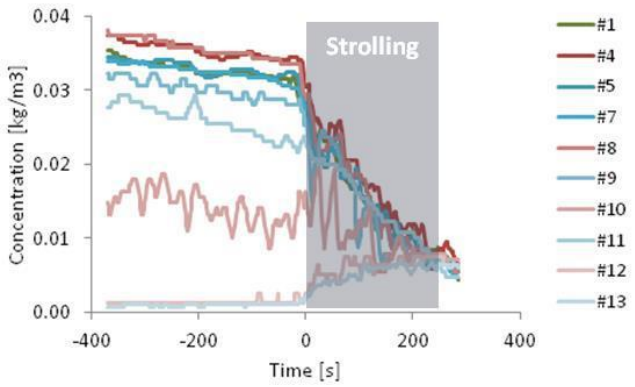

Figure 204: Example of dilution of concentration arising from 300 g of R290 released at 50 g/min from a height of 1 m.

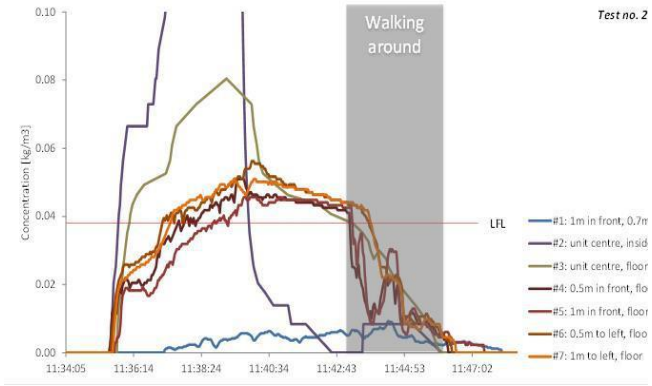

Figure 205: Example of dilution of concentration arising from 150 g of R290 released at 40 g/min from a height of 0.2 m.

A8.7 Final remarks

Ordinarily many of the sources of air movement discussed above are not normally taken into account and several of they are likely to be relatively ineffective in mixing releases that occur at higher mass flow rates. However, at least when lower mass flow rates (relative to a certain room size) occur, residual internal airflow, infiltration, thermal sources and movement of personnel can all have a notable effect on diminishing the size and duration of potentially flammable mixtures. Consideration of typical occupied spaces suggests that at least two of these sources of air movement will be present at leak 99.9% of the time (including residual internal airflow which is taken to be present continuously). Therefore, it is absolutely reasonable to rely on the effect of these to aid the dilution of a release under MSLR.

Furthermore, whilst leakage from real systems may be at MSLR and persist for a few moments, the decay in system pressure means that it gradually decays (to 0 g/min), thus posing less of a hazard than otherwise anticipated. Provided that any mitigation measure is set to intervene at or below MSLR, the majority of the release will be at a value below MSLR.

Further computational analyses were carried out for much larger rooms (56 m2), with an IDU height of 1 m; the proposed charge size calculation gives a charge of about 2500 g and the MSLR calculation results in about 63 g/min the factor ω = 0.50 and 45 g/min when ω = 0.35. Figure 206 shows results for a 65 g/min example and 40 g/min in Figure 207. With 65 g/min, the flammable volume hits the room floor at about 20 minutes/1200 g into the release, but by the time is reaches 30 mins/2000 g the flammable volume covers a large proportion of the room floor. Using 40 g/min, the flammable volume reaches the floor after 1600 g and begins to flor the floor at 2400 g. However, noting that residual air movement is not accounted for here and moreover with such a large room, it is much more likely that the aforementioned thermal convection and movement of personal are present in real situations. Nevertheless, if the maximum charge limit of “m2” (i.e., 26 m3 × 38 g/m3 = 988 g) is retained then both would be acceptable.

LIFE FRONT IS FUNDED BY THE EU UNDER THE LIFE CLIMATE ACTION PROGRAMME, PROJECT NUMBER LIFE16 CCM/BE/000054